Project funded by the European Commission under the 6th (EC) RTD Framework Programme (2002- 2006) within the framework of the specific research and technological development programme "Integrating and strengthening the European Research Area"

**Project UpWind**

Contract No.:
019945 (SES6)

"Integrated Wind Turbine Design"

# Final report WP 4.2
# Support Structure Concepts for Deep Water Sites

## Deliverable D4.2.8

## (WP4: Offshore Foundations and Support Structures)



| | |
|---|---|
| AUTHOR: | Wybren de Vries, |
| AFFILIATION: | Delft University of Technology |
| ADDRESS: | Stevinweg 1, Delft, The Netherlands |
| TEL.: | +31 15 2787568 |
| EMAIL: | w.e.devries@tudelft.nl |
| FURTHER AUTHORS: | Naveen Kumar Vemula & Patrik .Passon (Rambøll), Tim Fischer, Daniel. Kaufer & Denis Matha, (SWE Universität Stuttgart), Björn. Schmidt (Germanischer Lloyd), Fabian Vorpahl (Fraunhofer IWES) |
| REVIEWER: | B. Schmidt, F. Vorpahl, T. Fischer |
| APPROVER: | Jan van der Tempel (Delft University of Technology) |



Document Information

| | |
|---|---|
| DOCUMENT TYPE | Deliverable Report |
| DOCUMENT NAME: | UpWind_WP4_D4.2.8_Final Report WP4.2: Support Structure Concepts for Deep Water |
| REVISION: | - |
| REV.DATE: | - |
| CLASSIFICATION: | General Public (R0) |
| STATUS: | S0 - Approved/Released |

# Acknowledgement

The presented work was funded by the Commission of the European Communities, Research Directorate-General within the scope of the Integrated Project “UpWind – Integrated Wind Turbine Design” (Project No. 019945 (SES6).



| STATUS, CONFIDENTIALITY AND ACCESSIBILITY | | | | | | | | | | |
|---|---|---|---|---|---|---|---|---|---|---|
| **Status** | | | | **Confidentiality** | | | | **Accessibility** | | |
| **S0** | Approved/Released | **X** | | **R0** | General public | **X** | | Private web site | |
| **S1** | Reviewed | | | **R1** | Restricted to project members | | | Public web site | **X** |
| **S2** | Pending for review | | | **R2** | Restricted to European. Commission | | | Paper copy | **X** |
| **S3** | Draft for comments | | | **R3** | Restricted to WP members + PL | | | | |
| **S4** | Under preparation | | | **R4** | Restricted to Task members +WPL+PL | | | | |

**PL:** *Project leader* **WPL:** *Work package leader* **TL:** *Task leader*

# Summary

With the number of offshore wind farms rapidly increasing, in a wide variety of site conditions and using different turbine sizes, the need for alternative support structures other than the conventional monopile structure is apparent and several projects have been realised using other support structure types. In this report the results of Upwind Work Package 4, task 4.2 are reported. The aim of task 4.2 is to develop support structure concepts for large offshore wind turbines and deep water, including bottom mounted very soft and floating structures.

To meet this objective, first a survey of existing and proposed support structure concepts has been done. To establish the practical limitations and requirements for offshore wind turbine support structures, a review has been made of the fabrication process and installation methods for support structures. A description of the design methodology applied for monopile and multi-member structures is presented, including a review of design criteria.

Many concepts for support structures have been proposed, some of which have already been realised. Existing structures include fixed steel structures, concrete gravity foundations and floating structures and several other fixed and floating concepts can be envisaged.:

Existing concepts

- Monopile
- Tripod
- Jacket
- Tripile
- Gravity based foundation
- Spar floater
- Semisubmersible floater

Proposed concepts

- Suction bucket monotower
- Three-legged jacket
- Three or four legged full truss structures
- Hybrid monopile-truss structure
- Compliant structure
- Barge floater
- Tension leg platform

Based on these findings reference designs for a monopile structure in 25 m water depth and a jacket structure for 50 m deep water have been made. Sensitivity analyses showed how the loads and required dimensions for these structures vary as functions of the main environmental parameters and for key turbine parameters. Using these findings the mass and costs could be determined for a variety of conditions, leading to cost models for the monopile and jacket structures.
To look beyond the established concepts an analysis has been performed of more innovative bottom-fixed support structure concepts, including a tripod, a three-legged jacket, and a hybrid monopile-truss structure.
Finally, conceptual studies for support structures with fundamental frequencies outside the conventional soft-stiff range have been performed, first for compliant fixed structures, secondly for floating structures. Also a design solution for a support structure supporting a fictitious 20 MW turbine is presented.

The monopile reference design has been carried out for a shallow water site with conditions that lead to hydrodynamic dominated fatigue. The reference design approach included two stages. First, a preliminary design was made, based on superposition of hydrodynamic loads and predetermined aerodynamic loads. In the final design stage a fully integrated time domain analysis was performed for a large number of load cases, including extreme event and fatigue analyses.
The resulting design comprises a foundation pile with a bottom diameter of 6 m and a conical section tapering to a top diameter of 5.5 m. The embedded length is 24m and the total length is 54 m. The transition piece has an outer diameter of 5.8 m and a total length of 18.7 m. A tower of 68 m length is used, leading to a hub height of 85.2 m. The overall mass of the primary steel for the foundation pile is 542 tonnes and 147 tonnes for the transition piece. The required wall

thickness for the monopile and transition piece is driven by fatigue, whereas the penetration depth is driven by extreme loads and natural frequency requirements.

The Upwind reference jacket structure is intended to demonstrate a design solution for a support structure for an offshore wind turbine in 50 m of water and may be used for comparison with other support structure concepts and the demonstration of the sensitivity to environmental conditions and to structural parameters.
In a detailed design phase, time series of aerodynamic loads were combined with wave time series to establish the dynamic response to extreme event and fatigue load cases. The structure was optimised to fulfil the requirements for natural frequency, strength, stability and fatigue life. The final design shows that the critical locations for the ultimate limit state are in the X-braces at the jacket base, whereas for fatigue the critical joints are the connections of the top X-braces to the legs.
The interface level and hub height are set at 20.15 m and 90.55 m above MSL. A concrete transition piece is applied with length and width of 9.4 m and 4 m height. Due to the large water depth at this site, four levels of X-braces are implemented in order to comply with the requirement of the minimum angle between chord and brace. A jacket bottom width of 12.0 m is chosen. The mass of the concrete transition piece is 666 tons, while the overall mass of the primary steel for the jacket structure is 983 tonnes, the piles accounting for 438 tonnes and the jacket substructure contributing the remaining 545 tonnes.

A cost model has been established for monopile foundations. This allows for quick assessment of the impact of changing turbine parameters on the support structure costs. The model has been set up to determine the overall mass of the support structure based on a limited number of input parameters for the environment and the turbine. Parameters for the turbine are rotor diameter, rotor speed, and turbine mass. Environmental parameters included in the model are water depth, wave height and soil conditions. The dimensions of the support structure are determined on the basis of the natural frequency and a stress check for combined wind and wave loading. The overall costs are calculated based on material costs in which costs for the manufacturing are included.
A validation of the model has been performed using support structure mass data and the corresponding environmental data and turbine parameters of two existing projects and the monopile reference design. The results match the mass of the actual projects and the reference design within 20 %.
In a similar costing tool for a jacket structure the mass of a jacket support structure is determined as a function of the water depth, turbine size and soil conditions. This shows that the mass of a jacket structure increases approximately linearly with water depth. Limited data is available for verification, but comparisons with the jacket reference design and with a jacket design for the Alpha Ventus wind farm show that the resulting masses determined with the cost model are within 10% of the masses of the compared designs.

Apart from the reference designs for the monopile and jacket structures, several other support structure concepts have been assessed. Preliminary designs were made for a tripod, a three-legged jacket, and a monopile - truss hybrid in 50 m water depth. Also a monopile structure has been designed as a reference. The reference jacket structure is also included in the comparison. The results of this analysis show that three and four leg jackets are most suitable for deep water conditions, while a monopile -truss hybrid may also be feasible. The tripod structure appears to be less cost-effective than the jacket and truss structures, due to its increases sensitivity to hydrodynamic loads.

In order to achieve sufficient flexibility for a compliant structure to locate its first natural frequency inside the soft-soft range and below wave frequencies with high energy artificial soft spots are required. However, it is difficult to achieve strength and stability requirements for such a structure at the same time. Therefore additional restoring force is required. A study in which an extended monopile, a compliant piled tower and an articulated buoyant tower have been

evaluated showed that it is possible to design an articulated buoyant tower as a compliant structure in 50 m water depth. The mass savings compared to a soft stiff design for the same conditions were found to be approximately 100 tons in this preliminary assessment. For the other two concepts it has not been found possible to achieve a compliant design for the considered conditions, as the strength and stability requirements cannot be satisfied simultaneously with the natural frequency requirements.
Compliant structures for offshore wind turbines could be effective in intermediate water depths, where bottom-mounted structures may no longer be viable and floating structures might still need too much buoyancy to be cost effective.

A comparison of several floating support structure concepts has been made which includes a tension leg platform floater, a spar buoy and a barge floater. The concepts have been compared based on statistics, extreme event analysis, instabilities and fatigue life evaluations. The simple design of a barge floater may prove to be cost effective for benign sea conditions. The spar buoy is better suited for harsh sea conditions, but its deep draft and the large ballast make the structure relatively expensive. Regarding ultimate strength and fatigue considerations, the tension leg platform appears to perform best, but the installation procedure and the large mass makes it an expensive structure type. The results of these comparisons help to resolve fundamental design trade-offs between these floating concepts

A design for a jacket support structure for a 20MW turbine has been made. The 20 MW turbine used is the result of the application of classic upscaling coefficients rather than more realistic values as e.g. obtained from turbine development trends over the last years, leading to a very heavy, unrealistic design. Due to the low rotor speed of the 20 MW turbine the upper boundary of the 3P range is at 0.306 Hz. Therefore a stiff-stiff design is considered, rather than the conventional soft-stiff approach.
The foundation design is considered reasonably only in relation to the given tower and RNA configuration. Nevertheless, the designed foundation structure is very large and not expected to be a good representation of future jacket foundation structures for 20MW turbines. The resulting jacket structure has a top width of 28m and a base width of 42m. The overall structure mass, including piles, transition piece and jacket is 5610 tons. The associated first natural frequency is 0.297 Hz. As such the structure's first natural frequency falls within the 10% safety margin at the upper end of the 3P range. However, it is shown that it would be possible to achieve a design with a first natural frequency in the stiff-stiff range when the RNA mass and rotor diameter are scaled in more line with technological developments. Other possibilities for enabling the application of 20 MW wind turbines offshore is by employing lattice towers instead of the tubular tower used in this design.
Equipment and facilities for fabrication, transportation and installation of the designed foundation components are available even nowadays. Limitations arise in connection to the installation of the given tower and RNA components due to the large hub height as well as for fabrication of the tower segments due to the large diameter.

# Table of Contents

# 1. Introduction

## 1.1 The Upwind project

The offshore wind energy industry is turning out ever larger numbers of offshore wind turbines every year. Although significant progress has been made in making offshore wind energy more cost-effective, further cost reductions must be achieved to compete on equal terms with other sources of energy, such as gas and coal powered energy and land based wind energy. One way to achieve this is to turn to economies of scale, both in numbers and in terms of power output of turbines. To facilitate this development the EU funded research project was initiated in 2006. UpWind looks towards wind power of tomorrow; towards the design of very large turbines (8 to 10MW) standing in wind farms of several hundred MW, both on- and offshore.
The project brings together participants from universities, knowledge institutes and the industry from across Europe. Topics of research are gathered in work packages for example focussing on aerodynamics & aeroelastics, rotor structure & materials, control systems and electrical grids. One topic specifically geared towards the offshore development is the development of offshore support structures to enable the offshore application of large turbines in deep water sites.

## 1.2 Work Package 4: Offshore Support Structures and Foundations

The primary objective of the offshore support structure work package (WP4) is to develop innovative, cost-efficient wind turbine support structures to enable the large-scale implementation of offshore wind farms, for sites across the EU.
To achieve this objective, the work package focuses on the development of support structure concepts suitable for large turbines and for deep water which are insensitive to site conditions. Further focus lies on the assessment and enhancement of the design methods and the application of integrated design approaches to benefit from the integrated design of turbines and monopile support structures. The work package is divided into three tasks to execute the research for these subjects:

- Task 4.1: Integration of support structure and turbine design for monopile structures
- Task 4.2: Support structure concepts for deep-water sites
- Task 4.3: Enhancements of design methods and standards for floating support structures

To this end three main types of support structure concepts are addressed: monopile structures, braced structures and very soft and floating structures. The level of detail in the research reflects the state of current knowledge. The work package aims at making the “next step” in the development of these main concepts:

- For monopile structures focus will be on structural optimisation and pushing the boundaries of the range of application by integrated design.
- For braced support structures the focus is on structural development and making such structures suitable for large scale application.
- For very soft and floating structures the focus is on concept development and on the development of tools to assess these structure types

This report is part of a set of reports which together make up the final reporting of Work package 4. The work done in each task is documented in a separate final report. One encompassing report summarises the findings of the WP in an executive summary. The interrelation of the four reports is show in Figure 1.1.

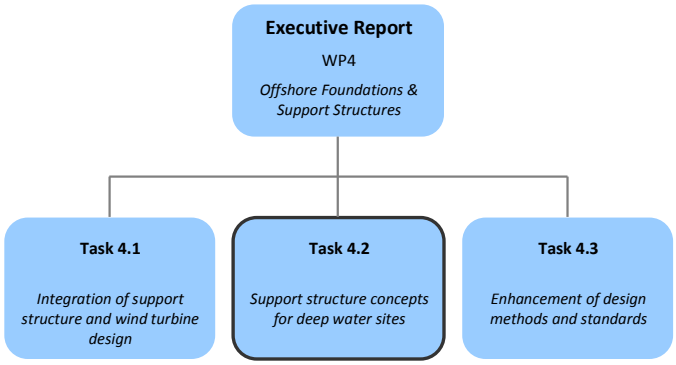


Figure 1.1: Context of reports in WP4

## 1.3 Task 4.2: Support structure concepts for deep water sites

The aim of the task 4.2 is to develop support structure concepts for large offshore wind turbines and deep water sites. The suitability of these concepts for varying water depths, site conditions and turbine sizes is also established. The work can be categorised as follows:

**Review of background and methods**

- Review identifying existing support structure concepts and presenting innovative braced and soft support structure concepts.
- Review of factors influencing design, such as site conditions, turbine parameters and fabrication and installation requirements.
- Review of design methodology.

**Design assessments**

Design assessments are performed for monopile and braced support structure concepts. Qualitative and conceptual analyses are made of innovative soft and stiff support structure types including compliant and floating structures for deep water and braced structures for very large turbines.

**Sensitivity analysis and cost modelling**

Sensitivity analyses of fixed support structures are performed with regard to environmental and structural parameters. The variation of costs for varying environmental conditions and turbine parameters is  and cost modelling of jacket and monopile structures is performed.

## 1.4 Report structure and context

This report starts off by giving an overview of existing and new support structure concepts. Subsequently, the background of support structure design, fabrication and installation is described. The site conditions and turbine parameters that will have impact on the design are identified and the applied design methodology for support structures for offshore wind turbines is described.

Subsequently the monopile support structure concept is treated in detail. A reference structure is design in two phases a preliminary design based using a non-integrated approach and a final design phase incorporating integrated time domain analyses for large number of load cases. A sensitivity analysis is performed. Finally a cost model is presented showing the variation of turbine mass with varying environmental conditions and turbine parameters.

A similar approach is taken for the next chapter, which deals with the reference braced support structure. A concept selection is performed to find the most suitable structure type for the analysis. A tripod and a jacket structure are considered revealing that the jacket is the most suitable structure type for the conditions. Subsequently a detailed design of the reference jacket structure for the 5.0MW UpWind reference turbine is described. Based on the final dimensions of the reference structure a sensitivity analysis is performed. Finally a cost model for jacket structures is presented indicating the variation of mass and costs for jacket structures for varying water depths and turbine parameters.

In the subsequent chapter preliminary designs for a number of alternative fixed support structure concepts are presented and a brief sensitivity analysis is given for each of the structures.
The next chapter deals with very soft or compliant structures with a first natural frequency below the wave frequencies with high energy content. Several possible concepts are presented and preliminary designs shown for a number of compliant structure concepts.
Similarly to compliant structures, floating structures can also be considered very soft structures. These are suitable for very deep waters. Three floating structure concepts based on different principles are presented in Chapter 10 and a comparison between the concepts is given.

Finally, an assessment is made of the requirements for support structures for very large wind turbines. To this end a preliminary design is presented for a 20 MW turbine in 50 m water depth. Apart from the design itself also considerations with respect to fabrication and installation of such large structures are discussed.

In the final chapter the conclusions for this report are presented and an outlook for support structures for large turbines and deep water is given.

# 2. Support structure concepts

## 2.1 Introduction

The primary function of the support structure is to keep the wind turbine in place and to transfer the loads from the turbine to the seabed. The presence of the structure itself attracts hydrodynamic and aerodynamic loads which should also be transferred to the soil.
Secondary functions are to allow for means of exporting the power produced by the turbine and to allow access to the turbine for inspection and maintenance purposes.
This chapter describes a variety of support structure concepts for offshore wind turbines, some of which are already in existence, others that are only proposed concepts.
Before a discussion of these support structure concepts can be given some definitions must be put forward regarding the support structure itself, its subcomponents and some important concepts.

## 2.2 Definitions

### 2.2.1 The support structure

Before support structure concepts are introduced a definition should be given of the 'support structure'. In its broadest sense it can mean the entire structure that carries the turbine. Sometimes the term foundation is used to indicate the entire structure as well. However, it may also be useful to define the foundation as the part of the structure that fixes it to the seabed. Usually the turbine tower is supplied by the turbine manufacturer. As such the tower is not the responsibility of the support structure designer. Therefore it is desirable to make a clear distinction between the tower, supplied by the turbine manufacturer and the structure designed by the offshore foundation designer.
To avoid confusion a definition of the support structure and the various components is given here, which will be maintained throughout this report. The support structure is defined as:

*The structure that supports the turbine and holds it in place and transfers the loads from the turbine to the ground*

The support structure is made up of three main components: the tower, the substructure and the foundation. For floating structures a mooring system is employed instead of a foundation. These components can be defined as follows:

| | |
|---|---|
| Tower | The tubular element(s) supplied by the turbine manufacturer on top of which the turbine is installed |
| Substructure | The part of the structure extending from the bottom of the tower down to the seabed |
| Foundation | The part of the structure in direct contact with the soil, transferring the loads from the structure to the soil[1] |

Mooring system The system of elements that connect the floating body to the seabed.

[1] For a monopile structure, the part of the pile embedded in the soil may be defined as the 'foundation', whereas the entire pile might be termed the 'foundation pile'. For a gravity based structure, the base slab can be defined as the foundation.

Figure 2.1 gives a representation of this definition of the support structure. This definition will be maintained in this chapter as it makes it easy to exchange one support structure concept for another.

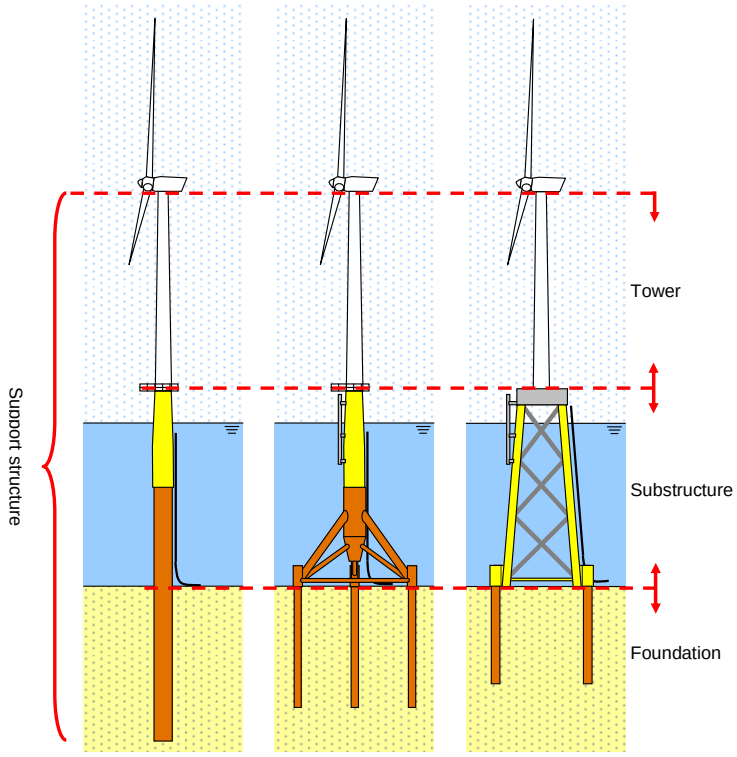


Figure 2.1: Definition of 'support structure' and main components

### 2.2.2 Design elevations

To facilitate communication between different parties involved in the design of an offshore wind turbine, two key elevations must be defined.

1. First the interface level is set. The interface level represents the interface between the turbine manufacturer's responsibility and that of the support structure designer in both a physical and an organisational sense. The interface level is located at the connection between the tower and the substructure. The elevation is chosen such that the main platform, which is generally situated at the level of the flange connection with the tower, cannot be hit by waves under extreme conditions.
2. The other elevation that must also be defined is the hub height. The hub height is the elevation at which the hub of the turbine is located.

### 2.2.3 Support structure components

#### Foundation

As part of different support structure concepts, various foundation concepts can be envisaged. Common solutions in the offshore oil and gas industry for bottom founded structures are the use of piles, suction cans and gravity base foundations. Piles and suction cans are also used to attach mooring lines for floating structures, as is the use of (drag) anchors.

Piles are open-ended hollow tubular elements that are installed vertically or at an inclination. Lateral loads are transferred to the soil by activating the horizontal active soil pressure, whereas axial loads are taken by shaft friction and end bearing.

Suction piles work along the same principles, although they have a distinctive method of installation. When the length of the pile is short in relation to the diameter, this type of foundation is also called a suction bucket or suction can. The suction can is a large diameter cylinder with a closed top. It is installed by placing it on the seabed and subsequently activating a pump that removes water from within the suction bucket. This creates a pressure difference with respect to the ambient pressure, which results in a downward force. This causes the suction can to be pressed down into the soil. Once the pump is deactivated skin friction and end bearing will keep the foundation in place and provide the required bearing capacity.

A gravity base foundation relies on the weight of the structure itself, if necessary in supplemented by ballast material to hold the structure in place on the seabed. The base is usually wide so that the resistance against overturning is large and also large resistance against sliding can be mobilised. Gravity foundations are integrated into the substructure and are usually made of concrete, but in principle ballasted steel structures are also possible.

**Secondary steel items**

The substructure usually comprises several secondary items to enable access, export of electricity and for protection of the structure itself. Depending on the structure type several or all of the following items will be present:

- Boat landings
- Ladders
- Platforms
- J-tubes
- Anodes

Boat landing — The boatlanding is the structure to which a vessel can moor to transfer personnel and equipment to the substructure. The boatlanding consists of two mainly vertical fenders connected by stubs to the main structure. Depending on the environmental conditions and on the maintenance strategy of the operator, there may be one or more boatlandings connected to a support structure.

Ladders — Ladders are required to allow personnel to access the main platform. If the distance to cover is larger than a certain limit, the ladder should be covered by a cage and have facilities for attaching fall arresters. Ladders for access to the main platform are usually combined with the boatlanding to provide protection for transferring personnel and to avoid difficult and dangerous steps to access the ladder from the vessel.

Platforms — Platforms are intended as safe working areas for personnel that need to work on the structure. Different functions can be identified; there are access platforms, resting platforms, and depending on the type of structures service platforms and airtight platforms. Platforms on offshore wind turbines are usually equipped with grating, to prevent excessive (air) pressure build up below the platform due to passing waves and to avoid accumulation of water that would render the floor slippery. Resting platforms are required for safety reasons when the vertical distance from the initial access point along a ladder to the next safe point exceeds a certain value. Service platforms are included for instance in the transition piece to facilitate the tightening of bolts at the base of the tower. Similarly, a service platform is installed at the level of the hydraulic jacks used to level the transition piece during installation. An airtight platform is required inside a transition piece for a monopile structure to close the flow of air towards the inside of the foundation pile, thereby limiting the process of corrosion.

J-tubes To protect and guide the export cable into the support structure, a J-tube is installed on the structure. The name derives from the shape that the tube makes as it curves to a horizontal orientation near the seabed. J-tubes can be either internal, only to protrude from the substructure at the seabed level, or external.

Anodes To provide cathodic protection against corrosion, blocks of aluminium may be installed as sacrificial anodes. Provisions must be made on the substructure to fix the anodes.

## 2.3 Overview of existing support structure concepts

In search of economic solutions for deeper water several new foundation concepts have been proposed. For inspiration, designers turned towards the offshore oil and gas sector. This sector has several decades of experience with various support structure types for all sorts of purposes; from the large deep water production platforms to small scale wellhead and monitoring platforms. Although loads on a turbine are very different than the loads on offshore platform topside facility, the concepts might be adapted to suit the needs of offshore wind energy production. These concepts can be divided into five main categories [1]:

- Monotower structure
- Tripod structure
- Jacket structure
- Gravity structure
- Floating structure

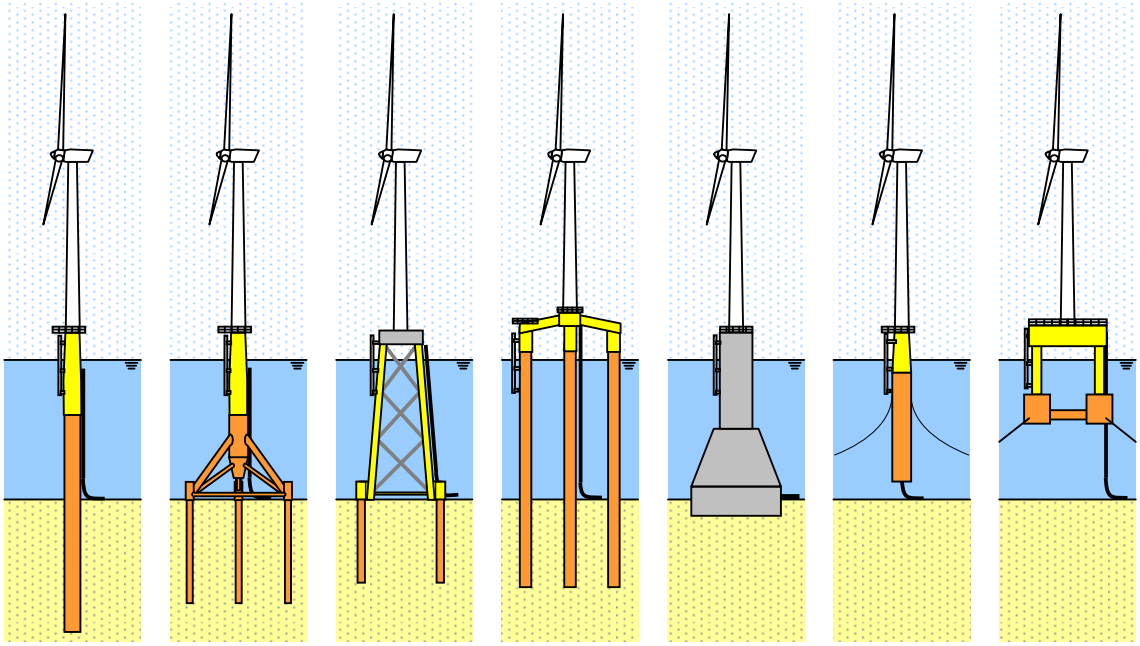

Figure 2.2: Existing support structure concepts (not to scale)

### 2.3.1 Monopile

The monopile foundation is more or less an extension of the onshore turbine tower below the sea surface and into the seabed. The vertical loads can easily be transferred to the soil through wall friction and tip resistance. The lateral loads, in comparison much larger, are conveyed to the foundation through bending. The loads are subsequently transferred laterally to the soil. To provide enough stiffness the diameter of the monopile foundation has to be large enough. This

attracts relatively high hydrodynamic loads. On the other hand, the monopile foundation is easy to fabricate and install. It is expected that monopile foundations will not be applicable beyond certain water depths. Stiffness requirements will result in such large diameters that it will be impossible to fabricate such a structure, due to limitations on the size of the steel plates that can be produced by steel mills. Difficulties due to limited sizes of pile driving equipment may also be expected.

### 2.3.2 Tripod

The lower portion of a tripod foundation consists of a framework of relatively slender members, connected to the main tubular by means of a joint section. This framework is fixed to the seabed by piles which are driven through pile sleeves at the end of each of the tripod legs. The main difference between the tripod and the monopile concepts is the way the loads are transferred to the seabed. From the main joint downwards the transfer of loads relies mainly on axial loading of the members. The piles are also mainly loaded axially. This allows the tripod foundation to be shallower and lighter than the monopile foundation. The main advantages are that the tripod has a larger base, which gives it a larger resistance against overturning. The base is also stiffer, leading to an overall stiffer structure. As the base is made up of relatively slender beams, it is transparent, allowing water mass to pass through the structure relatively unobstructed. However, this is not the case for the structure from the main joint upwards. Furthermore, the main joint is a complex element that is susceptible to fatigue and requires much effort in designing and engineering. The triple leg configuration makes directionality of wind and wave loads more of an issue, when compared to the monopile. From an installation point of view, the tripod poses challenges as it cannot be transported as easily as a monopile foundation.

### 2.3.3 Jacket

A jacket structure is made up of three or more legs connected by slender braces, making it a highly transparent structure. Loads are transferred through the members mainly in axial direction. The foundation is provided by piles driven through the pile sleeves at the bottom of each of the legs. The term ‘jacket’ has its origin in the oil and gas industry and is used to indicate a spaceframe structure which has the piles driven through the legs. The configuration as shown in Figure 2, which has the piles driven through pile sleeves at the base of the structure, would be termed a ‘tower’. However, the term ‘jacket’ will be maintained to avoid confusion with the turbine tower.

The large base offers large resistance to overturning. The space frame structure allows for light and efficient construction. However, each of the joints has to be specially fabricated, requiring many man-hours of welding. Furthermore, transportation will be an issue, particularly when installing a large number of turbines. A demonstrator project has been undertaken near the Beatrice oil field off the coast of Scotland, where two 5 MW turbines are installed on jackets in 45 m water depth. Four-legged jackets, or quattropods, were also used to support 5 MW turbines in the Alpha Ventus test fields. Two more jacket projects are underway with the Ormonde and Thornton bank wind farms awaiting installation in 2011.

### 2.3.4 Tripile

BARD Engineering has patented and applied an alternative concept, comprising three foundation piles which extend above the sea surface and are connected by a crosspiece with three struts. The struts are inserted in the foundation piles and connected by means of grouting. BARD claims that this type of structure is suitable for water depths between 25 and 40 m, while supporting the BARD 5.0 MW turbine.

An advantage of the concept is the fact that it can easily be adjusted to accommodate water depth variations, as the transition piece dimensions can be maintained and the pile dimensions can be adjusted to suit the site. Although the transition piece is relatively complex to manufacture, mass production benefits can be gained and while piles may have different dimensions for different sites or within one site, these simple tubular elements can be manufactured at relatively low cost. By placing the piles well away from the centre of the

structure smaller diameter piles can be used to achieve sufficient stiffness, leading to lower hydrodynamic loading.
The installation requires precision as the transition piece struts must fit inside the piles. Therefore a purpose built vessel employs a piling template to ensure good positioning of the piles.

### 2.3.5 Gravity Base Structure

A Gravity Base Structure (GBS) relies on a low centre of gravity combined with a large base to resist overturning. As the GBS requires a large mass it generally made of concrete as it is much cheaper than steel. The GBS is placed directly on the seabed. It can be equipped with vertical walls that protrude from below the actual base, called skirts, which penetrate into the soil below the base. These skirts increase resistance to base shear and help to avoid scour below the base. Liquefaction of the soil beneath the base due to cyclic loading is an issue that must be addressed when assessing the stability of the foundation.
The GBS can be extended to the platform level, thereby reducing the number of offshore installation activities, as no separate transition piece needs to be installed.

### 2.3.6 Spar floater

To date only one spar buoy type support structure has been applied to support an offshore wind turbine. This spar floater is part of the Hywind project. It is installed In Norwegian waters off the island of Karmøy in 120 m deep water, supporting a 2.3 MW turbine.
The spar buoy obtains its bearing capacity from the submerged volume. To achieve the required buoyancy the Hywind floater has a draft of 100m and a diameter of approximately 6.0m at the water line and 8.3 m at depth. The structure is held in place by three catenary mooring lines, anchored to the bottom by piles
The spar concept requires a large submerged volume to generate sufficient buoyancy and a low centre of gravity to maintain stability. This results in a slender structure with a large draft. The concept can be used in water depths up to 700 m. Difficulties for applying this concept on commercial scale are related to the power export cable spanning the water column, where it is susceptible to vortex induced vibrations.

### 2.3.7 Semisubmersible floater

Another type of floating structure that has been applied to support a wind turbine is the semisubmersible structure constructed by BlueH. It consists of several slender vertical columns protruding through the water line and which are connected to a central column above and below the water line. The elements below the water line are dimensioned such that sufficient buoyancy and stability is obtained, while the cross sectional area at the water line remains minimal in order to reduce heave motions. On top of the central column a wind turbine tower is installed. Currently a 220 kW machine is installed.

## 2.4 Alternative support structure concepts

Apart from the various concepts that have already been put into practice, a large number of alternative concepts have been proposed, by many different parties, ranging from concrete monopile and tripod structures to a wide variety of floating structures.
In this section only a selection of steel fixed and floating support structure concepts is presented.

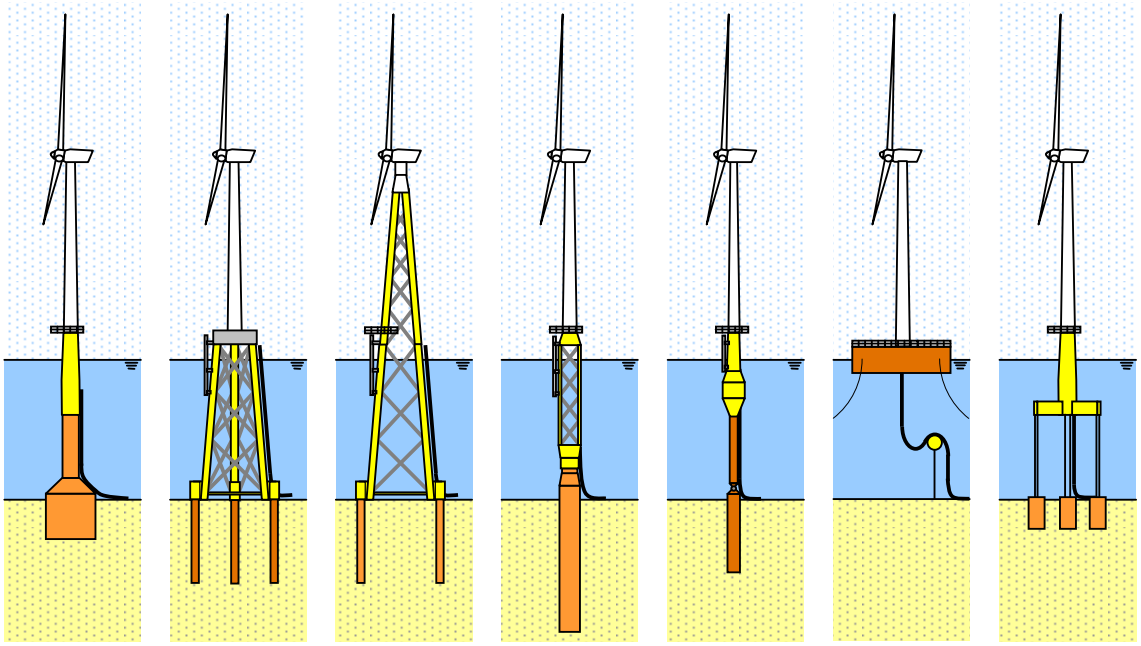

Figure 2.3: Alternative support structure concepts (not to scale)

### 2.4.1 Suction bucket monotower

The suction bucket concept is a monotower with a suction bucket at its base.. Because it is reliant on the pressure difference for installation, this concept is not suitable for very shallow water. It may be practical to integrate the suction bucket with the transition piece to reduce the number of offshore installation activities.

### 2.4.2 Three legged jacket

So far the jacket structures installed for offshore wind turbines are quattropods, having four legs. Alternatively, three-leg jackets could be used as has been done in the offshore oil & gas industry. Using a three-legged jacket could be beneficial as less material is required to build such a structure. However, the angle between braces at the legs will become smaller, requiring more attention to the detailing of joints at the legs.

For an equal footprint area a four-legged jacket will be better equipped to transfer the loads into the soil than a three-legged jacket, due to the extra pile and the larger distance between the piles across the diagonal.

Another critical aspect, which the three-legged jacket shares with the quattropod is the transition from the tubular tower to the jacket structure. The large moments from the tower supporting the wind turbine must be transferred to the jacket legs in a smooth manner. Careful detailing of this component is essential.

### 2.4.3 Full truss tower

In general a braced structure is lighter than a large diameter tubular structure with the same stiffness and strength. Therefore it has been proposed as an alternative to the three- and four-legged jackets as described above. However, the costs of manufacturing such a full truss structure will be considerable due to the large amount of joints. As the distance between the legs decreases with increasing height, the distance between brace joints decreases. This results in many braces and many joints that have to be manufactured. Another critical issue is the sensitivity to torsion loading, due to the limited torsion resistance of the structure.

For downwind turbine configurations the full truss tower is beneficial as it results in a significantly reduced tower shadow.

### 2.4.4 Compliant structure

The principle behind the aforementioned concepts is to have the first natural frequency above the wave frequencies with high energy to avoid resonance and thus high fatigue loads. In other words, the structure should be stiff enough. For a compliant tower the principle is opposite. The intention is to have the first natural frequency below the wave frequencies with high energy, in order to avoid resonance. This means a very soft structure is created. In turn, this implies that a light and slender structure can be achieved. Such a structure does not require a large diameter and therefore attracts relatively low hydrodynamic loads. On the other hand, due to its complexity, the concept has only been used a couple of times in the oil and gas industry and no projects are running or planned to apply this type of structure in the offshore wind industry. Apart from the complexity, other issues will have to be addressed. These include assessment of the stiffness and response of the upper section in relation to the turbine and in particular the blades. It should also be assessed whether the second natural frequency coincides with high energy wave frequencies. Another aspect that might pose problems is that the wind contains the most energy at low frequencies.

### 2.4.5 Barge floater

A floating structure relies on buoyancy to keep the turbine above the water. Different configurations, again derived from the oil and gas industry, can be envisaged. For instance; a turbine could be placed on a barge and attached to the seabed with anchor lines. The anchor line configuration can be either catenary or taut. The mooring can be completed using drag anchors, driven piles or suction anchors. The offshore wind turbine can be assembled on the barge floater at an onshore location. The assembly can be towed out to the required location. This concept may be suitable for large scale production as it can easily be adapted to different water depths. However, it may require at least a certain depth before the mooring concept can be applied. Furthermore, a barge type floater may have serious motion issues. Its large cross section at the water line makes it sensitive to hydrodynamic loads, which in turn makes it susceptible to heave, pitch, roll and sway.

### 2.4.6 Tension Leg Platform

Another option for a floating structure is a mini Tension Leg Platform (TLP), which is tethered to the seabed by means of pre-tensioned cables. The pre-tension greatly reduces heave motion and to a certain extent horizontal motion. The cables can be fixed to a template on the seabed or to individual piles or suction buckets. The TLP has a small cross section at the water line, keeping the hydrodynamic loads relatively small. The TLP requires well engineered connections of the cables to the floater. The tension legs will not be very suitable for shallow water

Spar floater

A spar type floating structure obtains its buoyancy from a cylinder that protrudes below the water line. This cylindrical body is generally long and slender in order to minimize the cross section at the water line. This greatly reduces the wave induced motion. It can be anchored to the seabed with chains in a catenary shape. A spar typically has a small surface cross-section, reducing heave motion. The draft of a spar is usually relatively large to ensure sufficient buoyancy. This may pose problems in small water depths. Because of this the spar may not be very cost effective for shallow water.

# 3. Fabrication and Installation

## 3.1 Introduction

In this chapter current manufacturing and installation methods for offshore wind turbines are described, with the aim of identifying requirements for the design of these support structure types. First the manufacturing process for the monopile tripod and jacket structures is discussed. Subsequently the installation process for these structures is treated. As the monopile is the most frequently used support structure concept, the full manufacturing sequence will be discussed for this type first. The subsequent sections deal with the fabrication of tripod and jacket structures, emphasizing the differences with the monopile. The same approach is followed for the installation process.

## 3.2 Fabrication

### 3.2.1 Manufacturing Process for monopile structures

For a monopile support structure the production process for support structures starts with creating the primary elements for the foundation pile and for the transition piece. Sheets of steel produced at a steel mill are delivered at the fabrication yard. Each sheet has been produced to the required dimensions for a particular tubular section.
The edges of plate are bevelled in preparation for welding. Subsequently the sheets are rolled into tubular sections. Several tack welds hold the ends of sheet together while the section is further prepared for welding. This includes welding on endplates at both ends of the longitudinal weld to ensure that no impurities end up in the welded joint.
The tubular section is welded at the seam from two sides. Whenever possible the welding is done in an automated process. The welds are ground if required to reduce stress concentrations. Tolerances with respect to out-of-roundness and eccentricities are checked and the quality of the weld is ascertained by non destructive testing, after which the section is ready for assembly.

Figure 3.1: Rollling and welding of a foundation pile

The sections are aligned into the predetermined order. Before welding can commence the edges of two adjoining sections are cut into the required weld shape. After preheating the steel surrounding the joint the two sections are welded together. This can be done automatically by rotating the pile while the welding machine remains stationary. Again, welds must be ground and tested
When all sections are assembled, the primary structure is ready. For the foundation pile it may be required to attach lifting trunnions at the pile top to facilitate upending in the installation phase. Furthermore, when internal J-tubes are applied, holes must be cut in the pile near the seabed level for the tubes to exit. Also, to ensure proper bonding at the grout to steel interface after installation, shear keys may have to be welded at the location of the grout overlap.

Several items are still to be attached to the transition piece. The flange at the transition piece top to which the tower will be bolted is welded on top of the transition piece. Care must be taken to ensure that the transition piece is perfectly round when the flange is attached, as current large

diameter structures have a tendency to ovalise under their own weight. Stubs with flanges to which the boatlandings and platforms can be connected at a later stage are welded to the primary structure. Brackets for the attachment of ladders and anodes are also welded onto the structure. The grout skirt at the bottom of the transition piece is attached and supports for the main platform are welded onto the structure. Before the coating can be applied, the surface of the structure is prepared by shot blasting. The structure is subsequently coated in a partly automated process.

Subsequently internal platforms are installed. If the J-tubes are internal, they are installed at this time as well. The J-tubes are not yet extended downwards to their full extent, as the transition pieces are transported upright. The final actions to be performed are the mounting of the main platform, the attachment of the boatlanding, resting platform and ladders and the attachment of a rubber grout seal at the base of the transition piece.

### 3.2.2 Manufacturing Process for tripods

To date the only tripods supporting offshore wind turbines are installed in the Alpha Ventus test field. Although the fabrication sequence might be different for other projects the general manufacturing process will be well illustrated by the example of the Alpha Ventus project.

The fabrication of the Alpha Ventus Tripods was carried out in two stages. In the first stage the main elements were prefabricated in the Netherlands, while the second stage, in which the tripod elements were assembled and the tripods were finished, took place in Norway.

**Phase 1: Prefabrication**

The tripod manufacturing process starts off with the sheets delivered at the yard, which have the edges bevelled in preparation of rolling and welding into large diameter tubular and conical sections for the main column, legs and lower braces.
For the connections of the legs and braces to the main column and to the pile sleeves, the ends of these sections must be cut into the exact predefined shape allowing a perfect fit.
To enhance the stiffness of the main joint, ring stiffeners are welded into the main column elements at the elevation of the heel and toe of the leg joints. A flange is fitted to the top of the main column to which the tower will be connected in the installation phase.
Several sections of the main column are lifted into alignment and welded together. Also the leg sections and the brace elements are assembled. Subsequently welds are ground and tested.
The pile sleeves are preassembled. This involves rolling and welding of sheets into tubular sections, fabricating mud mats, welding stiffeners and spacers to the sleeve top and attachment of pad eyes for lifting.
Before the elements could be shipped to the assembly yard in Norway, the legs and braces have been lifted into place to ensure that a correct fit is obtained at the joint. When all elements have been tested and match specifications, they are transported on barges to the assembly yard.

**Phase 2: Assembly**

At the Norwegian yard the main column elements have been assembled and welded together in an indoor environment. Here the internal platforms, the airtight platform and the internal J-Tubes are installed. Trunnions for lifting the tripod during the installation phase are attached to the top of the main column. The part of the main column from the bottom of the splash zone upwards is prepared for coating and the coating is applied.
The main column is transferred to the dockside where it is installed on elevated supports. In this way the legs and braces can be lifted into position before they are welded to the central column. Subsequently the pile sleeves are lifted into position and connected. Welding, grinding and testing are done in an enclosed space for safety and environmental reasons and to avoid the intrusion of moisture and contaminants in welds.

Final actions include the installation of the grout insertion tubes, the boatlanding, ladders and intermediate platform. Figure 3.2 shows various stages in the manufacturing process for tripod structures [42].

Figure 3.2: Various stages in the manufacturing of a tripod structure [42]

### 3.2.3 Manufacturing Process for jackets

As for tripods there may be different approaches to the fabrication of jacket structures. The following illustrates the multitude of activities that must be performed to create a jacket support structure. This example describes the fabrication of the jackets for the Beatrice project.

For jackets prefabricated tubular elements are delivered at the fabrication yard. Standard sized tubulars are available. These are cheaper than custom made tubulars of approximately the same dimensions.

The first step in the production process is to assemble the jacket joints. Three different joint types are to be prepared: double K-joints and double Y-joints for connections at the jacket legs and X-joints for the braces. The joints are prepared by cutting the brace stubs to fit the joint can at the angle defined in the design. The ends are bevelled and the joints are assembled by alignment of the elements and welding after the joint sections have been preheated. The welding speed and quality can be improved be ensuring easy access to the joint for the welder. If necessary the joints are ground smooth to reduce stress concentrations at the weld. Testing ensures that the quality of each weld is in accordance with specifications.
The tubular elements are coated before being assembled as it is more convenient to perform the coating procedure while the elements are still easy to handle.
When the leg joints have been assembled the legs are constructed. Simultaneously X-brace sections are assembled and anodes are attached. After placing the legs on elevated supports in a horizontal position, the first frame is assembled. Subsequently the X-braces of the adjacent frames are placed vertically on top of the brace stubs of the legs already in place. The braces are welded to the stubs.
The final frame is preassembled and lifted into position over the X-braces, so that the braces can be welded to the brace stubs on the final frame.
In the Beatrice projects the jackets were equipped with pile sleeves. These elements are created from steel sheets, rolled into tubular elements. Mud mats are attached as well as provisions to connect to the jacket legs. The pile sleeves are lifted into position to allow the attachment onto the jacket legs. Finally the joints and other parts of the structure requiring protection are coated.

In a separate process the transition joint is manufactured. The fabrication of this joint is a labour intensive process starting with rolling and welding of the main tubular sections. Also the tubular and conical sections for the stubs connecting the main column to the legs are created from steel sheets. The connection point for the stubs to the main column is strengthened by adding prefabricated stiffeners on the inside of the main column. Subsequently the flange for connection of the tower is connected to the top of the main column.

The support stubs and main column are assembled to form the transition piece. Subsequently internal platforms are installed inside the main column. Walkways for access and inspection are installed as well as a platform at the base of the transition piece. After blasting the transition piece is coated.

Finally the transition piece is mounted to the top of the jacket structure, still in horizontal position. Preassembled boatlandings, ladders, intermediate platforms and J-tubes are also connected to the structure.

Figure 3.3: Various stages in the production of a jacket structure [44]

## 3.3 Installation

### 3.3.1 Monopile installation sequence

The installation process varies significantly for the different support structure concepts. Monopile foundations may be transported to site by feeder barge, on the installation vessel itself or by floating the piles out to the site. Subsequently the pile must be upended, lifted into position, aligned and driven or drilled into the seabed. The next step is to install the transition piece onto the foundation pile. It is subsequently levelled and fixed by means of grouting the annulus between the pile and transition piece.
The turbine tower is installed, generally in two pieces and bolted. Finally the rotor-nacelle assembly is installed, sometimes with two blades pre-attached and lifting the final blade in place separately or by installing the nacelle first and the pre-assembled rotor later.

In general, the installation procedure of a monopile offshore wind turbine follows the steps as listed below. However, it should be noted that in some cases a slightly different approach may be adopted. For instance, it may be decided that scour protection may not be required. It is also possible to install the nacelle with (some) blades attached.

- Foundation pile
- Scour protection
- Transition piece
- Turbine tower
- Nacelle
- Rotor / blades

In the following each of these steps is treated in detail.

**Foundation pile**

Installation of a foundation pile can be done by driving or by drilling.

Driving
The most common way is to install the pile by driving. The foundation piles are delivered to the offshore site on a barge, usually several at a time. The pile is lifted off the barge using a crane

fitted with a lifting tool. The pile is lowered onto the seabed. The weight of the pile will usually cause the pile to penetrate the soil for a few meters. The pile is gripped with an alignment tool at a certain distance above the sea surface to ensure verticality of the pile during driving.

Figure 3.4: Pile driving at Offshore Wind Farm Egmond aan Zee

The hammer is lifted onto the pile, after which the pile driving can proceed. If required, driving can continue when the hammer is under water. Usually depth markings are applied to the pile before driving so that the penetration depth can be monitored visually. Driving can be done from a jack-up barge or from a stable floating system, although it should be noted that a floating system is very much dependent on favourable sea conditions. Figure 3.4 shows various stages of the pile driving process at the Egmond aan Zee offshore wind farm.

Drilling

When hard soils are encountered, drilling may be the preferred option. A hole is drilled at the desired location using a drilling tool operated from a jack-up barge. The pile can subsequently be inserted in the thus created hole. Alternatively, the pile is placed on the seabed and the drilling tool is inserted in the pile. The hole is drilled through the pile, while the pile is slowly lowered into the newly excavated space. The pile is aligned vertically using an alignment tool. Subsequently the pile is fixed in place by injecting grout into the space between the pile and the soil. During hardening of the grout the pile must be held in place to maintain the vertical alignment. When a foundation pile is installed by means of drilling the appurtenances can be pre-attached directly to the pile. Also the flange to which the turbine can be connected can be attached. In that case there is no need for a transition piece, reducing the number of offshore operations. Figure 3.5 shows the drilling equipment used at the Blyth offshore wind farm

Figure 3.5: Drilling equipment at Blyth

**Scour protection**

If a pile is situated in a current, the current is locally increased due to the disturbance in the flow caused by the presence of the pile. In combination with wave action this can cause sand particles to be picked up from the seabed and deposited further downstream. Eventually this can lead to a significant scour hole around the pile. To prevent this scour protection can be applied. An example of a scour protection design is given in Figure 3.6. This is generally in the form of a filter layer of relatively small stones to keep the sand in place on top of which an armour layer is dumped consisting of larger rocks to keep the filter layer in place. This is illustrated schematically in Figure 3.6 The scour protection is installed with the use of dedicated rock-dumping vessels.
With respect to installation two different approaches can be envisaged: static scour protection and dynamic scour protection.

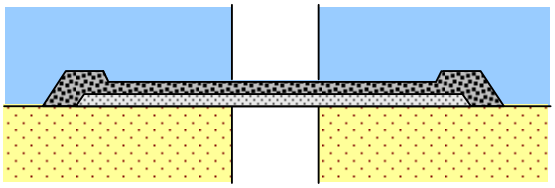

Figure 3.6: Schematic example of scour protection

*Static scour protection*

In the case of static scour protection, the filter layer is put in place prior to installation of the foundation pile. The pile is subsequently installed through the filter layer. Once the pile is in place the armour layer is applied. This approach is aimed at preventing the occurrence of a scour hole during the installation process.

*Dynamic scour protection*

When using dynamic scour protection the foundation pile is installed first. Only after the foundation installation is complete the scour protection is installed. Usually the scour protection is installed in one procedure for the entire wind farm. This implies that the installation of the scour protection is commenced once (almost) all of the piles have been installed. In this case it is likely that a scour hole will develop before the protective rock layers are installed. The scour protection then partially fills the scour hole.

*No scour protection*

Alternatively, it is possible to install an offshore wind farm without any scour protection. In this case the development of a large scour hole is taken into account in the design.

**Transition piece**

The transition piece sits on top of the foundation pile. Its main functions are to provide a flange for the connection of the turbine tower to the foundation, to correct any misalignment of the foundation and to hold the appurtenances, such as the boat landing, J-tube, ladder and anodes. A platform is located on top of the transition piece. The transition piece can be connected to the foundation in the following three ways: using grout, a flange or a slip joint. Transition pieces can be transported to the offshore location by barge along with the foundation piles. Alternatively, they can be carried by the installation vessel. Figure 3.7 shows the installation of a transition piece.

Figure 3.7: Transition piece installation [45]

*Grouted connection*

This is the most common way to make the connection between the foundation and the super structure. The transition piece is lifted from the barge and is slid over the top of the foundation pile. Spacers ensure that the required space remains between the pile and the transition piece. Hydraulic jacks are used to align the transition piece vertically. Grout seals close off the bottom of the annulus between pile and transition piece, after which the annulus is filled with grout. After the grout has hardened sufficiently the seals and jacks are removed.

*Flange*

The transition piece can also be connected to the foundation pile by means of flanges. The transition piece is lifted into place. Once the flanges are correctly aligned, bolts are used to connect the flanges. This procedure has the advantage that it can be performed quickly. However, great care must be taken to ensure that the flange is not damaged during pile driving.

*Slip joint*

A novel way of connecting two tubulars is by means of a slip joint. Both the top of the foundation pile and the bottom of the transition piece have a conical section of which the sides make a small angle with the vertical. The transition piece is lifted onto the foundation pile. Before the transition piece is slid into place, it must be ensured that it is exactly vertical. Once this is achieved the connection can be made by simply lowering the transition piece onto the foundation pile. The friction between the conical sections of the foundation pile and the transition piece due to the weight of the transition piece is sufficient to form a reliable connection. The advantage of this connection type is that it is simple to fabricate and allows for rapid installation. However, so far it has not been put to use for offshore wind turbines. Figure 3.8 shows a slip joint for an onshore turbine.

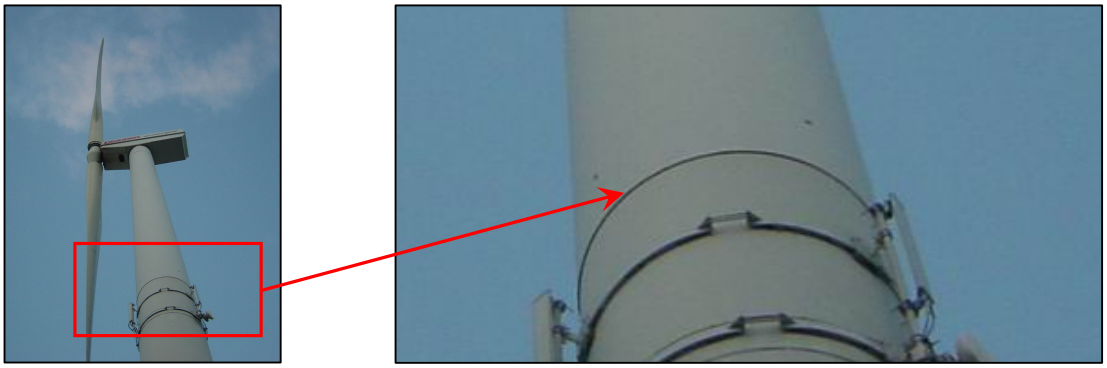

Figure 3.8: Slip joint on an onshore turbine

**Turbine tower**

The turbine tower is usually installed in two or three sections which are bolted together. Figure 3.9 shows such a tower section being lifted for installation. The connection between the transition piece and the turbine tower is also made by bolting two flanges together.

Figure 3.9: Lifting of a tower section for installation

**Rotor – nacelle assembly**

The rotor-nacelle assembly can be installed either separately or using the Bunny – Ear method. It should be noted that each turbine installation contractor has its preferred method.

*Separate*

The nacelle is lifted onto the top of the turbine tower. The flange beneath the yaw bearing of the turbine is bolted to the flange at the tower top when the nacelle is in place, the hub and the blades can be installed. These can be installed in one piece – the rotor assembly as shown in Figure 3.10, or separately. The blades are lifted in a frame that allows for easy manoeuvring. With the blade in a vertical position and with the blade root pointing upwards, the blade is carefully positioned in line with its connection point on the hub. The connection is achieved by bolting the blade to a flange in the hub. This procedure is repeated until all blades are connected.

Figure 3.10: Installation of a rotor in one piece

*Bunny - ear method*

In case of a triple bladed turbine two blades can already be attached onshore. These blades protrude upwards at an angle giving the rotor-nacelle assembly an appearance which has led to the method's distinct name. The advantage is that the rotor-nacelle assembly can be lifted into place with two blades already attached. Only one blade needs to be installed offshore, saving a lot of valuable offshore installation time.

Figure 3.11: Various stages in the installation of a turbine using the bunny-ear method [46]

### 3.3.2 Tripod installation sequence

The tripod support structure is installed in a very different way compared to the monopile support structure. The installation sequence for the main components is listed below.

- Lifting and landing of tripod structure
- Foundation piles
- Turbine tower
- Nacelle
- Rotor / blades

The tripod support structure is pre-assembled in an onshore construction yard. The entire structure is placed on a barge and towed out to the offshore location. There, it is lifted off the barge with a large crane. With the help of a smaller crane it is oriented in the right direction. The support structure is slowly lowered onto the seabed, ensuring that the structure is entirely level. Mud mats at the three corners of the tripod ensure that the structure settles onto the seabed in a stable manner, while providing support until the foundation piles are in place. The three foundation piles are each driven through pile sleeves at the three corners at the bottom of the structure using a submersible hammer. When the piles are at the required depth, a connection between the top of the pile and the pile sleeve is made by filling the annulus with grout.

Scour protection is generally not required as the foundation piles of a tripod support structure are loaded mainly in the axial direction. Therefore the effect of scour is relatively insignificant when compared to the monopile support structure, No separate transition piece is required, as the requirements for pile driving do not apply to the tripod and the appurtenances can be connected directly to the tripod support structure.

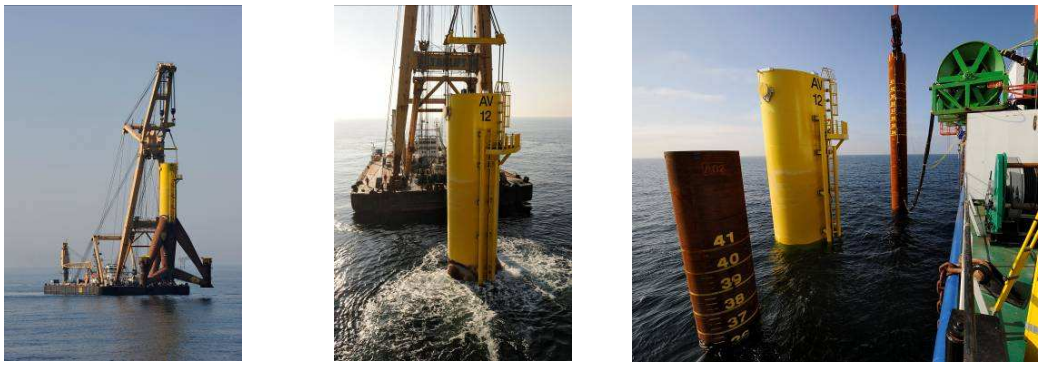


Figure 3.12: Installation of a tripod structure at the Alpha Ventus test field [42]

The turbine tower and the rotor - nacelle assembly are installed in the same manner as described in section 3.3.1.

### 3.3.3 Jacket installation sequence

The installation procedure for a jacket is very similar to the procedure for the tripod support structure. For the sake of completeness the sequence of installation is listed here again.

- Lifting and landing of tripod structure
- Foundation piles
- Turbine tower
- Nacelle
- Rotor / blades

Despite the similarities with the installation of a tripod structure, in some cases there is a significant difference regarding the installation of the foundation piles. In the oil and gas industry there are two ways of establishing the connection between piles and support structure. The piles can be driven through pile sleeves at the bottom of the structure a so-called ‘tower’ structure or the piles can be driven through the legs of the structure. In this case the connection is made at the top of the structure. Such a structure is called a ‘jacket’ structure. Although there is a difference in the way forces are directed to the foundation, in practice often no distinction is made between these two terms.
Usually the legs are inclined for a jacket structure. With respect to the installation procedure the difference lies in the fact that the piles are to be driven at an angle to the vertical in the case of a ‘jacket’ structure while they may be driven vertically for a ‘tower‘ structure.

To date only two projects using a jacket type support structure has been undertaken: the Beatrice Demonstrator Project and the Alpha Ventus test field and two projects in the preparatory stages: Ormonde and the Thornton Banks wind farms.
The Beatrice project involved two 5 MW turbines situated in 45 m water depth in Scottish waters. The electrical cables link the turbines to the nearby Beatrice oil field production platform. The turbines were installed as shown in Figure 3.13. The jacket support structure was transported to the offshore location on a barge. There, a heavy lifting vessel equipped with two cranes lifted the structure off the barge and tilted it until it was in an upright position. Subsequently, the support

structure was lowered onto the seabed and levelled, after which the piles were driven. The second part of the installation procedure involved installing the entire wind turbine, including the turbine tower, in one lift. The turbine was pre-assembled onshore on top of a soft landing system and lifted off the quayside using a specially designed lifting frame. At the offshore location the turbine was mated with the support structure, where the soft landing system compensated the motion of the turbine assembly during the set down phase. Finally, the lifting frame and the soft landing system were removed to complete the installation procedure.

Figure 3.13: Various stages of the installation at the Beatrice demonstrator project [47]

For the Alpha Ventus wind farm the installation sequence was slightly different as the jacket legs were designed to fit inside the pre-driven piles instead of the piles being inserted in the pile sleeves. Therefore the piles had to be preinstalled. This is done with the help of a piling template, through which the piles can be driven, thereby ensuring the correct distance of piles and verticality of the piles.
During the pile installation the template must be lifted and lowered onto the seabed in the correct position. Subsequently, piles are gripped at one end, lifted into a vertical position and lowered down to the piling template near the seabed. Cameras assist to ensure that the pile slots neatly into the template. When the pile is in position a submersible hydraulic hammer is lifted on top of the pile and the pile is driven to the predetermined depth. The hydraulic hammer is retrieved and the sequence is repeated for the remaining three piles. Finally the template is retrieved and the pile installation vessel or jack-up barge is moved to the next position.

If there is a significant time between installation of the piles and installation of the jacket, marine growth may accumulate on the pile heads. This could complicate installation of the jacket structure and therefore the status of the piles should be checked before installation commences. If the build up of marine growth is sizeable, steps should be taken to remove the growth.
The installation of the jacket substructure starts by lifting the jacket off of the transport barge or vessel. Subsequently the jacket is oriented in the right direction and lowered down to a short distance above the pile heads. The landing of the jacket is usually done when the tidal current is lowest. On the jacket legs, one stub is elongated. This leg is stabbed into the pile head of the associated pile first, allowing the crane operator to rotate the jacket to match the position of the other piles. Finally, when the jacket legs are positioned inside the piles the jacket is fixed into the piles by filling the annulus between the leg and the pile with grout.

While the turbine was installed in a single lift operation at the Beatrice project, the installation procedure for the wind turbine and the tower at the Alpha Ventus project was more conventional. The tower was installed in two sections, which were fixed by means of a bolted. The nacelle was lifted in place by a crane placed on a jacket barge. Subsequently the rotor was installed in one piece. This involved lifting the rotor from the deck of the barge, turning it to a vertical position and aligning it with the hub flange in the nacelle. Finally the rotor is bolted to a flange on the rotor shaft.

## 3.4 Conclusion

In this chapter the sequence of steps in the fabrication and installation process for monopiles, tripods and jackets structures have been described.

Although monopile structures are made up of large and heavy sections, the fabrication and assembly of these simple tubular elements is relatively straightforward and can be automated to a large degree.
Jacket structures require the fabrication of many joints. This process is labour intensive, but the tubular elements are relatively light and wall thicknesses are generally smaller than for monopile structures, meaning that each individual girth weld can be made relatively fast. Small diameter girth welds for the jacket structure can be performed automatically, but tubular joints and the transition joint will have to be hand welded.
The elements for tripods are large and require additional stiffeners at certain locations and some of the elements require cutting to fit the connecting tubular. Most joints will have to be hand welded and involve many weld passes in difficult to reach locations.

For these reasons the costs for producing a monopile structure is in the order of 2 €/kg, whereas the production costs for a jacket substructure are in the range of 4-6 €/kg. Tripod substructure manufacturing cost will be in a similar range. The fabrication of conical sections is more costly, than cylindrical sections, therefore the costs of towers can be estimated at 2-3 €/kg.

All three types of structures require the mounting of secondary items such as the J-tubes boatlanding, ladders, intermediate platforms and the main platform. The costs for fabrication are relatively independent of the chosen support structure concept, but are influenced more by the specific choice for the project, for instance the number of J-tubes and boatlandings may depend on operation and maintenance strategies.

For the installation phase the jacket and tripod structures require more or less the same approach in which the substructure is lifted off a barge onto the seabed and piles are driven into the seabed and grouted to the substructure - three for the tripod, one additional pile for the jacket. For the monopile structure there is only one pile to install. However, due to its large diameter and weight, lifting and handling are more cumbersome and the pile driving requires more energy and takes longer.

In the next chapter the design process and design criteria are discussed. Whenever relevant, the requirements due to the fabrication and installation process will be taken into account in the design criteria.

# 4. Design conditions

## 4.1 Introduction

The design of support structures is dictated by external conditions. These include wind and wave conditions, soil conditions, water depth and other local circumstances and the wind turbine. This chapter describes the site conditions relevant to the design of support structures for offshore wind turbines. Also wind turbine types for the offshore market are addressed. The critical turbine parameters for the design of support structures are highlighted and an outlook on future turbines is presented by discussing upscaling trends for wind turbines.

## 4.2 Site conditions

### 4.2.1 Overview of site conditions

For modelling of support structures and for load calculation purposes, the environmental parameters affecting the support structure must be defined. The data can be categorised under the following topics:

- Water level data
- Wave data
- Current data
- Wind data
- Soil data

In the following a brief description is given of the environmental data associated with these categories.

### 4.2.2 Water level data

Water levels can vary due to tides and storm surges. The variations due to tides are periodical, with semidiurnal and monthly effect as the most pronounced components. Spring tides define the highest astronomical tide (HAT) and lowest astronomical tide (LAT). The equilibrium water level is defined as the Mean Sea Level (MSL).
Storm surges occur in storm situations and have two principal causes. The strongest effect results from the friction of the wind on the water surface causing water to accumulate on the downwind shore of a basin, resulting in a water level rise at the downwind shore. At the upwind shore this can lead to lower water levels, called negative storm surge. The other effect is caused by the lower atmospheric pressure associated with a storm, leading to a rise in water levels.

Water levels are defined with respect to a certain reference level. Usually a convenient level such as MSL or LAT is used. Also the water depth is given with respect to the reference level. Water depths on bathymetric charts are noted relative to a chart datum (CD) the reference level for the chart. In many cases, the chart datum is equal to LAT, although different reference levels may be used.

Water levels may vary from point to point in a given area but also from time to time due to seabed morphological processes. A detailed survey of a prospected wind farm area is essential to establish not only the water depths at the time of the survey but also the expected seabed level changes. In some cases large scale ripples move though an area in the course of several years leading to water depth changes of several meters.

### 4.2.3 Wave data

Waves at sea are caused by wind acting on the sea surface, by which energy is transferred from the wind into the waves[2]. Waves occurring in the same area as in which they are generated are called sea. These waves have an irregular, short crested appearance. When waves travel outside the area where they were generated they are called swell waves. This type of waves tends to have a regular long crested pattern and large wave lengths.

The longer the fetch, the distance over which the wind blows over the sea, the higher the waves will grow. Also the duration that the wind blows over the surface and the wind speed influence the eventual size of the waves. For a given wind speed, if the duration and the fetch are long enough an equilibrium situation will occur in which the energy transferred from the wind to the waves is dissipated at the same rate. A sea state in such a condition is called fully developed. Sea states that have not yet reached this condition are called developing.

The wave height is also affected by the water depth. When the wave reaches a height of 0.78 times the water depth the wave breaks and will be depth limited. Waves may also break if the wave height becomes larger than 0.14 times the wave length.

Regular waves can be described by linear wave theory, in which the wave profile follows a sinusoidal shape. Linear wave theory can be applied for waves in deep water or intermediate water depth, when the waves are not too steep. Otherwise non-linear wave theories apply, in which the wave profile shows higher, narrower peaks and shallower, longer troughs.

Wave data is described in terms of the wave height, the wave period and the wave direction. Through the dispersion relation wave length and wave number are defined in relation to the wave period or frequency:

For sea states the wave conditions are given by the significant wave height and the zero crossing period. A sea state can be considered stationary up to three hours. Within that duration the maximum expected wave height is 1.86 times the significant wave height.

For extreme events, extreme wave heights must be defined, whereas operational conditions require the definition of the sea state parameters.

### 4.2.4 Currents

Currents may be caused by wind, tides and pressure or density gradients. Near the shore wave induced alongshore currents may occur. Wind induced current is most notable near the water surface, whereas tide induced currents are present over the major part of the water depth. Currents can be described in terms of the following parameters:

- Current profile $U_c(z)$
- Current velocity $U_c(T_{return})$
- Current direction $\theta_c$

[2] Apart from wind induced waves there are other types of waves, including earthquake induced waves (tsunamis), infragravity waves and seiches. These will not be treated here.

### 4.2.5 Wind data

Wind data relevant for determining the loads on the turbine and tower. For this purpose the maximum wind speed is needed as a function of the return period. Typically the one-year and 50-year values are required for evaluation of the extreme aerodynamic loads. Wind speed data is usually derived from a value given at 10 m above the sea level. The wind shear profile is required to translate the wind speed up to the hub height.
The wind speed distribution can be derived from measurements, but may also be approximated by assuming a Weibull distribution, for which the shape parameter and scale parameters should be known. The directional distribution of wind speeds is also required and can conveniently be represented in a wind rose diagram.

The wind data is given in terms of:

- Wind speed $V_w(T_{return})$
- Wind shear profile $V_w(z)$
- Wind distribution Weibull parameters
- Wind direction $\theta_{wind}$

Wind is characterised by local fluctuations of the wind speed and direction. This turbulence is described by the turbulence intensity, which is defined as the ratio of the standard deviation and the mean wind speed.

### 4.2.6 Soil data

Soil is generally a granular material, the product of erosion of rocks or the accumulation of organic material. Soil can be either cohesive such as clay, or non-cohesive such as sand. Other soil types that may be encountered are gravel, silt and peat. Due to its geological history soil can be very inhomogeneous.

For design of piled foundations, detailed knowledge is required regarding strength and bearing capacity of the soil. This is usually gathered through in-situ sampling and analysis of drilled samples in the laboratory. The first property measured for all types is the density $\gamma'_{soil}$, in kg/m$^3$, usually for submerged soil, which is the dry density minus the density of water. A typical value is between 4 and 10 kN/m$^3$. For clay, the undrained shear strength $s_u$ and the strain at 50% of the maximum stress $\varepsilon_{50}$ are measured.

For sand the friction angle $\varphi$ and the relative density of sand $D_r$ are derived directly from in-situ measurements. The initial modulus of horizontal subgrade reaction, $k_s$, can be derived from the friction angle [2].

Due to its discontinuous nature soil particles can move with respect to the surrounding particles, thereby altering the structure of the soil. This creates a significantly non-linear behaviour which is usually described in terms of load displacement diagrams. The main parameters for the description of the soil characteristics are as follows:

- Submerged unit weight of soil $\gamma'$
- Angle of internal friction (sand) $\varphi$
- Undrained shear strength (clay) $c_u$
- Strain at 50% of the maximum stress (clay) $\varepsilon_{50}$

## 4.3 Wind turbines

### 4.3.1 Wind turbines for the offshore market

To date only a limited number of turbine types have been installed offshore, in the range of 2.0 to 5.0 MW. Table 4.1 gives a list of turbines from a variety of turbine manufacturers that have been installed offshore. The most important turbine characteristics, the rotor diameter $D_{rotor}$, the top mass $M_{top}$ and the rated power $P_{rated}$ are also shown. All of the turbine types in Table 4.1 are variable speed, pitch regulated turbines.

Table 4.1: Turbine types currently installed offshore [3]

| Manufacturer | Type | $D_{rotor}$ [m] | $M_{top}$ [ton] | $P_{rated}$ [MW] |
|---|---|---|---|---|
| Areva Multibrid | M5000 | 116 | 309 | 5.0 |
| BARD Engineering | VM 5.0 | 122 | 436 | 5.0 |
| General Electric | GE 3.6 | 104 | 295 | 3.6 |
| Repower | RE5M | 126 | 410 | 5.0 |
| Siemens | SWT 2.3 | 93 | 142 | 2.3 |
| Siemens | SWT 3.6 | 107 | 220 | 3.6 |
| Vestas | V80 | 80 | 107 | 2.0 |
| Vestas | V90 | 90 | 112 | 3.0 |

### 4.3.2 Relevant turbine parameters for support structures

Apart from the parameters listed in Table 4.2 there are several other critical parameters that are required for adequate modelling of the support structure for dynamic analyses.
The turbine mass can be more accurately be modelled if a distinction can be made between the nacelle and rotor mass. Their respective eccentricities with respect to the tower centreline and the elevation above the tower top are required information. Also mass moments of inertia are needed to represent the eccentricity of blades from the rotor axis.

Particularly relevant for the design of the support structure is the rotational speed of the rotor. For a variable speed turbine this is given as a rotor speed range, from a minimum rotor speed to the nominal rotor speed. Other parameters of relevance are the rotor speed limits for turbine stops due to control of the safety system shut-downs. Together with the number of blades the blade passing frequency range can be determined, by which the allowable range for the structure natural frequency is known.

Table 4.2: List of turbine parameters relevant to support structure design [4]

| Parameter | Unit | Description |
|---|---|---|
| $N_{blades}$ | [ - ] | Number of blades |
| $h_{hub}$ | [m + MSL] | Design (initial) hub height |
| $D_{rotor}$ | [m] | Rotor diameter |
| $P_{rated}$ | [W] | Rated power |
| *RPM range* | [rpm] | Rotation speed range |
| *RPM limits* | [rpm] | Rotation speed limits for control and safety system stops |
| $M_{top}$ | [kg] | Top mass (rotor, hub, nacelle) |
| *c.o.g. of* $M_{top}$ | [m, m, m] | Top mass co-ordinates |
| $I_{top}$ | [$m^4$] | Top mass moments of inertia |

For a full definition of the turbine allowing full time domain simulations of turbine loads and response many more parameters must be known, including blade geometry, generator and drive train properties. For the UpWind project a Bladed model has been set-up in which all these parameters are included.

### 4.3.3 Upwind reference turbine

The turbine used for this project is the UpWind reference turbine, an updated version of the NREL 5.0 MW generic turbine [5]. It incorporates a three-bladed rotor, positioned upwind of the tower and relies on variable speed, pitch regulated control. In the UpWind reference turbine the original controller was replaced by an industry standard controller [6]. The UpWind turbine is a fictitious turbine, but the design is roughly consistent with current 5.0 MW wind turbines for the offshore market. The main parameters are listed in Table 4.3.

Table 4.3: Main parameters of the UpWind reference turbine

| Parameter description | Value |
|---|---|
| Rated power [MW] | 5.0 |
| Rotor diameter [m] | 126 |
| Minimum rotor speed[rpm] | 6.9 |
| Rated rotor speed [rpm] | 12.1 |
| Rotor mass [ton] | 110 |
| Nacelle mass [ton] | 240 |

### 4.3.4 Upscaling

While the Upwind reference design is representative for the current 5.0 MW wind turbines available for offshore application, future turbines will most likely have a higher power rating. This implies that future turbines will be larger in size and mass. Upscaling of existing turbines can give a good indication of the turbine properties representative of future turbines.

A study into mass scaling of wind turbines for the offshore market was performed in [3]. At the basis of this study was the assumption that the turbine concepts remain the same even as the power rating increases. The basis for the scaling is to maintain a constant tip speed ratio of $\lambda = 7$. For increasing rotor diameter, this implies that the rotor speed will vary inversely with the diameter.

The thrust force on the rotor with diameter $D$ in a steady wind $V$ is proportional to $V^2D^2$ and the power is proportional to $V^3D^2$.

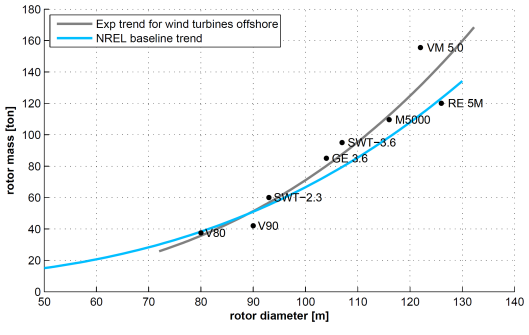


Figure 4.1: mass scaling of rotor [3]

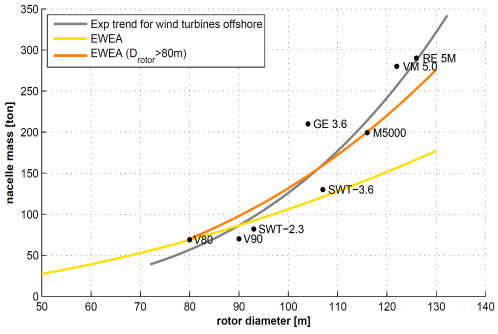


Figure 4.2: mass scaling of nacelle [3]

In [3] the mass of the rotor was found to vary according to $m_{rotor} = 0.0475 \cdot D^{3.09}$ and the nacelle mass varied following $m_{nacelle} = 0.00897 \cdot D^{3.57}$. It should be noted that in [7] a relation between tower top mass and rotor diameter is found following $m_{towertop} = 0.0167 \cdot D^{1.9988}$. However, this trend includes data from older, smaller turbine types. If only more recent turbines, with larger rotor diameters are taken into account the exponent exceeds 3, approximating the values given by [3].

Summarising, for turbines with in creasing diameter, the rotor speed decreases proportionally with the diameter, the thrust increases proportional to the square of the diameter, the power increases

proportionally with the cube of the diameter and the mass increases by approximately the cube of the diameter.

# 5. Design methodology

## 5.1 Introduction

In the previous chapters the background of offshore wind turbine support structures has been explained. When the requirements and design conditions for the support structure are known the structural integrity can be verified according to design criteria in accordance with design regulations and guidelines. These verifications are embedded in a sequence of design steps.
In this chapter the design methodology is explained by first addressing the design objective. Subsequently the process to arrive at a final design that meets the objective is explained. The design is subject to requirements and criteria, which are discussed in detail. There are different approaches to come to a support structure design, and various methods of analysis that can be applied. The chapter ends with a review of these approaches. Based on the approaches and criteria discussed in this chapter, design assessments can be made for the support structure concepts mentioned in Chapter 2.

## 5.2 Design objective

Before formulating a design objective the context of a support structure should be considered. The support structure can be seen as a part in the larger offshore wind farm development. For the offshore wind farm development the objective is to produce electricity at the lowest possible cost per produced kWh. To achieve this objective the energy yield should be as high as possible, while the costs of the overall development should be as low as possible.
For the individual components, such as the support structure this implies that the costs of the component should be as low as possible, without jeopardising up-time.

As stated in Chapter 2 the purpose of a support structure is to hold the wind turbine in place allowing it to produce electricity in a safe and reliable manner, such that the highest possible energy yield can be achieved. Therefore the offshore wind turbine should be able to:

- withstand all loads during envisaged lifetime
- remain operable in all intended operational conditions

Furthermore the structure should be able to fulfil all secondary functional requirements, such as accessibility and electricity export, while at the same time posing no threat to the environment and other users of the marine environment.

The objective of the design is therefore to define the geometric and material properties of the support structure, subject to requirements regarding the operability of the wind turbine, load resistance and economics.

## 5.3 Design process for offshore wind turbine support structures

### 5.3.1 Design sequence

According to [8] the design process for an offshore wind turbine is as depicted in Figure 5.1. This process is defined for a complete offshore wind turbine system, including rotor nacelle assembly (RNA). It assumes that the RNA is designed according to a standard wind turbine class (1) and as such has been type certified by a certification body. Once the design has been initiated (2) for a specific project, the external conditions for the project site must be defined (3). These include site-specific environmental data, local bathymetry, geotechnical information and other relevant oceanographic data. To allow different parties in the project to work with the same data the

environmental conditions, together with the design criteria for the RNA are recorded in a design basis (4). The design basis itself has to be certified by a certification body [1] [9].

To be able to apply a type certified turbine at a specific offshore site it must be demonstrated that the RNA still meets the design criteria for the site-specific loads. In the current industry practice the verification of the RNA design (6) will be the responsibility of the wind turbine manufacturer, whereas the support structure design (5) is the responsibility of the support structure designer.

The design process as illustrated in Figure 5.1 assumes that the support structure design and the verification of the RNA are performed in parallel. Both structures are modelled in structural analysis packages that can account for dynamic response of the structure to external loading. Preferably this entails a fully integrated analysis [10], but current industry practice also makes use of parallel models in which the interaction between RNA dynamics and the support structure dynamics as well as interactions between aero- and hydrodynamics and the structural response are taken into account.

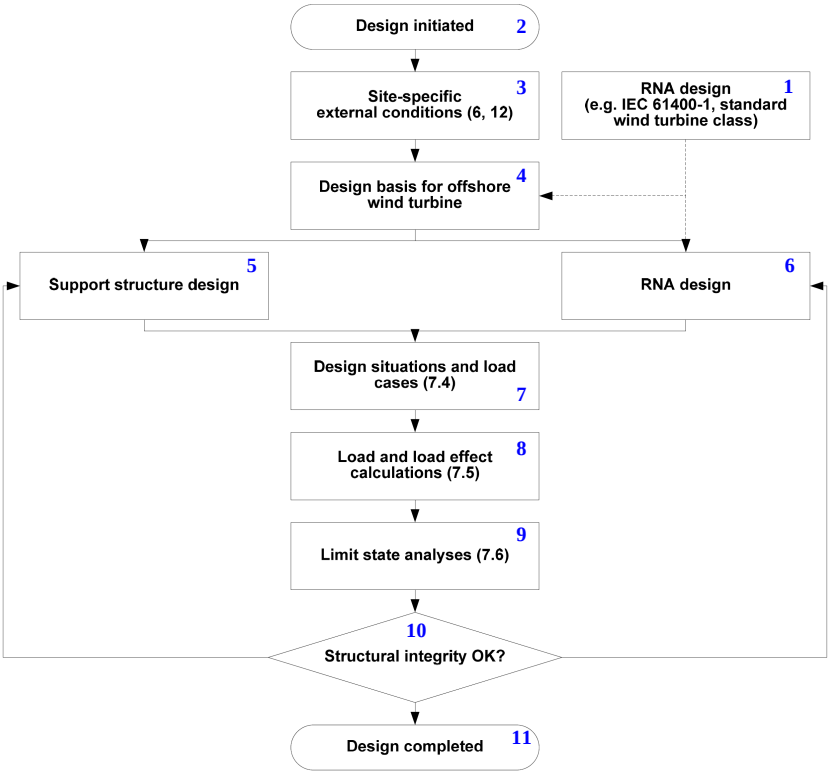


Figure 5.1: Design process for an offshore wind turbine [8]

### 5.3.2 Design Load Cases

When an initial support structure has been established, a series of Design Load Cases must be defined (7). Different design situations can be identified covering all expected operational situations as well as fault situations. These design situations are defined as follows in the standards for the design of offshore wind turbines [1] [8]:

1. Power production
2. Power production plus occurrence of fault
3. Start-up
4. Normal shut-down
5. Emergency shutdown
6. Parked (standing still/idling)
7. Parked and fault conditions
8. Transport, assembly, maintenance and repair

For each of the defined load cases loads and load effects are calculated (8). This usually entails time domain simulation of the wind and wave loads on a dynamic structural model, including the aero-hydro-servo-elastic behaviour of the turbine. The load effects are given by the response of the turbine to these loads in terms of displacements, velocities, accelerations and section forces at the nodes in the structural model.

### 5.3.3 Limit state checks

Once the load effects for each of the simulated design load cases have been determined the limit state analyses are performed. Four different limit states are distinguished:

- Ultimate limit state (ULS)
- Serviceability Limit State (SLS)
- Accidental Limit State (ALS)
- Fatigue Limit State (FLS)

The ALS and FLS are sometimes considered part of the ULS analysis. In the ULS analysis the structural strength of members and joints as well as the stability of members is checked. Also the strength of the foundation must be verified. The SLS is related to maximum acceptable deformations of the structure, the foundation and the RNA during operational conditions. For the ALS the effects of unintended impact loads such as ship impact and impacts due to dropped objects are evaluated. Finally, the ability of the structure to withstand the combined environmental loading over its intended design life must be verified in the FLS analysis.

The results from the limit state analyses are usually expressed as a utilisation ratio, defined as the design load divided by the characteristic resistance. A utilisation ratio larger than 1.0 implies that the structure has insufficient resistance to withstand the design load. If the utilisations for all load cases are less than 1.0 the structural integrity is guaranteed (10) and, according to Figure 5.1 the design is completed. If for some load cases the utilisation is larger than 1.0 the structural integrity of the system is not assured and changes to the support structure or the RNA must be made resulting in lower utilisations for the critical load cases. To this end either the loads may be reduced or the resistance of the structure may be increased.
To achieve either load reduction or increased resistance, the support structure design and the RNA design are revised. In some cases the design load cases well have to be redefined, for instance when a more detailed description of the DLCs may lead to less conservative loads and hence lower loads on the structure or RNA. Subsequently the load simulations are performed once again and the limit state checks are executed. This process is repeated until both the support structure and the RNA design meet the design criteria for all considered load cases and for all limit states.

### 5.3.4 Design evaluation

Figure 5.1 considers the design process to be complete when the structural integrity is shown to be satisfied. If this is the only requirement very robust designs may result. Economic considerations should also be taken into account, such that the contribution of the support structure and RNA to the total cost per produced kWh is minimal. Besides checking whether the structural integrity of the structure is guaranteed, it should also be ascertained if further reduction

of the overall cost is possible. Primarily this will be achieved by reducing the mass of the structure, thereby reducing the overall material costs. However, it should also be verified that reducing the mass of the support structure does not introduce unforeseen costs in other parts of the structure or for fabrication installation and maintenance issues. To reflect the economic considerations the process shown in Figure 5.1 should be updated to include a check for the minimum structure mass and costs. If the structural mass can be further reduced the dimensions should be changed and the structural integrity should be checked again. Only when the mass of the structure can be reduced no further without compromising the structural integrity the design may be considered completed.

## 5.4 Design criteria

### 5.4.1 From requirements to criteria

In section 5.2 the design objective is formulated as defining the geometric and material properties of the support structure subject to requirements regarding the operability of the wind turbine, load resistance and economics, thereby allowing safe, reliable and economical operation of the wind farm. To assess the suitability of the support structure design it should fulfil certain design criteria. These criteria are related to the requirements for the wind turbine and for the support structure itself. For the wind turbine the following requirements apply:

- The turbine should be situated at a certain elevation above the sea surface, for effective electricity production and to ensure sufficient safety
- The electricity produced by the generator must be fed into the electricity grid. For this purpose provisions for the exporting of the electricity must be incorporated.
- To allow reliable operation the turbine must regularly undergo maintenance and repair. Therefore provisions must be present for accessing the turbine.
- Sufficient clearance between the blades and the support structure must be maintained to reduce loads on the turbine and to avoid collision of the blades with the structure.
- To avoid damage to components in the wind turbine the tower head motions should be within predefined limits.

The support structure should ensure that all aforementioned requirements are fulfilled. Furthermore the structural integrity of the support structure must be guaranteed. Therefore the support structure must be able to withstand all loads from the wind turbine and from the environment onto itself and to transfer these loads to the soil.

To satisfy these requirements criteria can be formulated regarding natural frequencies, strength and deformations. In the following sections these criteria are discussed for the main components making up the overall support structure: tubular members, joints and foundation elements. Also requirements and criteria with regard to fabrication and installation are put forward.

### 5.4.2 Natural frequencies

Natural frequencies of the support structure are very important as they determine the dynamic behaviour of the offshore wind turbine. If the frequency of excitation is near a natural frequency, resonance occurs and the resulting response will be larger than in the quasi-static case. This leads to higher stresses in the support structure and, more importantly to higher stress ranges, an unfavourable situation with respect to the fatigue life of the offshore wind turbine. Therefore it is important to ensure that the excitation frequencies with high energy levels do not coincide with a natural frequency of the support structure.

In the case of an offshore wind turbine excitation is due to both wind and waves. For fatigue considerations sea states with a high frequency of occurrence have the largest effect. These are generally relatively short waves with a significant wave height $H_s$ of around 1 m to 1.5 m and a zero-crossing period $T_z$ of around 4 s to 5 s.

The wind excitation frequencies that should be avoided are those that coincide with the range of rotational frequencies of the rotor. This will be illustrated for the NREL 5 MW turbine which will be used during subsequent stages of this project. With a minimum rotational speed at the cut-in wind speed of 6.9 rpm and a maximum rotational speed of 12.1 rpm, the rotational frequency interval to stay clear of ranges from 0.222 Hz to 0.311 Hz. This interval is indicated with 1P. Furthermore, the blade-passing frequency interval should also be avoided. This interval, indicated with 3P for a triple bladed turbine is equal to the rotational frequency interval times the number of blades. As an example the allowable frequency range for the UpWind reference turbine is indicated in Figure 5.2. Taking the above into account, the first natural frequency is chosen at 0.29 Hz. The second natural frequency must be well above the 3P frequency range. Applying a 10% margin on the upper boundary of the 3P range the minimum second natural frequency is 0.666 Hz.

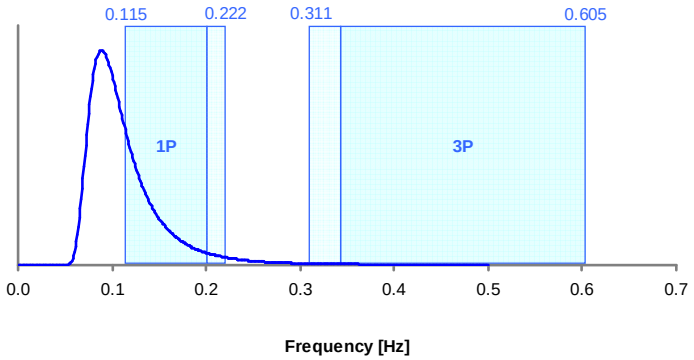


Figure 5.2: Diagram showing allowable frequency range and excitation frequencies

### 5.4.3 Strength criteria

**Yielding**

Stresses in elements must remain below the yield stress for metallic materials. Wind loads, wave loads, gravity and inertia loads and pressure differences between inside and outside of element (hoop stresses) all contribute to the acting stress in the element.
Buckling may occur before the full yield capacity of a cross section is reached. For foundation piles,, buckling is generally not considered a critical failure mode as the pile is normally supported by the soil on both the inside and outside. Pile strength should be checked under extreme compression loads.

**Buckling**

For monopiles the wall thickness can vary along the length of the pile as the bending moment increases from the top of the toward the seabed due to hydrodynamic and aerodynamic loading and then decreases as load is gradually transferred to the soil. For multi-member structures the load level will also not be the same throughout the entire structure, therefore the wall thickness of elements may vary.
The wall thickness should be sufficient to prevent buckling. Two forms of buckling can be identified: global or bar buckling and local or sheet buckling. In the case of global buckling the structure collapses in its entirety, whereas in the case of local buckling the buckling occurs only locally. However, the occurrence of local buckling may initiate global buckling. The most important parameters in the buckling analysis are:

- The buckling length, which is different for local and global buckling,
- The normal force in the structure or element under consideration
- The bending moment in the structure or element under consideration
- A slenderness parameter

The outcome of the buckling check is a usage factor, which indicates to what extent the cross section is utilised with respect to the buckling capacity. This value can be used to optimise the wall thickness. Furthermore, the top of the pile usually requires a large wall thickness to cope with the high stresses due to pile driving. The pile toe is usually also dimensioned with a larger wall thickness to prevent buckling during pile driving.

**Fatigue**

As the support structure is subjected to continuous load variations, the fatigue of the structure needs to be checked. Preferably all load combinations of wind and waves with their directions are incorporated in this check. But as the number of load cases is usually very large, it is desirable to use a reduced number of load cases. This can be achieved by two methods, preferably simultaneously. The first is by assuming that all loads act in the same direction. This approach is conservative as it leads to an accumulation of fatigue damage in a single location on the circumference of the pile. This is only valid in the power production state. For idling states (non-power producing states with unlocked rotor) wind-wave misalignment may result in higher loads than when wind and waves are aligned. The main reason for this is the lack of aerodynamic damping. Idling situations occur below cut-in and above cut-out but may also occur within the range of power production, due to non-availability of the wind turbine due to turbine errors. Therefore, the portion of idling state simulations must consider wind-wave misalignment for the fatigue analysis of the support structure, especially for monopiles.

In reality, the fatigue damage is lower than estimated by the first method, as the damage is spread over multiple locations on the circumference. In the second method, all the environmental states in a wind speed bin are grouped. The corresponding $H_s$ and $T_z$ are associated with the state within the wind speed bin with the largest probability of occurrence. The probability of occurrence of the grouped state is the summed probability of all contributing states. Sometimes it may be more realistic to group the environmental states in a wind speed bin into two or more grouped states. Either way, the resulting number of environmental states that serve as input for the fatigue analysis is significantly reduced.

For each of these environmental states a time domain simulation is performed and the bending stresses in the support structure are recorded. Near welds, where there are discontinuities in the structure, the local stress should be multiplied by an appropriate stress concentration factor. Using a stress cycle counting method, the number of cycles in each stress range bin is counted. With this information and using an *S-N* curve corresponding to the weld detail under consideration the fatigue damage due to environmental loads can be determined. Furthermore, fatigue damage due to transient events such as start-up and shutdown procedures and fatigue damage due to pile driving should be included in assessing the total fatigue damage.

### 5.4.4 Deformation criteria

**Joints and members**

For tubular elements which are part of the primary structure no specific deformation criteria can be stated. However, it should be kept in mind that the deflection at the tower top should remain within predefined limits and that deformation of tubular elements under axial loading may lead to second order moments, thereby contributing towards the occurrence of global buckling.

Excessive deformation of joints may induce joint failure and should therefore be avoided. Also the stiffness of the overall structure may be affected by the flexibility of joints, thereby influencing natural frequencies.

**Pile penetration depth and foundation stability**

For the formulation of deformation criteria for the foundation a distinction must be made between piles loaded mainly in lateral direction and piles loaded mainly in axial direction. For laterally loaded piles in sand the deformation at the pile head is more important than the ultimate capacity of the pile foundation. Under lateral loading at seabed the pile tends to rotate and deflect. However, though the soil may deform plastically quite significantly, new equilibrium is continuously achieved. At no point will the foundation suddenly and catastrophically collapse. Therefore laterally loaded pile foundations should be designed to have limited rotations and deflections at the mudline. According to GL [9] deformation limitations should also be set for the deflection of the pile toe. Additionally there should be a vertical tangent to the deflection curve. However, for large diameter piles this leads to very long piles, which does little to reduce the deflections at the tower top [11].

For axially loaded piles the deformation is not as critical as the ultimate capacity. If a pile is subjected to axial tension the pile will ultimately pulled out of the soil or if loaded in compression it may exceed the combined shaft friction and end bearing and it may lead to unacceptable settlements. However, to mobilise the shaft friction, some deformation of the pile is necessary. As the load is transferred to the soil, the load in the pile decreases and the deformations become less. Therefore the load transfer in the upper soil layers is the strongest. Axial pile deformations for multiple piled support structures may significantly influence the natural frequencies.

### 5.4.5 Design requirements for manufacturing and installation

Besides the design requirements listed so far there are also numerous practical limitations to what can be produced and installed. From the review of the manufacturing and installation processes in Chapter 3 it could be seen that many handling and lifting procedures must be performed and that accessibility during the fabrication and installation phases is important. Also during the operational phase requirements can be set for accessibility for inspection.

**Manufacturing**

The first limitation encountered in the manufacturing process is the size of the plates that can be handled. This is usually linked to a maximum mass, defined by the capacities of the steel mills producing the plates. This means that the height of a section with a certain diameter and wall thickness is limited. Usually segments of up to 4m are used in monopile fabrication. This affects the number of welds that have to be made.
Furthermore the maximum thickness of plates that can be rolled may limit the design.
Large diameter sections with high D/t ratios are susceptible to elastic deformation or ovalisation under their own weight. This may present additional costs during manufacturing. Therefore limits should be set for the maximum D/t ratios.
For the manufacturing of tubular joints, the angle between two connecting elements should not be less than 30°, to ensure that the joint is suita bly accessible for welding.

**Installation**

Structural elements are designed for their in-place situation. However, during transport and installation loads act on the structure, for instance dynamic wave loads leading to deformations and accelerations during transport and bending moments in piles during upending. Structural elements should therefore also be checked for transport and installation load situations.
Although strictly speaking not a technical limitation, but more related to the economics and the availability of vessels is the lifting capacity of the installation vessel. The weight of components

to be installed in one piece should not exceed the operational lifting capacity of a vessel that can be secured for the installation at an economically acceptable rate.
Pile driving equipment is currently limited to a maximum pile diameter that can be driven due to the limited size of anvils. The largest pile top diameter is currently 5.2 m.
The footprint of substructures and of piles on barges determines the number of structures that can be transported at one time, thereby influencing the logistics of the installation process.

It should be noted that the limitations mentioned in this section represent the current state of the industry. If the market requires the development of larger and more powerful equipment or facilities to increase cost effectiveness the industry will likely respond to meet this demand.

# 6. Monopile support structures

## 6.1 Introduction

As the monopile is currently the most frequently applied support structure concept it serves well as a reference to compare other support structure types with. To this end it is desirable to establish the development of loads and required dimensions for monopile structures in increasing water depths and for other varying site conditions or turbine parameters. Therefore this chapter presents a sensitivity analysis in which site parameters, turbine parameters and the water depth are varied. The resulting changes in loads, natural frequencies and eventually required dimensions are shown.

This sensitivity analysis requires a reference point, for which the parameters can be changed one by one to determine the sensitivity to each of these parameters. A realistic design is required for this. As the aim is to compare support structure concepts for deep water and large turbines with the results from the monopile sensitivity analysis, this reference design should be designed for the deepest water and largest turbine as possible. Although monopiles have been applied in water depths up to 35 m, the currently perceived water depth limit for a monopile supporting a 5 MW turbine is approximately 25 m. This is mainly due to the fact that large turbines are heavy and require an increased hub height. To avoid too low first natural frequencies the pile diameter is increased, in turn leading to larger hydrodynamic loads. The required dimensions for monopiles water depths beyond 25 m become restrictive in terms of installation and manufacturing capacity.

This chapter describes the design of a reference monopile structure in 25 m water depth and supporting the Upwind 5.0 MW reference turbine. The design conditions, approach and design results are presented. The reference monopile structure is designed as part of a study into the possibilities for load mitigation on a monopile structure through the use of adaptive control [12]. This design is also used in the sensitivity analysis described in Section 6.5. Finally a cost model is presented, showing not only the variation of the required dimensions for a variety of parameters, but also shows the costs for the monopile support structure based on material costs and production costs.

## 6.2 Design inputs for the monopile reference structure

### 6.2.1 Design data

For the monopile reference design a site in the Dutch sector of the North Sea has been chosen in approximately 25 m water depth. The wind and wave data have been selected from the K13 platform. These data have been obtained from the Rijkswaterstaat Waterdienst, formerly known as Rijksinstituut voor Kust en Zee [42]. This data source contains measurements of significant wave heights, wave periods, dominant wave directions, current velocities and directions and wind speed and directions over a period of 22 yrs. This data source has been selected as it is considered to be representative for environmental conditions in the southern part of the North Sea. Also the fact that the data is available for a long period of time at 3hr intervals for the wave conditions and 1 hr intervals for wind data adding to the reliability of the selected source.
Although the K13 measurements are real data, the selected site is artificial as the water depth has been altered and the significant wave heights in the scatter diagrams have been enhanced for the purpose of the load mitigation study. The site is dubbed the K13 shallow water site to distinguish it from the real site and from another artificial site using the K13 data in 50m, the K13 deep water site.
The rough data has been processed to establish the extreme values for wind wave and current data for different return periods. Also long term joint probabilities of sea states and wind speeds are determined from the data. These data, together with additional data on water levels, the

occurrence of marine growth, corrosion and definition of soil profiles and hydrodynamic coefficients are recorded in a design basis [13]. The extreme values for wind speed wave height and current velocity are given in Table 6.1:

Table 6.1: Main parameters for the K13 shallow water location [13]

| Parameter description | Value |
|---|---|
| 1 yr extreme wave height [m] | 11.25 |
| 50 yr extreme wave height [m] | 15.33 |
| 1 extreme wind speed [m/s] | 32.74 |
| 50 yr extreme wind speed [m/s] | 42.73 |
| Normal current velocity [m/s] | 0.6 |
| Extreme current velocity [m/s] | 1.2 |

In Figure 6.1 the wind speed distribution is given at an elevation of 80 m above sea level. The distribution of wind and wave directions is also indicated. The prevailing wind direction is approximately South West. Wave mainly approach from the same direction, but a significant portion of the distribution comes from northerly directions.

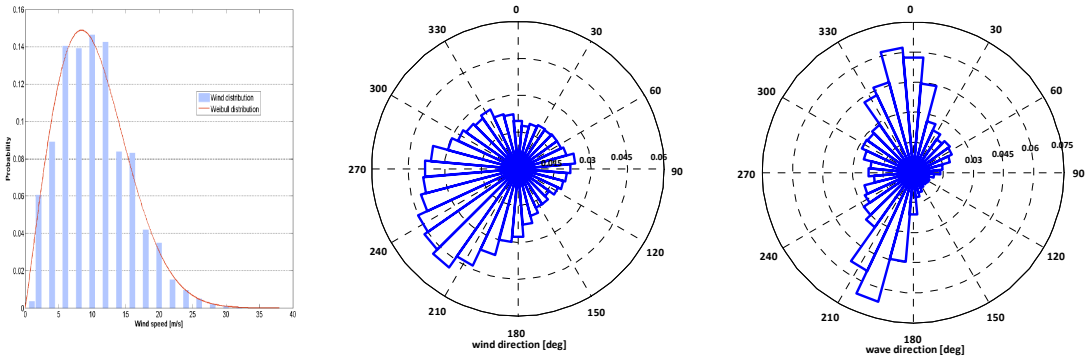


Figure 6.1: Wind speed distribution (left), wind rose (middle) and wave rose [13]

### 6.2.2 Design Load Cases

For the Ultimate Limit State (ULS) analysis the loads are obtained from integrated time domain simulations in GH Bladed [Ref Bladed]. Load cases are simulated according to the IEC standard [8]. A full analysis of all prescribed load cases involves a large number of simulations. To reduce the overall effort for the ULS analysis only those load cases deemed potentially design driving for the support structure are assessed here. As potentially design driving load cases, all load cases that might result in high values of rotor thrust or side-to-side force, corresponding with high tower bending moments, are chosen for the ULS load analysis. The Design Load Cases (DLC) considered for the ULS analysis are described below:

- DLC 1.3: Power production loading with Normal Sea State and Extreme Turbulence Model
- DLC 2.1: Power production loading with occurrence of fault. Pitch runaway with all blades pitching to fine at a constant rate of 6?s.
- DLC 2.3: Power production loading plus loss of electrical grid connection in combination with an Extreme Operating Gust
- DLC 6.1a: Normal idling conditions with Extreme Sea State model with constrained wave.
- DLC 6.2a: Idling conditions with loss of electrical network. Evaluation of idling conditions for yaw error ranging from 0° to 180

In the fatigue limit state analysis (FLS) the total damage incurred over the structure's design life is assessed by performing time domain simulations using GH Bladed for both operational and idling conditions, taking directionality and misalignment of wind and waves into account. For co-aligned wind and waves the effect of aerodynamic damping can significantly reduce fatigue damage. Therefore the availability of the turbine is taken into account in the post-processing by assuming the turbine to be in operation for 90% of the time. The Design Load Cases considered for the FLS analysis are described below:

- DLC 1.2: Power production loading
- DLC 6.4: Idling before cut-in and beyond cut-out
- DLC 7.2: Idling in cases of non-availability

### 6.2.3 Model dimensions

Before a design evaluation can be performed a preliminary geometry of the support structure must be available. This requires the definition of key elevations and dimensions and masses of various components. Some of these values are fixed, such as the interface level between the tower and the substructure and the hub height. Other elevations are dependent on the dimensions of the components. Also dimensions of one component can be dependent on dimensions of another component. Finally the dimensions of all components are dependent on the loads acting on the component. During the design process several design iterations are made, resulting in different loads and hence different support structure dimensions. Therefore it is convenient to parameterise the model to allow quick adjustment of the model dimensions based on a limited number of input variables.

#### Design elevations

The first elevation to establish is the interface level, the elevation of the interface between the tower and the substructure. The main platform is located at this elevation and it must be ensured that the platform is strong enough to withstand all hydrodynamic loads from waves coming into contact with the platform or alternatively that no waves can hit it. The latter is the most common approach and the elevation is determined by the highest still water level with a recurrence period of 50 years, combined with the highest crest elevation within a storm surge of the same recurrence period. To this an air gap is added to reduce loads from wave run-up and air pressure build up. Figure 6.2 illustrates the determination of the interface level. This elevation, set at 14.76m above MSL for the reference design, remains fixed throughout the design process. The platform is located at the interface level.

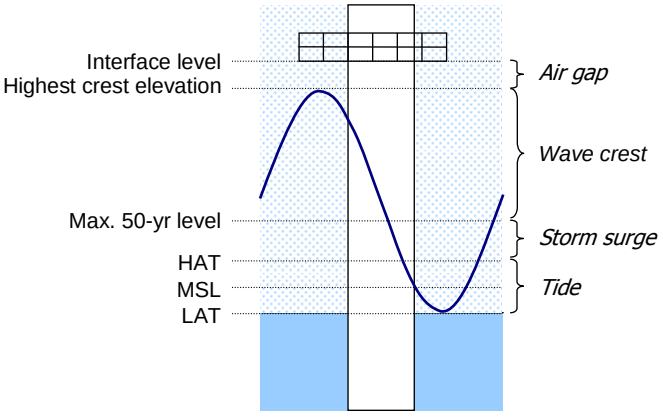


Figure 6.2: Determining the interface level

With the interface level established, the hub height can be determined. Contrary to onshore turbines, the hub height of offshore turbines should be selected as low as possible to avoid low

fundamental frequencies and large overturning moments. This does not come at the cost of energy production as the wind shear gradient at sea is reduced much steeper than onshore and the wind speed is generally higher due to the absence of obstacles. Therefore the requirement is that the blade tip at its lowest azimuthal position remains clear of the platform by a certain margin. In this design the margin is 7.4m and the hub height is 85.16m above MSL.

### Tower dimensions

In the reference design the tower is assumed to be supplied by the tower manufacturer. Therefore a separate design was made for the tower based on preliminary load data for the reference turbine. The resulting tower is made up of two 34 m sections. The outer diameter varies from 5.6 m at the bottom to 4m at the tower top and the wall thickness varies from 32 mm at the tower base to 20 mm at the tower top. An overview of the tower make up can be seen in Figure 6.3, while a more detailed description of the tower geometry is given in Appendix I.

### Pile dimensions

The support structure consists of a foundation pile and a transition piece. The transition piece is fixed over the top of the foundation pile by means of a grouted connection (the detailed assessment of the grout joint is not part of this study).
The pile top elevation is at 5.0m above MSL so that it is above the splash zone at all times in order to facilitate installation. The diameter at the top of the foundation pile is fixed at 5.5 m as larger diameter piles cannot be driven due to the limited size of anvils currently in the market. A conical section tapers outward to a larger diameter. This allows the stiffness of the foundation to be controlled by the pile diameter, while respecting installation limitations. A schematic representation of the pile model can be seen in Figure 6.3.

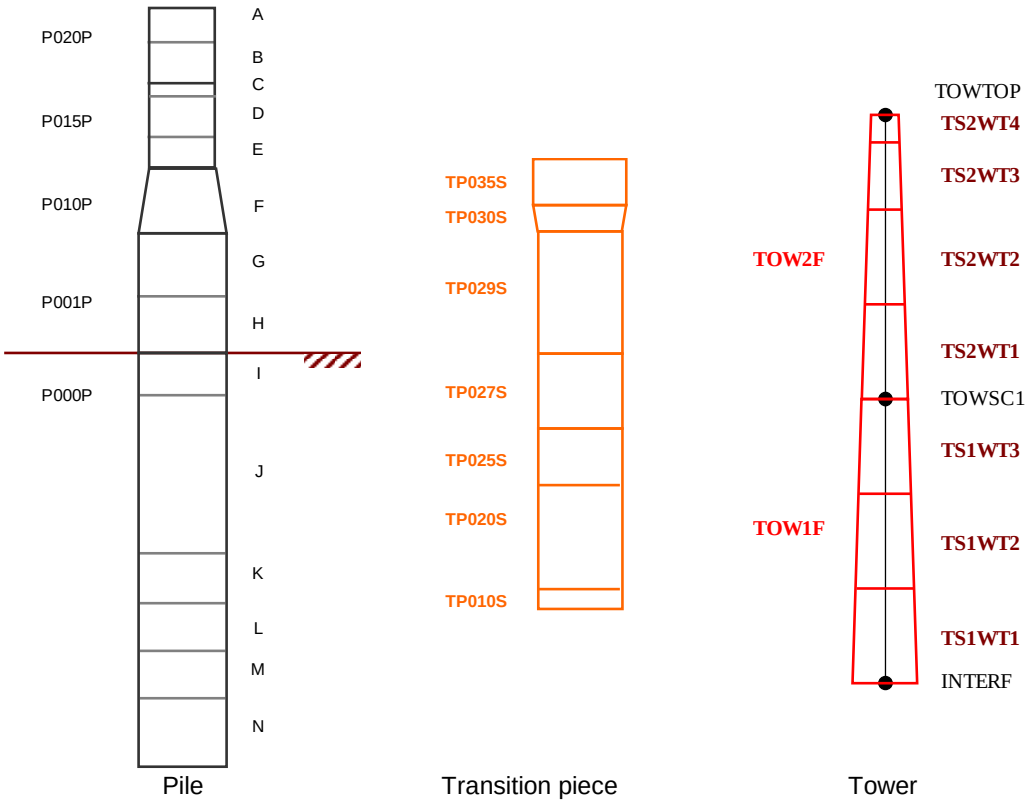


Figure 6.3: Parameterisation of the monopile support structure

**Transition piece dimensions**

The transition piece has an outer diameter of 5.9 m at the lower end to accommodate the required wall thickness of the transition piece itself and a minimum grout thickness of 75 mm. The length of the overlap is 1.5 times the pile top outer diameter, with an additional length of 0.5 m to represent the grout skirt. As such the bottom of the transition piece holding the sacrificial anodes is always below the splash zone. A conical section reduces to an upper diameter of 5.6 m, matching the diameter at the tower bottom. The distance of this cone above the overlap is fixed at 1.5 m. This same value is adopted for the distance between the bottom of the transition piece and the pile cone. In Figure 6.3 the parameterised model for the transition piece is depicted.
The presence of appurtenances on the support structure can attract significant hydrodynamic loading. Therefore the effect of the presence of the boat-landing and J-tube are taken into account by modifying the hydrodynamic coefficients. Additionally, equipment and additional non load-bearing elements are modelled as localised masses in the centreline of the structure.

**Foundation modelling**

The foundation is modelled using p-y curves to represent the lateral non-linear pile-soil interaction. The p-y curves have been modelled according to API [2]. The vertical foundation stiffness is modelled using t-z curves representing the shaft friction and with Q-z curves to model the end bearing at the pile tip. The torsional degree of freedom is constrained for the pile nodes. P-y curves and t-z curves are applied at every meter along the pile.

The occurrence of scour around the pile may significantly affect the dynamics of the support structure. A scour hole may develop up to a depth of 1.3 times the foundation pile diameter [14]. This will result in a smaller embedded pile length, leading to a softer foundation and in a larger unsupported structure length resulting in a softer structure. To avoid these effects it is assumed that scour protection is applied, thereby preventing the development of a scour hole.

## 6.3 Preliminary design for the monopile reference structure

### 6.3.1 Rosa model description

To generate a suitable preliminary geometry, use is made of the structural analysis package ROSAP [15]. ROSAP is the name of the Rambøll Offshore Structural Analysis Programme Package. It has been developed as a tool to solve the problems commonly arising in analyses of fixed offshore steel platforms. During recent years the programme package has been extended to solve problems regarding offshore wind turbine support structures. The structural analysis is carried out by the program ROSA. In addition there are several postprocessing programs within the ROSAP package.

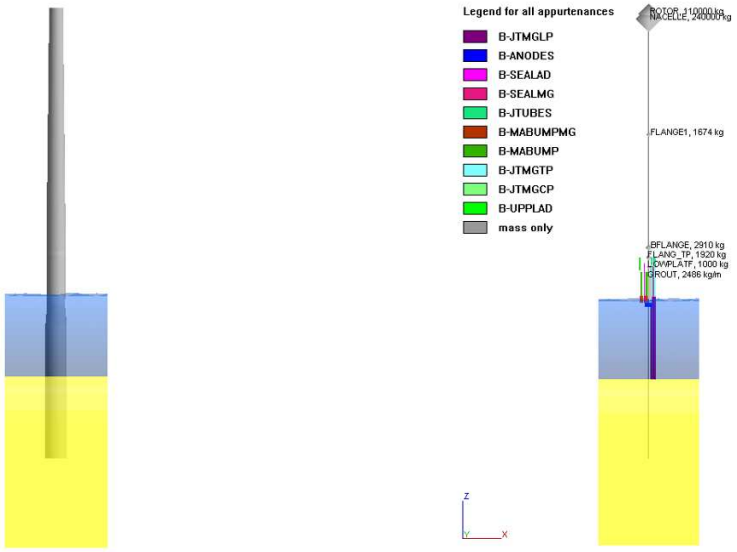


Figure 6.4: Rosa model of the support structure

A parameterised model is set up following the description in section 6.2.3. The RNA is included as a concentrated mass for the rotor and for the nacelle. The soil conditions are included in the form of p-y and t-z curves according to API [2]. The grouted connection is modelled using rigid links between the foundation pile and the transition piece in combination with a distributed mass representing the grout mass. Secondary steel structures such as boat landings, platforms and J-tubes are modelled as non structural elements having a mass and an area, in order to include their influence on dynamics and hydrodynamic loading. Figure 6.4 shows the ROSA model and the location of concentrated masses and appurtenances.

### 6.3.2 Natural frequency analysis

As stated in section 5.4.2, the allowable range for the support structure natural frequency for the Upwind reference turbine is 0.222 Hz - 0.311 Hz. In the natural frequency analysis the dimensions of the support structure have been varied to find a suitable configuration. Parameters that were varied were the pile diameter, penetration depth and elevations of the pile cone.

The outer diameter of the pile was varied in the range from 5.00 m to 6.75 m, while the pile diameter at the pile top was kept constant at 5.5 m. The wall thickness was kept constant in the analysis. The variation of the first natural frequency with penetration depth can be seen for the investigated pile diameters in Figure 6.11.
According to these results, the configuration with the lowest mass would be the most economic choice. However, the strength and stability requirements as well as the fatigue life requirements will also have to met, thereby reducing the possible number of combinations. In the next step the extreme load analysis is performed to determine which configurations meet the ULS requirements.

### 6.3.3 Ultimate limit state analysis

ROSA is capable of calculating wave loads and wind loads on static structures, but not aerodynamic loads on an operational wind turbine. Therefore a preliminary set of wind loads is generated with the use of GH Bladed [16]. For each degree of freedom (DOF) the maximum wind load in 6 DOF at the tower top is determined, as shown in Table 6.2.

Table 6.2: Aerodynamic loads at interface level determined with Bladed

| | | | Mx | My | Mz | Fx | Fy | Fz |
|---|---|---|---|---|---|---|---|---|
| | | Load case | kNm | kNm | kNm | kN | kN | kN |
| Mx | Max | 1.3ec_1 | 21067 | 24935 | -601.7 | 396.3 | -175.0 | -5593.2 |
| Mx | Min | 1.3ea_2 | -7293.9 | 9281.1 | -2235.2 | 316.2 | 115.9 | -5637.3 |
| My | Max | 1.3ca_3 | 7467.2 | 58379 | 2678.4 | 924.3 | -21.0 | -5722.4 |
| My | Min | 1.4aa | 12836 | -5283.1 | 276.0 | 36.6 | -149.3 | -5671.0 |
| Mz | Max | 1.3ec_3 | 10804 | 10907 | 7351.8 | 239.3 | -58.6 | -5887.8 |
| Mz | Min | 1.3ea_2 | 728.4 | 6838.1 | -11290 | 309.5 | 54.0 | -5563.3 |
| Fx | Max | 1.3aa_2 | 3158.9 | 50301 | 2140.9 | 972.1 | 20.1 | -5785.0 |
| Fx | Min | 1.4aa | 13135 | -4356.7 | 140.8 | 15.5 | -125.8 | -5675.1 |
| Fy | Max | 1.3ea_3 | -1904.7 | 14437 | -2588.9 | 406.0 | 202.1 | -5684.9 |
| Fy | Min | 1.4cc | 18210 | 18072 | 186.1 | 353.4 | -249.8 | -5648.9 |
| Fz | Max | 1.3ea_3 | 5388.8 | 18015 | -2858.3 | 358.4 | -8.59 | -5367.8 |
| Fz | Min | 1.3ec_3 | 8266.0 | 9548.0 | 6218.7 | 258.3 | -71.4 | -5921.0 |

The loads cases in Table 6.2 represent power production situations. The 1.3 cases correspond to extreme turbulence intensity in the wind conditions, whereas the 1.4 cases are concerned with the occurrence of an extreme coherent gust with change of direction. No hydrodynamic effects have been taken into account in the simulations, as these are calculated in the ULS analysis in Rosa.

These loads are combined with wave loads in Rosa in a static analysis. As for the natural frequency analysis a variety of configurations is tested, with the pile diameter varying from 4.5 m to 6.75 m and penetration depth varying from 20 m to 30 m. Gravity and buoyancy loads are also taken into consideration. Inertia loads are conservatively accounted for by applying a Dynamic Amplification Factor of 1.25. The load combinations are listed in Table 6.3. The loads at mudline are shown in Figure 6.5.

Table 6.3: Load combinations used in preliminary design

| Load | Aerodynamic | Vw | H/Hs* | T/Tp* | Uc |
|---|---|---|---|---|---|
| Combination | Load case | m/s | m | s | m/s |
| LC 1 | 1.3ec_1 | 24 | 5.30 | 7.80 | 1.2 |
| LC 2 | 1.3ea_2 | 24 | 5.30 | 7.80 | 1.2 |
| LC 3 | 1.3ca_3 | 14 | 2.80 | 6.07 | 1.2 |
| LC 4 | 1.4aa | 10 | 1.75 | 5.36 | 0.6 |
| LC 5 | 1.3ec_3 | 24 | 5.30 | 7.80 | 1.2 |
| LC 6 | 1.3ea_2 | 24 | 5.30 | 7.80 | 1.2 |
| LC 7 | 1.3aa_2 | 10 | 1.75 | 5.74 | 1.2 |
| LC 8 | 1.4aa | 10 | 1.75 | 5.36 | 0.6 |
| LC 9 | 1.3ea_3 | 24 | 5.30 | 7.80 | 1.2 |
| LC 10 | 1.4cc | 14 | 2.8 | 6.79 | 0.6 |
| LC 11 | 1.3ea_3 | 24 | 5.30 | 7.80 | 1.2 |
| LC 12 | 1.3ec_3 | 24 | 5.30 | 7.80 | 1.2 |

*$H_s$ and $T_p$ for all 1.3 cases, $H$ and $T$ for the 1.4 cases

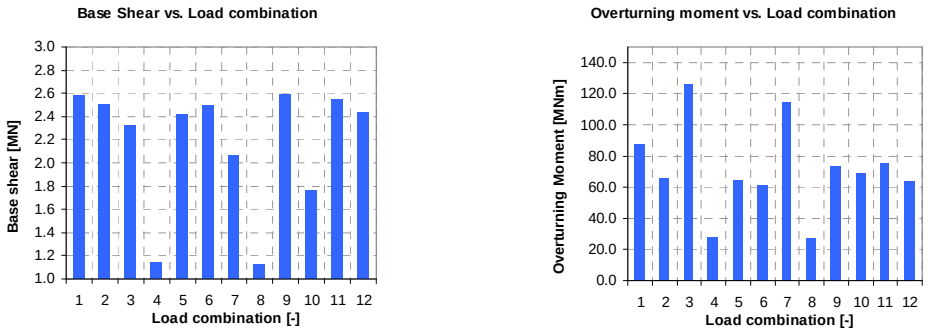


Figure 6.5: Loads at mudline for different load combinations for pile with outer diameter of 6000 mm

The 1.4 cases do not contribute much towards the maximum loads at seabed level. All of the 1.3 load cases give approximately the same base shear, but load combinations 3 and 7, corresponding to operational conditions around rated wind speed are governing for the overturning moment. The resulting utilisation ratios are recorded for each of the load cases.

Checks are performed for shell and column buckling, yield strength and according to NORSOK N004R2. Pile are checked for yield strength and lateral and axial stability. For the assessment of pile strength in the ULS the material factor applied for the soil strength parameters is 1.00.
For determining the pile penetration depth the design values of the soil strength parameters are reduced by applying a material factor of 1.35. When the calculation converges on a solution, equilibrium is achieved between applied forces and reaction forces and sufficient lateral resistance is available.

In a separate analysis the ROSA model has been used to determine the influence of appurtenances on hydrodynamic loads for a pile with lower diameter of 6.2 m, an upper diameter of 5.5 m and a transition piece outer diameter of 5.8 m. The loads on the pile have been determined for a regular streamfunction wave with wave height $H$ = 15.33 m and wave period $T$ = 10.174 s for different angles of attack. This way the contribution of the J-tubes and boatlanding on the hydrodynamic loads can be determined. The boatlanding and J-tubes are oriented towards 202.5° and 112.5° respectively (North = 0°, clockwise rotation is positive). The results from the analysis are shown in Figure 6.6.

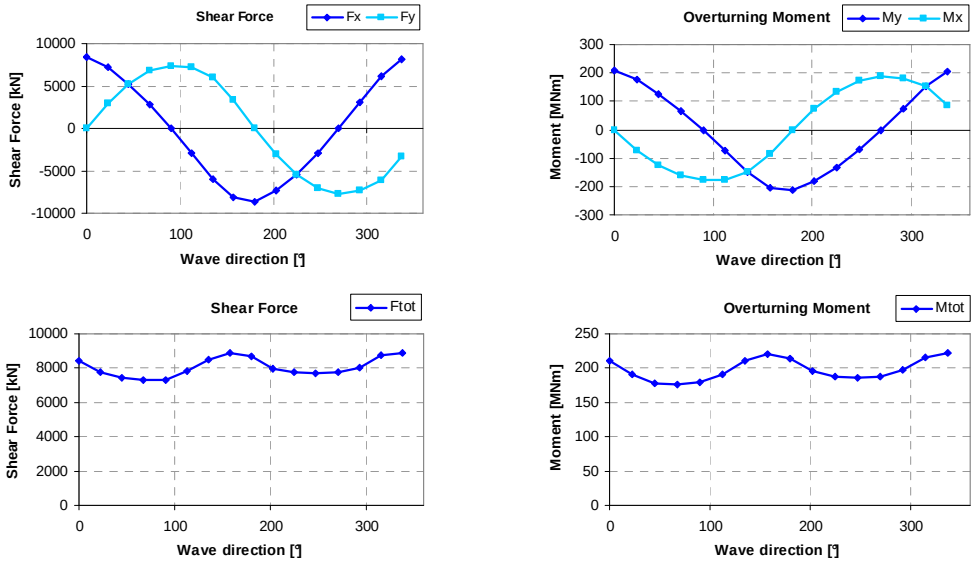


Figure 6.6: Influence of appurtenances on hydrodynamic loads for a monopile structure

The total shear force shows a peak at 157.5°, when the appurtenances are fully exposed and a minimum at 247.5° when the appurtenances are shield ed by the pile. The difference between these situations is approximately 17%. For the overturning moment the same pattern can be discerned, but the difference is slightly larger at approximately 21%. This clearly illustrates that the hydrodynamic load on monopile structures is significantly influenced by the presence of appurtenances. The appurtenances should therefore be taken into account in the analyses, at least in an ultimate load analysis.

### 6.3.4 Fatigue limit state analysis

In the ULS analysis the number of possible configurations was reduced. By fixing the penetration depth at 24 m, only four configurations remain, with pile outer diameters of 6000 mm to 6750 mm in steps of 250 mm. For these configurations a fatigue analysis has been carried out.

Damage equivalent loads have been determined in simulations using Bladed. In the fatigue analysis these loads are applied at the interface level to determine the fatigue damage due to aerodynamic loads. In a separate dynamic analysis the fatigue due to wave loading is determined by applying an irregular wave time series to the model for all wave load directions in the

To account for aerodynamic damping, which is not implicitly taken into account in Rosa, the structural damping for the first and second natural frequencies is enhanced by a conservative value of 4%, [17] leading to a total damping of 5% of the critical damping.

Directionality has not been taken into account in the preliminary design phase. For monopiles assuming the loading to come from a single direction for the entire design life is considered conservative, as usually the fatigue damage will be spread around the circumference of the pile instead of being concentrated in one direction. In some cases, severe misalignment between wind and waves may lead to reduced aerodynamic damping and thus to increased fatigue damage. However, this situation is not considered in the preliminary design phase.

For the main pile and transition piece elements no stress concentration factor was taken into account. However, at the transitions between cylindrical and conical sections stress

concentrations can be substantial. Therefore, stress concentration factors are included at the top and bottom of the pile cone and the transition piece cone, determined both for the tubular element side and for the cone side. The SCFs at these points range between approximately 1.4 and 1.7.
For the preliminary design S-N curves for tubular girth welds in seawater with cathodic protection have been applied according to DNV [1].

The fatigue results for the aerodynamic loads and the hydrodynamic loads are combined according to:

$$D_{tot} = (D_{aero}^{2/m} + D_{hydro}^{2/m})^{m/2}$$

Where $D_{aero}$ is the aerodynamically induce fatigue damage, $D_{hydro}$ is the hydrodynamically induced fatigue, $m$ is the Wöhler coefficient and $D_{tot}$ is the combined damage.

Four different structure configurations have been assessed for fatigue, with pile diameters in the range of 6.00 m to 6.75 m in steps of 0.25 m. The highest fatigue damage occurs near the pile cone transitions, due to the relatively high SCFs at those locations. This effect is to a lesser extent also visible near the transition piece cone, where the fatigue damage exceeds 0.5.
For all four considered models the fatigue life is less than the design life of 20 years at the top and bottom of the pile cone. However, at this stage the design is improved no further, as the used method is deemed conservative and the geometry found may prove to be adequate in the final design.

### 6.3.5 Preliminary design results

From the previous analyses the most suitable structure is found to be a monopile with a foundation pile diameter of 6 m, tapering to 5.2 m at the top and with a wall thickness of 80 mm. for the major part of the foundation pile and a wall thickness of 70 mm for the transition piece. The geometry can be seen in Figure 6.7.

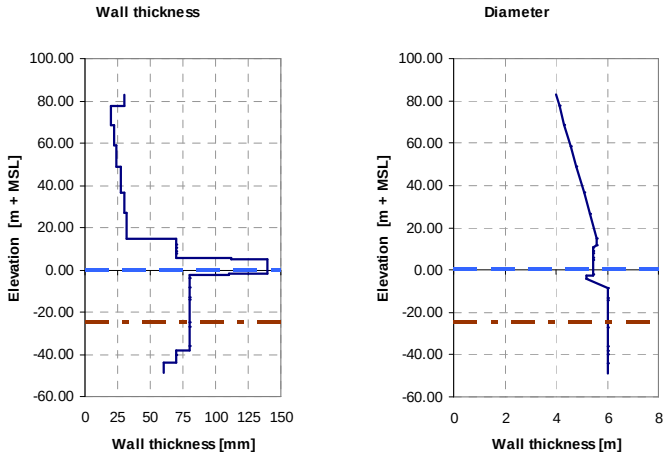


Figure 6.7: Resulting dimensions for the preliminary monopile design

The first and second bending frequencies of the structure are at 0.27 Hz and 1.22 Hz respectively. The overall mass of the foundation pile transition piece and tower is 964.62 ton. In a more detailed analysis this structure is further optimised as explained in the following section.

## 6.4 Final design for the reference monopile structure

### 6.4.1 Bladed model description

The detailed design of the reference monopile structure has been performed in an integrated analysis in Bladed. In this way the correct aerodynamic damping is taken into consideration in the dynamic analyses. While the turbine modelling and simulation capacity in GH Bladed is state-of-the art, the level of detail in modelling the support structure and the post processing capacity relating to stress checks are limited in the version of Bladed available at the time of this study in comparison with Rosa.
However, section forces can be extracted and post processed separately according to Germanischer Lloyd guidelines [9].

To account for the boatlanding and J-tubes the hydrodynamic coefficients in the Bladed model are adjusted for the ultimate load cases. The hydrodynamic loads are calculated with Morison's equation, in which the inertia force on a slender vertical element is determined as a function of the fluid particle acceleration and the square of the diameter and the drag force is calculated as a function of the diameter and the square of the fluid particle velocity.

The equivalent hydrodynamic coefficients $C_{M;eq}$ (drag) and $C_{D;eq}$ (inertia) are modified according to:

$$C_{M;eq} = C_M \frac{D_{pile}^2 + D_{bl}^2 + D_J^2}{D_{pile}^2} \text{ and } C_{D;eq} = C_D \frac{D_{pile} + D_{bl} + D_J}{D_{pile}},$$

where $D_{pile}$, $D_{bl}$ and $D_J$ are the diameter of the pile, boatlanding and J-tube as functions of elevation respectively. The relative increase of the drag coefficient is thus significantly larger than the increase of the inertia coefficient.
As a simplification the boatlanding is considered to consist of only one vertical cylinder, assuming that the second element is mainly shielded by the first. Furthermore, the same equivalent hydrodynamic coefficients have been applied for all angles of attack, whereas in reality the increase of the wave load is dependent on the angle of attack. This conservative approach can be justified by the fact that in the extreme load analysis the angle of attack producing the worst case loading should be considered, (unless this situation can be proven not to occur).

Masses of grout and contained water are modelled as additional masses at the nodes at the appropriate elevations. The masses of blades, hub and nacelle are accounted for in the turbine model.

The contribution of the grout to the stiffness of the grouted joint has been neglected and the overlap is modelled as a single tubular element with outer diameter of the transition piece and wall thickness equal to the wall thickness of transition piece and foundation pile combined.

To ascertain whether the Bladed model corresponds to the Rosa model, the first and second natural bending frequencies in the fore-aft and side-to-side directions have been checked. The first natural frequency showed an exact match, whereas the second natural frequency shows an error of 6%. As the first natural bending frequencies determine by far the greater share of loading compared to the second bending natural frequencies, the result of the natural frequency comparison between Rosa and Bladed model is considered satisfactory.

### 6.4.2 Ultimate limit state analysis

For the ULS analysis the following checks must be performed:

- Yield stress check for the pile, the transition piece and the tower
- Global buckling check for the pile above the mudline, the transition piece and the tower
- Local buckling check for the pile above the mudline, the transition piece and the tower
- Foundation stability check to determine the required penetration depth

For each of the above design checks the loads are found by performing time domain simulations for the relevant Design Load Cases (DLCs). For the yield and buckling checks the stresses are calculated for each relevant elevation, taking the appropriate load factors into account. Subsequently the maximum stress is found and the design check calculations are executed.

**Yield stress check**

In the yield check it is verified that the stress remains below the characteristic yield stress to avoid plastic deformations in the structure due to yielding of the steel. The check is performed by calculating the Von Mises stress at each node, taking the appropriate load factors into account and ascertaining that:

$$\sigma_i \leq f_y / \gamma_M$$

where $\sigma_i$ is the Von Mises stress at node $i$, $f_y$ is the yield stress and $\gamma_M$ is the material factor. The result is expressed as a utilisation ratio where the ratio between $\sigma_i$ and $f_y/\gamma_M$ should be less than 1.0. The characteristic yield stress is taken as 355 N/mm$^2$ for all elements of the primary structure, taking thickness effects into account according to Table 6.4:

Table 6.4: Characteristic yield strength including thickness effect

| | Characteristic yield strength as function of wall thickness | | | | | |
|---|---|---|---|---|---|---|
| | t > 100 mm | t > 80 mm | t > 63 mm | t > 40 mm | t > 16 mm | t > 0 mm |
| | t ≤ 150 mm | t ≤ 100 mm | t ≤ 80 mm | t ≤ 63 mm | t ≤ 40 mm | t ≤ 16 mm |
| fy [N/mm$^2$] | 295 | 315 | 325 | 335 | 345 | 355 |

**Global buckling check**

Under high compressive stress due to axial loading and bending, global buckling can occur. In the global buckling check it is verified that the overall stability of the structure is guaranteed. The global buckling check is carried out for each node according to [9].

$$\frac{N_d}{\kappa N_p} + \frac{\beta_m M_d}{M_p} + \Delta n \leq 1.0$$

where $N_d$ and $M_d$ are the factored axial compression force and bending moment respectively, $N_p$ and $M_p$ are the plastic compression resistance and the plastic resistance moment, $\kappa$ is a reduction factor for flexural buckling, $\beta_m$ is a bending moment coefficient and $\Delta n$ is calculated by $\Delta n = 0.25 \cdot \kappa \cdot \overline{\lambda}^2 \leq 0.1$, in which $\overline{\lambda}$ is the reduced slenderness.

**Local buckling check**

Thin walled tubular sections may be susceptible to local shell buckling. Compressive axial loads and bending moments together with compressive hoop stresses due to external pressure can cause unstiffened sections to fail locally. There is sufficient resistance against local buckling if the following interaction equation is satisfied [9]:

$$\left(\frac{\sigma_x}{\sigma_{xu}}\right)^{1.25} + \left(\frac{\sigma_\varphi}{\sigma_{\varphi u}}\right)^{1.25} \leq 1.0$$

In this equation $\sigma_x$ and $\sigma_\varphi$ are the acting axial compressive stress and circumferential stress due to external pressure respectively and $\sigma_{xu}$ and $\sigma_{\varphi u}$ are the ultimate compressive and circumferential stresses respectively. For the structure presented in this article the pressure difference between the inside and outside of the foundation pile due to water level variations is relatively small. Therefore the circumferential stress is neglected in the following.

**Foundation stability check**

To ensure the overall stability of the structure, the deformation of the foundation must be within certain limits for the deflection and rotation at mudline. Also the stiffness of the foundation should be such that the natural frequency of the entire structure lies within the frequency range that allows safe operation of the wind turbine. The verification of the foundation stability is usually performed after the diameter of the foundation pile is chosen. Therefore, this verification mainly involves determining the required embedded length.
To this end a model of the pile foundation is subjected to the maximum loads at seabed, found from all performed load case simulations. Initially the embedded length of the foundation pile is selected sufficiently long. In a finite element model of the pile including p-y curves, non-linear spring elements representing the pile-soil interaction, the loads are applied to the model at the seabed level and the resulting deflections and rotations are found. If the deflections and rotations are within the limits the embedded length is reduced. If the limits are exceeded, the penetration depth is increased. The design penetration depth is defined as the smallest embedded length for which the limits are still satisfied.

**Results of ULS Checks**

Figure 6.8 shows the results of the strength and buckling checks for all Design Load Cases. The figures show the maximum utilisation per elevation for each of the evaluated load combinations within the Design Load Case under consideration.

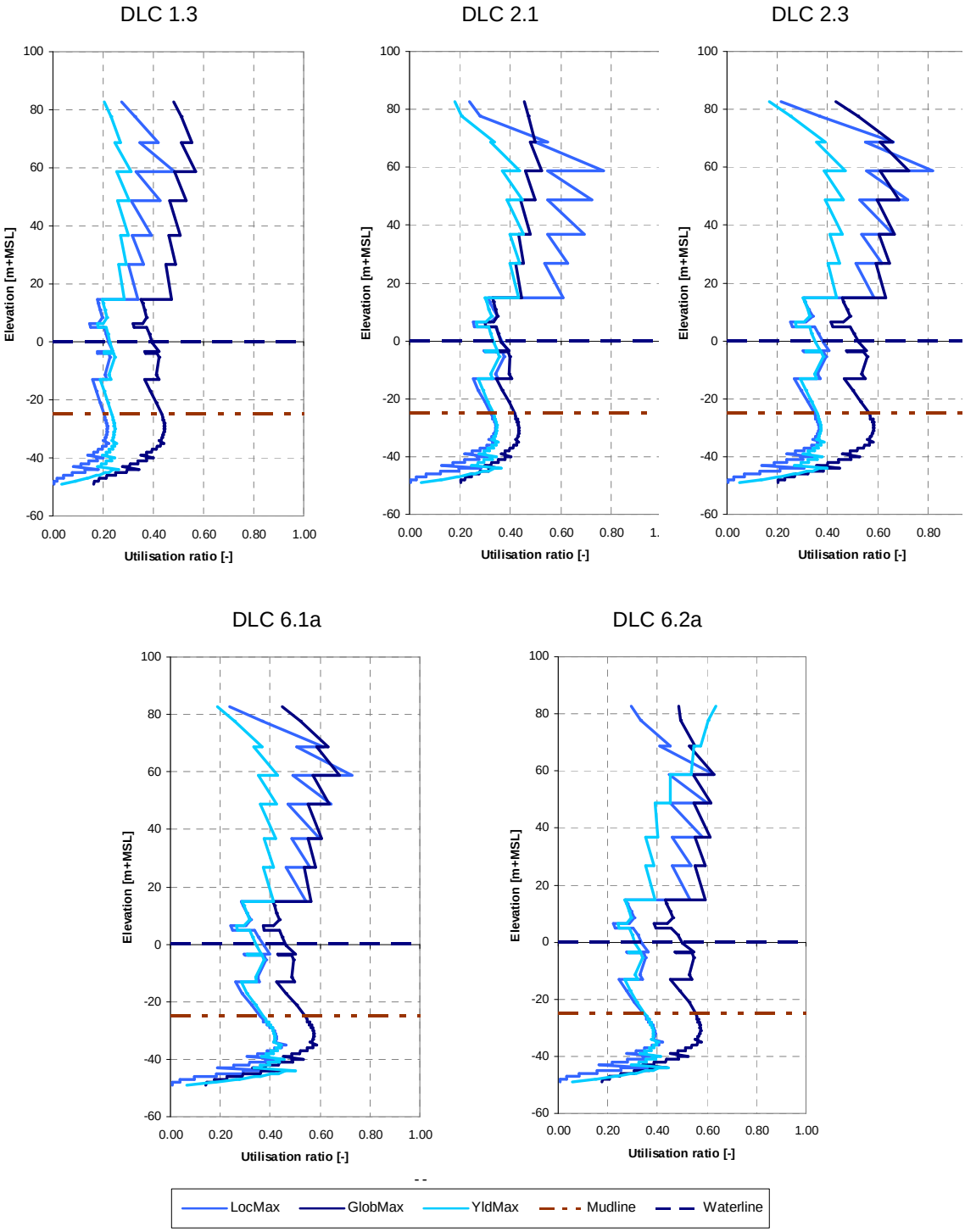


Figure 6.8: Results for strength and buckling checks

In reality the buckling checks below the mudline are not necessary as the support from the soil prevents buckling. Design Load Cases 6.1a and 6.2a appear to be governing for the pile and transition piece, while DLC 2.3 is governing for the tower. The utilisations for all checks are well below 1.0.

### 6.4.3 Fatigue limit state analysis

For the fatigue limit state analysis (FLS) a conservative approach is chosen. This implies a check for fatigue loads for a set reference cycle number and Wöhler coefficient, here $N=2\cdot10^7$ and $m=4$. The resulting equivalent stresses are then checked against S-N-curves according to GL [9]. For the pile and transition piece a curve with a FAT class '90' is chosen, for the tower '80' respectively. Furthermore an additional partial material safety factor is applied on the stress ranges according to the part's ability for inspection and accessibility. Here the pile and transition piece is chosen to be non fail-safe including no possibilities for monitoring and maintenance (safety factor of $\gamma_M=1.25$), and the tower as fail-safe including possible monitoring and maintenance actions (safety factor of $\gamma_M=1.0$).

For the fatigue analysis no effects of the presence of the secondary steel, such as boat-landing or J-tube, are taken into account. For the ULS this is done by modifying the hydrodynamic coefficients. The reason for disregarding this for FLS is that it was found that the attachment of appurtenances effects the drag part of the Morrison's equation by several percent, where the inertia part is nearly unchanged. As for fatigue the inertia part is important and this one is nearly unchanged due to the appurtenances, the attachment of secondary steel is neglected for the fatigue analysis. However, even if the loading would have been slightly increased, Figure 6.9 shows that around the pile there is still some buffer in fatigue utilisation to attach these structures.

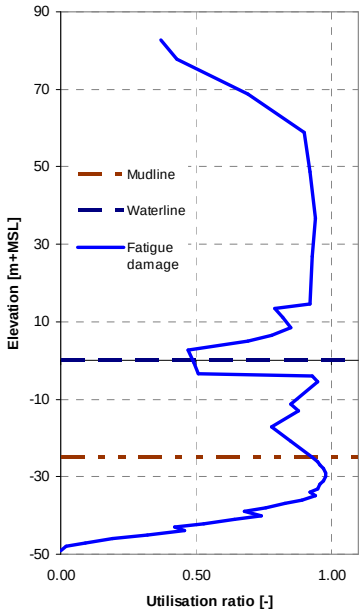


Figure 6.9: Fatigue results for final design

### 6.4.4 Final design results

The natural frequency for the reference structure is evaluated assuming FLS conditions: water level at MSL and half the corrosion expected over the lifetime. No seabed level variations or varying soil conditions were taken into account. The first bending mode in the fore-aft direction is

at 0.277 Hz and the corresponding mode in the side-to-side direction is at 0.279 Hz. The second bending modes are at 1.290 and 1.369 Hz for the fore-aft and the side-to-side directions respectively. These frequencies are safely outside the blade passing frequency range.

The simulations for the ultimate limit states reveal that the highest utilizations are found for DLC 6.1a. The highest utilizations are due to global buckling and are located in the tower. In Figure 6.8 the maximum utilization ratio along the height of the structure is depicted for 6.1a, with 30° wind wave-misalignment and a constrained streamfunction wave occurring 100s into the simulation. The figure shows the maximum utilisation due to local buckling, global buckling and for the yield criterion. The serrated appearance is due to the fact that the wall thickness is varied is steps instead of continuously.

For determining the stability of the pile the following criteria have been set:

- The deflection of the pile at mudline is less than 0.1m
- The rotation of the pile at mudline is less than 0.5°
- The ultimate lateral bearing capacity must be guaranteed when the characteristic soil strength parameters are reduced by a material factor 1.25 [1]

For the reference design the maximum overturning moment is 306 MNm and the corresponding base shear is 10 MN. Conservatively, these have been assumed to act in the same direction. The required minimum embedded length to withstand the ultimate loads is 24 m. It should be noted that the soil profile used for this reference design results in a stiff foundation. In practice, in most cases the foundation will be softer and pile lengths are usually longer.

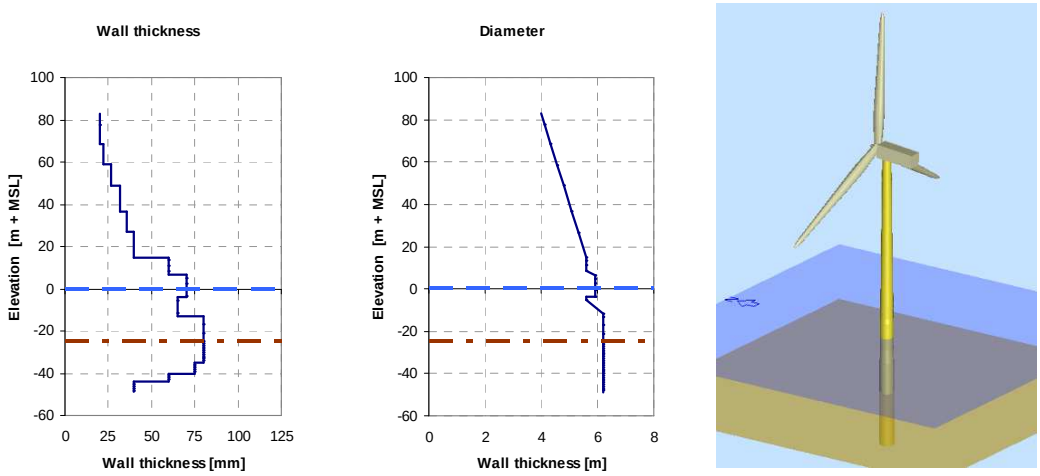


Figure 6.10: Final dimensions for the monopile reference design

## 6.5 Sensitivity analysis of structural parameters

In this section the sensitivity of monopile support structures to structural and environmental parameters in terms of natural frequencies, ultimate loads and fatigue loads is investigated. The following aspects are included in this study:

- Influence of pile dimensions on natural frequencies
- Influence of water depth on required dimensions
- Influence of pile diameter on fatigue loads

*Influence of pile dimensions on natural frequency*

For the reference monopile design presented in this chapter a parameter study has been done by varying foundation pile dimensions to show the influence of the pile penetration depth and of the pile diameter on the structure natural frequencies. The mass of the structure is also presented. The results are depicted in Figure 6.11.

The first and second natural frequencies show a quadratic relation with the penetration depth. This effect is stronger for smaller diameter pile, which behave in amore flexible manner than larger diameter piles. The first natural frequency also varies quadratically with the pile outer diameter, but the second natural frequency as a function of the pile outer diameter shows a distinctly cubic relation. The total structural mass, including pile mass, transition piece mass and tower mass, varies linearly with both the pile penetration depth and pile outer diameter.

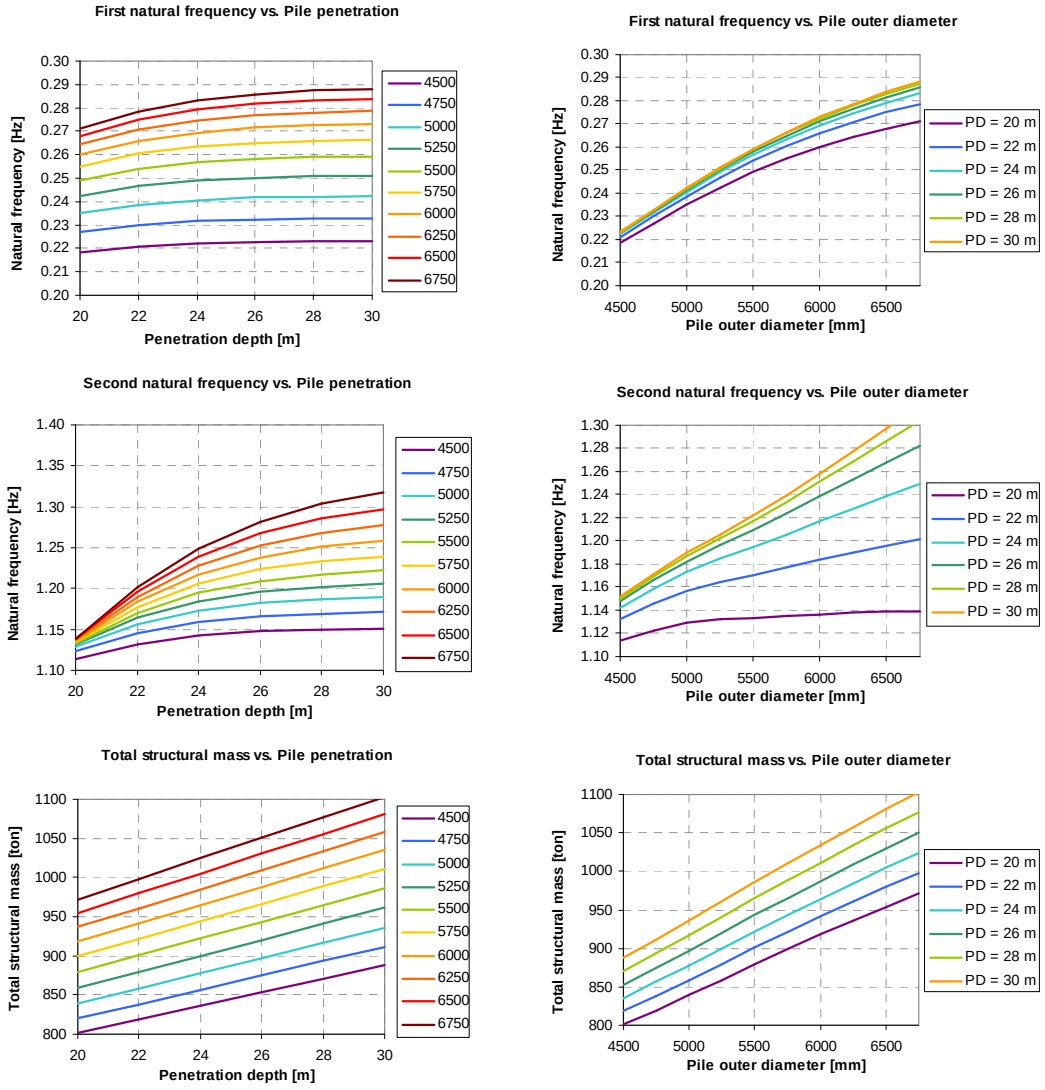


Figure 6.11: Variation of first natural frequency with penetration depth and pile outer diameter

For the same structure the maximum utilisation is checked for varying pile penetration depth. In Figure 6.12 it can clearly be seen that for sufficiently long piles the maximum utilisation in the

pile is no longer affected by the additional pile length. This is due to the fact that a longer pile behaves more flexibly and the loads are transferred to soil in the upper part of its length.

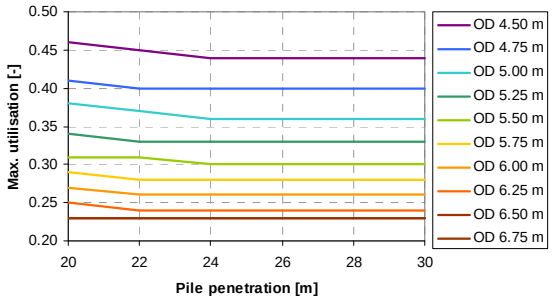


Figure 6.12: Maximum utilisation as function of penetration depth for various outer diameters

*Influence of water depth on structure mass*

In a separate study the influence of water depth on the required support structure dimensions has been investigated [19]. In this study a 3.0 MW class wind turbine was modelled on a monopile support structure for a site in the Dutch sector of the North Sea in approximately 40 m water depth. For a range of water depths from 20 to 50 m, a monopile structure has been designed to match a target first natural frequency of 0.32 Hz. The wall thickness is optimised for buckling. The variation of the foundation pile outer diameter and the wall thickness is shown in Figure 6.13.

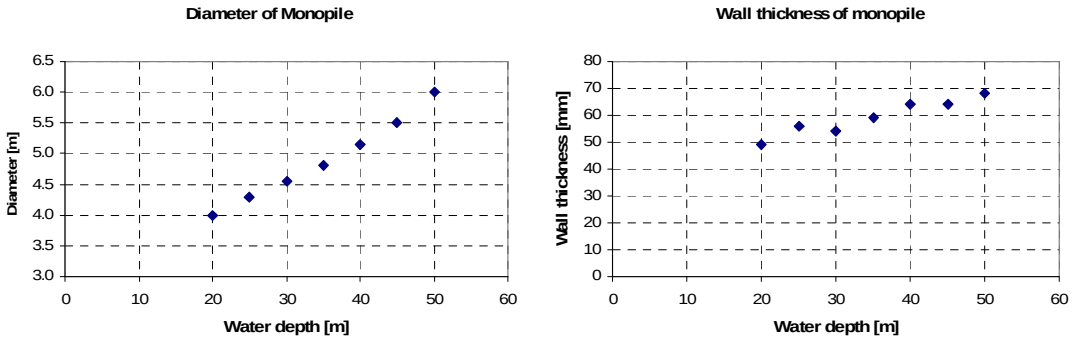


Figure 6.13: Variation of required diameter and wall thickness as function of water depth

Figure 6.14 shows the total overturning moment at the mudline as a function of the water depth and the contributions to the overturning moment of the wind loads and wave loads. The overturning moment due to wind loads, represented by the blue squares, show only a small increase with increasing water depth, whereas the overturning moment due to wave load, indicated by the green triangles, increases severely for larger water depths. This is due to the fact that with increasing water depth the length of the structure exposed to hydrodynamic loads becomes larger. Furthermore, the hydrodynamic loads are related to the diameter of the support structure, which increases rapidly for increasing depths.

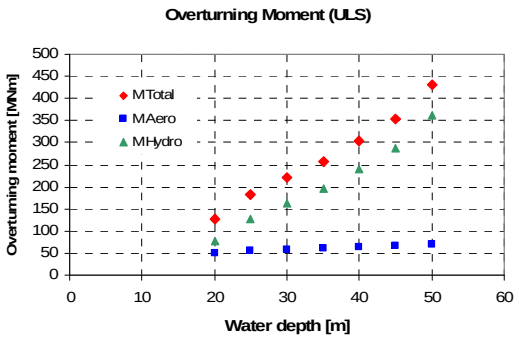


Figure 6.14: Overturning moment as function of depth

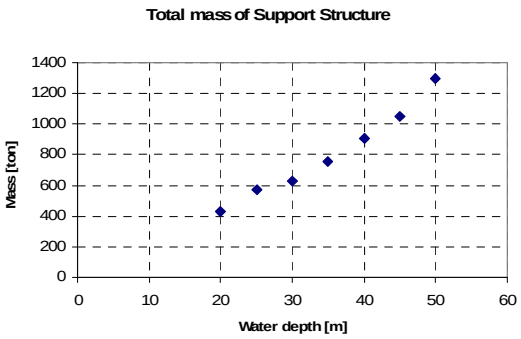


Figure 6.15: Mass of structure as function of water depth

It should be noted that fatigue has not been considered in this particular study. This implies that the wall thickness will be larger for larger water depths when the design becomes dominated by fatigue. This also reduces the likelihood of applying a monopile support structure in 50 m water depth, even for a comparatively small turbine. However it can be concluded that the support structure mass trend shows a quadratic relation with the water depth.

*Influence of diameter on fatigue damage*

In the preliminary design phase a fatigue analysis has been performed for four monopile designs with outer diameters in the range of 6.00 m to 6.75 m. Due to the varying diameter, hydrodynamic loads increase. At the same time the natural frequency increases making resonance due to waves with high energy content less likely. Furthermore the section modulus is increased, reducing the stresses in the pile. It should be noted that the diameter is increased only for the pile elements from P015P downward. The high fatigue utilisation for elements P015P and P010P is due to the relatively high stress concentration factor near the pile cone.

Figure 6.16 shows that for all elements the fatigue damage decreases as the pile diameter increases. As the cross section properties are not changed for the upper elements, the reduction in fatigue can only be related to the increase in the natural frequency and hence reduced dynamic amplification from wave loading. In this (particular) case increasing the pile outer diameter reduces fatigue damage. This may not hold true for structures with larger diameters near the water line.

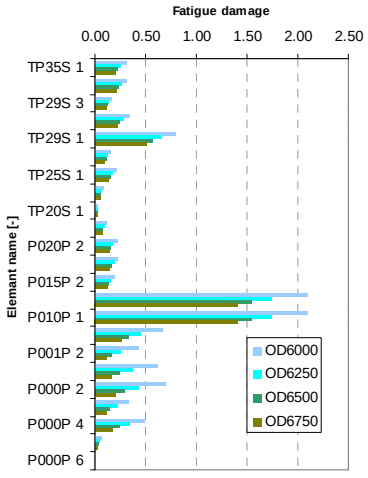


Figure 6.16: Influence of foundation pile diameter on fatigue

## 6.6 Cost modelling of monopile structures

### 6.6.1 Introduction

This section describes a cost model for offshore support structures. This cost model has been set up with three main objectives:

- To quickly assess the impact of changing turbine parameters on the support structure costs.
- To increase understanding of the importance of different parameters on the total mass of the support structure by performing rapid parameter studies for several variables for a large range of values.
- To give a rough estimate of the costs for fabrication of a monopile to allow comparison of costs with other structure types.

A further requirement is that the cost model should remain simple in its operation. Other parties should be able to use it without extensive knowledge of support structure design. Therefore the number of input variable is kept to a minimum. Only the turbine parameters that most strongly influence the design have been introduced as input variables. The environment is also expressed in a number of input variables. The output is given in a single value for the cost, based on the total mass of the support structure. Figure 6.17 shows the input/output screen for the monopile cost model. This chapter describes the cost model and how it can be used.

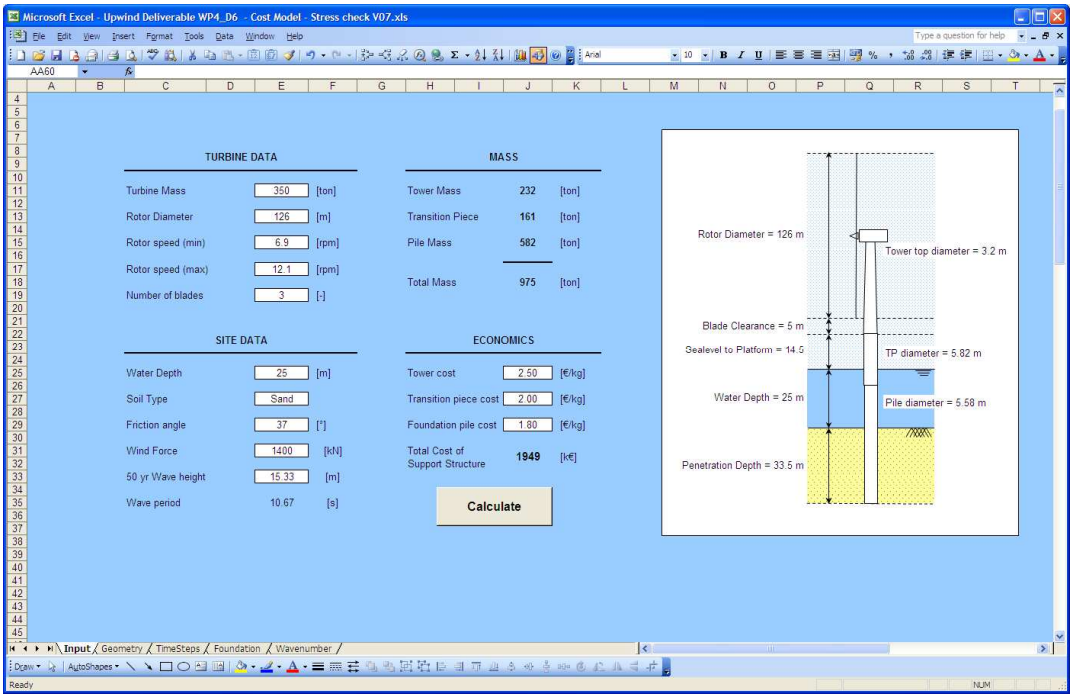


Figure 6.17: Input/Output screen for monopile cost model

### 6.6.2 Input parameters

The required input data falls within three categories: turbine parameters, site data and economics data.

**Turbine parameters**

The turbine parameters required are the turbine mass, the rotor diameter, the rotor operational speed range and the number of blades.

**Site data**

For the site data the following parameters are required: water depth, soil type, soil strength parameter, maximum thrust force on rotor and maximum wave height with 50 year return period. For the soil type sand or clay can be selected. If sand is selected, the soil strength parameter is the angle of internal friction and a value in the range of 32° to 42° can be chosen. If clay is selected the soil strength parameter is the undrained shear strength which has a value in the range of 50 to 500 kPa.

**Economics**

For the economic data the price per kg of primary steel for each component can be input. The overall value can be in the order of 2.00 €/kg including material costs, costs for blasting and coating and for fabrication and mounting of secondary items. A distinction can also be made between the various components. Due to the fact that tower sections are generally conical, they are more expensive to manufacture, which can be reflected by selecting a value of 2.50 - 3.00 €/kg for this component.

### 6.6.3 Approach

The support structure of a wind turbine is designed such that its natural frequencies do not coincide with excitation frequencies with high energy. Particularly the rotational frequency range and the blade passing frequency range are to be avoided. In addition to these ranges, it is also important to stay clear of the wave frequencies with high energy. Therefore a threshold value of 0.2 Hz is adopted. Based on these boundary conditions an allowable range for the first natural frequency is set.

The support structure is parameterised in the Excel file. First the interface elevation and hub height are determined based on the input parameters for turbine and environment. With these elevations set, all dimensions of the monopile support structure are determined as a function of the foundation pile diameter. The stiffness of the foundation at the seabed is dependent on the selected soil type and soil strength parameter and can be expressed in a single factor. Using Rayleigh's method, the first natural frequency of the support structure can be calculated.

Subsequently a stress check is performed. The loads are calculated based on the wave height and aerodynamic load parameters as entered in the input sheet. Based on the outcome of the stress check the D/t ratios for tower, transition piece and foundation pile are adjusted. The following steps are carried out:

1. Calculate initial dimensions
2. Perform natural frequency analysis
3. Adjust pile diameter
4. Calculate wave loads
5. Perform stress check
6. Adjust D/t ratios
7. Calculate structure mass

By employing a solver which repeats steps 2 to 7 the diameter of the pile and the *D/t* ratios for the tower, transition piece and the foundation pile can be adjusted until the configuration is found that has the minimum mass, satisfies the stress check and has a first natural frequency inside the allowable frequency range.

### 6.6.4 Assumptions

In order to set up the natural frequency calculation and the stress check a number of assumptions have been made. These can be grouped under the following categories:

- Frequencies
- Parameters
- Key levels
- Diameters
- D/t ratios
- Foundation
- Wave load calculation
- Stress check
- Pile diameter iteration

Frequencies The rotational speed range is expressed in Hz. The design frequency is determined as 1P max + 10%. This means that the first natural frequency is above the 1P region with a margin of 10%. It is also checked whether the first natural frequency is still lower than *n*P min -10% (where *n* represents the number of blades, which can be either 2 or 3, depending on the choice made in the input sheet). If this is not the case a warning is displayed in the input sheet. The threshold for the wave frequencies is set at 0.2 Hz.

Parameters The values for the blade clearance and the platform level currently cannot be given by the user. The blade clearance is currently defined as the distance between the platform level and a blade tip at its lowest point. This value is chosen as 5 m. The distance sea level to platform is determined based on the sum of the highest tide level (HAT) + storm surge + crest elevation associated with the 50 yr wave height. The highest tide level is assumed to be 2 m +MSL, the storm surge is assumed to be 2 m and the crest elevation is $0.68*H_{max;50}$, according to [9].

Key elevations The key levels indicate where each element starts and where it ends. From top to bottom, the tower starts at the hub height which is defined as Blade Clearance + Interface elevation + ½ Rotor Diameter. The tower ends at the interface with the transition piece. The transition piece in turn starts at the interface with the tower and ends at a level defined by $Z_{ref}$ - $L_{Overlap}$. The foundation pile starts at $Z_{ref}$ and ends at $Z_{ref}$ - water depth - penetration depth.

Diameters The diameters of the different parts of the support structure are all functions of the Foundation pile diameter. The transition piece diameter $D_{TP} = D_{MP} + 2*wt_{TP} + 2*t_{grout}$. The grout thickness $t_{grout}$ is assumed to be 0.05m. The diameter at the tower bottom is equal to the diameter of the transition piece whereas the diameter at the tower top is equal to $0.55*D_{TP}$.

D/t ratios The D/t ratios are not assumed constant over the entire height for the purpose of mass calculations. Three sections are defined: the tower, the transition piece and foundation pile, and the part of the foundation pile where the largest bending moments are to be expected in the region from 3D above the seabed to 2D below the seabed.

Foundation There are two contributions of the foundation on the support structure: the contribution of the mass to the overall structure mass and the contribution of the stiffness of the foundation to the overall stiffness of the structure. The stiffness of the foundation has a strong influence on the natural frequency. The penetration depth is estimated from an *L/D* ratio, as a function of the soil type

and strength. In the *L/D* ratio *L* represents the embedded length of the pile and *D* the diameter of the foundation pile.
The stiffness of the foundation is determined based on a look-up table in which the results of a parameter study are recorded. The look up table contains the lateral spring stiffness $K_{lat}$ and the rotational stiffness $K_{rot}$ at pile head for varying pile length, diameter and soil conditions for both sand and clay. With these values the foundation stiffness coefficient $C_{found}$ can be determined following:

$$C_{found} = \frac{3EI_{eq}}{K_{eq}L}, \qquad \text{where } K_{eq} = \frac{K_{rot}K_{lat}L^2}{K_{rot} + K_{lat}L^2}$$

Apart from the assumptions relating to the final design, the following steps in the optimisation can be identified:

Wave load calculation The wave load calculation in this model is based on linear Airy wave theory. The wave height used is the reduced wave height $H_{red;50}$ which is 1.1* $H_{s50}$, where $H_{s50}$ is determined as $H_{max;50}$/1.86. The associate wave period is taken as 11.1*$\sqrt{H_{red;50}}$. The wave load is calculated for each submerged element in the structure for 8 time steps in half a wave period.

Stress check Using the calculated wave loads and the maximum thrust force on the rotor, the stress in the structure can be determined for each elevation. A global buckling check according to GL [9] is included. The result is expressed as a utilisation ratio for the tower, the transition piece and the foundation pile.

Pile diameter iteration The pile diameter iteration is based on Rayleigh's method for a stepped monotower as described in.[20]. The foundation pile diameter is varied until the calculated natural frequency matches the target natural frequency. By varying the foundation pile diameter other dimensions of the support structure also change. The calculated natural frequency takes these changes into account.

Wall thickness adjustment:
The wall thicknesses are adjusted by changing the *D/t* ratios for the tower, the transition piece and the foundation near the mudline, such that the maximum utilisation is 1.0.

### 6.6.5 Verification

Before the cost model may be applied to estimate the costs of a monopile support structure it should be verified. To this end two options are available

- As the natural frequency calculation is the basis compare natural frequency calculation with results from FEM analyses for range of input values
- Compare Cost Model results with existing designs

**Natural frequency verification**

As the natural frequency calculation is at the heart of determining the dimensions of the support structure it is important that the estimation of the natural frequency using Rayleigh's method is within a certain margin of error. A margin of 10% can be considered acceptable. The natural frequency of the support structure was determined for several cases. Case 3 is the base case; its parameters are taken from the 5.0 MW reference turbine. These cases with the corresponding data are listed in Table 6.5:

Table 6.5: Natural frequency test cases

| Material Parameters | unit | Case 1 | Case 2 | Case 3 | Case 4 |
|---|---|---|---|---|---|
| Turbine mass | [ton] | 100 | 200 | 350 | 400 |
| Rotor diameter | [m] | 80 | 100 | 126 | 140 |
| Rotor speed range | [rpm] | 4.6-12.1 | 4.6-12.1 | 4.6-12.1 | 4.6-12.1 |
| Water depth | [m] | 20 | 30 | 40 | 50 |

The results are compared to the results obtained with a finite element program using the exact same geometry as in the cost model and with the foundation fixed at the seabed in both models. The results of this comparison can be viewed in Table 6.6.

Table 6.6: Natural frequency comparison with FEM analysis

| Material Parameters | unit | Case 1 | Case 2 | Case 3 | Case 4 |
|---|---|---|---|---|---|
| Fnat Cost Model | [Hz] | 0.2219 | 0.2215 | 0.2218 | 0.2216 |
| Fnat FEM analysis | [Hz] | 0.207 | 0.208 | 0.209 | 0.208 |
| Error | [%] | 6.74 | 6.11 | 5.78 | 6.13 |

Table 6.6 also shows the error between the natural frequencies determined using the cost model and the FEM results. The error is less than 10% for all investigated cases. This leads to the conclusion that the natural frequency is calculated correctly for a monopile support structure with the foundation fixed at the seabed and turbine and environmental data within the range spanned by the four cases.

The second step in the validation process entails the comparison of the mass of actual designs to the results from the cost model. For this step sufficiently detailed information about the input parameters should be available for actual design to allow a detailed comparison between the cost model and the actual designs. For the Arklow wind farm and for Offshore Wind Farm Egmond aan Zee these data were available to the Work Package. Furthermore, the reference design presented in this chapter allows for comparison as all details of the design are available.

**Reference monopile design**

In Table 6.7 the results for a verification of the cost model is shown by comparing the mass data from the monopile reference design with the cost model mass results.

Table 6.7: Verification of cost model for first natural frequency of 0.269 Hz as compared to reference design results

| | unit | Cost model | Reference design |
|---|---|---|---|
| Natural frequency | [Hz] | 0.269 | 0.279 |
| Pile diameter | [m] | 5.32 | 6.0 |
| Penetration depth | [m] | 29 | 24 |
| Tower mass | [tons] | 211 | 240 |
| Transition piece mass | [tons] | 143 | 148 |
| Pile mass | [tons] | 499 | 544 |
| Total mass | [tons] | 853 | 932 |

The natural frequency is slightly lower for the cost model although the difference is minor. A larger discrepancy can be found for the pile diameter. However, it should be noted that the reference design has a pile cone, reducing the diameter of the transition piece. No such feature is included in the cost model, so the pile diameter must be lower to compensate. The tower mass seems to be underestimated in comparison to the reference design, and the pile mass is overestimated. However, the differences are within 10% and the error in total mass is approximately 8 %. When the natural frequency is artificially increased to 0.279 Hz in the cost model, the overall mass increases to 889 tons. In this case the error is reduced to 4.6%.

**Egmond aan Zee**

In Table 6.8 the results for the verification for the Egmond aan Zee wind farm are shown. Although the overall mass compares well with an error of 5.2%, the natural frequency and the pile penetration are overestimated, while the pile diameter is underestimated. The latter is no surprise as the Egmond aan Zee employs an internal transition piece, which requires a larger pile diameter than when using an external transition piece.

Table 6.8: Verification of cost model as compared to Egmond aan Zee design results

| | unit | Cost model | OWEZ design |
|---|---|---|---|
| Natural frequency | [Hz] | 0.35 | 0.31 |
| Pile diameter | [m] | 4.2 | 4.60 |
| Penetration depth | [m] | 29 | 22 |
| Tower mass | [tons] | 110 | 80 |
| Transition piece mass | [tons] | 125 | 132 |
| Pile mass | [tons] | 230 | 230 |
| Total mass | [tons] | 465 | 442 |

**Arklow**

For the Arklow wind farm the results of the verification are shown in Table 6.9. In this case the error between the cost model and the project data is larger at approximately 14%. This is mainly due to the fact that at the Arklow site the water is relatively shallow, but the tidal range is quite large. However, as the main goal of this cost model is to show the trends in mass of monopile support structures with a minimum of input parameters, this is not further taken into account. The error is still within the limit considered acceptable of 20%.

Table 6.9: Verification of cost model as compared to Arklow design results

| | unit | Cost model | Arklow design |
|---|---|---|---|
| Natural frequency | [Hz] | 0.31 | 0.31 |
| Pile diameter | [m] | 4.35 | 5.1 |
| Penetration depth | [m] | 26 | 32 |
| Tower mass | [tons] | 132 | 156 |
| Transition piece mass | [tons] | 83 | 88 |
| Pile mass | [tons] | 220 | 280 |
| Total mass | [tons] | 435 | 506 |

The verification of the cost model by comparison with the reference design show that the results are within the 20% error margin. The agreement of the overall mass is good, but the dimensions may differ, depending on the circumstances in the field. Some situations, regarding extreme tide differences and alternative geometric configurations are not embedded within the assumptions in the cost model. However, for the purpose of the cost model, to indicate the mass trends for varying site and turbine parameters, the results are satisfactory.

**Comparison with several wind farms**

A comparison of the overall mass data with publicly available mass data for several existing projects has also been made. The results are listed in Table 6.10 and are displayed graphically in Figure 6.18. The data represents the total support structure mass, including the tower mass. In most cases the results obtained with the cost model match the mass data of the reference projects well. However, for the Princess Amalia, Robin Rigg and North Hoyle wind farms the error exceeds 20%. Although the error is more than the acceptable limit of 20% mentioned previously, it should be noted that not all required input data could be found in sufficiently reliable detail for all wind farms. In some cases this may have led to assumptions that underestimate the overall mass. Furthermore, it should be noted that in some cases the data on the hub height and interface level differed significantly from the assumptions in the cost model. In those cases the

cost model hub height and interface elevation entries have been adjusted to match the data from the reference projects.

Table 6.10: Cost model results compared with reference project results

| Project | Water depth | Total mass [ton] | | | |
|---|---|---|---|---|---|
| | | Reference projects | Cost Model | Error [ton] | Error [%] |
| Lynn | 11 | 570 | 564 | -6 | -1.1 |
| Inner Dowsing | 6 | 530 | 500 | -30 | -5.7 |
| Prinses Amalia | 25 | 534 | 403 | -131 | -24.5 |
| Horns Rev | 14 | 390 | 340 | -50 | -12.8 |
| Robin Rigg | 12 | 560 | 431 | -129 | -23.0 |
| Kentish Flats | 5 | 369 | 314 | -55 | -14.9 |
| Burbo Bank | 8 | 580 | 526 | -54 | -9.3 |
| Rhyl Flats | 12.5 | 630 | 632 | 2 | 0.3 |
| North Hoyle | 12 | 480 | 342 | -138 | -28.8 |
| Gunfleet Sands | 10 | 480 | 534 | 54 | 11.3 |

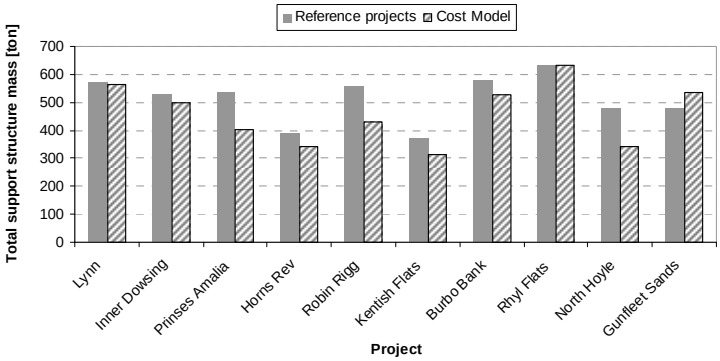


Figure 6.18: Comparison of cost model mass results with several existing projects

## 6.7 Conclusion

In this chapter a reference design for a monopile structure has been made for the UpWind reference turbine in 25 m water depth. The resulting design comprises a foundation pile with a bottom diameter of 6 m and a conical section tapering to a top diameter of 5.5 m. The embedded length is 24m and the total length is 54 m. The transition piece has an outer diameter of 5.8 m and a total length of 18.7 m. A tower of 68 m length is used, leading to a hub height of 85.2 m. The overall mass of the primary steel for the foundation pile is 542 tonnes and 147 tonnes for the transition piece. The required wall thickness for the monopile and transition piece is driven by fatigue, whereas the penetration depth is driven by ultimate loads and natural frequency requirements.

In general the first natural frequency is strongly influenced by the structure length and to a lesser degree by the turbine mass. When these values are fixed, which is the case when the turbine type and site conditions are known the natural frequency can be influenced by changing pile diameter and penetration depth.

For shallow waters fatigue is predominantly governed by aerodynamic loading, but for deeper waters the increase in diameter causes an increase in the hydrodynamically driven fatigue. However, this is very much dependent on the wave conditions on site and on the turbine size. The structure wall thickness is mostly governed by fatigue.

The structure mass increases following a square relation with the water depth and as this is mainly due to the increase in the length of the structure, this also holds true for increasing hub height. The overall costs for a monopile structure are mainly driven by the material costs, due to the sheer amount of steel required.
A cost model has been set up that calculates the structure mass based on a limited number of input parameters for the turbine and for the site conditions. A comparison with the monopile reference design and two actual projects shows that the error in overall structure mass is less than 10% in two cases and less than 15% in the remaining case, within the limits considered acceptable. A comparison with publicly available data shows good agreement for most cases, though in some cases the error is between 20 - 30%.

# 7. Jacket reference design

## 7.1 Introduction

In the previous chapter it was shown that the mass of monopile support structures increases by the square of the water depth. The increase is partly due to the larger diameter required to maintain a sufficiently high natural frequency and partly to the fact that the larger diameter attracts larger wave loads and hence requires larger wall thickness to withstand the stresses.
For large water depth this inevitably becomes prohibitive. Other support structure solutions are therefore required that are stiffer for the same amount of material used.

This chapter presents a support structure design that can be considered a reference for deep water locations. To this end a suitable structure concept is selected first, after which a detailed design can be created.

Of the support structures concepts described in Chapter 2 the jacket and the tripod structures are the most mature. This chapter describes the support structure selection, in which the jacket structure is found to be the most suitable for the turbine and site conditions considered. Subsequently the design of the jacket structure is described, followed by a sensitivity analysis and the definition of a simple cost model for jacket structures, describing the variation of mass and costs of a jacket structure for varying environmental conditions and turbine parameters.

## 7.2 Concept selection for reference design

### 7.2.1 Approach

The first step for this comparison study is to select a deep water location for which both extreme and long term environmental data is available. All required data will be compiled in a design basis. This document will subsequently provide input for setting up load cases and performing the turbine load calculations. The turbine load calculations are performed in the wind turbine simulation program GH Bladed. The resulting loads are recorded in a load document.
In the subsequent step the tripod and jacket configurations are selected and the structures are modelled in the offshore structural analysis package ROSAP.
Both models are tuned such that the natural frequency falls within the allowed frequency range for the selected turbine. When the natural frequency requirements are satisfied the extreme load analysis is performed. The turbine loads from the load document are combined with the wave loads to calculate the response of the support structures. Both models are checked for foundation stability and pile strength, strength and stability of members and strength of the joints against punching shear. When any of these checks is not satisfied, the structure dimensions must be adjusted to reduce the stress at the appropriate locations in the structure.
When the appropriate dimensions of the structures have been established a first order optimization is performed by reducing the wall thickness of members with low utilization ratios in order to reduce excess material use. Whenever the dimensions are adjusted the natural frequency must be reassessed to verify that it still falls within the allowed range.

### 7.2.2 Design Basis

For the comparison of the tripod and jacket support structures a representative deep water site was needed. A site in 50 m water depth on the border of the Dutch and British sectors was selected. The approximate location is indicated in Figure 7.1. Environmental data was taken from the K13 platform, located at a distance of 70 km from the selected site. This data is publicly available from the Dutch National Institute for Coastal and Marine Management [42]. The data includes 3-hourly wind, wave and water level measurements that have been collected over a 22 year period. Current data was taken from another nearby location. The data is processed in order to be included in the design basis. Key data will be presented briefly.


Figure 7.1: Selected deep water location (*map source: google*)

The water depth at the site is 50 m with respect to mean sea level (MSL). The tidal range is 2.22 m and the 50yr storm surge is 2.13 m (positive) and 1.31 m (negative).
The wind speed was translated to a hub height of 82 m to obtain the extreme and converted into 10 minute mean values and is presented in Table 7.1. The extreme wave heights are listed in Table 7.2, together with the design wave period.

Table 7.1: Extreme wind speeds as a function of return period

| $T_{return}$ [yr] | $V_w$ (10min) [m/s] |
|---|---|
| 5 | 41.29 |
| 50 | 48.62 |

Table 7.2: Extreme wave heights as a function of return period

| $T_{return}$ [yr] | $H_s$ [m] | $T_D$ [s] | $H_{max}$ [m] |
|---|---|---|---|
| 5 | 6.95 | 10.54 | 12.93 |
| 50 | 8.24 | 10.97 | 15.33 |

Two soil profiles have been assumed, intended to lead to a lower limit for the foundation stiffness and the other to give the upper boundary.
The turbine used in this research is the UpWind 5.0 MW reference turbine [5]. The nacelle weighs 240 tons, while the rotor assembly weighs 110 tons. The rotor diameter is 126m. A tower model suitable for offshore application was assumed. The key parameters are listed in Table 7.3.

Table 7.3: Key dimensions of tower

| | Diameter [mm] | Wall thickness [mm] |
|---|---|---|
| Top | 4000 | 20 |
| Bottom | 5500 | 34 |

### 7.2.3 Model

Parameterised models were set up for both the jacket and the tripod support structure in ROSAP. The configurations are shown in Figure 7.2.

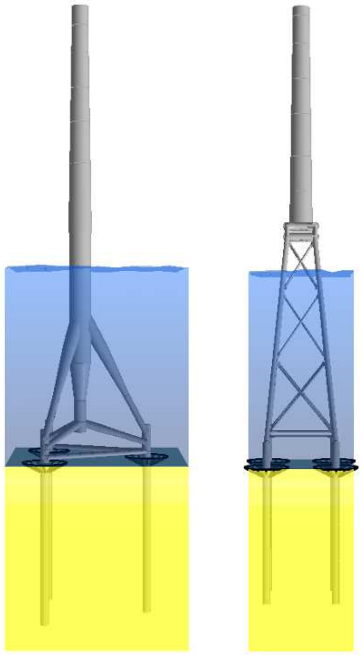

Figure 7.2: Jacket and tripod configurations

The interface level between support structure and tower is set at 14.75 above MSL. The hub height is at 82.75 m above MSL.
Key parameters in the tripod model are the interface level, the diameter of the main column, the depth below the sea surface of the main joint, the height above the seabed of the lower central joint and the radius of the tripod base as well as the pile penetration depth and the pile diameter.
For the jacket model, the key parameters are the interface level, the top width, the base width, the level of the lower horizontal brace above the seabed, the pile penetration depth and the pile diameter.
For the tripod the piles are modelled within a pile sleeve, while for the jacket the legs are inserted into the piles.

### 7.2.4 Load document

A load document is set up on the basis of simulations in the turbine simulation program Bladed. Load cases were set up on the basis of the IEC-61400-3 [8]. Only load cases that are considered design driving were assessed. These load cases are mainly cases where high thrust from the turbine can be expected. To this end an equivalent support structure was included in the turbine model with a natural frequency of 0.29 Hz. The simulations only include aerodynamic loads; the hydrodynamics are included later in the structural analysis. The following load cases are included in the load document.

- Power production with extreme turbulence model (ETM)
- Power production with extreme coherent gust with change of direction (ECD)
- Idling with loss of electrical network with extreme wind model (EWM)

### 7.2.5 Natural frequency analysis

For the natural frequency analysis the target natural frequency is determined on the basis of the turbine rotational speed as shown in Figure 7.3. A safety margin of 10% is adopted on the rotor speed range of 6.9 rpm to 12.1 rpm, giving an allowable natural frequency range between 0.22

Hz – 0.31 Hz. The target natural frequency is taken at the high end of the natural frequency range, at 0.29 Hz.

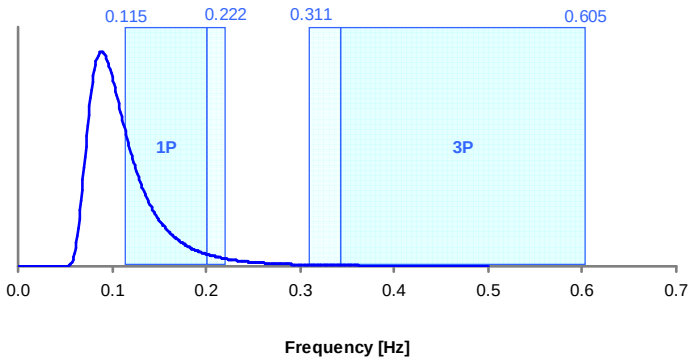


Figure 7.3: Allowable frequency range for UpWind reference turbine

The bottom radius and pile penetration depth are varied to find an envelope of combinations of parameters that fit the allowable natural frequency range. An upper limit for the stiffness is found by assuming the minimum water level, no marine growth and no corrosion, denoted 'stiff' in Figure 7.4 while a lower limit is found by using the maximum water level, full marine growth profile and full corrosion allowance denoted 'soft' in Figure 7.4. To evaluate the conditions corresponding to normal operational conditions, consistent with fatigue load cases, the water level at Mean Sea Level is considered together with half the corrosion allowance and full marine growth. This is denoted as 'fatigue' in Figure 7.4.

The results for the natural frequency as a function of the bottom radius for the tripod for a penetration depth of 30 m are shown in Figure 7.4 (a), while Figure 7.4 (b) shows the results for the jacket.. It can be seen that the mass increases approximately linearly with increasing base width, but the increase of the natural frequency becomes less with increasing base width. This effect is stronger for the tripod than for the jacket. However, at the target natural frequency the mass and natural frequency curves are almost parallel, indicating that the cost of increasing the natural frequency by increasing the base width is constant around the target natural frequency.

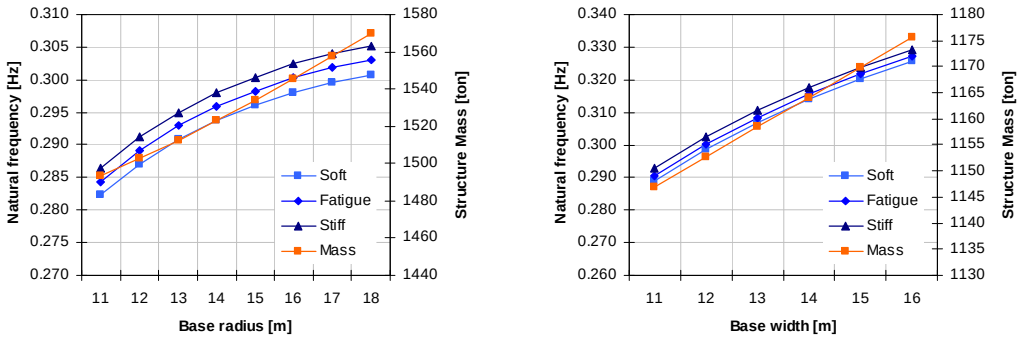


(a) (b)

Figure 7.4: Natural frequency for tripod (a) and jacket (b) as function of bottom radius/width

Figure 7.5 (a) shows the results as a function of the penetration depth for a bottom radius of 13 m. The results are also shown for the jacket in Figure 7.4 (b). It can be seen that the first natural frequency can be influenced by changing the pile length, but only to a certain depth. For the

tripod the effect of increasing the pile length becomes marginal at approximately 38 m penetration depth. For the jacket this occurs at a slightly lower penetration depth.

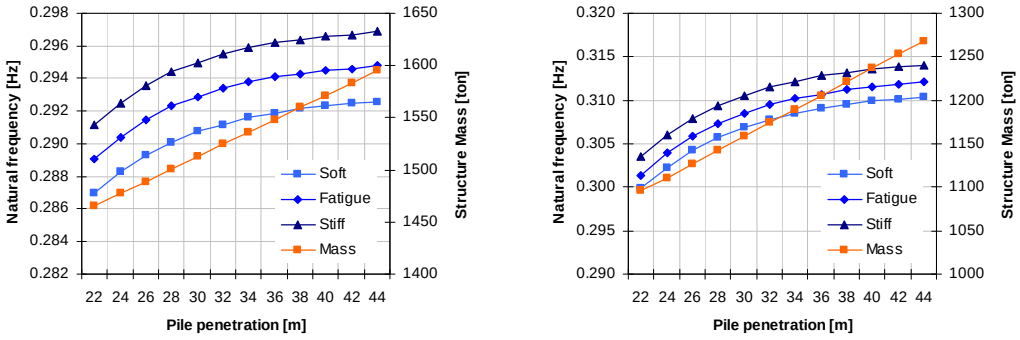


Figure 7.5: Natural frequency for tripod (a) and jacket (b) as function of penetration depth

### 7.2.6 Ultimate limit state analysis

For the ultimate limit state analysis both models are subjected to the same set of load combinations. For each load case from the load document for which the maximum aerodynamic loads are found the aerodynamic loads are combined with the corresponding values for the hydrodynamic loads. The structures are checked for strength and stability of members, punching shear at the joints and pile capacity in tension and compression.
First the most suitable basic dimensions are investigated by varying the pile penetration depth and the base width or in the case of the tripod, the base radius.

For the tripod the base radius is varied from 11 m to 15 m and the pile penetration from 26 m to 36 m. With these values, the pile utilisation of the pile in compression remains below 1 for all cases and only for a pile penetration of 26 m the punching shear criterion is not satisfied. This can be attributed to the fact that the loads are redistributed due to the softer foundation, thereby increasing the stress on the joints. Figure 7.6 shows the maximum Von Mises utilisation of the piles, while Figure 7.7 gives the maximum utilisation of the piles in tension for the tripod.

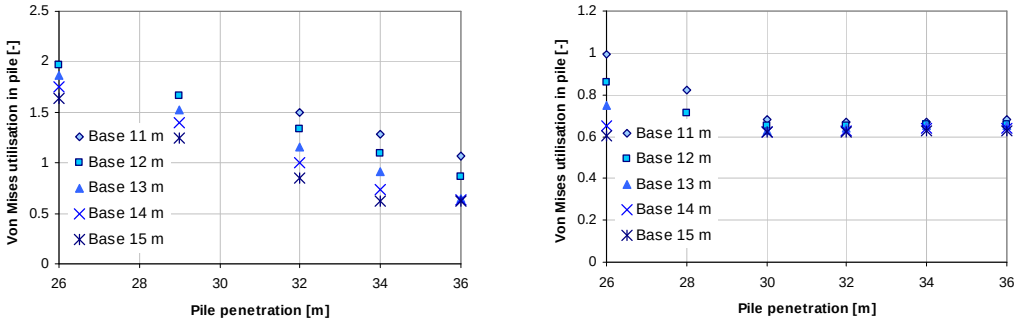


Figure 7.6: Maximum Von Mises utilisation for tripod piles (a) and jacket piles (b) as function of pile penetration

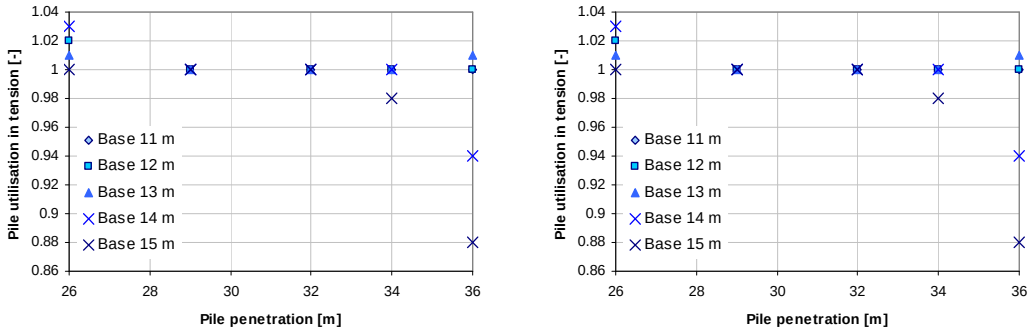


Figure 7.7: Maximum pile utilisation in tension for tripod (a) and jacket (b) as function of pile penetration

For the jacket the base width is varied from 11 m to 15 m and the pile penetration from 26 m to 36 m. The pile utilisation in tension is critical for penetration depths below 30 m as can be seen in Figure 7.6. The Von Mises utilisation is again given in Figure 7.7.

For the tripod the basic dimensions are selected as follows:

- Base radius: 13 m
- Pile penetration: 34 m

For the jacket these dimensions are:

- Base width: 12 m
- Pile penetration: 30 m

With the main dimensions now determined a further optimization on wall thickness of the members of the jacket and tripod structures can be performed. Through this optimization the mass of both structures is reduced further.

### 7.2.7 Fatigue limit state

In the final step of the concept analysis a simplified fatigue check has been performed. In this analysis the same environmental conditions have been used for both structures models.
Wind and wave loads are applied in two separate analyses and combined as explained in Section 6.3.4. A reduced number of sea states, taken from [13] and shown in Table 7.4 have been applied in a single direction corresponding with the prevailing wave direction.
For the assessment of the wind induced fatigue, the loads are based on damage equivalent loads. These loads have been determined in a separate integrated time domain analysis in GH Bladed. In this simulation only aerodynamic loads are taken into account. The damage equivalent loads are applied at $1.83 \cdot 10^6$ cycles, equivalent to the design life in seconds divided by the structure's first natural period.
Stress concentration factors have been calculated according to Efthymiou [21] and to determine the fatigue damage the GL-100 S-N [9] curve is applied. A safety factor of 1.25 is applied for all elements and joints of the substructure as no periodic inspection or maintenance is deemed possible.

Table 7.4: Reduced set of sea states used for fatigue analysis

| $V_w$ [m/s] | $H_s$ [m] | $T_p$ [s] | Probability [%] | Occurrences/year |
|---|---|---|---|---|
| 2 | 1.07 | 6.03 | 0.06071 | 531.8 |
| 4 | 1.1 | 5.88 | 0.08911 | 780.6 |
| 6 | 1.18 | 5.76 | 0.14048 | 1230.6 |
| 8 | 1.31 | 5.67 | 0.13923 | 1219.7 |
| 10 | 1.48 | 5.74 | 0.1444 | 1264.9 |
| 12 | 1.7 | 5.88 | 0.12806 | 1121.8 |
| 14 | 1.91 | 6.07 | 0.10061 | 881.3 |
| 16 | 2.19 | 6.37 | 0.07554 | 661.7 |
| 18 | 2.47 | 6.71 | 0.04878 | 427.3 |
| 20 | 2.76 | 6.99 | 0.03151 | 276.1 |
| 22 | 3.09 | 7.4 | 0.01924 | 168.6 |
| 24 | 3.42 | 7.8 | 0.00977 | 85.6 |
| 26 | 3.76 | 8.14 | 0.00474 | 41.6 |
| 28 | 4.17 | 8.49 | 0.00243 | 21.3 |
| 30 | 4.46 | 8.86 | 0.00093 | 8.2 |
| 32 | 4.79 | 9.12 | 0.00053 | 4.6 |
| 34-42 | 4.9 | 9.43 | 0.00019 | 1.6 |

In the first analysis both structures displayed fatigue lives less than 20 years for certain joints. For the jacket structure these were concentrated at the joints at the top of the bottom panel, as well as in the lower x-brace joints. Also considerable damage is found at the bottom of the legs below the mudbrace across the diagonal of the jacket. This corresponds to the direction of the fatigue loading. Relatively low damage is incurred at the middle and upper braces as these are located well above and below the splash zone.
For the tripod the highest damage is found at the central joint. Also the bottom joint experiences high fatigue damage as well as the connections of the mudbraces to the pile sleeves.
In a second iteration wall thicknesses at critical joints have been increased. For the jacket the fatigue damage is reduced to below 1.0 for all elements and joints apart from the jacket legs below the mudbrace.

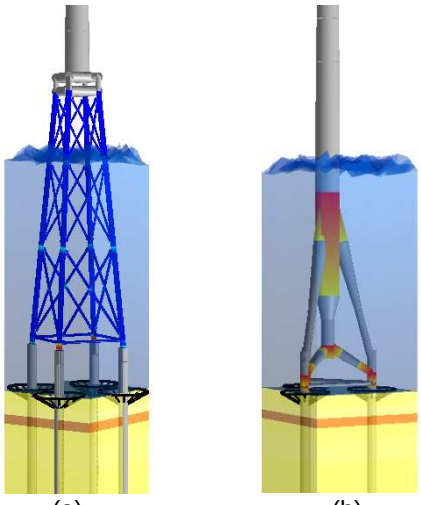

(a) (b)

Figure 7.8: Fatigue damage for jacket (a) and tripod (b) for first fatigue assessment

The tripod still has low fatigue life at the central joint, the bottom joint and the joints connecting the mudbraces to the pile sleeves. This is mainly due to high stress concentration factors at these locations.

### 7.2.8 Final results

The final mass of both structures can be viewed in Figure 2.13. It can be seen that the jacket is significantly lighter than the tripod. The pile masses of both structures are almost equal. However, it should be kept in mind that the tripod requires only three piles whereas the jacket is fitted with four piles.

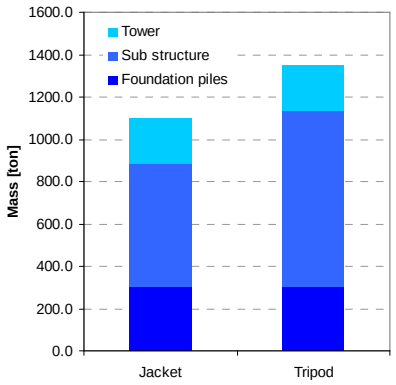


| | Mass [ton] | |
|---|---|---|
| | Jacket | Tripod |
| Tower | 216 | 216 |
| Substructure | 579 | 831 |
| Piles | 305 | 304 |
| Total | 1100 | 1351 |

Figure 7.9: Overall structure mass comparison between jacket and tripod

### 7.2.9 Conclusions

The general conclusion drawn from this study is that the jacket is significantly lighter than the tripod structure. It should be noted that for a real structure it is not simply the mass that governs the choice, but rather the cost. In general larger and heavier structures are more costly to install, while structures with many joints are labour intensive and therefore expensive to fabricate. However, large thick walled complex joints are also expensive. It is not straightforward to assess the costs other than the material costs for the jacket and tripod structures without a detailed assessment. However, based on a simplified cost analysis the jacket in this concept selection is shown to be cheaper. The following costs per unit mass of steel in the structure are used. The tower and piles are relatively simple structures and the cost of material and fabrication is estimated at 2 Euro/kg. The fabrication of substructures for both jackets and tripods is estimated at 4 Euro/kg.

Tower : 2.00 Euro/kg
Substructure : 4.00 Euro/kg
Piles : 2.00 Euro/kg

Figure 7.10: Costs for material and fabrication for jacket and tripod

| | Cost [kEuro] | |
|---|---|---|
| | Jacket | Tripod |
| Tower | 432 | 432 |
| Substructure | 2317 | 2493 |
| Piles | 610 | 607 |
| Total | 3359 | 3533 |

The costs for secondary steel items such as boatlandings, platforms and J-tubes are not included in Figure 7.10. Also not incorporated is the cost of installation. It is clear that the jacket is the cheaper structure type for the considered circumstances. Even if the cost of fabrication for the tripod is lowered to 3 Euro/kg the jacket is still the cheaper solution. On these considerations the jacket is selected as the reference structure.

Apart from this conclusion the following observations are done:

- The lower 3P boundary may be critical for the natural frequency of multi-member structures in combination with a stiff tower, in particular for the jacket. The tripod is more flexible than the jacket due to the lower location of its transition joint.
- Relatively deep foundation piles are required due to limited bottom width as a result of natural frequency constraints.
- Wave loads for the tripod are significantly higher due to large diameter members near the sea surface where the hydrodynamic loads are largest.

In the following sections the jacket structure is further evaluated. The load combinations are addressed in greater detail.

## 7.3 Design approach for reference structure

### 7.3.1 Design Requirements

As described in section 7.2.5 the first natural frequency of the entire structure must be located in the range of 0.22 Hz-0.310 Hz according to the design basis [13]. The penetration of the jacket pile into the soil is determined under consideration of the plastic soil capacity while the design of the pile steel is carried out under consideration of characteristic soil conditions. The design requirement for the jacket members and joints is that the maximum steel utilization ratio is below 1. The minimum fatigue life for all jacket members and joints has to be above 20 years. Soft soil conditions stated in [13] have been used for the design.

The design is carried out for a water depth of 50.0 m w.r.t. MSL. The interface level and hub height are set at 20.15 m and 90.55 m w.r.t. MSL [13].

### 7.3.2 Jacket Concept

For the present design a four legged jacket is applied with four levels of –braces, a horizontal brace and main piles. The legs are located inside the pile top and fixed by means of a grouted connection. The mud brace is placed close to the mud line to minimize the moments building up in the piles.

The X-bracings are designed in such a way that the angle between the brace and leg exceeds 30 degrees in accordance to the NORSOK recommendations [22]. Requirements from NORSOK regarding the minimum gap between braces at tubular joints (50 mm) and minimum distance between the brace-chord weld and the end of the can (the maximum of one fourth of the chord diameter or 300 mm) are fulfilled. Due to the large water depth (50 m) at this site, four levels of X-braces are implemented in order to comply with the requirement of the minimum angle between chord and brace.

The Timoshenko beam model is applied ROSA [15]. Moreover, a simple local joint flexibility (LJF) model is included; i.e all braces are calculated as simple T and Y joints, where the flexibility for each brace is calculated as if no other braces were present at the joint. Note that braces are automatically cut off at the brace centreline intersection with the chord wall, leading to a decrease in the stiffness of the joint itself. However, the shortening of the braces means that the braces themselves will become stiffer.

A concrete block transition piece is applied as a connection between the tower and the jacket structure. The material for the transition piece has been chosen as reinforced concrete rather than steel, which is based on a cost benefit evaluation. The concrete transition piece has the weight as a disadvantage. However, it is neither as susceptible to fatigue damage nor as labour intensive compared to a steel transition piece.
The width of 8.0 m at the jacket top/interface has been chosen in accordance to the required tower bottom diameter (5600 mm). The concrete transition piece dimensions estimated and used in this study are 9.6*9.6*4. Information regarding turbine parameters and tower geometry is provided in the design basis. The pile and jacket steel utilizations are also checked with the hard soil profile provided in design basis in order to confirm whether steel utilization ratio is below 1.

Furthermore, a detailed finite element analysis is necessary in order to verify that the grouted connection between the jacket and the piles is designed sufficiently for the transfer of axial loads and bending moments.

In general, jacket steel is more expensive than the pile steel (due to high yield strength of the steel). Hence, it is recommended to minimize the jacket steel mass by transferring mass into the pile so the total foundation cost will be reduced.

### 7.3.3 Structural Jacket Model

This section describes the overall jacket concept applied at 50 m water depth. Figure 7.11 shows a 3D-model of the jacket foundation and the superstructure, i.e. tower and rotor-nacelle-assembly (RNA). Secondary steel such as two boat landing bumpers, anodes and J-tubes are also shown in below figure. The background for the jacket design is presented in the following sections.

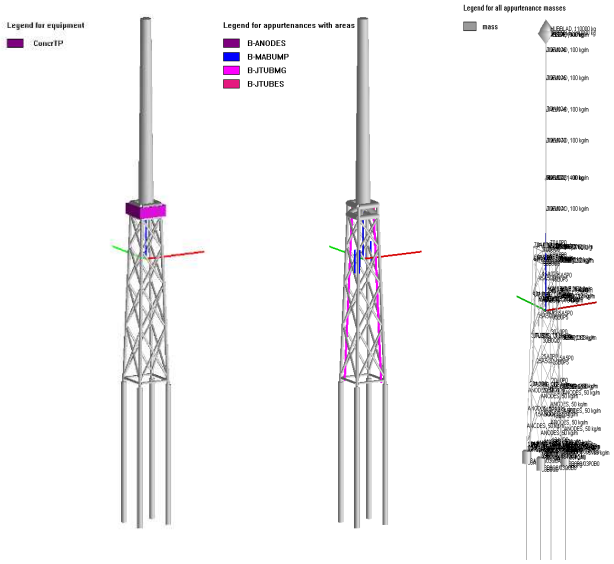


Figure 7.11: Jacket foundation model

The structure is modelled in the finite element program ROSA, the structural analysis program within ROSAP. The jacket FE-model consists of general non-linear beam and pile elements, and the load transfer from the concrete TP to the jacket legs is modelled by a stiff frame of fictitious elements resembling the stiffness of the reinforced concrete.

The jacket leg is located inside the pile while the mud braces are located at a certain elevation above the mud line. The distance between the mud brace and mudline for this design is 6.0 m

and the distance between the bottom of the grouted connection and the mud line is 0.5 m. In the model the connection between pile and leg is made with non-structural link elements at the top and bottom of the grouted connection.

Figure 7.12 shows the thicknesses, diameter over thickness (*D/t*)-ratios, material names and applied corrosion allowance for extreme event analysis in the splash zone. Note that the thicknesses and *D/t*-ratios have been adjusted for corrosion, whereas the steel amounts presented in chapter 5 corresponds to the uncorroded structure. It can be seen that the wall thicknesses in the vicinity of the tubular joints are locally increased by can sections in order to increase fatigue life and punching shear capacities. The *D/t* ratio is a key parameter for local buckling in the jacket structure. It is should be noted that the bottom part of the jacket legs are designed with high wall thicknesses and lower *D/t*-ratios in order to secure steel utilization ratios below 1.0. The fictitious material 'NOW' has no weight which is used for the fictive beam framework elements resembling the stiffness of the reinforced concrete TP. 'NOW' elements are therefore not checked with respect to the stresses.

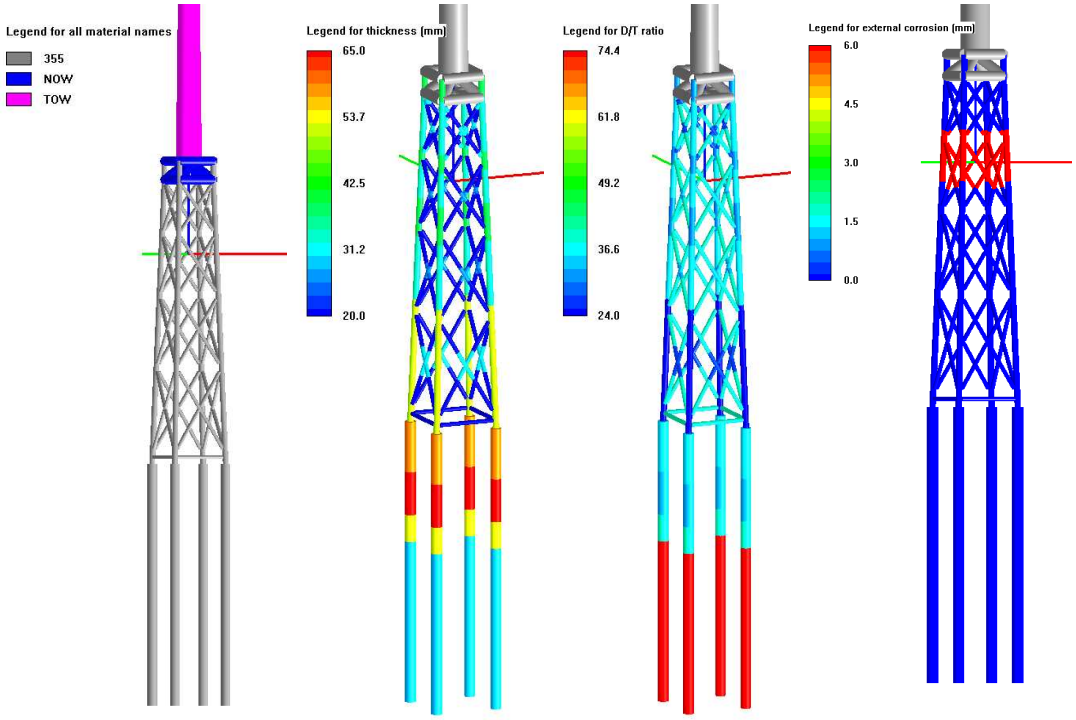


Figure 7.12: Material names, thicknesses, D/t-ratios and corrosion allowance for extreme event analysis in splash zone

### 7.3.4 Design Load Cases

In the different phases of the support structure design process, different approaches are followed with respect to the load analysis. As a first step, a preliminary design of the jacket is done in order to identify a first set of structural dimensions. In a second step, the structure will be analysed in more detail. For both cases the implemented design load cases are different. In the following the implemented load cases according to current standards are described and results for the turbine loads are shown. In all cases the used turbine is the Upwind reference turbine [5]. In the following a brief description of the load cases and method for generating the wind loads for the preliminary and final design phases is given. A full description can be found in [23].

**Wind load conditions for preliminary design phase**

In the preliminary design phase of the jacket design, damage equivalent loads are applied to the structural design tool as described in 7.3.5.
The generation of these preliminary turbine loads are done with the aid of an equivalent turbine model in the design water depths of 50 m. For the load calculations, a stiff monopile will be used, which has the target natural frequency of 0.29 Hz. This approach is valid here, as no hydrodynamic loading will be present (calm sea). By using a standard tubular steel tower of 68 m and a vertical offset in the nacelle of 2.4 m on top of the transitions piece with a elevation of 14.8 m above sea level, the support structure design results in a hub height of 85 m.

Based on the IEC-61400-3 standard [8], different load cases are simulated. As the generated loads shall deal as an input for the turbine loads only, no hydrodynamic effects are included (calm sea). Furthermore only a reduced number of design-driving load cases is simulated. The simulated load cases are

- dlc1.2 Power production + normal turbulence (Fatigue)
- dlc6.4 Idling + normal turbulence (Fatigue)

- dlc1.3 Power production + extreme turbulence (Extreme)
- dlc1.4 Power production + extreme coherent gust with change of direction (Extreme)
- dlc6.2 Idling with loss of electrical network, incl. dlc6.1 for wind direction=0° (Extreme)

The aero-elastic simulations are performed by the GH Bladed code [16]. All load simulations include:

- tower shadow
- 2 side-to-side and 2 fore-aft tower modes and 6 out of plane and 5 in plane blade modes
- three dimensional Kaimal turbulent wind field
- idling with pitch angle of 90°

The loads are given at the top of the transition piece, where the tower is mounted to the sub-structure.

**Wind load conditions for final design phase**

In the following the load case assumptions for the final design phase are discussed. The focus is on reducing the full set of required load cases according to standards to a range of cases, which will dominate the design for such a deep-water jacket design. Due to the non-rotational symmetry of the space frame jacket structure, wind and wave orientation influence the overall design. For fatigue design two methodologies may be applied:

1. Simplified method considering reduced directionality, but two support structure orientations

   The two support structure orientations (0° and 45°) are defined with regard to the rotor axis, while the rotor axis is assumed collinear with the wind direction. For conservative simplicity it is assumed that the rotor axis points north. The support is oriented accordingly to N (0°) or NE (45°).

2. Consideration of site environmental conditions for directional wind and wave distribution and directional load analysis

In order to reduce the sets of load cases, the for the extreme load calculation the first approach will be followed by using a reduced set of wind-wave-misalignments but by taking two different support structure orientations into account. For the fatigue load analyses, the more detailed second approach is done, where site-specific directionalities are taken into account.

### 7.3.5 Design process for Preliminary design phase

In this phase, a preliminary assessment of the jacket design has been carried out for the loads determined with loads in section 4.1 for the UpWind reference turbine.

A parameter study has been performed in order to determine a feasible configuration for the jacket dimensions, pile penetration and diameter. The intention of designing an optimal jacket structure is achieved by varying the base width at top and bottom of the jacket. The minimum pile diameter is chosen from the various jacket configurations. The well known behaviour of four legged structures has led to the selection of this base concept.

The following parameters have been considered.

- Two soil profiles (soft soil and hard soil, used for steel checks only).
- Six different jacket bottom base widths are chosen for the analysis.
- Three different pile diameter variations are chosen. The final pile diameter (1829 mm) has been chosen as an optimal pile diameter.
- Pile penetration variation from 40.0 m to 48.0 m. The optimal pile penetration 48.0 m is chosen.

The purpose of the extreme event analysis is to ensure that the jacket structure is able to withstand and transfer the loads to the piles. The jacket design is dependent on the applied loads which will influence the required base width at the bottom.

By varying the base width of the jacket, it is possible to determine the optimal diameter & penetration. The optimum pile diameter & penetration is chosen with respect to allowable utilization ratios and total weight of the structure from all above combinations.

The extreme wind loads provided are applied along and across (45°) the jacket structure together with the corresponding extreme wave as explained in section 7.3.4 for the preliminary design phase.

For fatigue analysis the damage equivalent loads provided for an inverse slope of the S-N curve of m=5 and a reference number of cycles of $N_{ref} = 10^7$ are applied at the interface level together with the wave loads.

### 7.3.6 Design process for Final design phase

The design procedure for natural frequency, extreme event and fatigue analyses in the final design phase is explained in this section.

**Natural Frequency Analysis**

In the natural frequency analysis it is checked whether the natural frequencies for the integrated structure (foundation + tower + RNA) are within the allowable frequency band of 0.22 Hz – 0.31 Hz for the present design as shown in Figure 7.3.

For offshore wind turbines on jacket foundations the natural frequency design in general tends to be more efficient when performed on the basis of tower variations rather than on basis of variations in the jacket structure, since jacket type foundations are relatively stiff and have relatively low masses compared to tubular steel towers. Especially, an increased tower length e.g. by an increased hub height while keeping the interface level unchanged can efficiently be used to reduce the eigenfrequency.

The natural frequency analyses are based on characteristic soil conditions, i.e. partial safety factors for soil are set to unity. It should be noted, that the particular type of a concrete transition piece applied for this design has a significant influence on the modal properties while e.g. conical steel transition pieces are significantly softer and also less heavy.

**Extreme Event Analysis**

The following steps briefly describe the analysis procedure.

*Computer Model Geometry*

The ROSA model of the jacket structure, transition piece and tower is modelled as one 3D-structure for the soil profiles as specified in [13]. In Figure 7.13, the model of the structure is shown in ROSA.

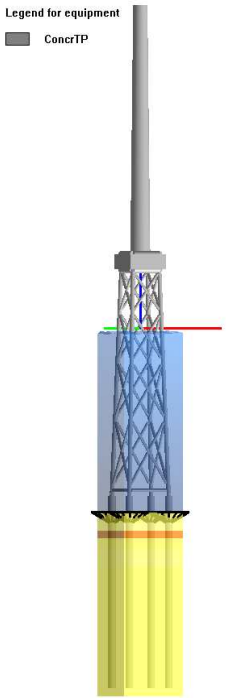


Figure 7.13: Integrated model of foundation and tower structure in ROSA

The tower structure has been modelled to obtain the correct stiffness and mass distribution for the global model, but no stress checks have been performed for the tower. Nacelle, rotor, tower accessories and secondary steel on the foundation have in general been modelled as appurtenances contributing with masses and wave load areas respectively.

*Soil-pile Interaction*

The load-carrying capacity of piles shall be based on strength and deformation properties of the pile material as well as on the ability of the soil to resist pile loads. For the requirements in extreme event analysis, the piles are designed as geotechnical elements by assuming the material safety factors as stated in Table 2 1 and the jacket elements are designed in the elastic ultimate limit state with material safety factors equal to unity. The non-linear soil-curves (p-y, t-z, q-w) are established in compliance with API [9].

Geotechnical Design

Material factors for the soil parameters are shown in Table 7.5 for the design of the pile as geotechnical element to consider for the plastic soil conditions.

Table 7.5: Material safety factors for pile as geotechnical element [5]

| Material Parameters | Material safety factor for the plastic soil conditions |
|---|---|
| Angle of internal friction $\varphi$ | 1.15 |
| Undrained shear strength $c_u$ | 1.25 |
| Axial load-carrying capacity | 1.25 |

For this analysis, equilibrium has to achieved between the load carrying capacity of the soil and the pile loads. Normally this design practice is crucial for the calculation of the necessary pile length and as well as pile diameter.

Elastic Pile Design
This analysis is based on the characteristic soil strength, i.e. soil strength parameters with material safety factors equal to unity. The purpose of this analysis is the verification of the capacity of the steel structure where the soil reaction acts as a boundary condition. Material safety factors for the steel in accordance to [5] are shown in Table 7.6. Normally this analysis is dimensioning for the wall thicknesses of the pile as required from the extreme event conditions.

Table 7.6: Partial material factors for structural steel design [5]

| | ULS |
|---|---|
| Steel strength | 1.15 |
| Modulus of elasticity | 1.00 |

*Load Generation*

Basic load cases are determined and combined in compliance with GL [9]. The permanent loading on the structure has been modelled as self generated weight for all tubular elements of the jacket, transition piece and tower structure. All other masses have been applied as appurtenances.
The wave loads on the support structure are computer generated and based on Morison's equation and appropriate wave kinematics. Aerodynamic load time series provided by GH Bladed are used for design purposes. The wave loads generated by ROSA including wave dynamics are combined with wind load time series in static analysis.
From the combined extreme loads ROSA searches for governing loads for each individual element in the structure.

*Static Analysis*

The static extreme event analysis is performed with ROSA. This analysis is non-linear due to the non-linear soil behaviour. The results of the analysis are nodal displacements as well as sectional forces and moments in the entire structure.

*Stress Check*

The steel stress check is performed in accordance with NORSOK [22] for the steel members by the use of STRECH, a ROSAP postprocessing program. The soil capacity is checked via the soil curves in accordance with the requirements in API [2].

The ROSA program generates all relevant loads except the wind loads, which are determined by Garrad Hassan using GH Bladed.
Based on the properties of the soil layers, the embedded part of the jacket pile is subdivided into a suitable number of elements. The soil-pile interface is described as a coupling between the

nodes of these elements and the surrounding soil in terms of soil curves. In each node the non-linear lateral (*p-y*) and axial skin friction (*t-z*) curves are generated based on the properties of the pile and the actual soil layer. Furthermore, the tip resistance is generated using (*q-w*) curves. ROSA finally determines the force distribution in the soil and displacements/rotations in all nodes and sectional forces/moments in all structural members.

**Fatigue Analysis**

The fatigue design approach is based on separate simulations of stochastic wind and stochastic waves under consideration of the aero-elastic interactions between both. These interactions are represented by an aerodynamic damping that influences the wave response.

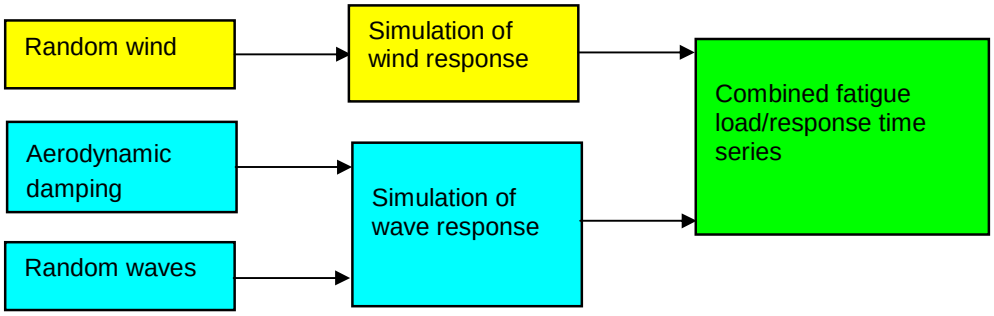


Figure 7.14: Fatigue analysis approach

*Wind Loading*

The wind loads are provided as load time series at the interface level for the given wind load combinations. The calculation approach is based on wind load time series including dynamics (inertial loads) determined by GH Bladed. The time series have been provided for different wind directions for the power production condition (DLC1.2, V=4-24 m /s) and for the idling conditions (DLC6.4, V=2; 26, 28 m/s).

*Wave Loading*

Time series for the wave loads are generated in ROSA, according to the representative wave situations. A time-series realisation of each selected scatter group sea state is performed assuming that the spectral density of the wave elevation can be described by the JONSWAP wave spectrum defined in DNV. The duration of this time series introduces an initialization time sufficiently long to allow for transient vibrations to be damped out followed by simulation time of 100 times $T_P$.

*Wind wave directional combination*

The jacket foundation structure is analysed with loading from different directional combinations of wind and waves. Table 7.7 illustrates the considered wind & wave directional combinations in the fatigue analysis, with the wind directions in the rows and the wave directions in the columns. Only 6 wave directions are considered for each of the 12 wind directions due to symmetry.

Table 7.7: Wind wave directional combination

| Wind /wave direction | N -0° | NNE -30° | ENE -60° | E -90° | ESE -120° | SSE -150° | S -180° | SSW -210° | WSW -240° | W -270° | WNW -300° | NNW -330° |
|---|---|---|---|---|---|---|---|---|---|---|---|---|
| N-0° | X | X | | | | | | | X | X | X | X |
| NNE-30° | X | X | X | | | | | | | X | X | X |
| ENE-60° | X | X | X | X | | | | | | | X | X |
| E-90° | X | X | X | X | X | | | | | | | X |
| ESE-120° | X | X | X | X | X | X | | | | | | |
| SSE-150° | | X | X | X | X | X | X | | | | | |
| S-180° | | | X | X | X | X | X | X | | | | |
| SSW-210° | | | | X | X | X | X | X | X | | | |
| WSW-240° | | | | | X | X | X | X | X | X | | |
| W-270° | | | | | | X | X | X | X | X | X | |
| WNW-300° | | | | | | | X | X | X | X | X | X |
| NNW-330° | X | | | | | | | X | X | X | X | X |

*Fatigue from combined wind and wave*

Wind and waves are combined according to the directional wind - wave combinations as described above. The wind response time series and the wave response time series, both including dynamics, are superimposed and subsequently post-processed to determine the total fatigue damage during the simulated period of time. Based on the annual and directional probabilities of occurrence, the fatigue damage from the combined wind and wave simulation is scaled to annual damages.

The fatigue damage is determined using an *S-N* curve approach combined with appropriate stress concentration factors (SCFs, e.g. for the joints) calculated according Efthymiou [21]. The cumulative damage is determined on basis of Miner's linear damage accumulation hypothesis. Eight equally spaced stress points around the circumference of the tubular section are considered. Nominal stresses due to axial forces, in-plane and out-of-plane bending moments are calculated based on Timoshenko beam theory. Variations of the nominal bending stresses along the circumference of the tubular section are considered to follow a cosine variation.

Hot spot stresses at each of the stress points are obtained by multiplying the above nominal stresses by SCFs.

**Damping**

For power production case where wind and wave are aligned (0°), the applied total damping is 4.5%, i.e. 4% of aerodynamic damping and 0.5% of structural damping. In case of 90° wind and wave misalignment, the applied total damping value is 0.5%. As an engineering approach, a cosine profile variation is reveals the aerodynamic damping values for the remaining misalignment. Applied total damping values for different wind and wave misalignment in fatigue analysis are shown in Table 7.8. For the idling case total damping value of 0.5% is applied i.e. only the structural damping value.

Table 7.8: Applied damping values for power production case

| Wind & wave misalignment | Aerodyamic damping [%] | Structural damping [%] | Total damping [%] |
|---|---|---|---|
| -30 | 3.46 | 0.5 | 3.96 |
| 0 | 4.00 | 0.5 | 4.5 |
| 30 | 3.46 | 0.5 | 3.96 |
| 60 | 2.00 | 0.5 | 2.5 |
| 90 | 0.00 | 0.5 | 0.5 |
| 120 | 2.00 | 0.5 | 2.5 |

**Hydrodynamic coefficients**

The hydrodynamic coefficients are calculated in ROSA for the individual elements dependent on the instantaneous Reynolds number (Re) and Keulegan - Carpenter number (KC). The maximum coefficients including marine growth are shown in Table 7.9 for the extreme and fatigue cases

Table 7.9: Hydrodynamic coefficients

| Fatigue | | Extreme | |
|---|---|---|---|
| $C_d$ | $C_m$ | $C_d$ | $C_m$ |
| 0.65 | 2.0 | 0.65 | 2.0 |

## 7.4 Preliminary design

In this section the results for the preliminary design phase are presented. For the preliminary design phase the dimensions following from this phase and the reasoning to come to these dimensions are discussed. The discussion of the final design phase is more extensive. The final dimensions are presented and the various steps in the design, including the natural frequency analysis, the extreme event analysis and the fatigue analysis are described.

An investigation has been carried out on support structure first natural frequency with varying jacket bottom width and remaining dimensions of the jacket foundation are kept constant.
Table 7.10 summarizes the first natural frequencies values found for different jacket bottom widths.

Table 7.10: 1st natural frequencies for different jacket bottom base widths

| Jacket bottom base width [m] | 1st Natural frequency [Hz] |
|---|---|
| 11.0 | 0.2762 |
| 12.0 | 0.2838 |
| 13.0 | 0.2903 |
| 14.0 | 0.2960 |
| 15.0 | 0.3009 |
| 16.0 | 0.3051 |

The total structural cost of the jacket foundation has been estimated for different jacket bottom base widths and remaining dimensions of the jacket foundation are kept constant. The following factors have been applied on the single component masses for the cost estimates of the individual foundations:

Jacket : 4.00 Euro/kg
Piles : 2.00 Euro/kg

Table 7.11 summarizes weight and cost distribution for different jacket bottom base widths.

Table 7.11:Total mass and cost for different jacket bottom base widths

| Jacket bottom base width [m] | | 11.0 | 12.0 | 13.0 | 14.0 | 15.0 | 16.0 |
|---|---|---|---|---|---|---|---|
| | | | | | | | |
| Piles | Mass [tons] | 380.04 | 380.04 | 380.04 | 380.04 | 380.04 | 380.04 |
| Jacket | | 569.87 | 575.42 | 581.00 | 586.63 | 592.32 | 598.07 |
| Total [piles+jacket] | | 949.91 | 959.46 | 965.04 | 970.67 | 976.36 | 982.11 |
| | | | | | | | |
| Piles | Cost estimate [k€] | 760.08 | 768.08 | 768.08 | 768.08 | 768.08 | 768.08 |
| Jacket | | 2279.48 | 2301.68 | 2324.00 | 2346.52 | 2369.28 | 2392.28 |
| Total [piles+jacket] | | 3039.56 | 3069.76 | 3092.08 | 3114.6 | 3137.36 | 3160.36 |

The 1st natural frequency and total cost variation for different jacket bottom base width is shown in Figure 7.15. From this, it can be concluded that the preliminary design jacket bottom base width of 12.0 m should be chosen in order to meet the requirements that the support structure first natural frequency should be within the range 0.22 Hz to 0.31 Hz and to obtain a total optimal cost of the structural steel.

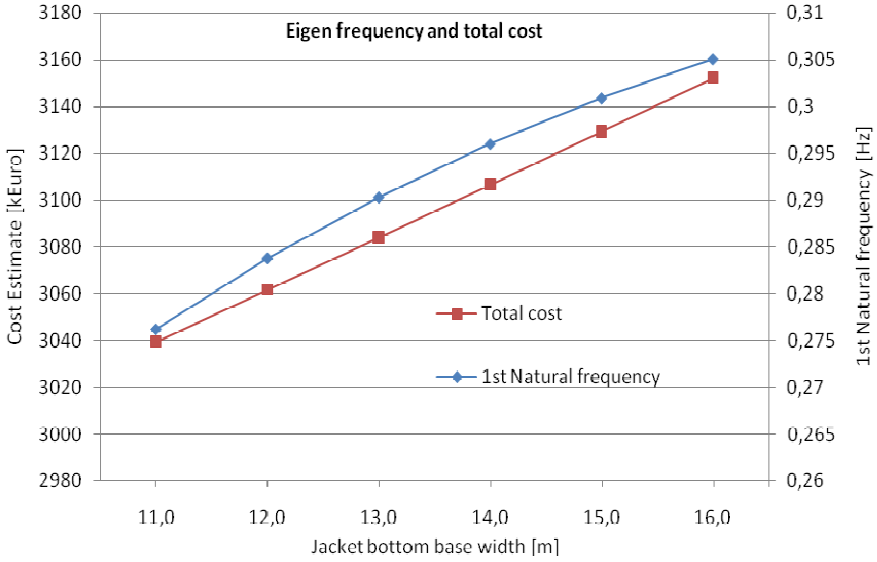


Figure 7.15: Eigen frequency and total cost for different jacket bottom base widths

The overall design summary of the preliminary design jacket foundation structure is presented in Table 7.12. The requirements of the structural steel utilization and minimum fatigue lives are at an acceptable limit for the preliminary design phase.

Table 7.12: Preliminary design jacket design summary with 50.0m water depth at soft soil conditions

| Base width | | Pile diameter | Pile penetration | Jacket only weight (excl. piles) | All 4 piles | Total jacket weight (incl. piles |
|---|---|---|---|---|---|---|
| Top | Bottom | | | | | |
| 12 m | 8 m | 1829 mm/74" | 48 m | 576 tons | 380 tons | 956 tons |

## 7.5 Reference jacket design

Based on the dimensions found in the preliminary design and described in Table 7.12 a more detailed analysis is made involving a more detailed analysis for both ultimate loads and fatigue. Also the structure is optimised to a higher degree. In the following sections the results for the analyses regarding natural frequencies, extreme events and fatigue are described.

### 7.5.1 Natural Frequency Analysis

In the natural frequency analysis a variety of conditions must be evaluated leading to different natural frequencies, depending on the stiffness and mass properties of the structure considered. These properties are not constant as over time corrosion decrease stiffness, marine growth may accumulate, thereby increasing the mass and water levels may vary leading to different values for added and entrained water mass. For the structure considered, the natural frequency is close to the 3P lower boundary. Therefore it is important to consider the stiffest possible conditions, leading to the highest natural frequency.
To this end the natural frequency analysis (NFA) has been carried out for a foundation with the jacket legs flooded and without consideration of corrosion and marine growth in order to get the upper bound natural frequencies, leading to a relatively stiff structure. This situation is referred to as “stiff foundation” in Table 7.13. The NFA has been carried out also for the "rigid foundation" (Structure clamped at the bottom) as a reference case to quantify the major influence of the superstructure on the modal properties in comparison to the “stiff” configuration.

Table 7.13 summarizes the natural frequency values for the “rigid foundation” and for the “stiff foundation”. The corresponding top view mode shapes are shown in Figure 7.16 and the side view mode shapes are shown in Appendix II. It can be seen that the modal displacements of the tower are large, while the jacket only deforms slightly for the first 2 modes.

Table 7.13: Natural frequency values for rigid and inflexible foundation

| Tower Mode | Rigid foundation [Hz] | With marine growth, LJF, added mass, flooded jacket leg members, “stiff” foundation [Hz] |
|---|---|---|
| 1st Tower Fore-Aft | 0.310 | 0.291 |
| 1st Tower Side-to-Side | 0.308 | 0.290 |
| 2nd Tower Fore-Aft | 1.104 | 0.813 |
| 2nd Tower Side-to-Side | 1.088 | 0.806 |
| 3rd Tower Fore-Aft | 2.622 | 2.001 |
| 3rd Tower Side-to-Side | 2.375 | 1.936 |
| 1st Tower Torsion | 1.291 | 1.038 |

From Table 7.13, it can be seen that the resulting natural frequencies for the “rigid foundation” are relatively close to the natural frequencies for the “stiff foundation” case for the first mode, indicating a dominating influence of the tower and rotor-nacelle-assembly properties on the modal properties. The first five mode shapes can be seen in top view in Figure 7.16. The side views of the mode shapes in Figure 7.16 are given in Appendix II.

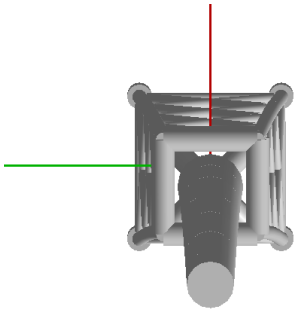

(a) 1st tower fore- aft: $f_1$ = 0.291 Hz

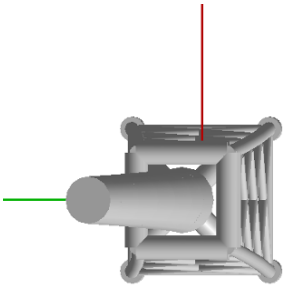

(b) 1st tower side to side: $f_2$ = 0.290 Hz

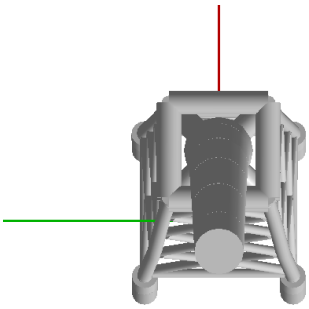

(c) 2nd tower fore aft: $f_3$ = 0.813 Hz

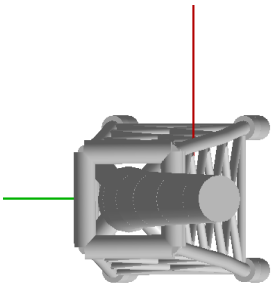

(d) 2nd tower side to side: $f_4$ = 0.806 Hz

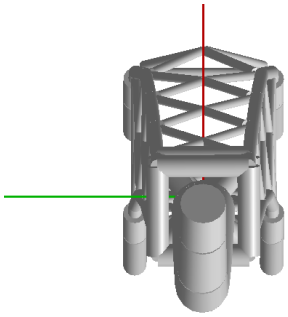

(e) 3rd tower fore-aft: $f_5$ = 2.001 Hz

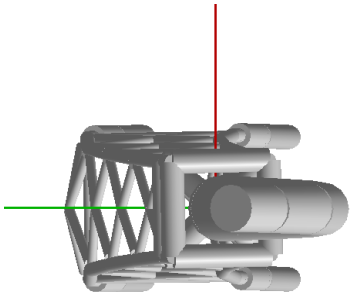

(f) 3rd tower side to side: $f_6$ = 1.936 Hz

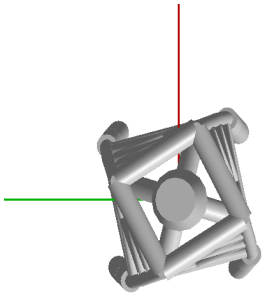

(g) 1st tower torsion: $f_7$ = 0.291 Hz

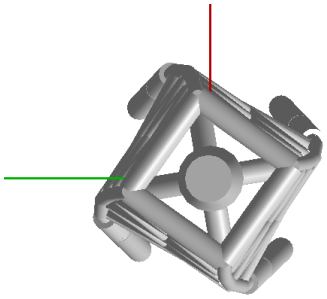

(h) 2nd tower torsion: $f_8$ = 0.291 Hz

Figure 7.16: First 5 Eigen mode shapes for 50 m of water depth

A mass comparison has been done for the inflexible foundation without local joint flexibility (LJF) and with local joint flexibility. The corresponding masses for the support structure are shown in Table 7.14 where lower weight is observed for jacket with LJF. This is due to the fact that when joint flexibilities are applied, the braces are cut off at the chord surface and the link to the chord is made with a non-structural (massless) member.

Table 7.14: Jacket structural masses

| | Without LJF [tons] | With LJF [tons] |
|---|---|---|
| Jacket | 584 | 545 |
| Pile | 438 | 438 |
| Tower | 216 | 216 |
| Transition Piece | 666 | 666 |
| Appurtenances | 346 | 346 |

### 7.5.2 Extreme Event Analysis

In the extreme event analysis the jacket structure model is subjected to various load cases. In the following the design load cases are briefly described. Subsequently the governing load cases are identified and the design results in terms of utilisation ratios are presented

#### Design load cases

The design load cases are implemented as described in section 7.3.4. The considered load cases for extreme and fatigue are shown in Table 7.15. These reduced set of extreme and fatigue load cases are expected to drive support structure loads.

Table 7.15: Design load cases used for extreme and fatigue analysis (ULS/FLS)

| | Description | Type |
|---|---|---|
| DLC1.6 | Power production in 50 year sea state | ULS |
| DLC2.2 | Safety system fault | ULS |
| DLC2.3 | Generator cut-out | ULS |
| DLC6.1 | Idling in storm | ULS |
| DLC6.2 | Idling in storm during grid loss | ULS |

Table 7.16 presents the design extreme load case DLC6.1 used for the combined wind and wave load calculations for final design. A full description regarding combined wind and wave load calculations for design load cases is given in [23].

Table 7.16: Combined wind and wave conditions used for extreme load DLC6.1

| | | | | | | |
|---|---|---|---|---|---|---|
| Design load case (DLC): | 6.1 | | | | | |
| Operating condition: | Idling | | | | | |
| Wind conditions: | Extreme wind model (turbulent) ($V_{hub} = V_{50}$) | | | | | |
| Sea conditions: | Extreme sea state ($H_s = H_{s50}$), extreme current model (50yr return), EWLR | | | | | |
| Type of analysis: | Ultimate | | | | | |
| Partial safety factors: | Normal | | | | | |
| Description of simulations: | | | | | | |
| | Wind conditions | | Wave conditions | | | |
| | Mean wind speed (m/s) | Longitudinal turbulence intensity (%) | Significant wave height (m) | Peak spectral period (s) | Yaw error | Wind/wave misalignment |
| 6.1a1-6 | 42.73 | 11.00 | 9.40 | 13.70 | 8 deg | 0 deg |
| 6.1b1-6 | | | | | | 30 deg |
| 6.1c1-6 | | | | | | 60 deg |
| 6.1d1-6 | | | | | | 90 deg |
| 6.1e1-6 | | | | | | 120 deg |
| 6.1f1-6 | | | | | | 150 deg |
| Comments: | Three dimensional three component Kaimal turbulent wind field (10 min sample).<br>First 20s of output discarded to allow initial transients to decay<br>Six turbulent wind seeds per wind speed bin (indexed 1-6)<br>Simulations run with support structure at 0deg and 45deg orientation from North<br>Wind gradient exponent (exponential model), α = 0.11<br>Extreme sea state with irregular waves defined using Jonswap spectrum with γ = 3.3<br>Extreme current with 50-year return period of 1.2 m/s applied<br>50-year extreme water level (HSWL) of 53.29m<br>Constrained extreme non-linear wave included in irregular wave history:<br>- Constrained wave height = H50 = 17.48m<br>- Constrained wave period = T50 = 10.87s<br>- Time of constrained wave crest: 100s<br>The characteristic loads for each load case group are calculated as the mean of the maxima from each of the six seeds. | | | | | |

From the extreme analysis it can be concluded that the load case DLC6.1 is the governing load for the jacket design.

**Combined load cases**

Extreme wind loads determined using GH Bladed are combined with corresponding sea states for each of the extreme load case (e.g. DLC 6.1, 6.2 etc.) using ROSA. The maximum absolute wind forces, moments defined at interface are added to loads from irregular waves and the combined loads have subsequently been used to search for the governing loads in all individual elements in the structure. In total, 72 different wind load combinations have been used for DLC6.1 and are given in full in [23].

**Governing load case**

The governing load combinations of DLC6.1 for most of the jacket members with respect to wind and wave directions are shown in Table 7.17. For a four legged jacket, the smallest pile capacities can typically be found in a diagonal direction, which means that the highest utilizations of the jacket legs can be found in the diagonal direction. This is why the load case DLC6.1 with wind from 45° and waves from 195° results in the most severe load. The locations of the appurtenances do also have a significant influence on the governing load direction.

For load case DLC6.2 apart from support structure orientation and wind-wave misalignment, the remaining load setup is same as DLC6.1 as described earlier. It is assumed that DLC6.1 identifies the worst support structure positions in terms of incoming waves. The support orientation shall be determined for DLC6.2 by the support orientation for DLC6.1 that resulted in maximum loads. See a full description on governing design load cases in the design basis.

The support structure orientation of 45° (wind from 45°) and wind-wave misalignment of 150° (with wind from 45° and waves from 195°) results in maximum loads for DLC6.1. The governing wind and wave load direction from DLC6.1 is used to calculate the maximum loads for DLC6.2.

Table 7.17: Governing load occurrence on jacket member for DLC6.1

| Compass Direction | | Rosa Direction | | Amount | |
|---|---|---|---|---|---|
| Wind | Wave | Wind | Wave | Combined load case no. | Occurrence on jacket member |
| 45° (NNE-ENE) | 195° (S-SSW) | 135° | 345° | 332 | 48 |
| 45° (NNE-ENE) | 165° (SSE-S) | 135° | 15° | 73 | 40 |
| 45° (NNE-ENE ) | 135° (ESE-SSE) | 135° | 45° | 66 | 35 |

The extreme event analysis showed that the governing loads for most of the jacket elements and joints result from DLC6.1. This is summarized in more detail together with individual element utilizations and their corresponding governing load cases in [23]

The maximum shear force and overturning moment at interface are shown in Table 7.18. The extreme event analysis comprises investigations on the capacities of the structure and soil to withstand extreme loads. Analyses of pile-soil interactions are performed on the basis of plastic soil conditions and analyses of the pile steel and jacket steel are performed on the basis of characteristic soil conditions. In addition, the pile steel and jacket steel utilization ratios are also checked with the hard soil profile. However, the largest steel utilizations occur for the soft soil conditions.

Table 7.18: Maximum resultant shear force and moment at interface level

| DLC6.1 | |
|---|---|
| Maximum shear force[kN] | Maximum moment [kNm] |
| 900 | 57146 |

**Analysis results**

The capacities of the piles in the soil are checked under consideration of plastic soil conditions as stated in section 7.3.1. Steel stresses in the jacket structure are checked under consideration of characteristic soil conditions. Furthermore punching shear stresses are checked for all tubular joints by using TUBJOI, a ROSAP postprocessing program.

In Figure 7.17 & Figure 7.18, lateral and axial soil capacities and reactions are shown for the worst load condition (DLC6.1, load combination 332). The size of each disk represents the reaction in the soil while the colour represents the utilisation of that particular soil layer. It can be seen that the soil just below mudline is fully utilized due to rather high deformations and low capacities of the corresponding layers.

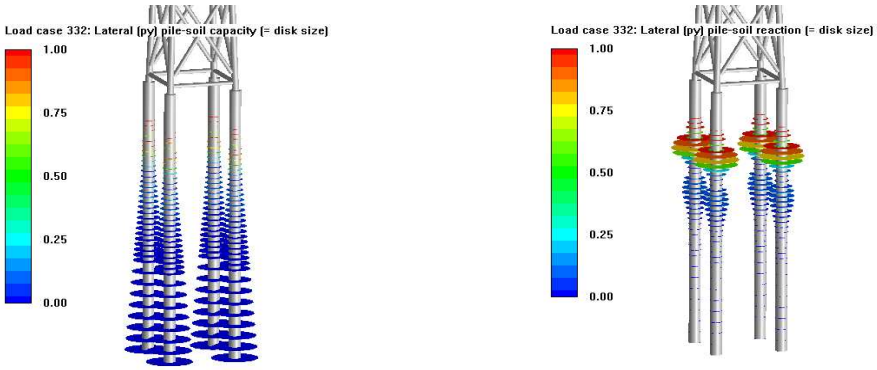


(a) (b)

Figure 7.17: Lateral soil (a) capacities and (b) reactions for worst load combination 332

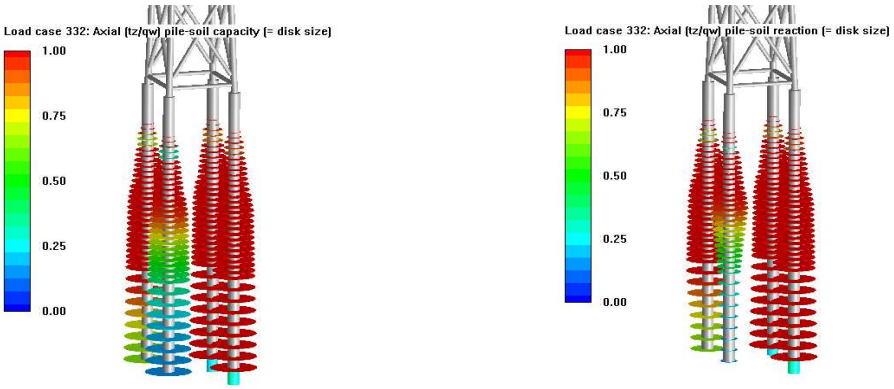


(a) (b)

Figure 7.18: Axial soil (a) reactions and (b) capacities for worst load combination 332

The steel utilization plots for members, joints and piles are shown in Figure 7.19. Individual steel member utilization ratios and tubular joint utilization ratios can be found in [23].

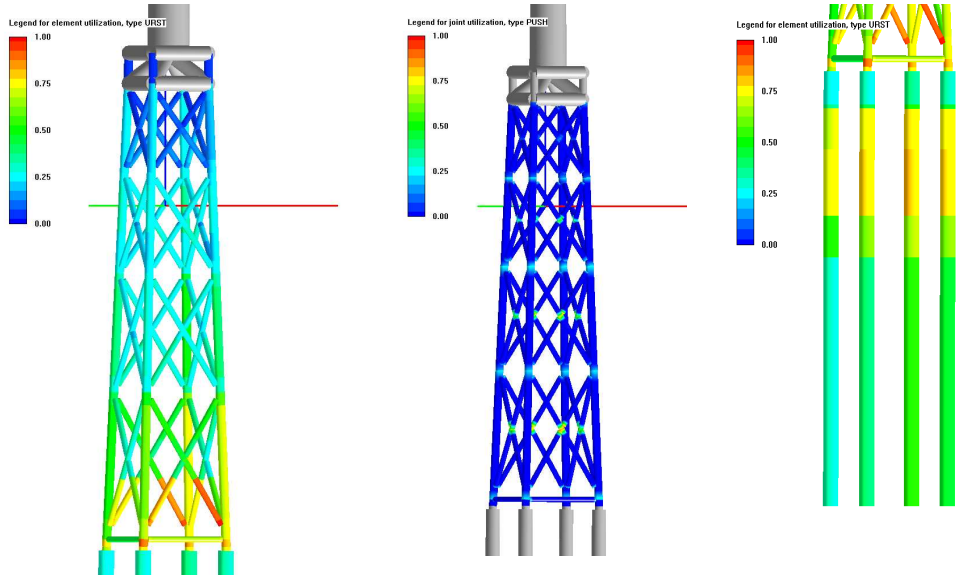


Figure 7.19: Maximum utilization ratios for elements, tubular joints and piles

### 7.5.3 Fatigue Analysis

**Analysis results**

A fatigue analysis is performed for the tubular joints, elements and attachments in the jacket structure. Fatigue lives are improved by increasing the can section thickness at middle X-braces. The tubular joints, upper parts of the jacket legs and bracings are optimized with respect to the fatigue loads. The tubular joints, elements and circumferential welds are analysed on basis of a GL-90 curve [9], i.e. without weld toe grinding. Boat landing attachment fatigue lives are analysed under consideration of a mean stress reduction factor of 0.77 on basis of GL [9] for the GL- 63 curve. The fatigue analysis shows that the fatigue lives are above the minimum fatigue life of 20 years.

It is important to check the fatigue lives for both joints as well as for members in order to extract minimum fatigue lives in entire structure. The minimum fatigue lives are observed for joints on the chord of the connection of the top X-brace with the leg. The maximum damages can be seen where wind and wave come from SSW. The maximum fatigue lives for joints are observed at bottom X-brace. The maximum and minimum fatigue lives for joints are shown in Figure 7.20 and Figure 7.21 respectively. Fatigue lives for individual members and joints can be found in [23].

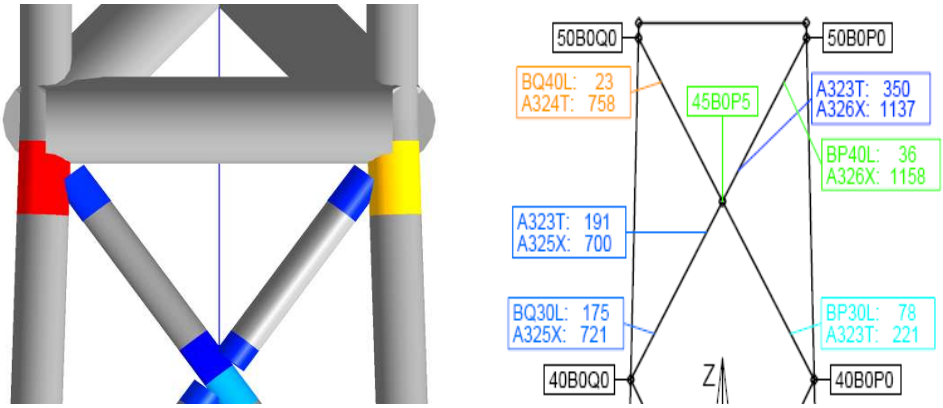


Figure 7.20: Maximum joint fatigue lives at top x-brace

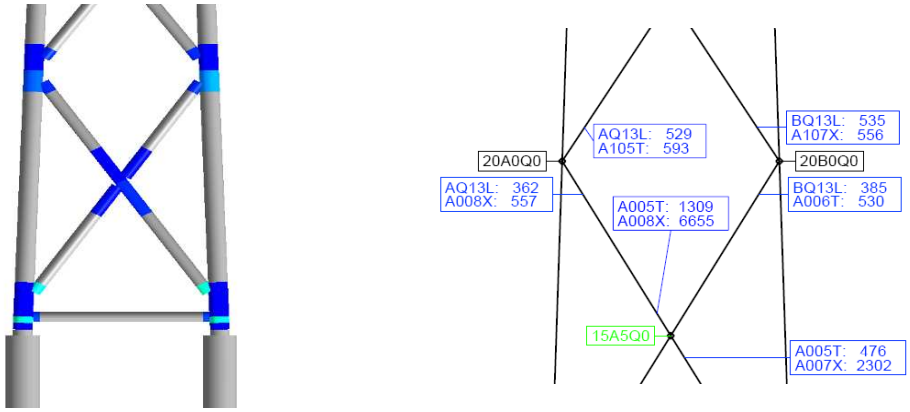


Figure 7.21: Maximum joint fatigue lives at bottom x-brace

The damage equivalent moment (DEM) provided in Table 7.19 for the preliminary design phase and from the final design phase are shown in the below table. The damage equivalent moment provided for preliminary design phase is, however, valid for a monopile structure and therefore not comparable with the damage equivalent moment for the jacket structure in the final design phase. However, the monopile DEM for wind only is very close to the jacket DEM for combined wind & waves indicating that the contribution of the wave loading to the fatigue damage is small in comparison to the contribution of the wind.

Table 7.19: Damage equivalent moments

| | Final design-jacket (combined wind & wave loads) | Preliminary design |
|---|---|---|
| Level | $M_{eq}$ [kNm], ($m$ = 5, $N_{eq}$ = $10^7$) | $M_{eq}$ [kNm], ($m$=5, $N$=$10^7$) |
| Interface | 900 | 57146 |

### 7.5.4 Final Design Structural Dimensions

The overall design summary of the jacket foundation structure for final design is presented in Table 7.20 for 50m water depth w.r.t to MSL for the soft soil conditions according to the Design Basis [13].

Table 7.20: Final design jacket design summary with 50.0m water depth at soft soil conditions

| Base width | | Pile diameter | Pile penetration | Jacket only weight (excl. piles) | All 4 piles | Total jacket weight (incl. piles |
|---|---|---|---|---|---|---|
| Top | Bottom | | | | | |
| 12 m | 8 m | 2082 mm/82'' | 48 m | 545 tons | 438 tons | 983 tons |

The wall thicknesses of the piles are 65 mm in the upper part of the piles and 28 mm at the lower part as shown in Appendix III.

According to DNV recommendations [1], it is reasonable to assume local scour depth of 1.3 times the pile diameter for sand if no detailed scour information is available. In this study a local scour of 1.3 times the pile diameter and no global scour is considered for the jacket design. The obtained first natural frequency of the entire structure is 0.291 Hz which is in the allowable range.

From previous experience with jacket design, the estimated concrete transition piece weight 666 tons is considered in this design. Table 7.21: shows the maximum utilization ratios (ULR) as well as minimum fatigue lives for members and joints. The utilization ratios are within the allowable limit for both, the soil capacity and the steel capacity. The maximum utilization ratios are found at the bottom X-braces for the members and joints, whereas the minimum fatigue lives are found at the top of the jacket joints.

Table 7.21: Maximum utilization ratios (ULR) and minimum fatigue lives for members, joints

| | Members | Joints |
|---|---|---|
| Steel Utilization ratios | 0.99 | 0.91 |
| Minimum fatigue lives | 152 | 23 |

### 7.5.5 Conclusions

In general jacket foundations are found to relatively insensitive to wave loads and introduce high stiffness and low soil dependency. Therefore such foundations are well suited to deeper water sites with soft soil condition such as the site under consideration within this report. The jacket structure is optimized with respect to the natural frequency, extreme event and fatigue conditions i.e. the natural frequency of the overall structure is within the allowed range and all member and joint utilizations as well as the fatigue lives are within the allowable limits.

Naturally, not all jacket members and joints can be designed optimally, i.e. fully utilized in terms of fatigue lives and limit states for the extreme events. This results in member diameters and thicknesses that are in some cases fully utilized and in other cases conservative.

With increased hub height the natural frequency can efficiently be reduced. The interface level and hub height are set at 20.15 m and 90.55 m w.r.t. MSL The transition piece dimensions are estimated and used in this study are 9.6*9.6*4. Due to the large water depth (50 m) at this site, four levels of X-braces are implemented in order to comply with the requirement of the minimum angle between chord and brace.
The jacket structure is modelled with simplified local joint flexibility (LJF) assumptions i.e. all braces are calculated as simple T and Y joints, where the flexibility for each brace is calculated as if no other braces were present at the joint. The braces are automatically cut-off at the brace centreline intersection with the chord wall, so the global stiffness is reduced. A mass comparison has been done for inflexible foundation without LJF and with LJF. The lower weight is observed for the jacket with the LJF assumption.

In the preliminary design phase, provided preliminary design extreme loads are applied at interface along and across the jacket foundation in order to extract the governing loads for jacket foundation design. A parameter study has been performed with variations of the jacket bottom width and remaining dimensions of the jacket foundation are kept constant. A jacket bottom base width of 12.0 m is chosen in order to meet the requirements from the support structure 1$^{st}$ natural frequency and total optimal cost of the structural steel.

It should be noted that, the type of transition piece may have an influence on the modal properties e.g. conical steel transition pieces are significantly softer, but less heavy than the concrete transition piece used in this study. The transition piece is considered a major cost item for the jacket type foundation. Moreover, installation of such heavy concrete transition piece adds additional cost to the foundation. Hence, various transition piece solutions should be discussed and tested for offshore wind turbines with jacket foundations.

It is recommended that further studies should be carried on grouted connection and total cost reduction possibilities. A detailed finite element analysis is necessary to check whether the transition piece will withstand the interface loads as well as to verify that the grouted connection between the jacket and the piles is designed sufficiently for the transfer of axial loads and bending moments.

In general, jacket steel is more expensive than the pile (due to high yield strength of the steel). Hence, it is recommended to minimize the jacket steel mass by transferring mass into the pile so the total foundation cost will be reduced.

It can be concluded that no significant dynamics introduced by the hydrodynamic excitations, illustrated by the fact that the damage equivalent moment for a monopile determined at interface for wind loading only is similar to the damage equivalent moment at interface for the jacket determined at interface for wind and wave loading combined.

It is worth mentioning that the applied wind loads at interface are without accelerations i.e. neglecting the influence of the foundation inertia loads on the total dynamic response. However, especially in case of large masses connected to the foundation, such as the transition piece in this example, the overall fatigue lives might significantly be influenced by the foundation inertia loads as explained in detail in [24].

## 7.6 Sensitivity analysis

### 7.6.1 Introduction

To make more general statements about the range of application of jacket structures a more thorough analysis of the sensitivity of the reference design described in the previous section to structural and environmental parameters is performed. Also some modelling aspects that may influence dynamics and loads on the structure are addressed. The sensitivity analysis focuses on the following issues:

- Turbine parameters
- Environmental conditions
- Structure dimensions
- Modelling of joint stiffness
- Modelling of environmental influences

**Turbine parameters**

Parameters influencing the structure are the mass of rotor and nacelle, the rotor diameter, the thrust force and other aerodynamic loads on the turbine. The change of loads can only be assessed to limited degree, as it is not straightforward to change the design of the reference

turbine for the purpose of this sensitivity study. Other effects, such as changing turbine mass and changing hub height due to change in diameter of the rotor can more easily be incorporated and will be considered in particular in the natural frequency analysis.

**Site conditions**

The number of environmental parameters associated with load calculations on offshore wind turbines is large. Not all of these parameters can be assessed separately. However, some parameters in particular affect the design of the support structure and these are included in the sensitivity analysis The soil conditions affect the foundation of the jacket, both in terms of dynamic behaviour and required penetration depth to withstand extreme loads. The water depth affects the structure in many ways; especially in terms of larger hydrodynamic loading and dynamic behaviour. This also holds for the water level, but to a lesser extent, as the geometry does not change when the water level rises or falls.

**Structural dimensions**

This category of parameters includes all changes to the dimensions of the substructure and foundation that affect the dynamic behaviour, the loading, in particular from hydrodynamic loads and the stresses of joints and elements. Parameters that will be considered are the pile diameter, penetration depth, diameters and wall thicknesses of legs and braces and overall dimensions, governed by the bottom and top width of the jacket structure.

**Modelling of environmental influences**

The environment can influence a support structure in other ways than direct loading, for instance through corrosion, reducing the strength of a cross section of by affecting the stiffness of members. Also the presence of water in or around a structure in terms of internal or hydrodynamic added mass, can lead to additional inertial loading on the structure. Finally marine growth can lead to more severe hydrodynamic loading caused by the increased diameter and roughness. Several investigations are performed to determine the influence of these parameters on the natural frequencies extreme loading and in some cases fatigue.

**Modelling of joint stiffness**

Finally, the dynamic behaviour of the support structure is affected by the stiffness of joints. The modelling of joints as beams rigidly connected at the centreline may misrepresent the actual stiffness of the joints. Deformation of the braces and chord in particular lead to higher flexibility. This effect is called local joint flexibility and can be represented by parametric equations to modify the stiffness of the join, or - more accurately - using so-called superelements derived from detailed finite element models.
Another point of concern is the stiffness of the transition joint. This is usually modelled with very stiff elements, possibly overestimating the stiffness of this part of the structure. As the deflection of the tower top is strongly dependent on the stiffness of the transition joint this can significantly affect the dynamics.

In the following sections the influence of changing the mentioned parameters on the first and second natural frequencies[3] is established. Also the torsion natural frequency is recorded as well as the mass of pile elements and structural elements if they are affected by the parameter variations.

[3] The Jacket structure is highly symmetric, leading to almost equal frequencies in x- and y-direction. Therefore only the bending frequencies in the x-direction are considered.

To this end a parameterised model of the reference jacket structure is set up in Rosa. For each parameter the value is changed to +/- 10%, +/- 20% and +/- 30%.

### 7.6.2 Turbine parameters

Figure 7.22 shows the influence of large concentrated masses on the first, second and torsion natural frequencies. The first natural frequency is indicated with $f_1$, the second with $f_2$ and the first torsion natural frequency is designated $f_t$. In Figure 7.22 (a) the nacelle mass is varied +/- 30 % with respect to the reference value of 240 tons, while the rotor mass does not change.
It is clear that $f_2$ and $f_t$ are not affected significantly the variation of the nacelle mass. This is as expected as the nacelle mass is modelled close to the centreline of the tower axis and contributes little to torsional inertia. The deflections at tower top for the second mode are small and hence the variations also do not contribute much to the second natural frequency. The first natural frequency is most strongly affected and the relation is linear.

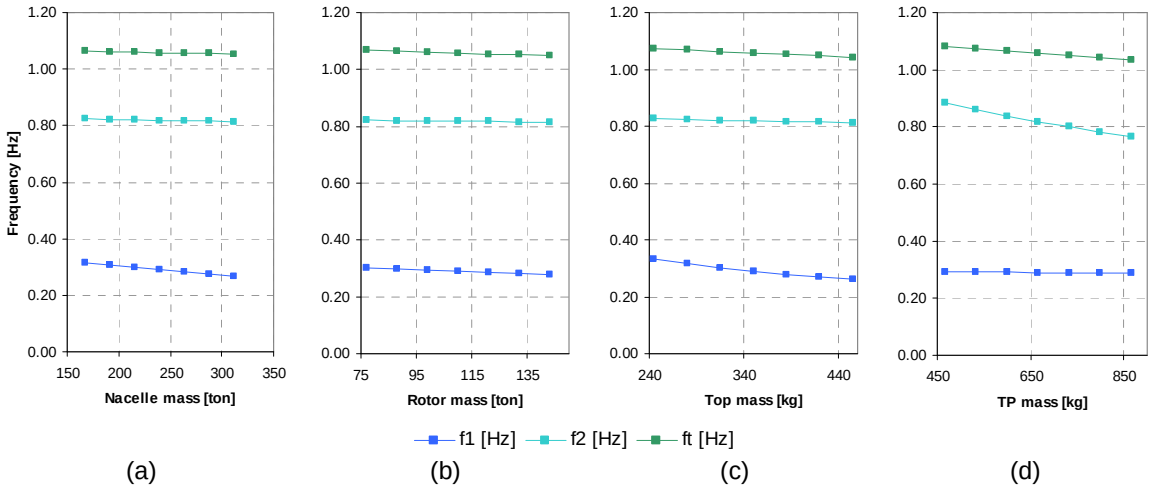


Figure 7.22: Influence of mass variation on natural frequencies

Variation of the rotor mass, shown in Figure 7.22 (b), hardly affects the second natural frequency but f1 and ft are affected. Due to the increased mass moments of inertia around the tower axis the torsion frequency decreases and the increase in mass leads to a lower first natural frequency.

Figure 7.22 (c) shows the combined effects of increased rotor mass and nacelle mass. The behaviour is consistent with the increase of rotor and nacelle mass separately.
At 666 tons the transition piece used in the jacket design is a substantial mass. Figure 7.22 (d) illustrates the variation of the natural frequencies due to a variation of the transition piece mass in the range of +/- 30%. The first natural frequency is hardly affected, but the second natural frequency is, as the displacements for the associated mode shape are the largest in this area. Also the torsion frequency is influenced, due to the considerable mass moment of inertia of the transition piece as modelled in the reference jacket structure.

Figure 7.23 (a) shows the variation of natural frequencies as function of the hub height. Here the interface level is kept at 20.15 m + MSL and the hub height is changed by +/- 30%. Also plotted is the mass of the structure, which is in this case due to the change in tower mass. The structure has not been altered apart from the change in tower length. All three natural frequencies are affected strongly by this change.
Also the change of the interface level was investigated; see Figure 7.23 (b). The interface level was changed by +/-30 % and the hub height is kept at 88.15 m above MSL. The first and second

natural frequencies decrease, but the first natural frequency increases, as the overall bending stiffness becomes larger. The decrease in the torsion frequency can be explained by the fact that the torsion stiffness of the jacket part is lower than that of the tower part. The decrease in second natural frequency can be explained from the fact that the mass of the transition piece is now closer to the part of the second mode shape with largest deflections. The mass of the structure actually increases, with an increase of the interface level, indicating that the mass per meter of the jacket is larger than the mass per meter of the tower.

Finally Figure 7.23 (c) illustrates the variation of natural frequencies when the interface level is varied, but the tower length is kept constant. The pattern is similar to Figure 7.23 (b), but variations are slightly stronger. Only the first natural frequency is now decreasing slightly with increasing interface elevation instead of increasing as was the case in Figure 7.23 (b). The mass shown is excluding the piles of 384 ton in total.

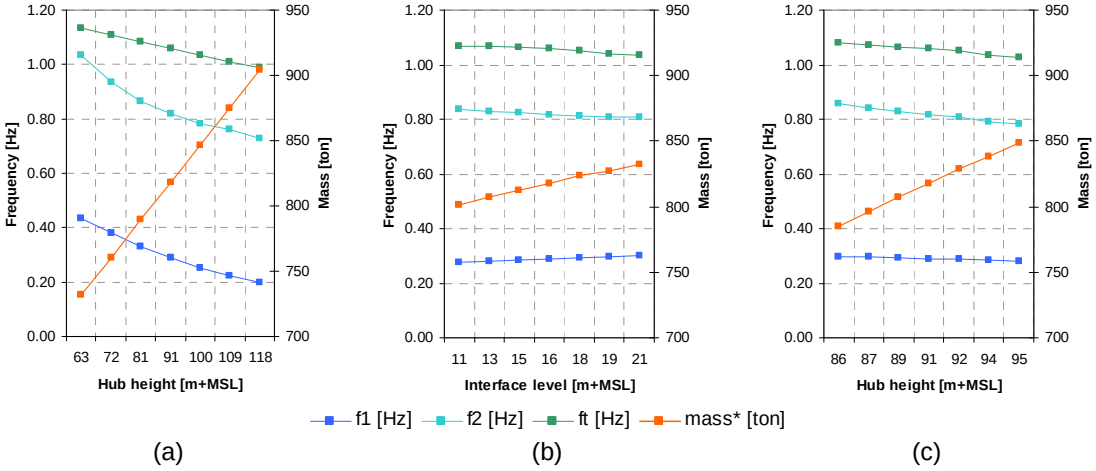


Figure 7.23: Influence of hub height and interface level on natural frequencies

### 7.6.3 Site conditions

Figure 7.24 shows the variation of natural frequency for varying soil conditions. In Figure 7.24 (a) the soil profile was assumed to consist entirely of sand, with the angle of internal friction $\varphi$ as the parameter being varied. The range of variation was taken from 28° to 42° while the submerged unit weight $\gamma'$ was kept constant at 10 kN/m$^3$. Figure 7.24 (b) illustrates the variation of frequencies for a profile consisting entirely of clay. Here the parameter varied is the undrained shear strength $c_u$ in the range of 35 to 125 kPa. Again $\gamma'$ is kept constant. The influence on natural frequencies is roughly similar for sand and clay. For the range considered the first natural frequency remains approximately constant. The second bending frequency and the torsion frequency decrease with decreasing $\varphi$ and $c_u$, first slowly and for lower values more rapidly. This is consistent with the fact that the second and torsion mode shapes generally show relatively large displacements near the mudline compared to the first mode shape and will therefore be affected more strongly.

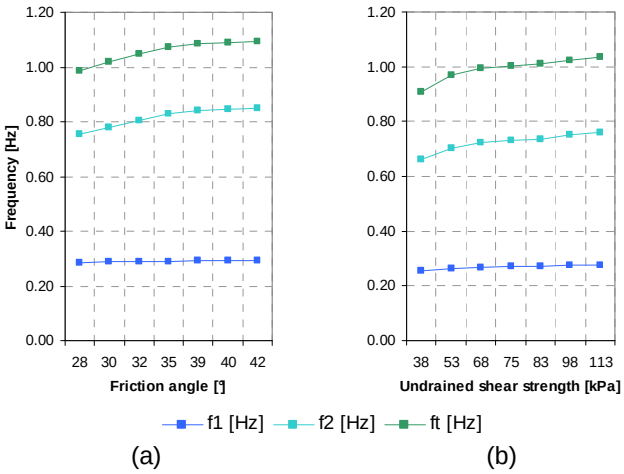


Figure 7.24: Influence of soil conditions on natural frequencies

The variation of frequencies and masses for water depth is shown in Figure 7.25. Here the range of water depth covered is from 25 to 75 m. The structure geometry has only been altered by changing the length of the structure below the waterline to match the water depth change. The variation of the first natural frequency is linear with the water depth, whereas the variation of the second natural frequency is quadratic with water depth, the effect being the strongest at low water depths. The torsion frequency is also affected in a quadratic relation with water depth, but in this case the effect is strongest at larger water depths. The increase in mass with water depth follows a linear trend. The mass shown is excluding the piles of 384 ton in total.

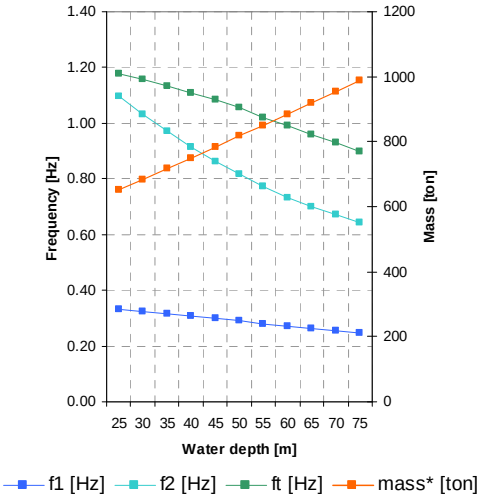


Figure 7.25: Influence of water depth on natural frequencies and mass

### 7.6.4 Structural dimensions

To demonstrate which measures are effective when attempting to change the natural frequencies of the structure by changing the geometry, an sensitivity analysis of structural dimension parameters is performed. In Figure 7.26 the influence of top and base width are investigated. An increase in bottom width results in an increase of the first, second and torsion natural frequencies. The variation follows the square of the base width for $f_1$ and $f_t$. For $f_2$ the

variation approaches a linear trend. Also the mass of the structure increases linearly with base width. Figure 7.26 (b) shows that the first natural frequency increases marginally with increasing top width and that the second and torsion frequencies decrease slightly. The increase of mass is less pronounced than for an increase in top width, but still considerable. The mass shown is excluding the piles of 384 ton in total.

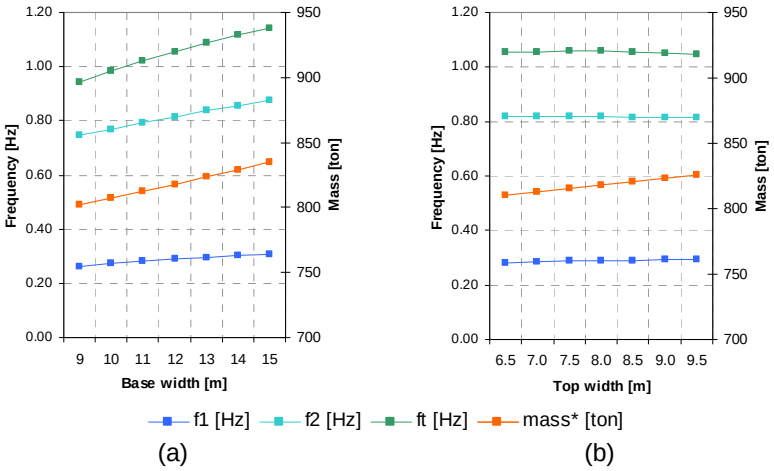


Figure 7.26: Influence of top width and base width on natural frequencies and mass

Figure 7.27 illustrates the influence of changing diameters of various elements on the natural frequencies and on the structure mass. In Figure 7.27 (a) the influence of the leg diameter on the frequencies and masses is investigated. The first natural frequency increases slightly, while the second frequency and the torsion frequency remain nearly constant. The mass variation is considerable, ranging from 725 to 910 tons.

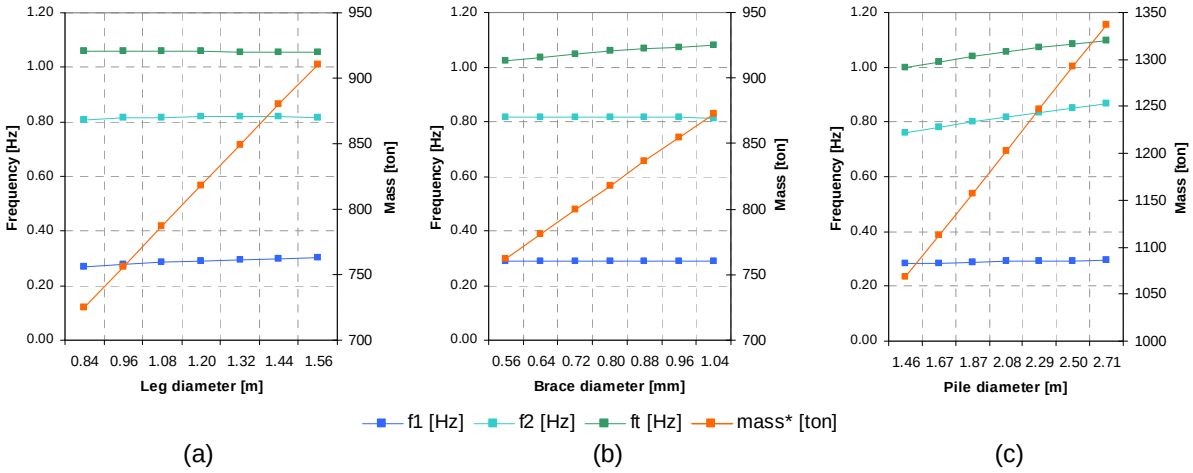


Figure 7.27: Influence of element diameters on natural frequencies and mass

In Figure 7.27 (b) the variation of natural frequencies and masses is shown for varying brace diameters. It can be seen that only the torsion natural frequency is noticeably affected, showing an increase for larger brace diameters. The mass of the structure increases linearly with increasing brace diameter.

The variation of the pile diameter has relatively little influence on the first natural frequency, but relatively strong influence on the second natural frequency and the torsion frequency. This is consistent with Figure 7.24, where the modes with relatively large lateral deflections near the mudline are affected the strongest. The mass increases linearly with penetration depth. As the mass increase is only caused by increase of pile mass here the total mass of the support structure is shown in Figure 7.27 (c).

Figure 7.28 shows the variation of natural frequency with penetration depth for the soft soil profile (a) and the hard soil profile (b), as documented in [13]. The natural frequencies are hardly affected by the penetration depth, at least not in the range of depths considered. The mass increases linearly with penetration depth.

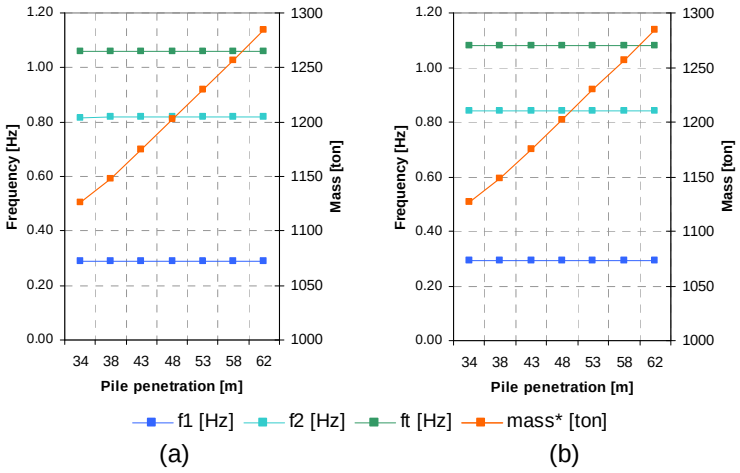


Figure 7.28: Influence of penetration depth on natural frequencies and mass

### Corrosion

Corrosion deteriorates material by diminishing its thickness. This then affects load carrying abilities of a member. It is therefore important to check the influence of different corrosion rates. For the jacket, the corrosion is defined in the splash zone region. As the legs are defined as flooded, the corrosion rate is doubled for legs. The following corrosion rates are studied:

- 3mm as reference according to DNV [1]
- 2.25mm for 75% of the reference value
- 1.5mm for 50% of the reference value
- No corrosion (0mm)

The corrosion rate influence is presented in terms of normalized stress. The changes in stresses are shown for different members and nodes in the jacket, as illustrated in Figure 7.29.

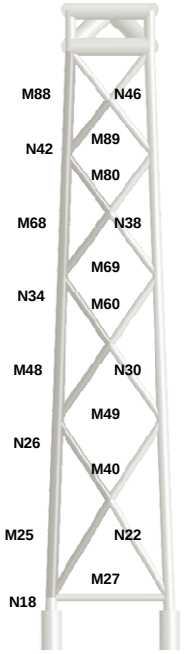


Figure 7.29: Elements for load studies [25]

The results of the analysis using GH Bladed are shown in Figure 7.30. The results obtained are not conclusive with respect to the influence of corrosion on the sub-structure. For nodes 22, 26, 38 and 46, the stress magnitude is visibly increased, whereas for nodes 34 and 18 the stress decreases when the corrosion rate is higher. For some other nodes the influence of the corrosion rate is almost insignificant. However, many diverse factors influence fatigue loading of such complex support structure types.

Even if the global natural frequencies of the jacket are slightly decreased for higher corrosion rates, this cannot be directly transferred to lower fatigue lifetimes. This is different to monopiles, where a clear influence can be seen. Corrosion results in a reduced stiffness of a member, which may lead to changes in its natural frequency. Different frequencies might be induced by coupling with other structural frequencies resulting in increased or decreased stresses. Thus, no clear tendencies for a jacket can be discerned.

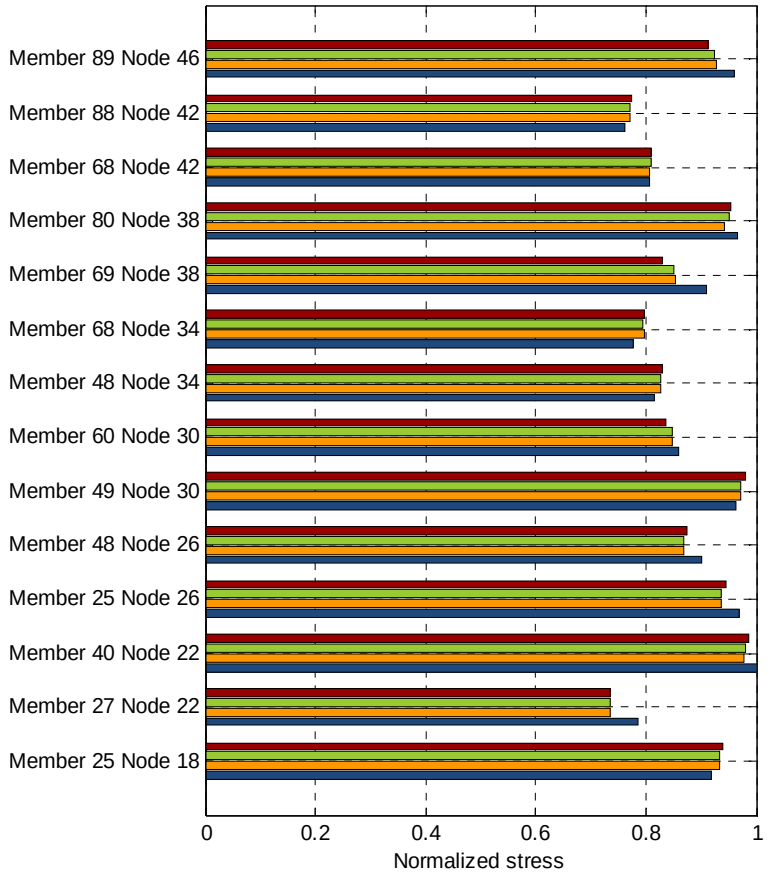


Figure 7.30: Different corrosion rate influence in terms of normalized stresses at nodes [25]

Table 7.22 shows the variation of the very first structural natural frequencies depending on applied corrosion rate. As already stated, the presented variation of the main natural frequencies is quite small. However the local, much higher frequencies may change significantly. It is not possible to check the local frequencies of particular members in GH Bladed.

Table 7.22: Corrosion influence on the structural frequencies

| Frequencies [Hz] | 3mm corrosion | 2.25mm corrosion | 1.5mm corrosion | No corrosion |
|---|---|---|---|---|
| 1st tower fore-aft | 0.286 | 0.287 | 0.288 | 0.289 |
| 1st tower side-to-side | 0.289 | 0.290 | 0.290 | 0.291 |
| 2nd tower fore-aft | 0.944 | 0.944 | 0.944 | 0.944 |
| 2nd tower side-to-side | 0.969 | 0.969 | 0.969 | 0.968 |
| 3rd tower fore-aft | 2.502 | 2.504 | 2.504 | 2.505 |
| 3rd tower side-to-side | 3.567 | 3.573 | 3.574 | 3.580 |
| 1st tower torsion | 1.412 | 1.413 | 1.414 | 1.415 |
| 2nd tower torsion | 4.078 | 4.079 | 4.074 | 4.057 |

**Marine growth**

The marine growth increases thickness of members by affecting hydrodynamic loading. Higher hydrodynamic loading is expected to have an influence on the fatigue lifetime of a structure. The load analysis is based on the same assumptions as the corrosion study, using again normalized

stresses at the same nodes and members. The following marine growth rates are applied from the upper splash zone down to mudline:

- 100mm as reference according to DNV [1]
- 50mm for 50% of the reference value
- No marine growth (0mm)

Figure 7.31 shows the results obtained for different rates of marine growth, where a similar pattern as for those from the corrosion influence study can be seen. In the case of 100mm marine growth, the stress magnitude is visibly increased for nodes 22, 26, 38 and 46, whereas for nodes 18, 34, and 42 stress decreases. For node 30 the influence of marine growth is almost insignificant. Interestingly, the stress magnitude does not increase or decrease linearly for different marine growth rates as expected for structure types like monopiles.

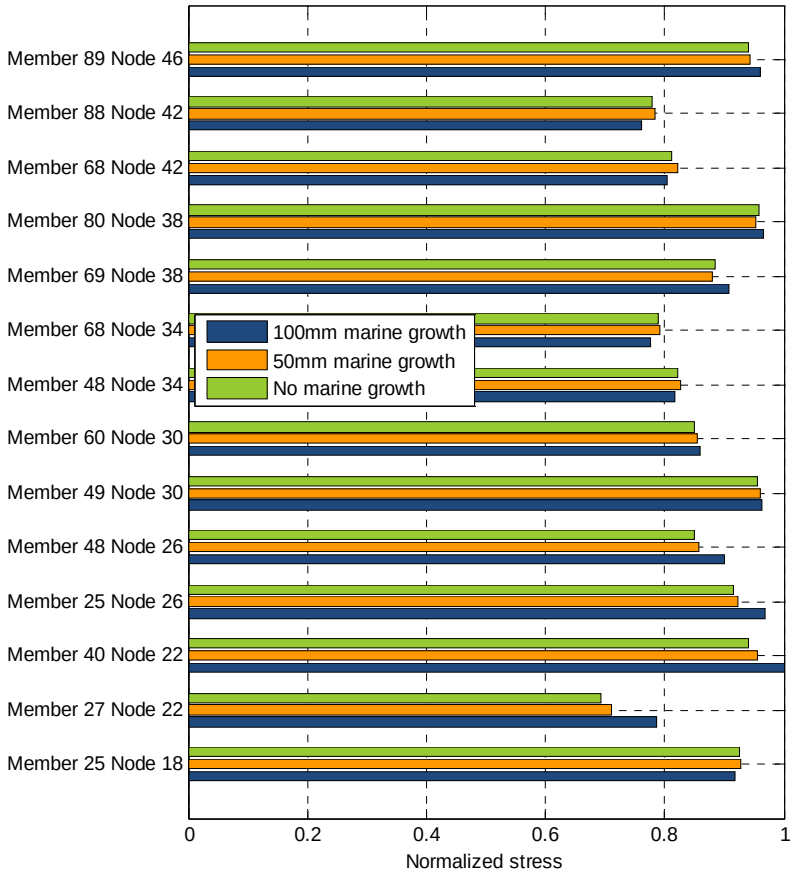


Figure 7.31: Marine growth rate influence in terms of normalized stresses at nodes [25]

Marine growth increases mass and thickness of members. This influences the natural frequency of the structure and leads to slightly lower frequencies in cases of applied marine growth. But as for the corrosion analysis, this change in global support structure natural frequencies does not lead to higher loadings in general. Again, this is probably due to induced changes in local modes and couplings with other structural frequencies.

Table 7.23: Marine growth influence on the structural frequencies

| Frequencies [Hz] | 100mm marine growth | 50mm marine growth | No marine growth |
|---|---|---|---|
| 1st tower fore-aft | 0.286 | 0.286 | 0.286 |
| 1st tower side-to-side | 0.289 | 0.289 | 0.289 |
| 2nd tower fore-aft | 0.944 | 0.947 | 0.949 |
| 2nd tower side-to-side | 0.969 | 0.972 | 0.975 |
| 3rd tower fore-aft | 2.502 | 2.512 | 2.519 |
| 3rd tower side-to-side | 3.567 | 3.673 | 3.758 |
| 1st tower torsion | 1.412 | 1.414 | 1.415 |
| 2nd tower torsion | 4.078 | 4.263 | 4.435 |

**Hydrodynamic added water mass**

A structure surrounded by water experiences loads due to the relative velocities and accelerations between the structure and the medium. One effect is called hydrodynamic added water mass [26]. A certain volume around the structure is oscillating with the structure and thus adds an additional mass, which is acting perpendicular to the direct axis of the element. As a simplification of what is happening physically the amount of added water on an element can be calculated according to the following equation:

$$m_{added} = \underbrace{\left(c_m - 1\right)}_{c_a} p_{water} \cdot V_{body}$$

This means that the added water mass is equal to the displaced water volume $V_{body}$ of a structural element times the water density $\rho_{water}$ times the mass coefficient $c_a$. The mass coefficient $c_a$ is equal to the inertia coefficient $c_m$ minus 1. The inertia coefficient is a parameter for calculating the hydrodynamic loading according to the Morison equation. The hydrodynamic added water mass can be introduced as additional mass on the structure or as a force term, which is more a matter of implementation in the equations of motion. The expression above needs to be multiplied by the acceleration of the element in the case that the hydrodynamic mass shall be considered as a force term, i.e. $F_{added} = -m_{added} \cdot \ddot{x}$ , where $\ddot{x}$ is the acceleration of the element. The minus sign denotes that the loading due to the hydrodynamic added mass acts in the opposite direction to the acceleration.

The influence on simulations is shown on masses, natural frequencies and damage equivalent loads [26]. The calculation of damage equivalent loads is based on the power production design load case 1.2 according to the guideline IEC 61400-3 [8].
The reference jacket of the Upwind project has a water added mass of 507.8t in total, which is 83% of the mass of the primary steel parts of the jacket. This mass has been calculated with a mass coefficient $c_a$ = 1, which means the displaced water is equal to the added water mass. Table 7.24 shows the first 15 natural frequencies of the wind turbine models with and without hydrodynamic added water mass. It can be seen that lower natural frequencies do not significantly change. Only high frequencies above 3 Hz show a larger difference. Table 7.25 shows the influence on damage equivalent loads of 8 exemplary sensors. Four sensors are located in the jacket as indicated in Figure 7.32. The remaining four sensors are the in-plane and out-of-plane bending moment of blade one and the fore-aft and side-side bending moment at the tower bottom.

Table 7.24: Natural frequencies of the reference model with and without hydrodynamic added water mass

| # | | 1 | 2 | 3 | 4 | 5 | 6 | 7 | 8 | 9 | 10 | 11 | 12 | 13 | 14 | 15 |
|---|---|---|---|---|---|---|---|---|---|---|---|---|---|---|---|---|
| Reference model | [Hz] | 0.299 | 0.302 | 0.655 | 0.668 | 0.694 | 1.083 | 1.090 | 1.147 | 1.154 | 1.718 | 1.818 | 1.925 | 1.978 | 2.995 | 3.650 |
| With water added mass | [Hz] | 0.299 | 0.302 | 0.655 | 0.668 | 0.694 | 1.080 | 1.085 | 1.127 | 1.136 | 1.716 | 1.814 | 1.923 | 1.978 | 2.990 | 3.407 |
| Deviation | | 0.00% | 0.00% | 0.00% | 0.00% | 0.00% | -0.28% | -0.46% | -1.74% | -1.56% | -0.12% | -0.22% | -0.10% | 0.00% | -0.17% | -6.66% |

Table 7.25: Damage equivalent loads of the reference model with and without hydrodynamic added water mass

| Sensor | Reference model | with water added mass |
|---|---|---|
| Bld 1 in-plane bending [kNm] | 10176 | 10173<br>-0.03% |
| Bld 1 out-of-plane bending [kNm] | 9835 | 9831<br>-0.04% |
| Tower fore-aft bending [kNm] | 33003 | 32718<br>-0.86% |
| Tower side-side bending [kNm] | 17618 | 17547<br>-0.40% |
| Jacket #1 [kN] | 3749.9 | 3688<br>-1.64% |
| Jacket #2 [kN] | 3294.4 | 3231<br>-1.93% |
| Jacket #3 [kN] | 432.48 | 428<br>-0.87% |
| Jacket #4 [kN] | 553.06 | 532<br>-3.78% |

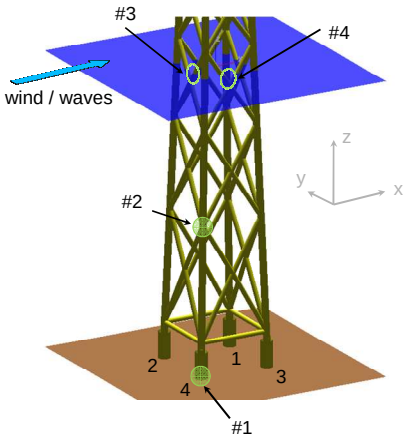


Figure 7.32: Position of the four jacket sensors

In general the damage equivalent loads of the model with water added mass are smaller than the reference case without water added mass. However the blade bending moments are almost unchanged. The damage equivalent loads at the support structure decreased more. The largest decrease of up to 3.8% can be found in the bracings pointing in the direction of wind and waves. It can be said that the behaviour of the rotor-nacelle-assembly is independent from hydrodynamic water added mass on the substructure. For the design of the support structure it is recommended to consider this parameter.

### Flooded members of the jacket

The reference jacket design considers flooded main legs until mean sea level to lower the buoyancy of the jacket. This subsection will show the influence on simulations if the main legs are filled with water or not. For this reason the jacket has been modelled with and without flooded main legs.

The influence on simulations is explained for masses, natural frequencies and damage equivalent loads in [27]. The calculation of damage equivalent loads is based on the power production design load case 1.2 according to the guideline IEC 61400-3 [8]. The position of the eight sensors is as shown in Figure 7.32.

Table 7.26: Natural frequencies of the reference model with and without flooded main legs

| # | | 1 | 2 | 3 | 4 | 5 | 6 | 7 | 8 | 9 | 10 | 11 | 12 | 13 | 14 | 15 |
|---|---|---|---|---|---|---|---|---|---|---|---|---|---|---|---|---|
| Reference model | [Hz] | 0.299 | 0.302 | 0.655 | 0.668 | 0.694 | 1.083 | 1.090 | 1.147 | 1.154 | 1.718 | 1.818 | 1.925 | 1.978 | 2.995 | 3.650 |
| with flooded legs | [Hz] | 0.299 | 0.302 | 0.655 | 0.668 | 0.694 | 1.082 | 1.088 | 1.138 | 1.146 | 1.717 | 1.817 | 1.924 | 1.978 | 2.993 | 3.535 |
| Deviation | | 0.00% | 0.00% | 0.00% | 0.00% | 0.00% | -0.09% | -0.18% | -0.78% | -0.69% | -0.06% | -0.06% | -0.05% | 0.00% | -0.07% | -3.15% |

Table 7.27: Damage equivalent loads of the reference model with and without flooded main legs

| Sensor | Reference model | with flooded main legs |
|---|---|---|
| Bld 1 in-plane bending [kNm] | 10176 | 10173<br>-0.03% |
| Bld 1 out-of-plane bending [kNm] | 9835 | 9834.3<br>-0.01% |
| Tower fore-aft bending [kNm] | 33003 | 32894<br>-0.33% |
| Tower side-side bending [kNm] | 17618 | 17593<br>-0.14% |
| Jacket #1 [kN] | 3749.9 | 3721.4<br>-0.76% |
| Jacket #2 [kN] | 3294.4 | 3264.9<br>-0.90% |
| Jacket #3 [kN] | 432.48 | 431.25<br>-0.28% |
| Jacket #4 [kN] | 553.06 | 544.12<br>-1.62% |

The total mass of water inside the four legs accounts for 255t, which is almost 42% of the mass of the primary steel parts of the jacket. The first 15 natural frequencies are shown in Table 3. It can be seen, that lower natural frequencies do not significantly change. Only high frequencies above 3 Hz show a difference. The damage equivalent loads of the eight sensors are shown in Table 7.27. Flooded main legs result in lower damage equivalent loads. Most differences occur in the bracings, which is similar to the findings in the hydrodynamic added mass effect. The influence on the rotor-nacelle-assembly is negligible small. For the design of the support structure it is recommended to consider this parameter.

### 7.6.5 Modelling of joint stiffness

**Stiffness of main joint**

The influence on the dynamics of the stiffness of the transition joint is shown in Figure 7.33. In Figure 7.33 (a) the stiffness of the transition has been varied +/- 30% by changing Young's Modulus for the elements of the transition joint. The effect on all three natural frequencies can hardly be discerned. In Figure 7.33 (b) the results for a larger variation of Young's Modulus are shown. The stiffness of the joint as it is currently is can only be increased marginally. However, a decrease of the stiffness of the joint by a factor 10 results in a decrease of the first natural frequency of 20%, a decrease of 5.7% for the second natural frequency and 3.6% for the torsion frequency.

These results show that the transition piece is modelled very stiff. In reality this structure may be softer, thereby lowering the natural frequencies. However, without quantification of the stiffness of a real transition piece, No conclusive statements can be made here regarding the accuracy of the modelled transition piece.

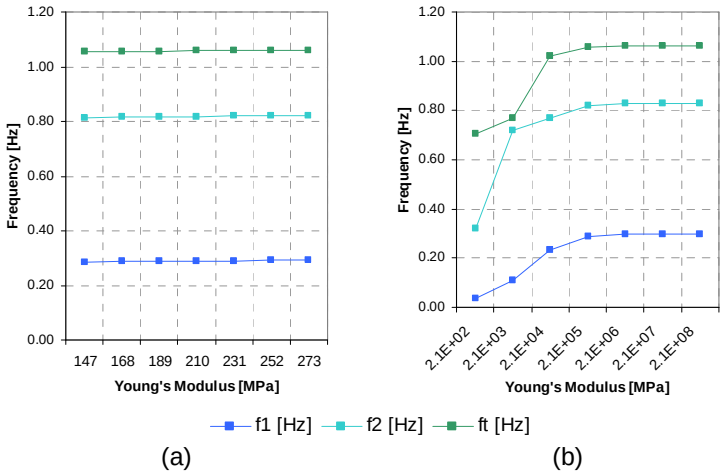


Figure 7.33: Influence of transition joint stiffness on the natural frequencies

### Influence of joint can modelling

Investigations were carried out to determine the influence of joint can modeling on the global dynamic simulation of a jacket support structure. The UpWind 5MW reference wind turbine [5] was used, mounted on the Upwind reference jacket structure [23].

In this preliminary study the turbine was simulated with two different jacket models in the ADCoS-Offshore design tool [28], as shown in Figure 7.34. Firstly a basic model was created in which all tubular members are modelled with the constant properties of the braces and legs, and secondly a model was created including the joint cans.

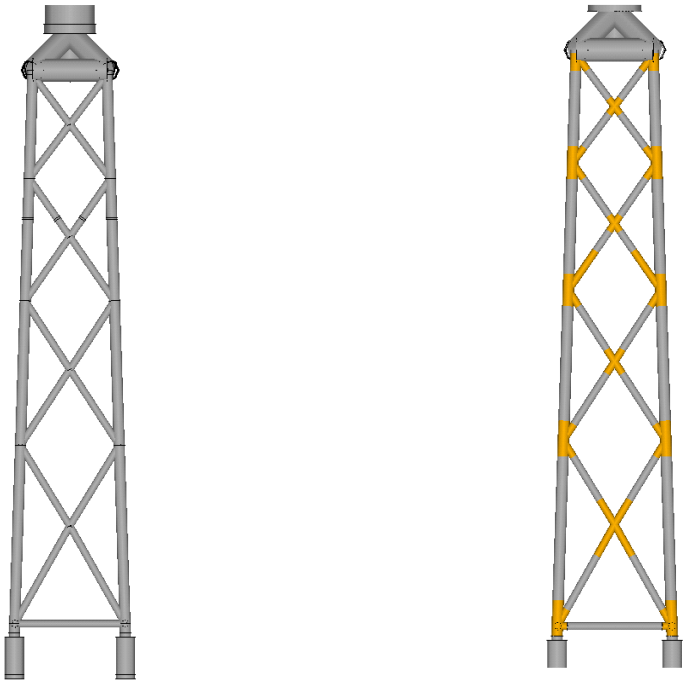

Figure 7.34: Basic jacket model without joint cans (left) and more detailed model including joint cans (right).

The joint can properties differ compared to the basic tube properties in terms of increased wall thicknesses as described in [23]. In both models, only the primary steel of the jacket is included. This is expected to be a conservative approach as supplementary masses e.g. resulting from marine growth or water in free flooded members would increase the total mass significantly and therefore reduce the relative mass difference due to joint cans and the resulting effects. The effects on the stiffness would be the same in both cases. The basic model includes 90 nodes (528 DOF) for the structure from tower top to mudline, and the model including joint cans features 270 nodes (1608 DOF).

In a first step the mass difference due to the joint cans is checked via direct comparison of the total dead weights of the jacket structure. The mass difference is about 5% (referred to the jacket mass) or approximately 1.7% (referred to the total mass of the offshore wind turbine from blade tip to mudline). Not only the masses, but also the stiffnesses of the members are changed due to the treatment of the joint cans in the model. Both the mass and stiffness distribution may affect the dynamic behaviour of the offshore wind turbine. This possible influence is investigated via comparison of the first 18 natural frequencies of the total system in ADCoS-Offshore, which corresponds to a frequency range between the lowest global natural frequencies of 0.3Hz up to approximately 3.5Hz. The results are shown in Table 7.28. All differences are under 0.8%.

Table 7.28: Relative differences of the first 18 natural frequencies comparing a model of the NREL 5-MW reference turbine on the Upwind reference jacket with and without joint cans in ADCoS-Offshore.

| Number of order natural frequency [-] | 1 | 2 | 3 | 4 | 5 | 6 | 7 | 8 | 9 | 10 | 11 | 12 | 13 | 14 | 15 | 16 | 17 | 18 |
|---|---|---|---|---|---|---|---|---|---|---|---|---|---|---|---|---|---|---|
| Difference [%] | -0.67 | -0.68 | -0.18 | -0.04 | -0.03 | -0.14 | -0.32 | -0.15 | -0.14 | -0.18 | -0.26 | 0 | 0 | -0.02 | 0.13 | 0.48 | 0.19 | 0.74 |

To conclude, the mass difference due to joint can modelling is approximately 1.7% w.r.t. the offshore wind turbine as a whole and the differences concerning the first 18 natural frequencies are under 0.8%. These are minor differences that are not expected to lead to significant changes in the loads in more detailed investigations. Furthermore, the increase of model complexity (528 DOF in the simple model vs. 1608 DOF in the detailed model) leads to considerably higher computational costs in an FE based tool like ADCoS-Offshore, and in other tools that treat at least the structure as a FE model. Therefore it is proposed to carry out further investigations with a basic model neglecting joint cans.

**Influence of parametric Local Joint Flexibilities**

In this analysis the influence of applying local joint flexibilities on the structure natural frequencies is investigated. In the reference design the local joint flexibilities are included following a simple joint classification in which the joints are considered as simple T and Y joints as if no other braces are present at the joint. The Buitrago local joint formula is used. In a second case no local joint flexibility is applied. The results for the first and second bending modes in the x-direction and for the first torsion frequency are listed in Table 7.29.

Table 7.29: Infuence of local joint flexibilities on natural frequencies

| | | 1st mode | 2nd mode | Torsion mode |
|---|---|---|---|---|
| Reference - with LJF | [Hz] | 0.2898 | 0.8180 | 1.0578 |
| Without LJF | [Hz] | 0.2899 | 0.8168 | 1.0976 |
| Difference | [%] | 0.03 | -0.15 | 3.76 |

The difference for the first and second bending modes is very small. The torsion mode shows a larger difference of approximately 4%. The reason for the small error can be found in the fact that, while the joint flexibility reduces the stiffness of the joints, the length of the braces is also reduced, leading to a stiffer behaviour of the braces.

## 7.7 Cost modelling of jacket structures

### 7.7.1 Approach

From the sensitivity analysis it can be concluded that the local water depth has a strong influence on a jacket structure's first natural frequency. Additionally, the required hub height and the mass of the rotor nacelle assembly significantly affect the structure dynamics.
From a design point of view, the main parameter of the substructure to influence the natural frequency is the base width. The length of the foundation piles can also be used to influence the first natural frequency.

The aim of the cost model is to indicate how cost of the support structure change for varying site conditions and for varying turbine parameters. Costs can be expressed in material cost and cost for manufacturing. Of course costs installation and inspection and maintenance also contribute to the costs, but these will not be considered here.

The cost model is based on a parameter analysis for the jacket substructure for a large number of different cases. In these cases the parameters being varied are the water depth, rotor diameter, hub height, turbine mass and thrust force. The structure dimensions are determined based on the dimensions of the reference structure. By changing the base width the natural frequency is tuned to match the allowable frequency range. Finally a simplified ultimate limit state check is performed. All configurations that fulfil both the natural frequency requirements and the ultimate limit state requirements are entered in the cost model. Figure 7.35 shows the input/output screen of the Excel based jacket cost model

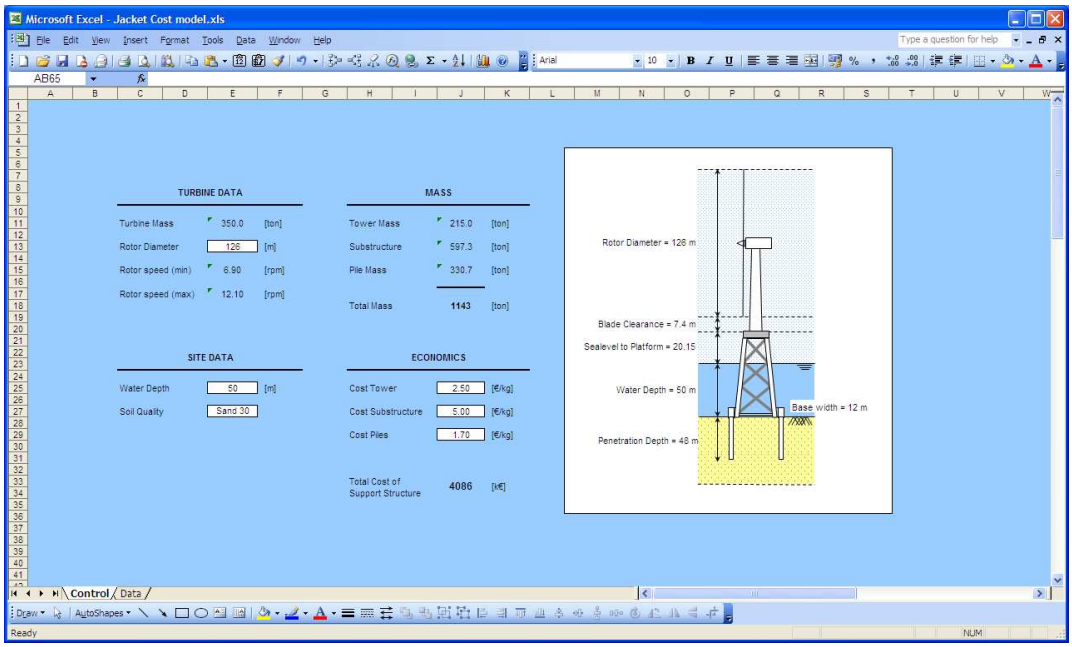


Figure 7.35: Input/output screen of jacket cost model

### 7.7.2 Definition of fictive turbines

As the mentioned turbine parameters are usually correlated via the rotor diameter, a set of fictive turbines is established, with rotor diameters ranging from 90 to 150 m in 10 m intervals. Also the UpWind reference turbine is included in this range. Based on the reference turbine, the mass and thrust force are scaled. A study into mass scaling of turbine components [3] showed the

rotor and nacelle mass to vary as a function of rotor diameter as described by the following equations:

$$m_{rotor} = 0.0475 \cdot D^{3.09}$$
$$m_{nacelle} = 0.090 \cdot D^{3.57}$$

In order to fit these relations to the mass of the UpWind reference turbine the coefficients are scaled to obtain:

$$m_{rotor} = 0.0355 \cdot D^{3.09}$$
$$m_{nacelle} = 0.076 \cdot D^{3.57}$$

As was shown in [29] the first natural frequency has significant influence on the fatigue damage of a jacket structure. When the first natural frequency lies closer to the 1P frequency this leads to higher fatigue damage. Therefore it is important to consider the first natural frequency as a critical design parameter. To define the allowable frequency range the rotor speed range of the turbine is also required. Therefore the rotor speed is scaled as a function of the rotor diameter and a constant tip speed ratio using the rotor speed range of the UpWind reference design.

In [29] it was also shown that the fatigue loading in a jacket structure is for the major part due to aerodynamic loading. This, in combination with the fact that a lower natural frequency leads to higher fatigue damage, leads to the consideration that the tower should be as short as possible to reduce fatigue loading. The hub height is therefore determined by the following relation:

$$z_{hub} = z_{interface} + \tfrac{1}{2} D_{rotor} + \Delta z_{clearance}$$

And the tower length can be found following:

$$L_{tower} = z_{hub} - \Delta z_{towertop-hub} - z_{interface}$$

Finally, the turbine loads are also scaled as a function of the rotor diameter. The maximum total load on the turbine is simply considered to be the maximum thrust force during operation. Since the thrust force is proportional to $D^2$ the thrust force for a turbine with rotor diameter $F_D$ is:

$$F_D = D^2 \cdot F_{ref} / D_{ref}^2$$

The resulting fictive turbine parameters are listed in Table 7.30. The rotor speed range and the allowable natural frequency range are listed in table Table 7.31, where $1P_{low}$.and $1P_{high}$ denote the limits of the 1P range, $3P_{low}$ and $3P_{high}$ the limits of the 3P range and *1P+10%* and *3P-10%* indicate the upper and lower boundary of the 1P and 3P ranges including safety margin, marking the boundaries of the allowable frequency range.
As a check the parameters of the fictive turbine with rotor diameter 90 m are considered. The mass of the rotor and nacelle, the thrust force and the rotor speed range appear to be in the correct range for a 3.0 MW class turbine with 90 m rotor diameter.

Table 7.30: Fictive turbine parameters for use in turbine model

| $D_{rotor}$ | $M_{rotor}$ | $M_{nacelle}$ | $M_{Total}$ | $z_{hub}$ | $F_{thrust}$ | $M_{y:interface}$ |
|---|---|---|---|---|---|---|
| [m] | [ton] | [ton] | [ton] | [m+MSL] | [kN] | [kNm] |
| 90 | 38.9 | 72.2 | 111.1 | 72.55 | 714 | 37429 |
| 100 | 53.9 | 105.2 | 159.0 | 77.55 | 882 | 50617 |
| 110 | 72.3 | 147.8 | 220.1 | 82.55 | 1067 | 66582 |
| 120 | 94.6 | 201.6 | 296.2 | 87.55 | 1270 | 85587 |
| 126 | 110.0 | 240.0 | 350.0 | 90.55 | 1400 | 98560 |
| 130 | 121.2 | 268.3 | 389.5 | 92.55 | 1490 | 107898 |
| 140 | 152.3 | 349.6 | 501.9 | 97.55 | 1728 | 133778 |
| 150 | 188.5 | 447.2 | 635.8 | 102.55 | 1984 | 163492 |

Table 7.31: Rotor speed ranges and allowable frequency ranges for fictive turbines

| $D_{rotor}$ | $1P_{low}$ | $1P_{high}$ | $3P_{low}$ | $3P_{high}$ | 1P +10% | 3P-10% |
|---|---|---|---|---|---|---|
| [m] | [Hz] | [Hz] | [Hz] | [Hz] | [Hz] | [Hz] |
| 90 | 0.161 | 0.282 | 0.483 | 0.847 | 0.310 | 0.435 |
| 100 | 0.145 | 0.254 | 0.435 | 0.762 | 0.279 | 0.391 |
| 110 | 0.132 | 0.231 | 0.395 | 0.693 | 0.254 | 0.356 |
| 120 | 0.121 | 0.212 | 0.362 | 0.635 | 0.233 | 0.326 |
| 126 | 0.115 | 0.202 | 0.345 | 0.605 | 0.222 | 0.311 |
| 130 | 0.112 | 0.195 | 0.335 | 0.586 | 0.215 | 0.301 |
| 140 | 0.104 | 0.181 | 0.311 | 0.544 | 0.200 | 0.280 |
| 150 | 0.097 | 0.169 | 0.290 | 0.508 | 0.186 | 0.261 |

Finally the tower diameter and wall thickness were scaled under the assumption that the stress at the tower base remains constant. According to [7] the scaling of the tower diameter is proportional to $D^{1/3}$ assuming a constant thrust force. The wall thickness is taken linearly proportional to the diameter.

### 7.7.3 Natural frequency analysis

For each of the fictive turbines listed in Table 7.30 and Table 7.31 the natural frequency for a range of water depths (20 m to 70 m in 10 m intervals) is determined. Simultaneously, the base width is varied from 8 to 16 m in 2 m steps, the penetration depth is varied from 30 to 55 m in steps of 5 m and the wall thickness is scaled by factors of 0.8, 0,9 1.0, 1.1 and 1.2. The natural frequency analysis is carried out for 6 soil profiles, of which three are clay profiles with undrained shear strength of 50, 200 and 500 kPa and the other three are sand profiles with friction angles of 30, 35 and 40°. For each combination of parameters the first natural frequency is recorded, together with the structural mass. This leads to approximately 36000 combinations from which only the results that fall within the allowable natural frequency range for each turbine are selected..

### 7.7.4 Ultimate limit state analysis

Besides the natural frequency analysis the structure is also checked to determine whether it can withstand the extreme loads. To this end a simplified load case is set up consisting of the maximum wind load during operation at rated wind speed together with a streamfunction wave at reduced wave height. According to the design basis [1] the reduced wave height associated with the 50 year return period is 10.34 m and the corresponding wave period is 10.87 s. This load case is applied co-aligned in two directions. In the first case the loading is parallel to a panel of the jacket (0°) and in the second case the loading is applied parallel to the diagonal of the jacket base (45°).

**Penetration depth**

To avoid an excessive number of permutations to check for the ULS, the required minimum penetration depth is evaluated separately. This involves two steps, one to determine the loads acting on the pile and the other to determine the minimum required penetration depth for a given combination of load and soil type.
For jacket structures the loading in the piles is mainly in axial direction. Therefore the penetration depth in this study is determined based on the axial load on the piles only. The maximum axial load on the pile generally occurs when the jacket is loaded in the diagonal direction. As such, the overturning moment resulting from coaligned wind and wave loads is taken up by only two piles. The contribution of the wind load to the overturning moment is known from the maximum thrust and the hub height and water depth. The contribution of the wave load is determined by performing a wave load analysis for 9 base width steps and 11 water depth steps. The resulting maximum pile load is given in Figure 7.36. With increasing water depth the load on the pile increases. With increasing base width the load on the pile decreases.

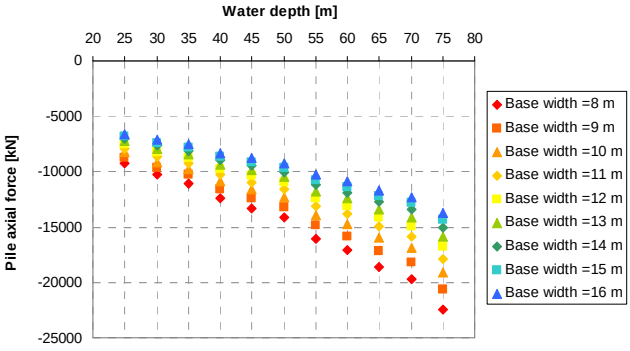


Figure 7.36: Maximum axial pile load for varying water depth and base width.

By combining the maximum axial pile load found in the wave load analysis with the contribution from the wind load the load on the pile is in the range of 10MN to 70 MN. For a step size of 1 MN all load steps in the range are evaluated for 6 soil types to determine the minimum required penetration depth. This analysis is performed in ROSA where the pile axial resistance is modelled with *t-z* curves to represent the shaft friction and *q-w* curves to represent the end bearing.

**Strength and stability**

In a separate analysis in ROSA the strength and stability for all combinations of water depth, base width, turbine size and wall thickness is checked. The maximum utilisation ratio for members found from the simplified ultimate load analysis using the reference design dimensions is 0.45. This is lower than the value found in the detailed design described in Section 7.5. However, the load applied in this analysis is simplified to reduce computational effort and since obtaining the exact design dimensions is not the objective, but instead to find the trends in support structure mass with varying external parameters this is deemed acceptable. A utilisation ratio of 0.45 is therefore the target for all combinations considered in the ULS analysis. For each combination of water depth, base width and turbine, the combinations resulting in the utilisation closest to this value are selected.

### 7.7.5 Results

For each of the resulting configurations, the maximum load in the pile is calculated and the associated minimum pile penetration depth is determined. With the support structure configuration and the pile penetration depth known, the total mass of the support structure is known. For each combination of water depth, soil type and turbine the minimum overall

structural mass is selected. These results are incorporated in the cost model sheet as shown in Figure 7.35, that allows the extraction of mass data of tower, substructure and piles for different combinations of turbine size, soil type and water depth. It should be noted that the presented mass results account only for the primary structure. No secondary steel items or equipment is included in the mass data presented.

The mass of the substructure as function of water depth is shown in Figure 7.37. The mass increase shows a generally linear trend with increasing water depth. Also the mass increases with water depth

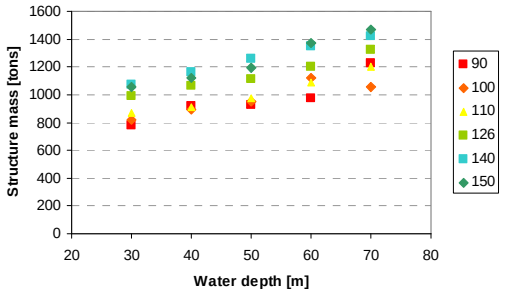


Figure 7.37: Structure mass as function of water depth and turbine size for soil type sand 35°

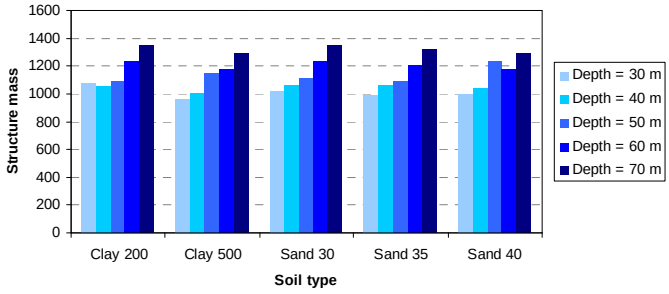


Figure 7.38: structure mass for varying water depth and soil type for turbine with rotor diameter 126m.

### 7.7.6 Verification

Not much data from actual projects is available for verification. However, the reference design gives one point for comparison and a second point in 30 m water depth is obtained from [31] in which a mass break down for a jacket structure for the Alpha Ventus test field is presented. The turbine employed in this case has a rotor diameter of 126 m. The soil type is considered to be average sand with a friction angle of 35°. The results of the comparison are shown in Table 7.32. The tower mass data is not stated in [31], hence the tower mass data is omitted from the comparison for Case 2 in Table 7.32. For Case 1 the error in total mass is approximately 5%. The jacket structure mass determined by the cost model is heavier than the reference jacket, however the piles are lighter. As the cost model is looking for the lowest mass that satisfies the ULS and natural frequency requirements it may find a configuration that is slightly heavier for the jacket, but lighter for the piles. Also it should be considered that the ultimate load analysis is very simplified and that no fatigue has been taken into account. For the second case the error in total mass is also approximately 5%.

Table 7.32: Mass data comparison for jacket cost model verification

| | Case 1 | | Case 2 | |
|---|---|---|---|---|
| | Reference jacket | Cost model | Alpha Ventus [31] | Cost model |
| Tower mass | 216 | 215 | - | - |
| Jacket mass | 545 | 597 | 425 | 472 |
| Pile mass | 438 | 331 | 315 | 303 |
| Total mass | 1199 | 1143 | 740 | 775 |

Although the data for comparison is limited, the mass data seem to compare sufficiently accurate to accept the results. It should be kept in mind that the cost model is meant to show trends rather than predicting actual mass and cost for a given situation.

## 7.8 Conclusion

In this chapter an assessment has been performed on a jacket and a tripod support structure in 50 m water depth and supporting the UpWind 5.0 MW reference turbine. Based on a rough cost estimate it has been shown that a jacket structure is both lighter and cheaper than a tripod structure in the considered circumstances.

The design of a reference jacket structure is described. The design methodology and the preliminary and final design results are presented. The final structure has a bottom width of 12 m and a top width of 8 m. The legs fit inside the four pre-piled piles with outer diameter of 2082 mm that penetrate 48 m into the soil. The mass of the substructure is 545 tons and the combined mass of the foundation piles is 438 tons. The structure is intended to be used as a reference for sensitivity analyses or comparisons to other concept. A particular use will be the incorporation of the jacket model in the Offshore Code Comparison Collaboration project follow-up OC4 [30].

The maximum utilisation ratios for the extreme event analyses are found in the bottom members of the lower X-braces, whereas the maximum fatigue damage is found in the legs near the top of the upper X-brace. The fatigue damage is dominated by aerodynamic loading.

The sensitivity analysis for the jacket structures focuses on the influence on the required dimensions of the support structure of site conditions such as water depth and soil conditions and turbine parameters. It shows that the first natural frequency is highly dependent on water depth. The hub height and turbine mass also strongly influence the structural dynamics. In order to influence the natural frequencies changing bottom width is the most effective. To a lesser extent the variation of pile diameter and pile penetration depth can be used to influence the frequencies. Corrosion and marine growth affect the global structural natural frequencies, but have no clear impact on fatigue loading. The inclusion of hydrodynamic added mass and internal water in the structural model may help reduce the fatigue loading on the jacket slightly in a fatigue analysis. Finally the modelling of the stiffness of the transition joint can be critical if not sufficiently stiff enough.

A simplified cost model draws on these observations to determine the mass and cost of a jacket support structure as a function of water depth and turbine size. For each turbine size the increase is support structure mass as function of water depth is approximately linear.

# 8. A comparison of soft-stiff structure concepts

## 8.1 Introduction

In Chapters 6 and 7 an extensive description of the design process, design results and sensitivity of structural and environmental parameters has been presented for monopile and jacket structures.
As mentioned in Chapter 2 many other support structure concepts can be identified. In this chapter, two alternative support structure concepts are introduced. Preliminary designs have been made, based on preliminary design approaches as explained in Chapters 6 and 7 for each of these concepts. In this chapter these concepts are compared for a water depth of 50 m. In this comparison the focus will be on overall required structural mass and hydrodynamic loads.

## 8.2 Approach

Four structures have been modelled in ROSA. Additionally the reference design for the jacket is included in the comparison at the end of this chapter.

- Monopile,
- Monopile - truss hybrid
- Tripod
- 3-leg jacket

For each of these structures a preliminary design is made. The structures are designed for the UpWind 5.0 MW reference turbine and for the K13 deep water site as described in [1]. The design water depth is 50 m.
Simplified load cases as described in Section 7.2 are applied. Extreme loads are applied in the governing directions for each model, 0° and 45° for four-leg structures, 0° and 30° for three-leg structures.
Each of these models is dimensioned to have a first natural frequency in the allowable range of 0.22 Hz to 0.31 Hz. To this end several key structural parameters are varied to obtain an envelope for structural configurations that satisfy the natural frequency requirements.

To determine the minimum required penetration depth the ultimate limit state check is performed with increased material factors for the soil strength parameters. The penetration depth is sufficient if a solution can be found.
Subsequently, the material factors for the soil are set to unity to determine pile stresses and to check the overall structure strength. The structures are checked for buckling, ultimate strength and where relevant for punching shear.

Finally a fatigue analysis is performed. Here wind and wave fatigue are determined separately and combined following:

$$D_{tot} = (D_{aero}^{2/m} + D_{hydro}^{2/m})^{m/2}$$

Where $D_{aero}$ is the aerodynamically induce fatigue damage, $D_{hydro}$ is the hydrodynamically induced fatigue, $m$ is the Wöhler coefficient and $D_{tot}$ is the combined damage. The aerodynamic loading is applied at the interface level in the form of damage equivalent loads. The applied damping ratio is 5%, including 4% aerodynamic damping and 1% structural damping. The total fatigue life for each joint and element must be above 20 years design life.

Based on the aforementioned checks the structure is optimised and the overall mass results are determined.

## 8.3 Models

### 8.3.1 Monopile

The monopile structure is modelled in Rosa as shown in Figure 8.1. The foundation pile is modelled with a constant outer diameter from the pile tip upwards until several meters below the sea surface. Here a pile cone tapers to an outer diameter of 5.5 m. The top part of the pile has a constant outer diameter, over which the transition piece is fitted. The connection between the pile and the transition piece is modelled with rigid link elements. In Figure 8.1 the appurtenances included in the model can also be seen. Concentrated masses representing the turbine, flanges and the grout mass are included. The boatlanding, ladders and J-tubes cause additional loads on the structure. These are taken into account by modelling these appurtenances as areas.

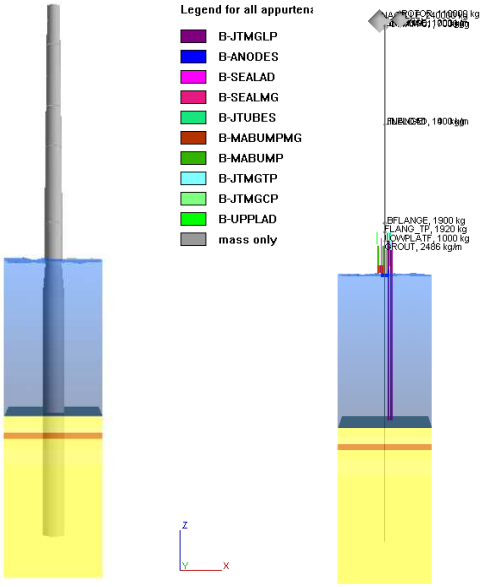


Figure 8.1: Rosa model of Monopile

### 8.3.2 Monopile - truss hybrid

The monopile - truss hybrid structure is modelled with a foundation pile similar to the pile in the monopile model. Onto the pile top section the truss transition piece is fitted. This element is modelled with five identical sections consisting of four legs and four X-bracings. The width of each section is equal to the height. The parts forming the transition between the legs and the tower (at the top) and the pile (at the bottom) are modelled using stiff members. As is done for the monopile, the connection between the pile and the transition piece is modelled with rigid link elements. Also the appurtenances are modelled similarly. Local joint flexibilities are modelled following a simple classification using Buitrago parametric formula, where each joint is calculated as a simple T or Y joint as if no other members are present.

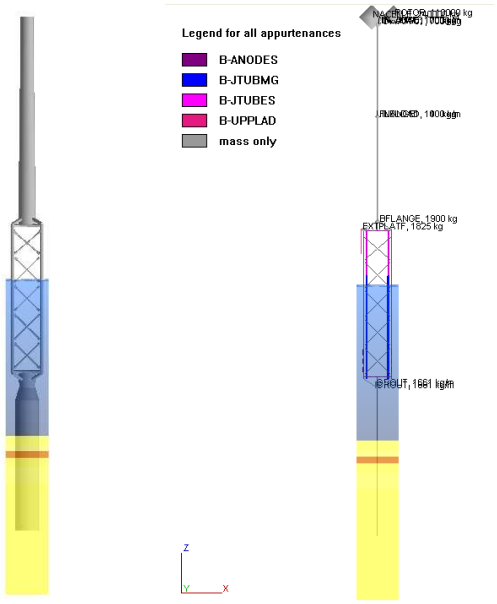


Figure 8.2: Rosa model of Monopile - truss hybrid

### 8.3.3 Tripod

The tripod model is shown in Figure 8.3. The tower sits on a central column with outer diameter equal to the tower base diameter. The central column is supported by three legs and tapers to a smaller diameter at the bottom, where it is supported by three braces. The braces and legs are attached to vertical pile sleeves. Three mud braces connect the pile sleeves near the mudline. Appurtenances are modelled as was done for the monopile and monopile - truss hybrid, but J-tubes are not included as they are assumed to be guided through the central column and will therefore not contribute to hydrodynamic loading. The main parameter governing the dimensions of the structure is the base radius, the distance from the pile to the central column centreline. Local joint flexibilities are applied following a simple classification.

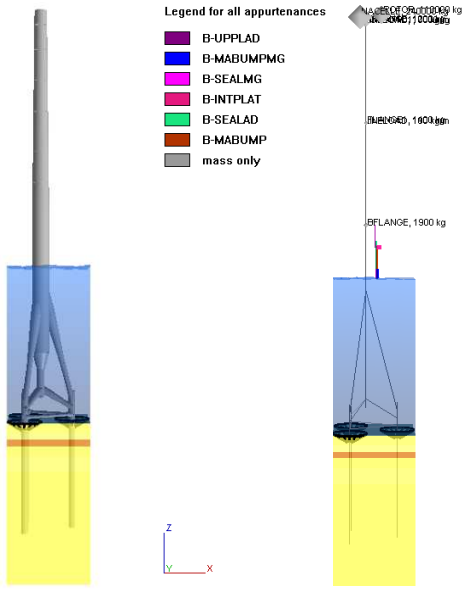


Figure 8.3: Rosa model of Tripod

### 8.3.4 Three leg jacket

The three- leg jacket is an adaptation of the four leg jacket, with one leg less. The remaining three legs are connected with four levels of X-braces. As for all previously mentioned models. Local joint flexibilities and appurtenances are included. The dimensions are mainly determined by the base radius, the distance between the leg and the jacket centreline.

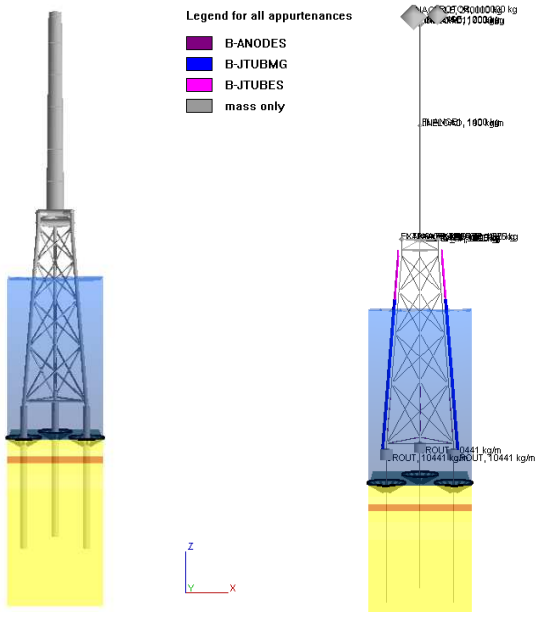


Figure 8.4: Rosa model of Three-leg jacket

## 8.4 Results

### 8.4.1 Monopile

The monopile is not very well suited for large water depths. The resulting structure found in this study requires very large wall thicknesses and is therefore not very realistic, both from an economic point of view and in relation to practical aspects such as fabrication and installation. However, it serves well as a reference, particularly for comparing the monopile - truss hybrid with.

#### Natural frequency analysis

The natural frequency analysis showed that a pile diameter of at least 7.0 m was required to achieve a first natural frequency of 0.22 Hz. However, subsequent iterations resulted in substantially larger wall thicknesses and the first natural frequency increased to 0.26 Hz. The second natural frequency is at 0.694 Hz. The mode shapes associated with the first and second bending natural frequencies are shown in Figure 8.5

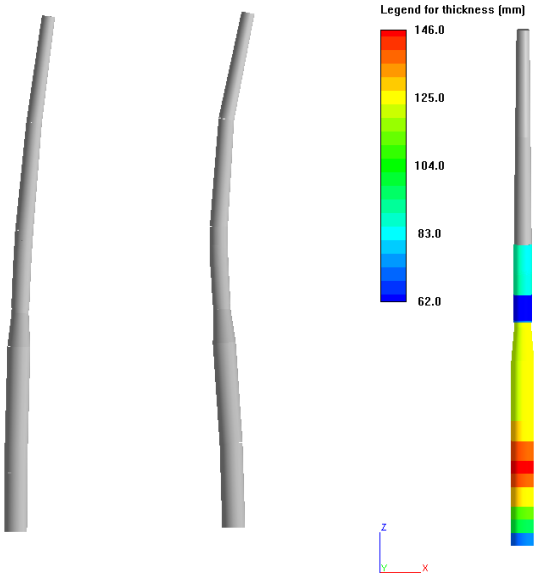


Figure 8.5: Results for Monopile: First (a) and second (b) mode shapes, wall thickness (c)

### Ultimate limit state

The ultimate limit state check revealed that the minimum required penetration depth is 28 m in combination with a 7.0 m diameter pile. The maximum base shear is 16.3 MN and is found for load case 25, in which only the 50 year wave height is considered. The maximum overturning moment is 779 MNm. The highest utilisations are found near the seabed.

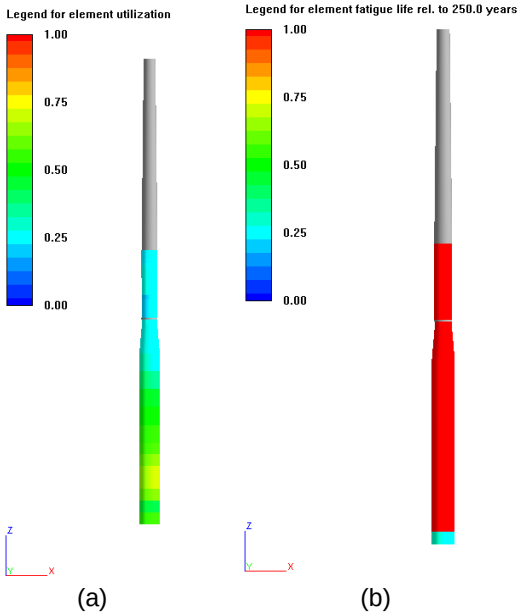


Figure 8.6: Monopile: element utilisation (a) and element fatigue damage (b)

### Fatigue limit state

The fatigue analysis showed that the fatigue lives are very low, below the required design life of 20 years, even when increasing the wall thickness to values above 120 mm. It was therefore decided not to fully optimise the monopile for fatigue. The lowest resulting fatigue life is 3.73 years, at the bottom of the pile cone.

#### Structure mass

The resulting structure mass is 2133 tons. This includes the tower of 216 tons, the transition piece of 438 tons and the pile of 1479 tons.

### 8.4.2 Monopile - truss hybrid

For the monopile - truss hybrid the hydrodynamic loads are significantly lower than for the monopile, this leads to a significantly lower mass. Also a truss structure can be constructed lighter for the same stiffness.

#### Natural frequency analysis

For the first natural frequency to be in the allowable frequency range the pile diameter must be at least 7.5 m in diameter. This indicates that the truss transition piece is softer than the pile and transition piece of the monopile described in the previous section. To exceed the lower boundary of the allowable frequency range for both soils a penetration depth of 34 m is required. This results in a first natural frequency of 0.22 Hz and a second natural frequency of 0.95 Hz. The mode shapes can be seen in Figure 8.7 (a) and (b). The first torsion mode (c) is also shown. The torsion frequency is at 2.44 Hz.

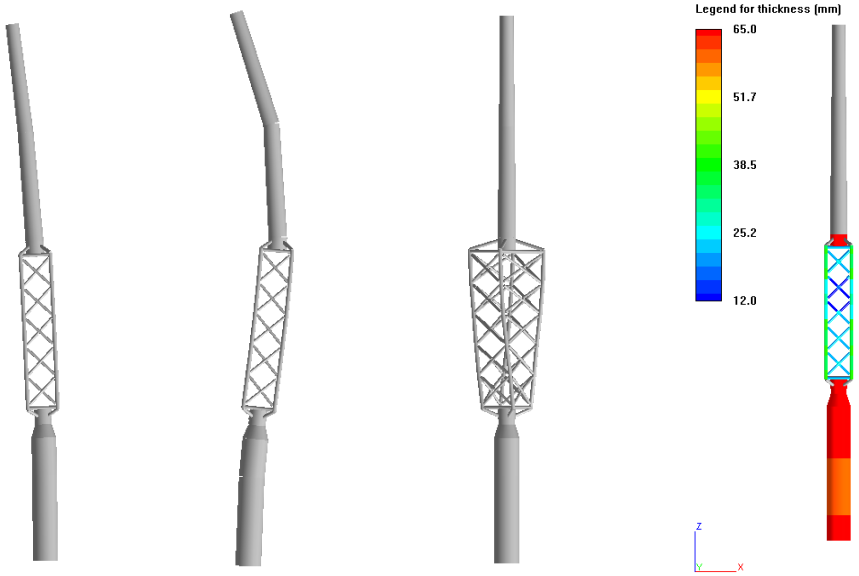


Figure 8.7: Results for Monopile - truss hybrid: First (a) and second (b) fore-aft bending mode shapes, first torsion mode (c), wall thickness (d)

#### Ultimate limit state

The required penetration depth for the monopile truss hybrid is 28 m. The maximum base shear is 7.4 MN and the maximum overturning moment is 345 MNm, both occurring for the maximum 50 year wave height. While still sizeable, these values are significantly less than for the monopile structure. The highest utilisations are found in the pile near the seabed.

### Fatigue limit state

The fatigue analysis shows that also the hydrodynamically induced fatigue is significantly reduced. Near the seabed the fatigue life is lowest, but still sufficient at 21.1 years. In the lower part of the vertical members of the truss the fatigue life is slightly higher at 27.7 years. For all other members the fatigue life is substantially higher than the required 20 years.

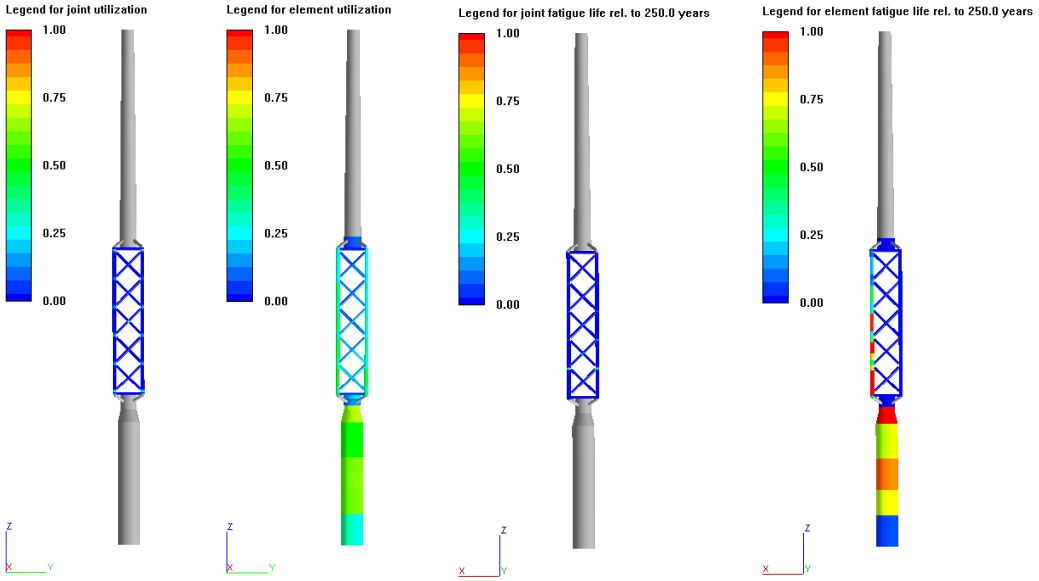


Figure 8.8: Monopile -truss hybrid: Joint utilisation (a), element utilisation (b), element fatigue damage (c) and joint fatigue damage (d)

### Structure mass

The overall structure mass for the monopile - truss structure is 1221 ton, including the tower (216 tons), the truss transition piece at 350 tons and the foundation pile at 656 tons. The width of the truss transition piece is 9 m. and the foundation pile diameter is 7.5 m.

## 8.4.3 Tripod

### Natural frequency analysis

The first natural frequency for the tripod is at 0.28 Hz and the second natural frequency is at 0.944 Hz. The first two bending mode shapes in the fore-aft direction are shown in Figure 8.9 (a) and (b) and the torsion mode is shown in Figure 8.9 (c).

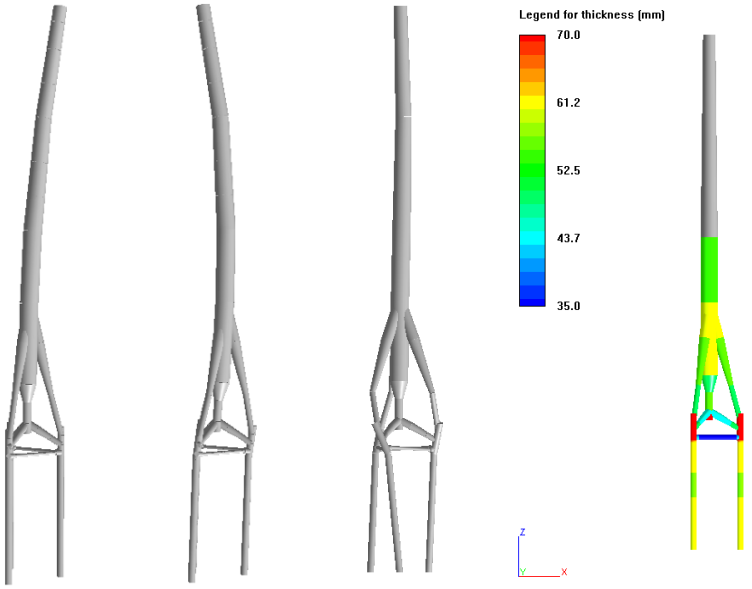


Figure 8.9: Results Tripod: First (a) and second (b) fore-aft bending mode shapes, first torsion mode shape (c),

### Ultimate limit state

For the ultimate limit state a maximum base shear of 8.6 MN is found and a maximum overturning moment of 352 MNm. The values both occur for the maximum 50 yr wave height. The required penetration depth is 30 m.

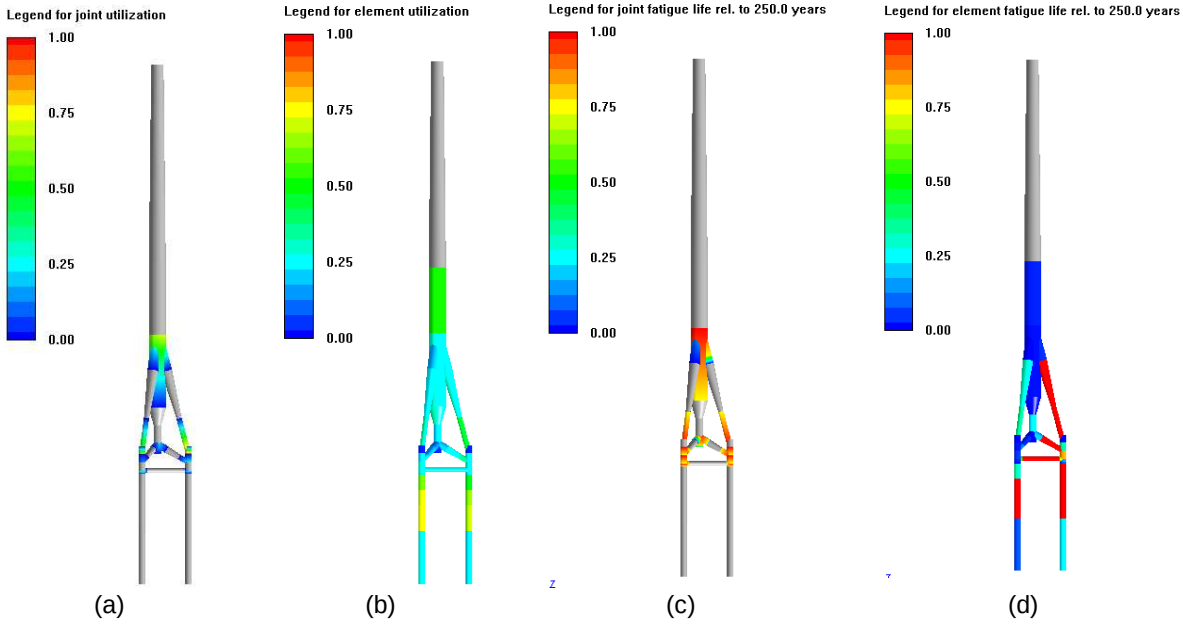


Figure 8.10: Joint utilisation (a), element utilisation (b), element fatigue damage (c) and joint fatigue damage (d)

**Fatigue limit state**

The fatigue limit state analysis for the tripod structure shows some very low fatigue lives both for joints, as seen in Figure 8.10 (d). These are partly due to high stress concentration factors. Also the high wave loading leads to large stress ranges.
In the study presented these fatigue lives have not been reduced to meet the fatigue requirements.

**Structure mass**

The overall structure mass is 1631 tons, of which 1074 is the substructure and 340 tons accounts for the piles. Finally the tower complements the mass with 216 tons.

### 8.4.4 3-leg jacket

The three leg-jacket appears to be suitable for the given conditions. However, fatigue is pronounced near the leg joints. This is partly due to the higher stress concentration factors due to the proximity along the circumference of the leg of the incoming braces. In this case the piles seem to be relatively heavy. There is room for further optimisation of the wall thickness of the piles.

**Natural frequency analysis**

For the three-leg jacket a base radius of 10 m and a penetration depth of 34 m leads to a first natural frequency of 0.30 Hz. To avoid getting into the 3P range at 0.31 Hz the radius cannot be larger.

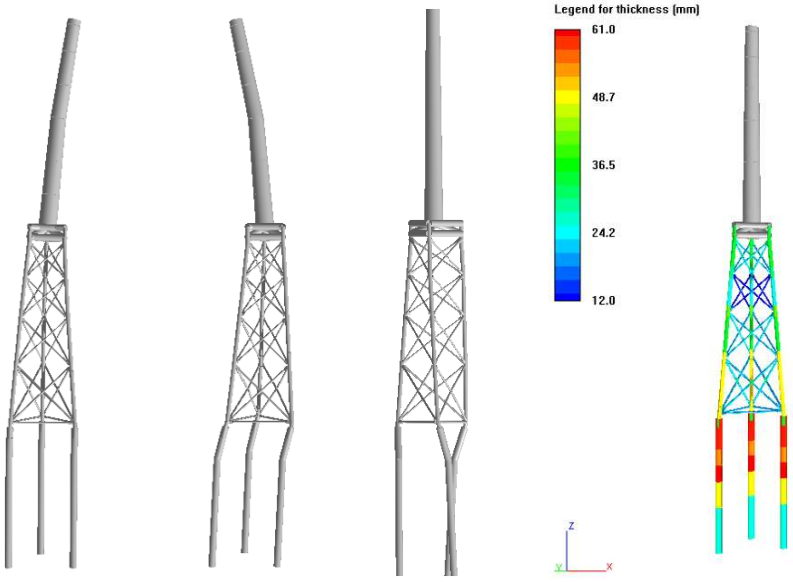


Figure 8.11: Results for Three-leg jacket: First (a), second (b) and torsion (c) mode shapes and wall thickness (d)

**Ultimate limit state**

From the ultimate limit state analysis it becomes clear that the base width must be at least 10 m to avoid overstressing the piles. The pile penetration is 32 m to satisfy the requirements for both soft and hard soil. The maximum base shear is 6.1 MN and the overturning moment is 260 MNm. The maximum utilisation in the jacket substructure is located in the lower X - braces near the legs

**Fatigue limit state**

For the Three-leg jacket the fatigue damage concentrates at the joints on the legs, in particular around the water line and at the legs between the mudbrace and the pile. The lowest fatigue life found is 15.61 years at the connections of the X braces with the legs at the top of the third X-brace panel from the seabed. The fatigue results are shown in Figure 8.2 (c) and (d).

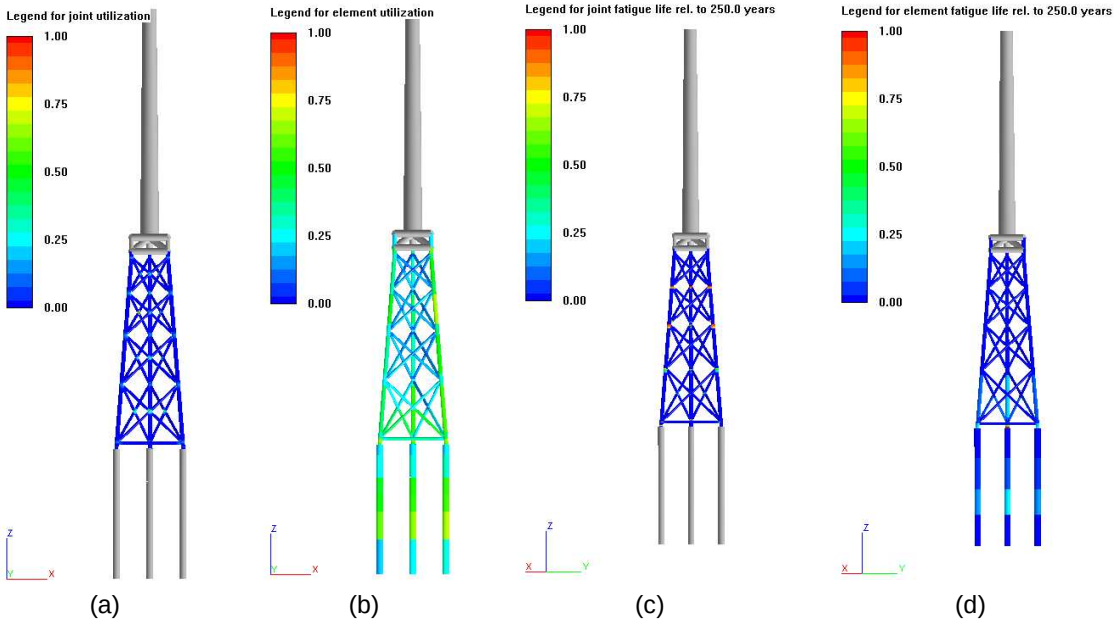


Figure 8.12: Joint utilisation (a), element utilisation (b), element fatigue damage (c) and joint fatigue damage (d)

**Structure mass**

The total structural mass is 929 tons. Of this value 301 tons are contributed by the piles and 414 tons by the substructure itself. The tower makes up the remaining 216 tons.

## 8.5 Conclusions

Figure 8.13 shows an overview of the masses of the support structures presented in this chapter, together with the mass of the reference jacket from Chapter 7.
In some cases the differences between the concepts investigated are substantial. In particular the reference monopile has a very large mass.
The three leg jacket is lighter than the four leg jacket, due to the fact that it has one leg and one set of X-braces less than the four leg jacket. However, it should be kept in mind that for the analysis of the three-leg jacket only a simplified approach is followed whereas the reference design has been subjected to an extensive load case set, and a more detailed analysis may have yielded more severe loads. From a mass perspective the three-leg jacket may be competitive with the four leg jacket. Whether this can be achieved is eventually very much dependent on detailing and production costs.

The tripod is significantly heavier than both jacket structures. In this analysis the optimisation of the tripod is not taken into sufficient detail to give a final statement about the overall mass for the given conditions. However, it seems unlikely that the tripod concept presented here can be sufficiently reduced in mass to compare favourably with the other concepts (save the monopile) in the given conditions

The monopile - truss hybrid is slightly heavier than the four-leg jacket concept, but substantially lighter than the tripod. Also the difference in required mass compared to the reference monopile is very large showing that the application of a truss transition piece can significantly reduce hydrodynamic loading. This may prove more effective in intermediate shallower waters. To enable more reliable statements regarding this concept, time domain simulations should be performed, to check whether the application of 5% aerodynamic damping is justified, since the excitation of the structure by waves is significantly reduced.
Finally, whether such a structure is suitable for offshore application depends highly on production costs. The concept is developed with mass production of the truss transition pieces in mind, so that the costs of producing multi-jointed structures can be produced. The remaining element is a large diameter pile, which is relatively simple to produce, provided that its dimensions do not exceed manufacturing capabilities.

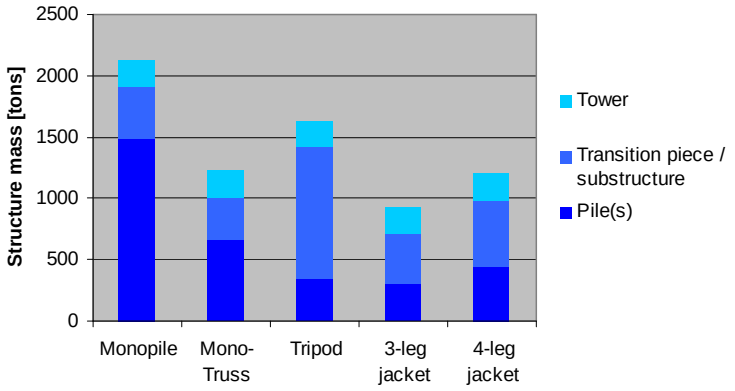


Figure 8.13: Overview of structural mass for the five concepts

It is emphasized that the analysis of the structures in this chapter is based on a simplified approach. To determine the loads more accurately an integrated time domain analysis must be performed, both for the ultimate limit state as for the fatigue limit state. After optimising the structures based on such a detailed analysis, more conclusive remarks can be made regarding the relative suitability of the three leg jacket and four leg jacket and the monopile-truss hybrid.

# 9. Compliant structures

## 9.1 Introduction

### 9.1.1 Soft-soft bottom mounted structures

As stated in Section 5.4 the most common way to design a support structure for an offshore wind turbine is to tune the structure to have the first natural frequency within the soft-stiff range. Conceivably the structure can also be designed to have a first natural frequency in the soft-soft range, below the rotor frequency. This has the advantage that less material is required to achieve the required stiffness of the structure. However, for offshore wind turbines the lower bound of the 1P range usually lies around the peak of the wave spectrum, where the energy in the waves is largest. To design a soft-soft offshore wind turbine support structure the first natural frequency must be well below the wave frequencies with appreciable energy, making it a true compliant structure.

This type of structure is known from the offshore oil and gas industry where it has been applied for deep water developments where rigid fixed support structures would be prohibitively large and expensive.

In this chapter the feasibility of applying this concept for offshore wind turbines is investigated. Therefore the lessons from the oil and gas industry are heeded to develop concepts for compliant offshore wind support structures. Also a preliminary assessment is made of several promising concepts.

### 9.1.2 Definition of compliant structures

Compliance can be defined as “degree of yielding under applied force”. Applying this definition to offshore structure implies the following definition for compliant offshore structures:

“A compliant offshore structure is a structure in the marine environment that accommodates the (dynamic) forces by flexibility instead of resisting the loads rigidly, thereby limiting the internal (dynamic) loads.”

### 9.1.3 Approach

As the compliant offshore structure concept originates in the offshore oil and gas industry, this chapter starts off in with a look into the history of compliant structures in that field of engineering. In the following sections the theory behind compliant structures is described. Subsequently the boundary conditions of offshore compliant structures are described as well as how they can how they can be met. A preliminary assessment of selected compliant support structure concepts for offshore wind turbines is presented

## 9.2 Overview of compliant structures in the offshore oil industry

In the mid 1970s developments in the oil & gas industry were taking place in increasingly deep water. Particularly in the Gulf of Mexico, the traditional approach of designing bottom mounted support structures with a natural frequency higher than the prevailing wave frequencies became more and more challenging. In 1978 the Cognac platform was installed in 312 m of water depth. At the time it seemed that the depth limit was reached for fixed (steel) structures. Eventually the record set by the Cognac development was to be surpassed by the Bullwinkle platform in 1988. Standing in 412 m of water, it was a gargantuan undertaking. Building and installing this structure was extremely expensive, drawing on the largest equipment available to get it in its final position over the Manatee field. It was clear that other solutions were needed and engineers were wondering whether the support structure could be designed to be slender and flexible enough to move with the waves instead of resisting them. This resulted in a design for a guyed tower for the Lena field in the Gulf of Mexico which was installed in 1983. Plunging oil prices in

the mid 1980s meant that massive projects in deep water were suddenly highly unattractive and the guyed tower concept was not to be repeated again. But the idea of the compliant tower as a more cost-effective alternative to a jacket structure in deep water lingered and was finally put to practice in 1998. In that year two compliant structures were installed, pushing the depth record for bottom mounted support structures to 535 m. After the Baldpate and Petronius structures no compliant towers were constructed for a decade, preference being given to floating structures for deep water developments. The compliant structure made its comeback with the construction and installation of the Benguela/Belize compliant tower off the coast of Angola. The recent installation of the compliant tower for the Tombua Landana field, again off the coast of Angola, shows that the compliant structure is still a viable solution for deep water hydrocarbon production developments. In the following a brief description is given of the compliant structures installed to date.

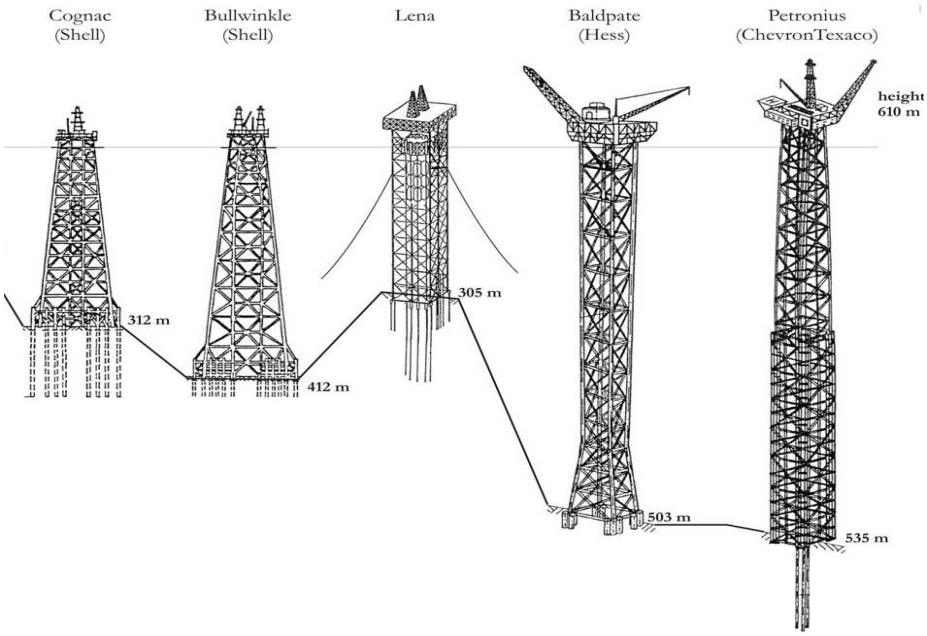


Figure 9.1: Comparison of different support structures [32]

**Lena guyed tower**

The first compliant structure to be installed was the Lena guyed tower in the Mississippi Canyon. It relies on a flexible foundation pile arrangement at the tower base to ensure sufficient bending flexibility and was fitted with guy wires, with clump weights lying on th seabed. During storms the weights would be lifted off the seabed, giving the structure a more flexible behaviour, decreasing its natural frequency away from the wave frequencies. Twelve buoyancy cans were incorporated in the upper part of the structure [32] [33]

**Baldpate**

In 1998 the Baldpate platform was installed in the Gulf of Mexico in water 503 m deep. The structure is free standing, transferring lateral and vertical loads to the seabed through its foundation piles. To ensure sufficient flexibility an articulation point that acts as a hinge allows the upper section to be compliant under storm conditions.

**Petronius**

The Petronius Compliant structure is located in the Viosca Knoll block in the Gulf of Mexico. It stands in 535 m of water and is composed of two tower sections. It is the tallest bottom mounted offshore structure ever built.. The structure relies on flex piles to give the structure its flexibility. The flex piles - three at each corner - are fixed to the structure only at the top of the piles and near the base. Guides provide lateral restraint at regular intermediate intervals.

**Benguela/Belize**

In 2005 the Benguela/Belize compliant piled tower was installed for Chevron off the Coast of Angola. Similar to the Petronius structure it is supported by 12 flex piles. The Flex piles are connected to the space frame at a point 120 m below the sea surface. To ensure sufficient flexibility the piles are not restricted in their axial motion. This is achieved by running the piles through a series of guides, providing lateral support of the piles.

**Tombua Landana**

The latest compliant tower to be installed is the support structure of the Tombua Landana field. This structure of the Compliant Piled tower type is situated off the coast of Angola in approximately 370 m water depth. It was installed in several phases in the course of 2008.

An overview of the key data for the aforementioned projects can be found in Table 9.1. To illustrate the size and general layout of a compliant structure in the offshore oil industry the Baldpate platform can be seen in Figure 9.2. Also depicted is the support structure on transport.

Table 9.1: Key data of compliant structures in the offshore oil and gas industry

| Description | | Lena Guyed tower | Baldpate | Petronius | Benguela/ Belize | Tombua Landana |
|---|---|---|---|---|---|---|
| Year of installation | | 1983 | 1998 | 1998 | 2005 | 2008 |
| Water depth | m | 305 | 503 | 535 | 390 | 366 |
| Topsides | ton | 4,900 | 2,400 | 7,500 | 35,000 | 30,000 |
| Structure weight | ton | 27,000 | 28,900 | 43,000 | 49,300 | 36,700 |

Figure 9.2: Baldpate platform in place (left) [9] and tower section during transport [48]

It is clear that in the offshore oil and gas industry compliant structures are sizeable structures. However, they are suited for water depths where normal fixed structures become uneconomic. In the described projects several features were incorporated that may also be applicable for compliant structures for offshore wind turbines.

## 9.3 Theory of compliant structures

### 9.3.1 Dynamics of a single degree of freedom system

Figure 9.3 (a) shows a single degree of freedom mass-spring-damper system. In Figure 9.3 (b) its response to harmonic loading is given. In the low frequency range the mass responds quasi-statically. With increasing frequency, the system starts behaving dynamically. When the load frequency approaches the natural frequency of the system, resonance occurs. Beyond the natural frequency the phase difference between the load and the response of the system becomes opposed and the magnitude of the response displacements decreases. Eventually, the displacements become smaller than the quasi-static displacements. The three different frequency ranges described here are the stiffness controlled zone, the damping controlled zone (as the level of damping present in the system determines the height of the resonance peak) and the inertia controlled zone respectively, as illustrated in Figure 9.3 (b). By dividing the dynamic response by the static response for each frequency, the dynamic amplification factor (DAF) is obtained.

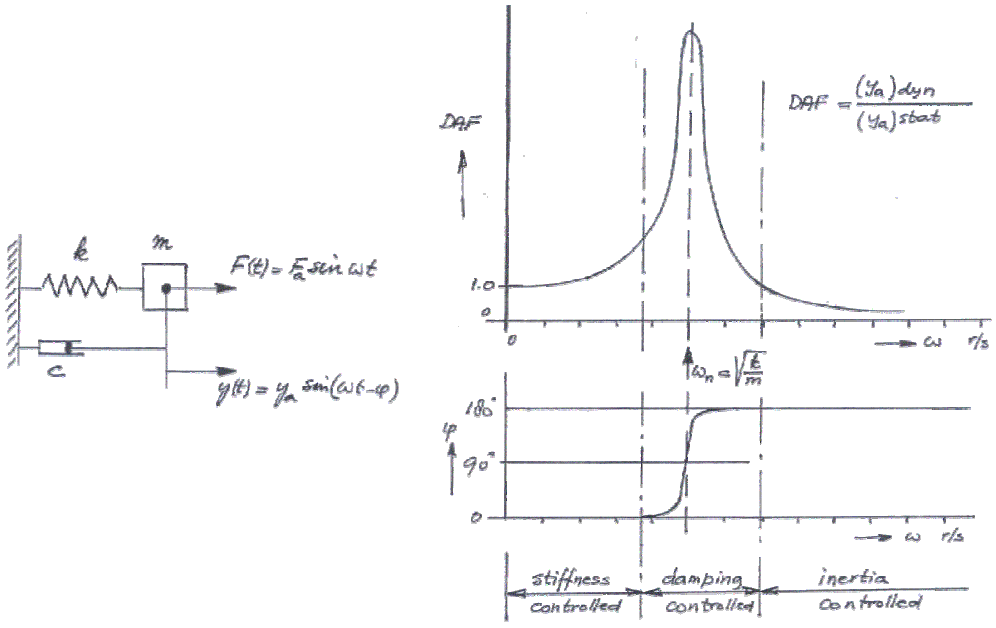


Figure 9.3: Dynamics of a single degree of freedom mass-spring-damper system [34]

### 9.3.2 Response to wave loads on offshore structures

The previous section shows how a single degree of freedom system behaves when it is excited by a harmonic load. While simplified, this behaviour is representative for most offshore structures. However, as an offshore structure can be considered to be made up of many elements it will in reality have an unlimited number of natural frequencies. Most of these are in the high frequency range, well outside the wave excitation range. Therefore considering only the first few mode shapes and frequencies will be acceptable in order to describe the structure's dynamic response.

In the offshore environment the waves will usually not be regular harmonic. Instead the sea surface elevation may be described as the result of many different superimposed harmonic waves, each with their own frequency, wave height and direction. If the wave components are assumed to be coming mainly from a single direction, the sea state can be described by a single wave spectrum. This wave spectrum shows the relation between the wave amplitudes and the wave frequencies, in essence showing the distribution of wave energy over the frequencies.

For each of the considered modes the structure's response to every single frequency present in the wave spectrum can be determined, thus obtaining the wave response spectrum. This is shown schematically in Figure 9.4. The response spectrum shows a peak at the wave spectrum peak and at the natural frequency of the structure.

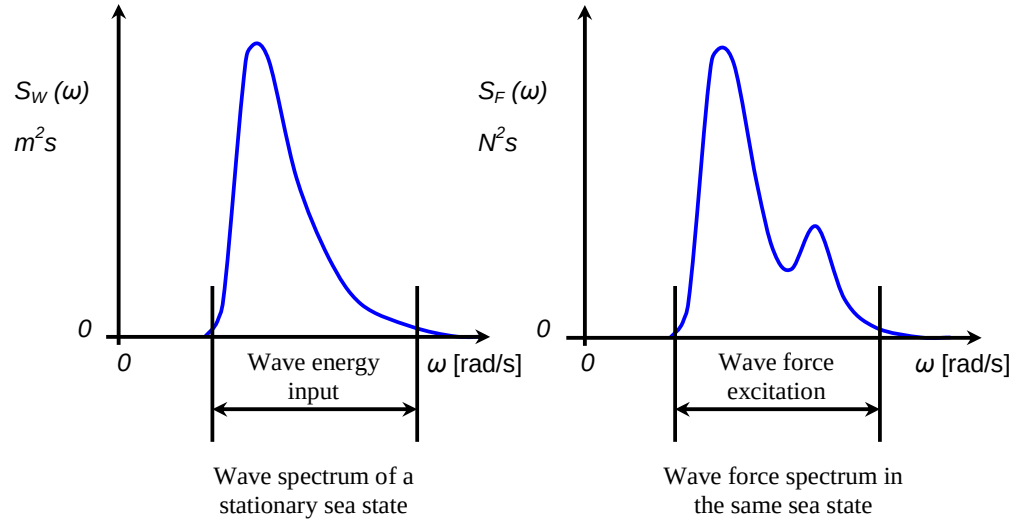


Figure 9.4: Schematic model of response at sea [34]

The magnitude of the response peak at the natural frequency depends both on the structure's dynamic response at the natural frequency as given by the DAF and the magnitude of the energy present in the waves at frequencies around the natural frequency. This is illustrated in more detail in Figure 9.5. Structure 1 has a natural frequency of approximately 0.33 Hz. This is well above wave frequencies with appreciable wave energy. Consequently the response at its natural frequency is small. However, the quasi-static response at lower frequencies is significant. For decreasing natural frequency it can be seen that the response for frequencies larger than the natural frequency decreases as this is in the inertia dominated range, but the resonance peak increases due to the increased energy content at that frequency. Structure 5 has a frequency below the frequencies with any significant energy content. It can clearly be seen that the resonance peak is relatively low and there is no longer any quasi static response as there is no energy content in the wave spectrum for those frequencies.

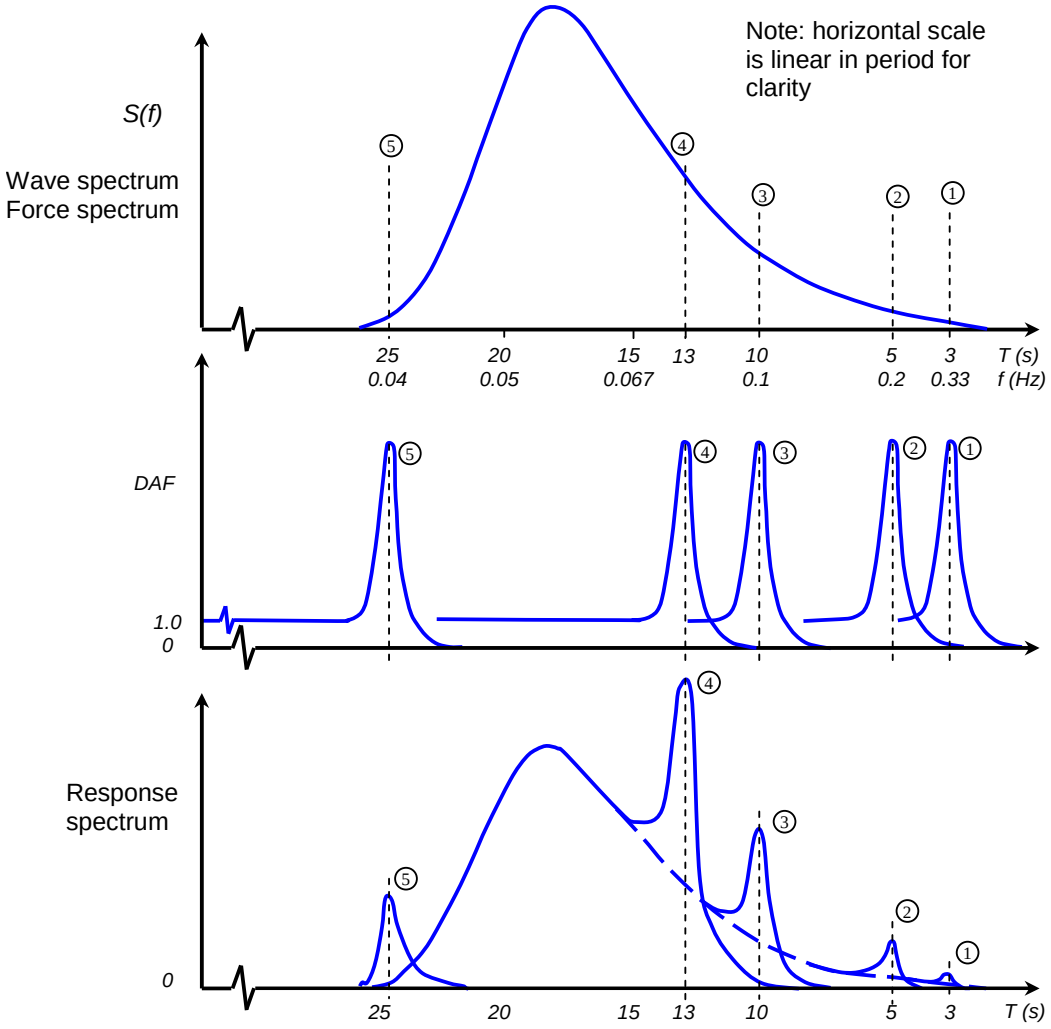


Figure 9.5: Response for structures with different natural frequencies [34]]

### 9.3.3 Design of fixed offshore structures

For fixed offshore platforms the general approach is to design the structure such that the fundamental natural frequency is higher than the wave frequencies with high energy content in order to avoid resonance. Resonance can lead to excessive dynamic response under extreme conditions, but also under operational conditions, which in turn leads to a reduced fatigue life.

This approach requires the support structure to be sufficiently stiff. The stiffness requirement can usually be achieved by placing the legs far apart in order to achieve a high area moment of inertia and by giving the legs sufficiently large diameter.

For shallow water this is a practical approach, but for deep water this results in impractical dimensions and excessive material use, which adversely influence the costs, both for fabrication as well as for installation.

### 9.3.4 The principle of compliant structures

In Figure 9.5 it can be seen that the response of a structure is significantly reduced when the fundamental frequency is below the lower boundary of the wave energy spectrum. This principle is adopted for the design of compliant structures, where the first natural frequency is positioned below the lowest wave frequencies with appreciable wave energy. At the same time it should be

avoided that the second natural frequency coincides with wave frequencies in the high end of the spectrum. Therefore the structure must also be designed such that the second natural frequency is positioned above the highest frequency with appreciable wave excitation. This principle is illustrated in Figure 9.6.

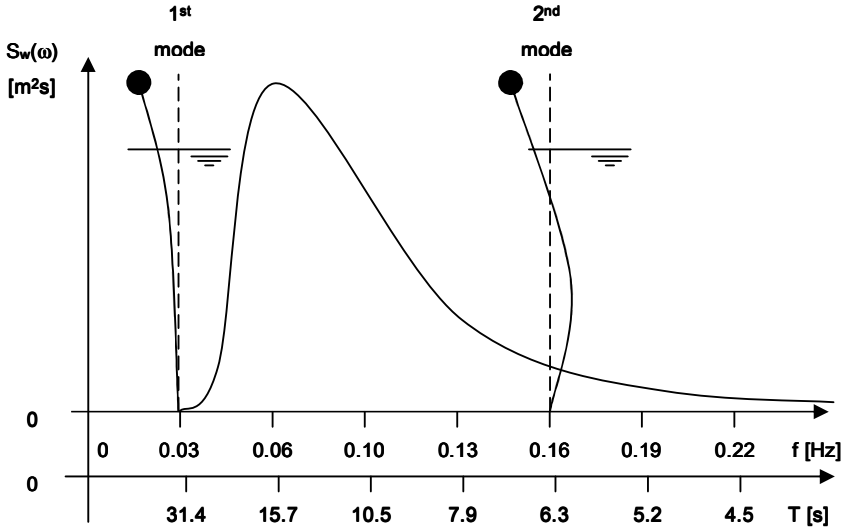


Figure 9.6: Principle of compliant structure design

For the design of the structure this means that the mass and stiffness distribution in the structure should be such that the first natural frequency lies below the lowest frequencies in a severe sea state whereas the second natural frequency lies above the highest frequencies with appreciable excitation in that severe state.
The challenge in designing a compliant structure lies in the fact that the first and second natural frequency should be sufficiently far apart and at the same time the structure should be able to withstand (quasi)-static loading from wind, currents and mean wave drift forces. Some form of restoring force will therefore be necessary.

## 9.4 Modelling aspects for compliant structures

### 9.4.1 Introduction

This chapter describes several aspects that should be considered when modelling a compliant structure. First, general modelling considerations such as influence of water depth and mass modelling are described. Subsequently, the boundary conditions relevant to compliant structures are discussed. Ways of achieving these requirements are also treated.

### 9.4.2 General modelling considerations

**Water depth**

Water depth strongly influences the natural frequency as it determines the length of the structure from seabed to topsides. This length in turn influences the flexibility of the structure. The longer the structure is, the lower its natural frequency.

**Mass modelling**

The top mass of the structure influences the natural frequencies of the structure strongly. The larger the top mass the lower the natural frequency. The top mass represents any large masses that can be assumed to be concentrated in a local centre of gravity. In the case of an offshore oil

platform this could be the deck, accommodation, and processing equipment. In the case of an offshore wind turbine this is usually the rotor nacelle assembly.
The mass of the support structure cannot be assumed to be concentrated in a single point, due to the influence of the position of the mass on the natural frequency. Therefore the support structure is usually modelled as a distributed mass. This in turn can be modelled as a series of concentrated masses at regular intervals. The distributed mass is made up of the mass per unit length of the primary support structure, any marine growth or contained water in flooded members and additional elements that span the length of the support structure such as risers or cables.
Any other elements on the support structure that have large mass can be represented by lump masses.

### 9.4.3 Boundary conditions

#### Foundation

The foundation transfers loads from the support structure to the seabed. The foundation must always be designed such that the vertical loads as well as the base shear can be directed into the soil. In some cases the foundation should be able to transfer bending moments to the soil as well. For certain concepts the foundation should provide the flexibility required to make the structure compliant. Three means of creating a flexible foundation are mentioned in the following sections.

#### Restoring force

While the compliant tower requires sufficient flexibility for the dynamics, it should also have a restoring force of some sort in order to reduce the deflections of the structure under extreme loading. As these static deflections will usually be largest at the top of the structure, the restoring force should act as high up as possible. The restoring force acts as a spring. With increasing deflection, the restoring force also increases thereby causing the structure to move towards the neutral position. Two main ways of generating a restoring force are discussed in the following.

### 9.4.4 Foundation solutions

#### Hinge

The application of a hinge can be achieved by a true hinge in the form of an articulated joint or by deliberately incorporating soft spots into the structure. The articulated joint has been applied in the past in several offshore structures such as mooring towers and flare towers. Most notably an articulated joint was applied on the North East Frigg platform in the North Sea. The application of the soft points in the structure was applied on the Baldpate compliant tower. It should be noted that the hinge need not necessarily be located at the seabed.

#### Piles

Another way of introducing flexibility into the support structure is to design the foundation piles to allow the structure to rotate around the seabed, acting like a pin joint. To obtain this behaviour, the piles should not be spaced too far apart. This approach was applied for the Lena guyed tower where 12 piles were installed in a circle at the centre of the base of the support structure. Unfortunately, placing the piles close to the centre reduces their capacity to transfer torsion loads to the soil. This was solved at the Lena tower by placing a number of torsion piles at the corners of the structure base. These torsion piles should not be allowed to transfer significant loads in axial direction.
A foundation can also be compliant piled. Flex piles are connected to the space frame at a point below the sea surface. To ensure sufficient flexibility the piles are not restricted in their axial motion. This can be achieved by running the piles through a series of guides, providing lateral support of the piles.

**Spud can**

A spud can is a large diameter conical shell that penetrates slightly into the soil and relies on end bearing to transfer the vertical loads to the soil. This type of foundation is common in jack-up structures. If a single spud can is used, its behaviour will resemble a hinge. However, it is not particularly well suited to transferring lateral loads, which may result in slip.

### 9.4.5 Restoring force solutions

**Buoyancy**

By including a buoyancy tank in the support structure an upward buoyant force is present. When a lateral load causes an excursion of the structure from its neutral position, the structure is under a slight angle with the vertical. The buoyant force can be decomposed in a component parallel to the structure main axis and a component perpendicular to the axis. The perpendicular component causes a moment around the pivoting point of the structure, returning the structure towards the neutral position. Buoyancy tanks are preferably located below the zone of significant wave action to avoid excessive wave loading, yet high enough to generate sufficient restoring force.

**Guy wires**

The restoring force can also be achieved by using guy wires. Guy wires can either be taut or follow a catenary shape. Taut wires will give the system too high spring stiffness, however, so for compliant structures the catenary configuration must be employed. The catenary wire system obtains its stiffness from the weight of the mooring system. In the neutral position a considerable length of the cable is lying on the seafloor. When the structure moves away from its neutral position a larger part of the cable is suspended and more of its weight contributes to the tension in the cable. The force at the end of the cable can be decomposed into a horizontal contribution and a vertical contribution. The more taut the line becomes, the larger the horizontal component and the larger the restoring force.
Occasionally, clump weights are added to the guy wire system. Under normal operational conditions these will be lying on the seabed, causing the system to behave stiffer. During extreme sea states, when compliant behaviour requires a lower stiffness the forces generated are large enough to pick the clump weight off of the seabed. The additional length of line thus mobilised, the system behaves more compliant.

**Structure stiffness**

Naturally, the stiffness of the structure itself can also be used to serve as a restoring force. It is however a challenge to accommodate both the dynamic requirements and to keep the displacements in check during extreme loading conditions. A possible way to overcome this is to rely not only on the structural stiffness but additionally on a restoring force such as buoyancy.

## 9.5 Compliant support structure concepts

### 9.5.1 Concepts for offshore wind

**Introduction**

In [35] compliant structure concepts employed in and proposed for the offshore oil and gas industry were described. These concepts can also be applied for offshore wind turbines. However, due to differences in boundary conditions, most notably top mass, required (deck) space, water depth, lateral loads and cost efficiency requirements, the eventual shape will be different than the equivalent concepts in the oil and gas industry. The concepts found in the offshore oil & gas industry are as depicted in Figure 9.7.

a) "Dumb" tower
b) Compliant piled tower
c) Compliant tower with 'mass trap'
d) Buoyant tower with flex joint
e) Guyed tower with flex joint
f) Articulated column

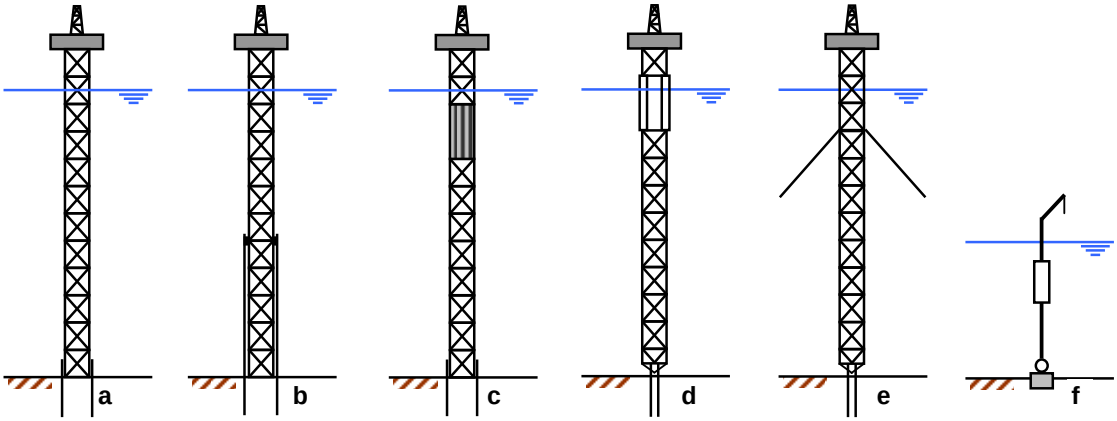


Figure 9.7: Compliant tower concepts in the oil and gas industry

**Slender monopile ("dumb tower")**

The "dumb" tower could be a simple extension of the monopile concept, where the diameter of the monopile could be reduced to attain the desired fundamental frequency, resulting in a slender monopile. An illustration of this concept can be seen in Figure 14a. However, great care should be taken that the second natural frequency is still in the right range and that the structure does not succumb to buckling due to the large bending moments in combination with the small section modulus. Furthermore, it should be ascertained that the structure has sufficient static resistance to keep top deflections within tolerable limits.

**Guyed tower**

One way to mitigate the problems mentioned in the previous section is to add a restoring force in the form of guy wires, as illustrated in Figure 14b. While this can alleviate the internal stresses due to quasi static loads, the practical issues associated with guy wires make it a challenge for installation, particularly for offshore wind, where the structures are to be installed in large numbers.

**Buoyant tower**

Another option for the restoring force is the inclusion of a buoyancy can. This is shown in Figure 14c. Not only does this help to accommodate the quasi static loads, but it also exerts an upward force on the structure, thereby reducing the risk of buckling. Incorporating a buoyant section in the tower may also be beneficial from an installation point of view. It should be noted that to make this option effective, the remainder of the structure should be flooded below the sea surface.

**Articulated buoyant tower**

While the buoyant tower as indicated in the previous section may be viable for large water depths, it may still suffer from the same problems as the "dumb" tower for shallower sites. To increase the flexibility of the support structure an articulated joint can be included near the seabed. (See Figure 14d) This situation gives the designer sufficient possibilities to tune the structure to achieve the appropriate dynamic and static behaviour.

**Tower with mass trap**

As for the offshore oil and gas concepts it is also possible for offshore wind turbine structures to influence the natural frequencies by adjusting the mass properties. Including a mass trap may however be more difficult to achieve as the structure should be transparent to avoid vertically supporting the enclosed water mass by the structure itself. A truss type structure is one way to achieve this. (See Figure 14e)

**Compliant piled tower**

Finally, the compliant piled tower concept may be adopted to ensure compliant behaviour. However, as this structure relies on several piles connecting to the structure at certain elevation above the seabed, this can likely only be achieved for a spaceframe structure as depicted in Figure 14f.

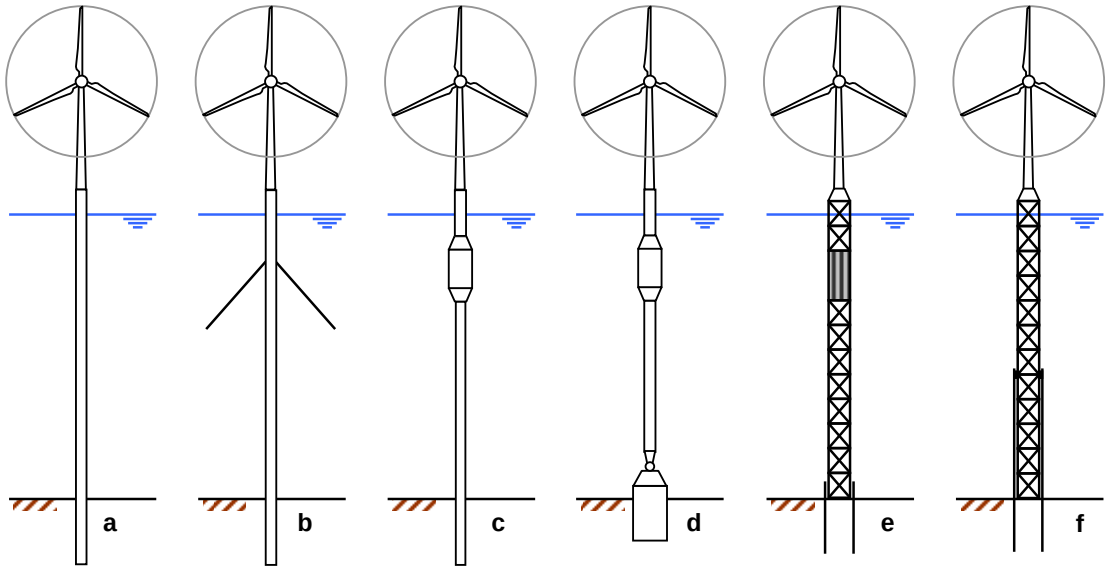


Figure 9.8: Compliant tower concepts for the offshore wind industry

a) Extended monopile (“dumb tower”)
b) Guyed tower
c) Buoyant tower
d) Articulated buoyant tower
e) Tower with mass trap
f) Compliant piled tower

## 9.6 Preliminary designs

### 9.6.1 Introduction

From the concepts shown in Figure 9.8, 3 concepts have been selected for closer investigation. These are the extended monopile, the compliant piled tower and the articulated buoyant tower. The extended monopile is selected as it is the simplest possible structure, with only the diameter and wall thickness as parameters for tuning the dynamics of the structure. This concept serves well as a reference, also for comparison with regular monopile structures.
Secondly, the compliant piled structure is selected as it is the most frequently applied structure type in the offshore oil industry.

In the previous two concepts the restoring force is derived from the structural stiffness alone. In the third concept the restoring force is derived from the buoyancy provided by the buoyancy can. Because of the entirely different concept this is an attractive alternative concept to be included in the study.
Figure 9.9 gives a graphic representation of the concepts as used in the study.

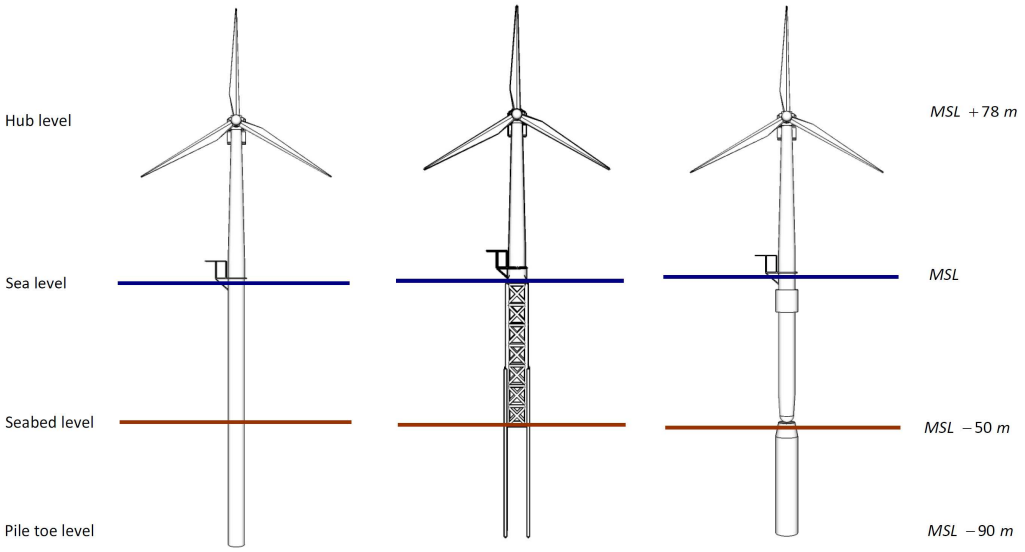


Figure 9.9: Illustration of selected compliant structure concepts [36]

### 9.6.2 Design data

As seen in the examples for the offshore oil and gas industry, compliant structures are well suited for deep waters as the increased length leads to increased flexibility of the support structure. For this study the K13 deep water site was used [13]. The most important design parameters for this study are repeated here:

#### Turbine

The turbine used in this study is the UpWind 5.0 MW Reference turbine [5].Only mass data, the required minimum hub height, the maximum thrust force and the allowable frequency range are incorporated here. The allowable frequency range and target natural frequencies, marked in red, are illustrated in Figure 9.10. The first natural frequency should be below 0.1 Hz while the second natural frequency should be between the 1P and 3P ranges (0.22 Hz - 0.31 Hz) or above the 3P range (0.67 Hz).

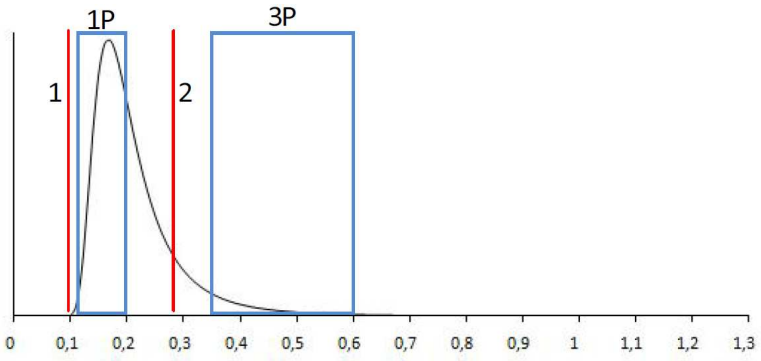


Figure 9.10: Allowable frequency range and target frequencies [36]

**Water depth**

The water depth at the site is 50 m.

**Soil**

For the analyses in this chapter the hard soil conditions as described in [13] were taken. This soil profile, consisting of sand with friction angles in the range of 38.0° to 42.5° is considered conservative for the purpose of designing a compliant structure as it will result in a higher first natural frequency than the soft profile.

**Load cases**

For the ultimate limit state the structure is subjected to a single conservative, simplified load case in which wind loads, current and extreme wave loads are applied together. Also the self generated weight is included.

Table 9.2: Key parameters used in compliant structure study

| Description | Unit | Value |
|---|---|---|
| Water depth | [m] | 50 |
| 100-yr extreme wave height | [m] | 18.41 |
| Associated wave period | [s] | 11.15 |
| Current velocity | [m/s | 1.2 |
| Maximum thrust force | [kN] | 1500 |

### 9.6.3 Models

**Extended Monopile**

The extended monopile is modelled in the DNV offshore structural analysis program Sesam [37] as a tubular with constant diameter and wall thickness up to the interface elevation. From the interface upwards to the tower top a conical tower is applied, with a tower top diameter of 4.7 m. The tower bottom diameter is scaled to match the diameter of the monopile. In this simplified model no transition piece is modelled.
The pile soil-interaction is modelled as p-y springs, with one spring placed every meter of the pile in the soil. The pile tip is constrained in the vertical direction, as is the torsion degree of freedom. In Figure 9.11 (a) the Sesam model of the extended monopile can be seen.

**Compliant Piled Tower**

For the compliant piled tower the substructure is modelled as a truss with seven levels of X-bracings. The structure is supported at the four corners by piles. The pile tips are fixed in the

vertical and torsional direction. The piles are fixed to the substructure at the top of the third X-brace level by hinges, with the translations in x, y and z direction equal to the translations of the substructure at the connection point and the rotations in all directions free. The piles are also connected to the structure base by means of hinges. For these connections also the vertical translations are released. The pile-soil interaction is again modelled by p- y curves. In Figure 9.11 (b) the Sesam model of the compliant structure can be seen.

**Articulated Buoyant Tower**

The articulated buoyant tower is an adaptation of the extended monopile. To increase the flexibility of the sub structure, a hinge is introduced at the base of the structure. Translations in x,y and z direction are constrained as well as rotations around the z axis. For the rotations around the x- and y-axes a low stiffness is applied.
This concept also requires a restoring force. This force is generated by buoyancy in the form of a buoyancy tank, located close to the sea surface. The buoyancy tank is modelled as a non-flooded member with an enlarged diameter. The modelling of the foundation is identical to the modelling for the extended monopile.

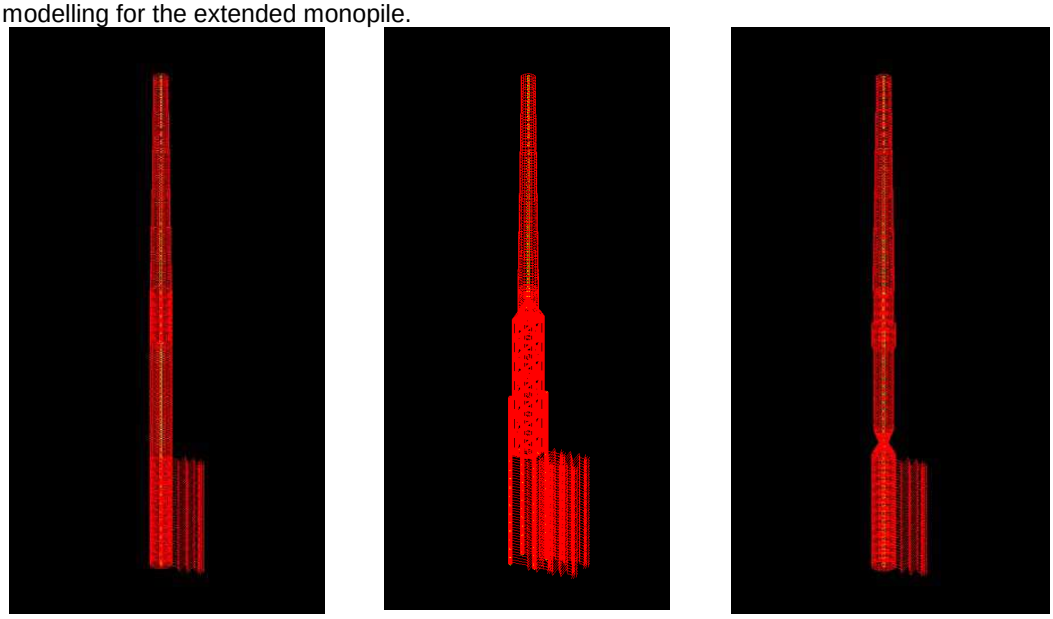

(a) (b) (c)

Figure 9.11: Sesam models of Extended monopile (a), Compliant piled tower (b) and Articulated buoyant tower (c) [36]

### 9.6.4 Approach

For each of the three descried models the structure is checked for the ultimate limit state. When the structure satisfies the criteria the first and second natural frequencies associated with the resulting designs are checked as well as the deflections at the tower top and the mudline.

### 9.6.5 Results

**Extended Monopile**

For the extended monopile in the conditions used in this study, it proved impossible to satisfy both the target natural frequency requirement and the criteria for the ultimate limit state. In Figure 9.12 the natural frequency results for the structure are shown. At 0.258 Hz the first natural falls within the soft-stiff range. This is due to the fact that the structure is optimised to satisfy the ultimate limit state requirements, requiring large diameter and wall thickness. The second natural frequency is at 0.883 Hz. The overall mass of the structure is 1779 tons, including the mass of the tower.

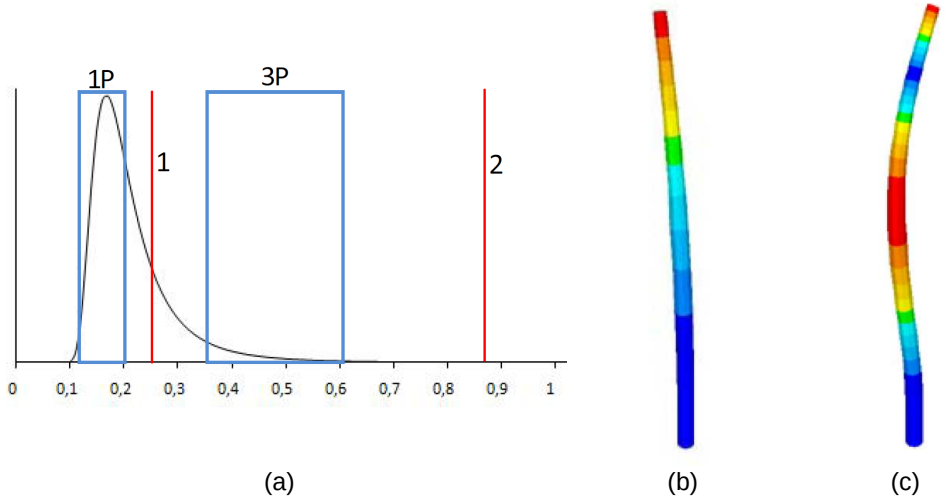


Figure 9.12: Natural frequency results (a), first (b) and second (c) mode shape for extended monopile [36]

**Compliant piled tower**

The compliant piled tower shows similar difficulties as the extended monotower in getting a sufficiently low first natural frequency while at the same time satisfying strength and stability criteria. The original width of the braced sections is increased from the original 7 meters to 10 m to reduce loads in the legs. The structure is optimised to satisfy the buckling and yield criteria, but thereby becomes too stiff for the first natural frequency to fall within the soft-soft range. In this case the first natural frequency, at 0.399 Hz even lies within the 3P range, as is shown in Figure 9.13. The second natural frequency is 1.160 Hz, well above the 3P range. The overall structure mass is 2100 tons.

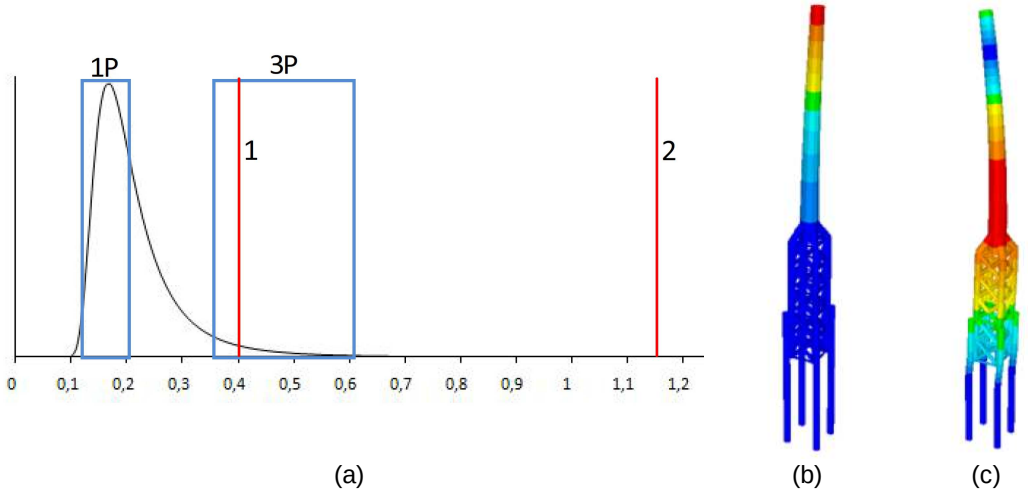


Figure 9.13: Natural frequency results (a), first (b) and second (c) mode shape for compliant piled tower [36]

**Articulated buoyant tower**

For the articulated buoyant tower the natural frequency requirements could be satisfied alongside the ultimate limits state requirements. The first natural frequency is 0.109 Hz, which puts it in the soft-soft region. Also the first natural frequency is below the wave frequencies with

appreciable energy, as shown in Figure 9.14 (a). The second frequency is relatively high at 0.850 Hz, safely above the 3P range. The structure is optimised to meet the strength and stability criteria. The resulting mass of the structure is 1688 tons.

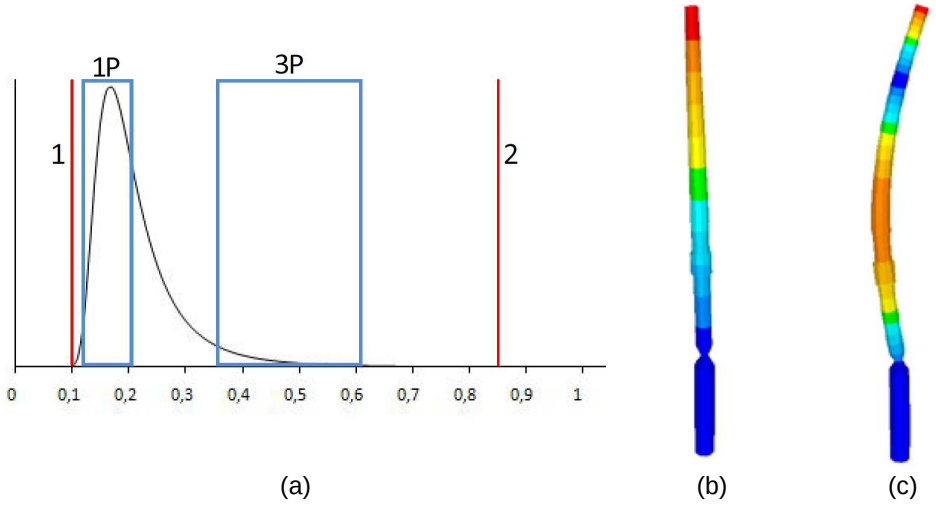


Figure 9.14: Natural frequency results (a), first (b) and second (c) mode shape for articulated buoyant tower [36]

### 9.6.6 Discussion

In the previous it is shown that it is possible to design a compliant tower for an offshore wind turbine in 50 m water depth satisfying both ultimate limit state as well as natural frequency requirements, though only for the articulated buoyant tower. The mass saving compared to the extended monopile, which is essentially a soft-stiff monopile in 50 m water depth, is approximately 100 tons. For the extended monopile and compliant piled tower concepts, designing for extreme loads results in overly stiff structures, which do not meet the natural frequency requirements for a compliant structure. However, several remarks must be made regarding the assumptions in the described study.

First, the load case considered for the ultimate limit state is very conservative. Combining the maximum thrust force with the extreme wave height leads to overestimation of the maximum loads likely to occur during the structure's intended lifetime. Furthermore the 100 year return period selected for the extreme wave is too high. With a less conservative extreme load case, particularly the extended monopile and the compliant piled tower might have been designed softer.

Secondly, the optimisation procedure followed is simplified. The main elements are designed with constant wall thickness, dimensioned for the maximum occurring stress, but leaving other sections under utilised. Also the pile foundation is not optimised. A more detailed optimisation of the structures will allow a better comparison of the concepts with each other and with other fixed support structure concepts.

Thirdly, the load analysis is static. A dynamic analysis will do more justice to show the benefits of a soft-soft design compared to a soft-stiff monopile, for instance.

No fatigue analysis is included. For the articulated buoyant tower a frequency domain fatigue analysis based on wave loading only should show very low fatigue damage, in accordance with the theory. However, for the other concepts, with natural frequencies in the soft-stiff range the fatigue damage may become dominant, making the comparison of these concepts with the articulated buoyant tower less favourable.

Furthermore, apart from the static thrust force no effects of wind loading are incorporated in the presented study. This will remain an important factor in determining the feasibility of compliant structures in general, a feature shared with floating structures.

Finally, in this study only a water depth of 50 m has been considered. The proposed structures, particularly the compliant piled tower will become softer in larger water depths. It remains to be seen whether it will be possible to satisfy the extreme load criteria as well. The feasibility of the compliant pile tower is therefore inconclusive.

## 9.7 Limitations

### 9.7.1 Introduction

After analysing three concepts in the previous chapter some limitations will be mentioned briefly. These limitations are connected to the validity of load assumptions and to the limitations due to the incorporation of wind turbines

### 9.7.2 Validity of wind load assumptions

When dealing with simulating low frequency motions in aero-elastic tools, several limitations should be considered. The first problem is that low frequency motions tend to be large displacement motions that cannot be modelled by the strictly modal-based codes which require small displacements.

The second problem is that low-frequency motions have an aero-elastic influence on the rotor wake that is different than the influence caused by high-frequency motions. This is a problem because many of the aero-elastic models use an implementation that assumes that the time-scales of the turbine motions (vibrations) are much faster than the time-scales of the rotor wake. When modelling a wind turbine on a compliant support structure in such a program, the result of this is that the low-frequency motions will be modelled with less aerodynamic damping than is physical.

The third problem with low-frequency motions is that in nonlinear time-domain analysis it is required to run longer simulations in order to capture a statistically significant number of response cycles. For example, 10 minutes may be a good length for modelling stationary turbulence, but may not be long enough to capture a lot of cycles of very low-frequency motions.

### 9.7.3 Limitations for turbines

**Closest blade to tower approach**

One of the more obvious limitations of the application of wind turbines on compliant support structures is the closest distance of the blades to the tower during operation or in severe sea states during non operational states. Due to the large deflections of the tower the blades may hit the tower. To avoid this, a larger precone or tilt can be applied or the turbine may have a downwind configuration. The latter option may introduce more challenges than it is meant to solve, however.

**Other excitation sources**

In the previous it is indicated that the natural frequencies should not coincide with excitation frequencies. The focus was mainly on the wave frequency ranges with high energy content. Other excitation sources should also be considered.

Wind excitation has the highest energy content at low frequencies, leading to large quasi static response. Although the number of cycles in this range is relatively low and may therefore not significantly contribute to fatigue damage to the structure, it should be verified that no resonance

occurs. In any case the quasi static excitation can be significant and must be counteracted by some restoring force.

Secondly, most turbines operate at variable speed, thereby generating excitations corresponding to the rotational frequency of the rotor. This creates a frequency interval corresponding to the rotational frequency range (1P) in which the natural frequency may not be situated. Furthermore, each time a blade passes the tower an additional excitation is experienced, giving rise to an additional 'forbidden" frequency interval, the so called 3P range. The challenge now lies in the fact that the first natural frequency should be below the low frequency end of the wave spectrum and above the frequencies of the wind spectrum with high energy, while at the same time positioning the second natural frequency above the wave frequencies with appreciable wave energy, but avoiding the 1P and 3P frequency ranges. Furthermore it should be verified that further rotational frequency multiples do not coincide with higher modes.

**Control adaptation**

Controllers of wind turbines currently in the market are tuned to operation in the soft-stiff range. Adapting the control to operate in the soft-soft range is possible, but considering the low frequency motions associated with compliant structures, a significantly different approach is required. Lessons can be learnt from studies on floating structures, where large low frequency motions are also present

**Position of turbine**

The turbine is always located at a relatively large elevation above the sea level due to the fact that the entrance to the tower is at a sufficiently high location above the wave and that the tip of the blade in its lowest position should be a safe distance above that level. Therefore both the top mass and the thrust force on the rotor are at a large elevation above the sea level, resulting in a large overturning moment, without an effective form of restoring force.

## 9.8 Discussion and outlook

### 9.8.1 Feasibility of compliant offshore wind turbine support structures

Considering the principles of compliant towers, the boundary conditions and the limitations presented in this report it appears that applying compliant towers for offshore wind turbines will be challenging. The offshore industry has paved the way in terms of concepts, several of which can be adapted to suit the needs for offshore wind turbines.

Three concepts have been subjected to a preliminary evaluation: an extended monopile, a compliant piled tower and an articulated buoyant tower. Of these three concepts, only the articulated buoyant tower satisfies both the ultimate limit state analysis and the natural frequency requirements. The total structural mass of this concept is 1688 tons, heavier than most other fixed structures in 50 m water depth. However, further optimisation and less conservative load cases will reduce the mass. Also, for larger water depths the comparison with regular soft-stiff structures may become more favourable.

Some of the concepts suggested in this report, most notably the articulated buoyant tower show considerable similarities with floating structures, in particular with so called Tension Leg Platforms. Further research should take note of the work done in the field of floating offshore wind turbines. For the moment the economic feasibility of compliant structures can not be wholly confirmed or denied, although compliant structures could possibly be attractive when hybrid solutions of floating and bottom mounted structures are applied. These could be effective in intermediate water depths, where bottom mounted structures may no longer be viable and floating structures might still need too much buoyancy to be cost effective.

### 9.8.2 Avenues for further research

Several suggestions for further research can be distilled from the work presented in this report. First of all an evaluation of the mentioned concepts in terms of actual response under realistic operational conditions should be performed to determine the suitability of the proposed concepts.

Secondly, the impact of resonance of higher order modes with rotor frequency multiples should be determined and ways of avoiding this should be investigated. Also the response due to non-linear mean wave drift forces and low frequency wind excitation should be established.

Subsequently full time domain analysis of the behaviour of most promising compliant structure concepts, including (non-linear) boundary conditions should be performed.

Based on these considerations an assessment can be done and the more promising concepts can be selected for optimisation. Only then could a preliminary cost comparison be done to ascertain the attractiveness of the compliant structure with respect to bottom mounted or floating concepts.

# 10. Floating structures

Several support platform configurations are possible for floating offshore wind turbines, particularly considering the variety of the mooring systems, tanks, and ballast options that are used in the offshore oil and gas industries.

## 10.1 Floating support structure concepts

The three principal concepts—classified in terms of how the concepts achieve static stability—are:

1. A shallow drafted barge, achieving pitch restoring via waterplane area moment;
2. A ballasted deep-drafted spar buoy with pitch restoring by ballasting; and
3. An unballasted tension leg platform, for which pitch restoring mainly is provided by the mooring system.

Figure 10.1 shows this classification in a simple symbolic triangle plot. In Section 2 a quantified, more detailed plot of the design space is given. Figure 10.2 gives a short indicative comparison of the relative advantages and disadvantages of each concept.

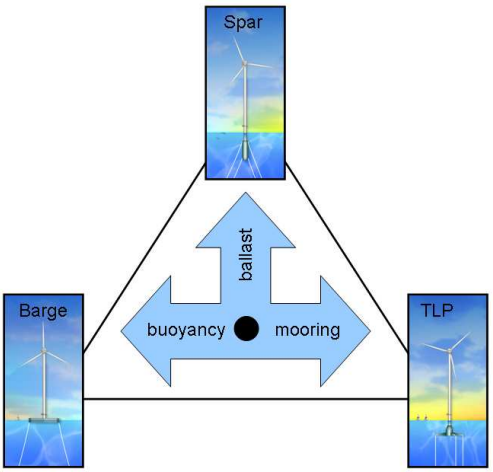


Figure 10.1: Floating wind turbine concepts

+ relative advantage
0 neutral
– relative disvantage

| | TLP | Spar | Barge |
|---|---|---|---|
| Pitch Stability | Mooring | Ballast | Buoyancy |
| Natural Periods | + | 0 | – |
| Coupled Motion | + | 0 | – |
| Wave Sensitivity | 0 | + | – |
| Turbine Weight | 0 | – | + |
| Moorings | + | – | – |
| Anchors | – | + | + |
| Construction & Installation | – | – | + |
| O&M | + | 0 | – |

Figure 10.2: Relative advantages of concepts

The barge and spar-buoy types can be anchored to the seabed either with slack catenary or with taut vertical mooring lines, but the TLP must be equipped with taut mooring lines. There are various types of possible mooring cables, such as chains, steel or synthetic fibres, or a combination of these. Numerous anchor systems exist, ranging from simple deadweight anchors and conventional “mushroom” anchors to more sophisticated screw-in and suction anchors.

One major hybrid-concept not mentioned above due to its hybrid status is the semi-submersible platform with catenary mooring lines, e.g. the Dutch Trifloater concept or Principal Power’s WindFloat concept. Semi-submersibles in general have distributed buoyancy tanks attached to the central tower through truss arms. This achieves stability primarily through weighted water plane area but weight of the steel tanks and truss structure also provides significant mass to resist overturning moments. The catenary moorings provide some additional resistance to overturning, mainly due to the mass of the lengthy chain.

## 10.2 Concept Comparison

In a study conducted at the National Renewable Energy Laboratory (NREL), three different FOWT concepts were compared, the ITI Barge, OC3 Hywind Spar-Buoy and MIT/NREL TLP, representing the three primary FOWT concepts. Figure 10.3 presents the three investigated concepts. The following sections provide a short overview of the concept comparison study, documented in detail by Jonkman [38] and Matha [39].

### 10.2.1 Overview of the three concepts investigated

Each analyzed platform concept supported the NREL 5-MW baseline wind turbine, representing a typical state-of-the-art multi-megawatt turbine. An in-depth description of the turbine can be found in Jonkman [5]. All calculations were performed in the fully coupled time-domain aero-hydro-servo-elastic design code FAST with AeroDyn and HydroDyn. This code has the capability of simulating all relevant time-domain hydrodynamic effects important for the dynamic behavior of floating offshore structures. Linear hydrostatic restoring and added-mass and damping contributions from linear radiation, including free-surface memory effects, are considered, as well as incident-wave excitation from linear diffraction. Nonlinear viscous drag, including sea-current loading, is also accounted for. The code also includes a nonlinear quasi-static mooring line module. The models have been verified and compared to frequency-domain calculations in terms of response amplitude operators and probability density functions.
An extensive load and stability analysis for ultimate and fatigue loads according to the procedures of the IEC 61400-3 offshore wind turbine design standard was performed with the verified models. Response statistics, extreme event tables, fatigue lifetimes, and selected time histories of design-driving extreme events were analyzed. A short summary of the results is given in section 10.2.2.

| **TLP Properties** | |
|---|---|
| Platform Diameter: | 18 [m] |
| Displaced Volume: | 12,180 [$m^3$] |
| Platform Draft: | 47.89 [m] |
| Freeboard: | 5.0 [m] |
| Water Depth: | 200 [m] |
| Platform Mass: | 8,600 [tons] |
| Taut Mooring System: Distance to Fairleads from Tower Centerline: | 27 [m] |

***TLP design based on MIT study***

| **Spar Buoy Properties** | |
|---|---|
| Platform Diameter: | 6.5-9.4 [m] |
| Displaced Volume: | 8,029 [$m^3$] |
| Platform Draft: | 120.0 [m] |
| Freeboard: | 10.0 [m] |
| Water Depth: | 320 [m] |
| Platform Mass: | 7,466 [tons] |
| Catenary Mooring System: Distance to Fairleads from Tower Centerline: | 5.2 [m] |

***Spar Buoy design based on StatoilHydro's Hywind concept; used in Phase IV of the IEA OC3 project***

| **Barge Properties** | |
|---|---|
| Platform Size: | 40x40x10 [m] |
| Displaced Volume: | 6,000 [$m^3$] |
| Platform Draft: | 6.0 [m] |
| Freeboard: | 4.0 [m] |
| Water Depth: | 150 [m] |
| Platform Mass: | 5,450 [tons] |
| Catenary Mooring System: Distance to Fairleads from Tower Centerline: | 28.3 [m] |

***Barge design based on ITI Energy's concept***

Figure 10.3: Analyzed FOWT Concepts

### 10.2.2 Floating Wind Turbines Stability Triangle

The concepts described above achieve static stability by different means. The previous section discussed the classifications made based on how the concepts achieve static stability: (1) The barge concept, represented by the ITI Energy barge, achieves restoring from buoyancy via waterplane area moment; (2) the spar buoy, represented by the OC3-Hywind concept, is statically stable because restoring primarily is provided by ballast; and (3) for the tension leg

platform, here represented by the MIT/NREL TLP, restoring mainly is provided by the mooring system. The static restoring coefficient in pitch $C_{55}$ is used to quantify this classification. The stiffness matrices for each component were obtained by linearization of the WT model and the platform. For each concept, the restoring moments due to:

- hydrostatics (buoyancy) $C_{55}^{Buoyancy}$,
- weight (ballast) $C_{55}^{Ballast}$, and
- the mooring system $C_{55}^{Mooring}$

are determined. These moments each then are normalized by the total restoring in pitch $C_{55}^{Total} = C_{55}^{Buoyancy} + C_{55}^{Ballast} + C_{55}^{Mooring}$ and plotted in a so-called ternary plot.

The ternary plot is a barycentric plot of three variables which sum to a constant, in this case chosen to be unity or 100%. It graphically depicts the ratios of the three variables as positions in an equilateral triangle. These plots typically are used to show the compositions of systems composed of three species and can be used as a valuable tool used to graphically show how a specific floating wind turbine concept achieves static stability.

In the floating wind turbine design space ternary plot the proportions of the three variables buoyancy, ballast, and mooring sum to one (100%) for each concept. The three proportions cannot vary independently. Therefore it is possible to graph the intersection of all three variables in only two dimensions. Each base - or side of the triangle - represents a proportion of 0 (0%), with the point of the triangle opposite that base representing a proportion of 1 (100%). As a proportion increases from 0, the point representing that sample moves from the base to the opposite point of the triangle.

Table 10.1: Stability Triangle - non-dimensional pitch restoring

| Concept | $C_{55}^{Buoyancy}$ | $C_{55}^{Ballast}$ | $C_{55}^{Mooring}$ |
|---|---|---|---|
| MIT/NREL tension leg platform | -0.126 | 0.130 | 0.995 |
| OC3-Hywind spar buoy | -3.374 | 4.164 | 0.210 |
| ITI Energy barge | 1.244 | -0.260 | 0.016 |

The ternary plot for the concepts investigated in this project is shown in Figure 10.4. Important points and lines of the triangle are annotated to make the plot more easily readable. The underlying data, normalized to unity, is presented in Table 10.1. The TLP and ITI Energy barge concept appear very close to the associated, previously predicted corners of the triangle. The TLP is located close to the mooring = 1 corner, and most of the static restoring (99.5%) for the TLP is provided by the mooring system. The contributions from buoyancy and ballast restoring - ±13% of the total restoring - cancel each other out.

Restoring for the ITI Energy barge is primarily (+1.24) provided by the water-plane area effect from buoyancy of the platform, therefore the barge is located in the proximity of the left corner of the triangle representing buoyancy = 1. The excess buoyancy of 24% is similar to the TLP cancelled out by the -26% negative restoring from weight. The mooring-line restoring contribution for the barge concept is negligible at 1.6%.

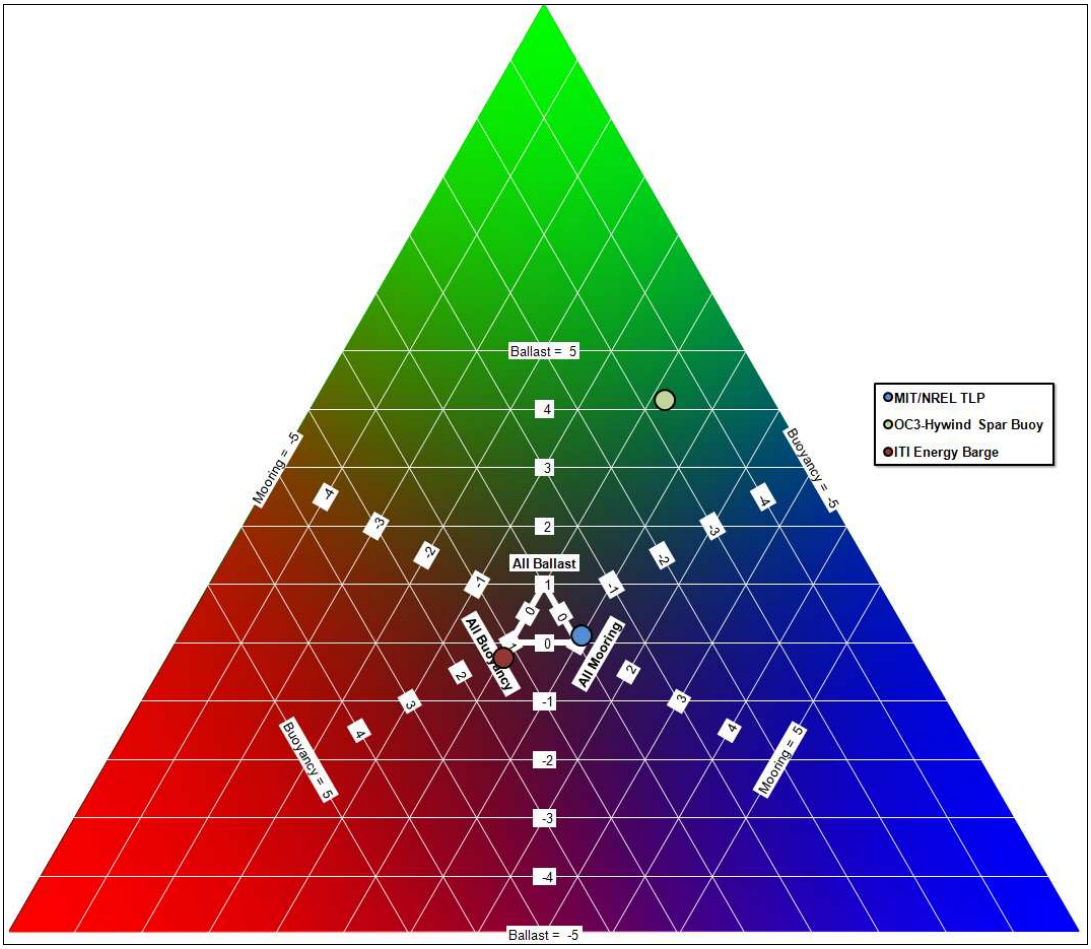


Figure 10.4: Floating wind turbine stability triangle (ternary plot)

At first glance, the OC3-Hywind concept appears at an odd location - far away from the upper corner of the triangle, where restoring by ballast is equal to 1. However, the location far from the core triangle illustrates the different restoring contributions very well. The positive restoring from ballast of 416% of the total restoring is counteracted by -337% of negative restoring originating from hydrostatic buoyancy. That is, without ballast the spar statically would be extremely unstable. The ballast provides enough restoring to more than compensate for this effect. In contrast to the slack catenary barge moorings, the slack catenary mooring lines of the OC3-Hywind contribute with 21% positive restoring to the spar's static stability.

The locations of the different concepts on the stability triangle illustrate the different restoring contributions for each concept graphically. The positions in the ternary plot, however, do not provide a basis for determining the quality of the specific design. That is, the TLP—which is positioned almost perfectly in the mooring = 1 corner of the triangle—is not an optimized design. For example, the absolute value of the ballast restoring for the TLP is much greater as compared to the ITI Energy barge. A TLP design with much less ballast probably could be designed and would be placed at almost the exact same position as the MIT/NREL TLP, but would have a much more economic design. This example illustrates that no statements on design quality can be derived from the concept's position in the stability triangle. However, for concept comparisons, the plot provides a powerful tool to classify novel platform designs, especially designs incorporating hybrid features.

### 10.2.3 Summary of Results

Based on the analysis described in section 10.1, the three basic floating wind turbine concepts - represented by the MIT/NREL TLP#1, the ITI Energy barge, and the OC3-Hywind spar buoy - are compared to each other. It is important to note that the TLP design investigated in this study is not a “pure” TLP, but rather a hybrid between a TLP and a spar buoy.

**ITI Energy Barge**

The ITI Energy barge primarily has the advantage that the platform design is easy to manufacture and install. It consists mainly of inexpensive off-the-shelf flat steel panels and can be assembled in almost any coastal facility due to the shallow draft. The slack catenary mooring system allows for a simple inexpensive anchoring system. The stability analysis also showed fewer instabilities for the barge than for the other two concepts.
In harsh contrast to these advantages are the results from the ultimate and fatigue load comparisons. Here, the barge is by far the concept with the highest ultimate loads and lowest fatigue lifetimes. These high loads are mainly caused by the barge’s extreme motions and accelerations in high waves, which means that the barge design is affected greatly by extreme seas. Nakim [40] showed that using a control system with individual blade pitching on the floating barge wind turbine system, significant reduction in platform pitching motion could be achieved without affecting power regulation in the above rated wind speed region. Economic cost analysis must show to what extent the savings due to the simple design are outweighed by the need for a strengthened turbine. Particularly for sites that have less severe sea states, such as the Great Lakes, an improved barge design could provide the most cost-effective choice.

**OC3-Hywind Spar Buoy**

Of the three concepts investigated, the OC3-Hywind is the only system which is close to a real system, Statoil Hydro’s Hywind concept, which actually is being tested full-scale in the North Sea since 2009. The OC3-Hywind model is not completely identical to the real Hywind design and also lacks certain details, which (most likely) make the real design superior to the investigated OC3 model. Nevertheless, compared to the other two floating concepts investigated, the OC3-Hywind design can be assumed to be optimized to relatively high degree. The analysis of the ultimate and especially the fatigue ratios however indicate that the concept, although experiencing significantly less loads than the ITI Energy barge, yields higher loads than the investigated TLP design. The fatigue ratios - which differ up to one order from the TLP - indicate a great need for improvements in the tower strength or the control system. Additionally, the spar buoy has the disadvantage that it is very deep drafted and could require deep-water harbours for manufacturing and assembly. The amount of ballast needed also adds to total costs. Compared to the TLP, the design has the advantage of a simpler anchoring system, due to the slack catenary mooring and the slender cylindrical body, which results in a small cross-section at the water line, it also has advantages regarding drag forces. The spar’s natural frequencies also are placed well outside the energy-rich wave spectra. Further iterations, economic design analysis, and experimental data will help to clarify the pros and cons of the spar concept, particularly as compared to the TLP.

**MIT/NREL Tension Leg Platform**

The investigated tension leg platform showed the best ratios for ultimate and fatigue loads of all investigated concepts. It is the floating concept closest to the land-based system and therefore requires the least effort for strengthening the turbine, which saves costs. A disadvantage of all TLP designs is the expensive tension leg mooring system and expensive anchors needed. This particular TLP also has the disadvantage of a large amount of ballast and a very high volume of the platform - the largest of all three concepts. The big cross-section at mean sea level also poses a significant obstacle for incident-waves and adds to drag. The long spokes are a source of failure; to build them with the necessary strength requires additional costly material and manufacturing work. Installation also is the most difficult of the three designs because the design is fairly deep drafted, the tension leg anchors are difficult to install, and without adding

additional ballast the design is quite unstable without a mooring system (which makes the towing-out process challenging). Nevertheless, the TLP design yields the lowest ultimate and fatigue loads for all other concepts. The great potential for optimization of the TLP adds to its advantages, especially regarding a possible decrease of the amount of ballast required, or development of alternative installation and anchoring methods. The present study only provides initial information on the loads for, and stability of, each concept. A thorough cost analysis, improvements in the control system, further design optimization, and analysis of more concepts can lead to a conclusion on the optimal concept.

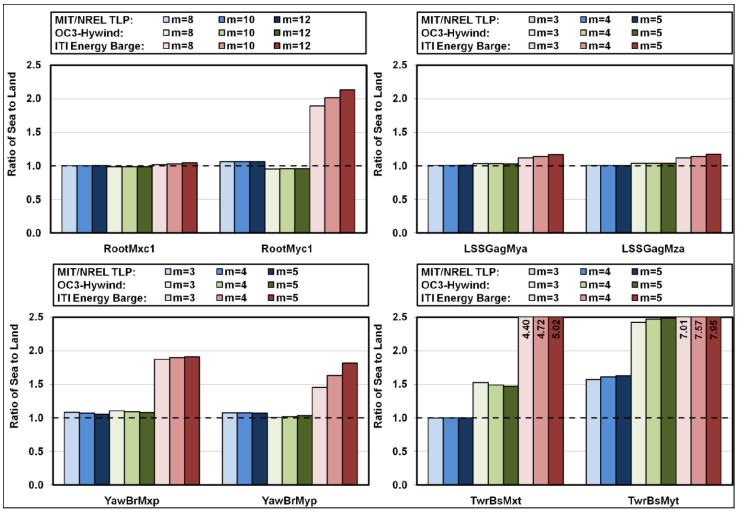


Figure 10.5: Ratios of tension leg platform, OC3-Hywind, and ITI Energy barge fatigue DELs to land-based turbine from normal operation DLCs

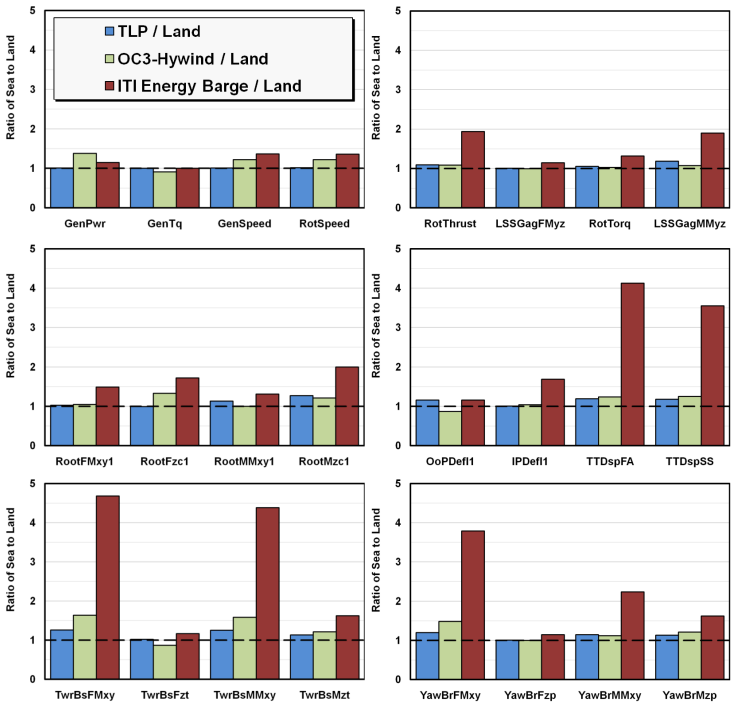


Figure 10.6: Ratios of TLP, barge, and Hywind concepts to land-based loads for normal operation DLCs

## 10.3 Overview of current Developments

Floating offshore wind turbines are becoming increasingly important for research and industry. Table 10.2 represents an overview on current research and industry projects focusing on FOWT. In December 2010, Statoil's Hywind spar-buoy concept with a 2.3 MW Siemens wind turbine, installed in 2009, represents the only operating full scale FOWT, but several other FOWT projects have announced prototypes to be installed in 2011-2015. Supporting the strong interest in FOWT in industry and research, the European Union has announced the FP-7 Call (ENERGY.2011.2.3-1) "Demonstration of innovative off-shore wind electricity generation structure", primarily focused on FOWT technology demonstration.
In summary these developments indicate, that within 5-10 years FOWT could complement fixed-bottom offshore wind turbines to generate electricity from wind in both shallow water (<50m, near-shore) areas, as well as at deep water (>50m, near- & far-shore) locations.

Table 10.2: Selection of current FOWT projects

| Concept | Project leader | Platform concept | Turbine | Country | Status (announced) |
|---|---|---|---|---|---|
| Blue H | Blue H USA | Submerged Deepwater Platform (SDP) | 80KW Demonstrator | USA | Prototype installed in Italy, 2007 |
| Hywind | Statoil ASA | Spar-Buoy with catenary moorings | Siemens SWT-2.3-82 | Norway | Prototype installed in Norway, 2009 |
| SWAY | SWAY | Spar-Buoy with single taut tether | SWAY TURBINE, 10MW | Norway | Prototype in 2013 |
| WindFloat | Principal Power | Semi-Submersible | 3.6-10MW | USA | Prototype in 2011 |
| HiPRWind | Fraunhofer IWES | various designs, in design phase | 1MW (1:10 scaled) | Germany | Prototype within 5 years |
| DeepCwind | DeepCwind Consortium | TLP, Spar-buoy, Barge investigated | 100KW demonstrator | USA | Prototype in 2012 |

# 11. Jacket foundation design for a 20MW turbine

## 11.1 Introduction

Offshore wind turbine sizes on the market have been increased up to 6.0MW over the last years. Furthermore, some manufacturers have already built prototypes of higher power rating and even prototypes of 10 MW are currently under development highlighting the trend to further increased turbine sizes. The Upscaling work package of the UpWind project focus on the development of a 20MW 'Lighthouse' turbine. Main objectives of this Lighthouse design are to show the challenges and possible solutions for future developments of very large turbines. In the same context a jacket foundation structure is designed for a 20MW offshore wind turbine. However, it is explicitly stated here that the 20MW 'Lighthouse' wind turbine model from the UpWind Upscaling work package is not used for the foundation design addressed in this chapter since it has not been available when the foundation design activities had to be carried out. Instead, the foundation design has been based on an alternative 20MW wind turbine as derived by application of classical similarity rules for upscaling on the UpWind 5MW turbine [13].
This chapter introduces the jacket and pile foundation design for the 20MW turbine for a 50m water depth site. Furthermore, it addresses the related technical challenges and possible solutions, advantages of an integrated design approach as well as the advantages and need of intensive R&D efforts in order to achieve more beneficial 20MW solutions than obtained by application of the classical similarity rules for upscaling.

## 11.2 Foundation Design Approach

The design of an offshore wind turbine support structure depends on various aspects such as turbine characteristics, site specific conditions, available installation methods and tools and fabrication requirements. Clearly, not all of these aspects can be properly addressed at this conceptual stage since the turbine generation under consideration represents a medium to long term future development. Therefore the results of this study must be considered as only indicative with respect to dimensions, mass and loads. Certain practical limitations of e.g. present transport, fabrication and installation possibilities are explicitly not taken into account for the 20MW foundation design. Nevertheless, the results of this study can be used to identify challenges in terms of design, fabrication, transportation as well as installation and subsequently focus on the development of sophisticated solutions and advanced technologies in early design stages. Consideration of implications from the turbine design on the aforementioned aspects and vice versa forms an essential step towards integrated design solutions resulting in more competitive offshore wind turbines.

The design approach for the 20MW foundation, i.e. transition piece, jacket and piles, basically corresponds to the approach taken for the design of the UpWind 5MW reference jacket structure [23]. However, only a reduced set of load cases as well as a less sophisticated combination of aerodynamic and hydrodynamic loads is applied. Initially, a preliminary support structure geometry has been established with a natural frequency within allowable frequency range for the 20MW turbine. Subsequently, aerodynamic extreme loads and fatigue loads in terms of damage equivalent loads are determined for the turbine by time domain simulations in GH BLADED. These loads are superimposed to hydrodynamic design loads in ROSA as calculated by dynamic analyses resulting in the design loads for the foundation structure optimization. Hydrodynamic fatigue and extreme loads are re-calculated and superimposed to the aerodynamic loads again in case of structural changes of the foundation. The models, tools and load cases applied for the 20MW foundation design correspond to those applied for the UpWind 5MW reference jacket structure as explained in more detail in UpWind report "Design solution for the UpWind reference offshore support structure" [23]. Furthermore, the

environmental conditions for this design study can be found in the data description for the 'K13 deep water site' in the UpWind design basis [13].

## 11.3 Definition of a 20MW turbine and tower

Development of increased turbine sizes in terms of rated power requires larger turbine dimensions such as rotor diameter, hub height and mass. A fast, but rough, estimation of the corresponding turbine dimensions can be made by upscaling of an existing turbine on basis of classical similarity rules. Here, the rated turbine power is proportional to the square of the rotor radius R while the mass of the turbine increases cubically with the rotor radius. Furthermore, the hub height will increase proportionally with the rotor radius. The thrust force increases with the square of the rotor diameter and consequently the moments at the tower base increase cubically. However, it can be stated that those classic upscaling coefficients seem to be by far too conservative in reality e.g. due to improved technologies which is also supported by trends of turbine developments over the past decade. Scaling coefficients on power and mass based on the rotor radius R for the classic similarity theory are provided together with average estimations on more realistic upscaling coefficients in Table 11.1. Implications of those different upscaling coefficients for the present design are discussed in more detail at a latter part of this chapter.

Table 11.1: Upscaling coefficients on power and mass

| | Classic theory | Average of realistic values |
|---|---|---|
| Power | $R^{2.0}$ | $R^{2.25}$ |
| Mass | $R^{3.0}$ | $R^{2.40}$ |

It is obvious that design, manufacturing, installation and operation of structures for upscaled 20MW turbines will introduce tough challenges especially when based on classic upscaling coefficients.

The 20MW turbine used for the foundation design in this chapter is an artificial 3-bladed upwind variable speed machine with collective pitch control prepared as by P. Jamieson from Garrad Hassan following classical similarity rules. The resulting turbine appears to be rather conservative, with a rotor mass of 1203 tons and a total top mass of 3565 tons. The main turbine parameters are summarized in Table 11.2.

Table 11.2: Properties of the 20MW turbine

| | |
|---|---|
| power rating | 20MW |
| rotor orientation, configuration | upwind, 3 blades |
| control | variable speed, collective pitch |
| drivetrain | high speed, multiple-stage gearbox |
| rotor, hub diameter | 258 m, 6.9 m |
| cut-in, rated, cut-out wind speed | 3 m/s, 11.6 m/s, 25 m/s |
| cut-in, rated rotor speed | 2.79 rpm, 5.58 rpm |
| overhang, shaft tilt, precone | 11.18 m, 6º, 0º |
| | |
| rotor mass | 1203 t |
| nacelle and rotor mass | 3565 t |
| | |
| hub height | 159.0 m |
| platform/interface level | 25. 0 m |
| height of tower top flange | 5.5 m below hub height i.e. 153.5 m |
| | |
| tower bottom diameter | 14.0 m |
| tower top diameter | 8.0 m |
| tower mass | 4024 t |

The interface elevation between tower and substructure is set to 25.0m allowing only for a limited clearance between a blade tip in its lowest azimuthal position and the platform level. Furthermore, the hub height is set at 159.0 m above MSL. The vertical offset between the hub and the tower top is 5.5 m, resulting in a tower length of 128.5 m. Figure 11.1shows the tower structure.

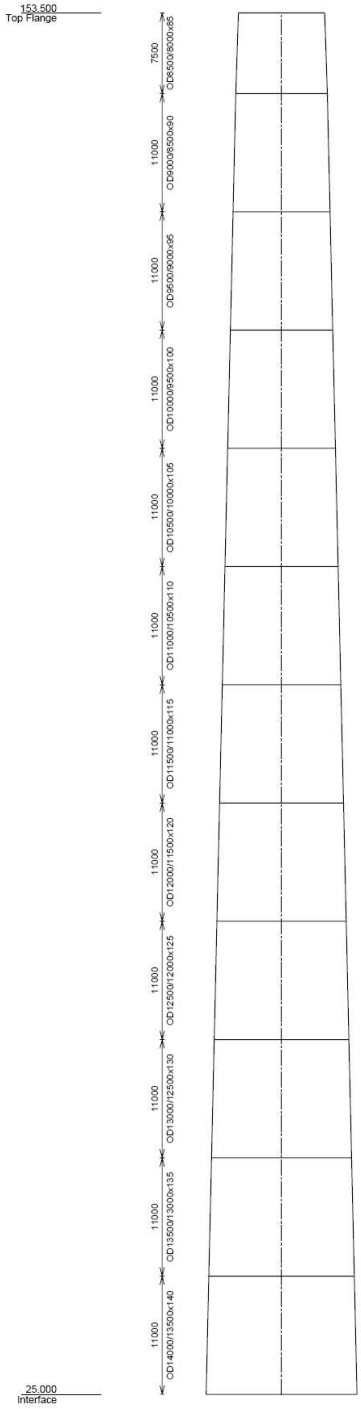


Figure 11.1: Tower dimensions for the 20MW turbine for offshore application

As the focus in this study is on the foundation structure, these main parameters for the superstructure, i.e. turbine and tower, are used as they are, i.e. no modifications based on foundation design requirements will be made in order to allow for a more optimized overall system. Basically the studies presented here can be considered as the first loop of a design iteration for the 20MW offshore wind turbine.

## 11.4 Modal properties

The large rotor diameter of the 20MW turbine leads to low rotor speeds as well as a rather large hub height. Figure 11.2 shows the resulting allowable frequency ranges under consideration of 10% safety margins together with an exemplarily wave energy spectrum representing a severe sea state with a peak period of approx. 10s. It can be seen that a significant amount of the wave energy is located in the soft-stiff region from 0.102Hz to 0.126Hz.

A natural frequency of 0.361Hz has been calculated in preliminary investigations of the tower and RNA with a rigid foundation, i.e. structure fully fixed at tower bottom.

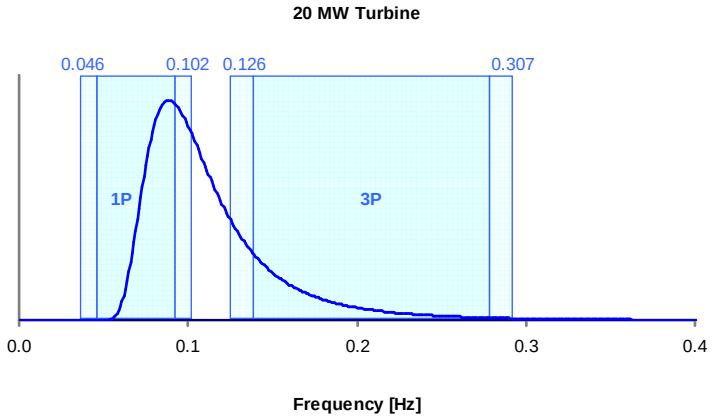


Figure 11.2: Allowable frequency range for the 20MW turbine

There are three possible design solutions in order to avoid 1P and 3P excitations of the structure.

**Soft-soft**

This design solution has a very low natural frequency, i.e. below 1P excitations and preferably also below wave frequencies with high energy contents. The latter mentioned aspect would automatically be fulfilled for the case of a soft-soft design of the present 20MW turbine as the rotor speed is very low. A soft-soft design solution would need to have a natural frequency below 0.042 Hz introducing characteristics of a compliant structure. This could only be achieved by an extremely low structural stiffness which is not expected to be able to cope with the extreme aerodynamic and hydrodynamic loads. Soft-soft solutions for bottom-mounted offshore structures have so far been applied mainly in the offshore oil & gas industry whereas soft-soft solutions in the offshore wind industry have mainly been discussed in relation to floating structures.

**Soft-stiff**

It has become common practices for today's offshore wind turbines to design the structures with a natural frequency in the soft-stiff range (i.e. between the 1P and 3P ranges). Allowable

frequencies for existing offshore wind turbines approximately range from 0.2Hz to 0.35Hz. This typically allows ensuring that the natural frequency is located outside the frequency range of high wave energy contents as well as a sufficiently high stiffness of the structure.
However, in case of this 20MW structure it can be assumed that the structure would experience severe fatigue damage from hydrodynamic excitations for a soft-stiff design solution due to the significantly reduced frequencies, i.e. between 0.102Hz to 0.126Hz, compared to a 5MW turbine. This is due to the fact that typical peak periods of the fatigue sea states at the reference site [1] vary from 6.9s to 9.5s corresponding to peak frequencies of 0.105Hz to 0.146Hz, i.e. very well within the soft-stiff design range.

**Stiff-stiff**

Natural frequencies are beyond the 3P excitation for stiff-stiff designs. This design solution typically requires extremely stiff support structures. Therefore, a stiff-stiff solution is usually not applied nor desired for today's offshore wind turbines[4] since it would result in significantly larger amounts of material compared to a soft-stiff design solution. However, the situation is different in case of the present 20MW turbine since the stiff-stiff region starts at 0.306Hz which e.g. corresponds to the soft-stiff region of today's turbines. Both, enough structural stiffness as well as a sufficiently large frequency distance to the waves with high energy contents is expected when designing the 20MW jacket foundation for this frequency region. However, it needs to be kept in mind that a natural frequency of 0.361Hz has been calculated for the tower and RNA with a rigid foundation resulting in severe stiffness requirements on the foundation in order to obtain a natural frequency in the stiff-stiff region.

## 11.5 Design load cases

A reduced selection of typical IEC61400-3 [8] design driving load cases have been taken from the design basis of the 5MW reference structure [1] in order to generate the fatigue and extreme design loads for the present 20MW turbine. Furthermore, additional load cases have been defined in accordance to Germanischer Lloyd [9].

- dlc1.2 Power production + normal turbulence (Extreme)
- dlc6.4 Idling + normal turbulence (Extreme & Fatigue)
- dlc1.3 Power production + extreme turbulence (Extreme)
- dlc1.6 Power production + extreme operating gust; here according to GL, as the 50yrs gust is assumed to be critical and this case is not in IEC61400-3 (Extreme)
- dlc1.8 Power production + extreme directional change; here acc. to GL, as the 50yrs gust is assumed to be critical and this load case is not included in the IEC61400-3 (Extreme)

Aerodynamic loads and hydrodynamic loads are generated individually and are subsequently superimposed in order to obtain the total design loads as outlined before, e.g. no hydrodynamic effects are included for the calculation of the aerodynamic extreme and fatigue loads. However, aerodynamic damping has been applied as additional structural damping in order to address the aero-elastic behaviour of the offshore wind turbine for the calculation of the hydrodynamic loads. Details on the resulting aerodynamic loads as well as on the calculation of the hydrodynamic loads and the superposition of both are provided in the following sections.

[4] Typically, 3 to 6 MW turbines with tubular steel towers and monopile, tripod or jacket foundations.

### 11.5.1 Extreme Loads

Table 11.3 provides an overview of the aerodynamic extreme loads at tower bottom over all load cases in terms of minimum and maximum value for each load component together with the contemporaneous values of the other load components. A load safety factor of 1.35 has been considered for the relevant load cases 1.6 and 1.3 which is already included in the table values.

Table 11.3: Aerodynamic extreme loads at interface including safety factor

| | | Load case | Fx [MN] | Fy [MN] | Fz [MN] | Mx [MNm] | My [MNm] | Mz [MNm] |
|---|---|---|---|---|---|---|---|---|
| Fx | Max | 1.6 | 31.2 | 0.3 | -104.3 | 61.7 | 4182.5 | 46.1 |
| Fx | Min | 1.3 | -3 | 2 | -101.2 | -198.7 | -396 | -26.8 |
| Fy | Max | 1.3 | 0.2 | 2.5 | -101.2 | -226.1 | -69 | 0.1 |
| Fy | Min | 1.3 | 1.5 | -2.5 | -101.4 | 310 | 69 | 6.5 |
| Fz | Max | 1.3 | 0 | 1.1 | -100.8 | -90 | -98.2 | -13.6 |
| Fz | Min | 1.6 | 29.7 | 0.3 | -104.6 | 61.5 | 4044.9 | 79.1 |
| Mx | Max | 1.3 | 2.8 | -2.3 | -101.4 | 338.8 | 197.2 | -4 |
| Mx | Min | 1.3 | 0.3 | 2.5 | -101.3 | -226.9 | -67.3 | -0.3 |
| My | Max | 1.6 | 31.2 | 0.3 | -104.3 | 62.4 | 4183.1 | 45.8 |
| My | Min | 1.3 | -2.9 | 1.6 | -101.6 | -174.6 | -432.3 | -25.4 |
| Mz | Max | 1.6 | 29.3 | 0.2 | -104.3 | 78.3 | 3998.9 | 85.4 |
| Mz | Min | 1.3 | -0.2 | 1 | -101.1 | 73.4 | -110.7 | -46.9 |

The aerodynamic extreme loads are added to loads from a representative extreme wave and current. However, a combination of the maximum 50-year wave load with the maximum wind load is considered too conservative since the simultaneous occurrence of both maxima is highly unlikely. Therefore, the 1-year wave according to Table 1.4 has been applied instead, together with an extreme current velocity of 1.20 m/s according to the 5MW Jacket Design Basis [1]. The aerodynamic loads are strongly dominating for the present site, turbine and foundation structure. Therefore, further load combinations with a 50-year wave and reduced wind are not considered.

Table 11.4: Extreme wave properties

| | |
|---|---|
| Wave height Hmax | 13.21 m |
| Wave period T | 9.44 s |

Conservatively, wind, wave and current directions are assumed fully aligned and are applied along and across the jacket foundation according to Figure 11.3 in order to extract the governing design loads.


Figure 11.3: Wind and wave direction relative to the jacket structure configuration

### 11.5.2 Fatigue Loads

Aerodynamic and hydrodynamic fatigue loads are calculated individually and are subsequently superimposed in order to obtain the total fatigue loads for the foundation design. Calculations of the aerodynamic fatigue loads are based on the wind speed distribution in Table 11.5.

Table 11.5: Wind speed distribution

| Mean wind speed | Turbulence intensity (longitudinal) | Probability |
|---|---|---|
| [m/s] | [%] | [%] |
| < 2 | 20 | 5.04 |
| 4 | 13.7 | 9.88 |
| 6 | 11.8 | 13.15 |
| 8 | 10.9 | 12.13 |
| 10 | 10.5 | 12.13 |
| 12 | 10.3 | 13.48 |
| 14 | 10.1 | 10.8 |
| 16 | 10.1 | 8.7 |
| 18 | 10.1 | 5.01 |
| 20 | 10.1 | 4.02 |
| 22 | 10.1 | 2.43 |
| 24 | 10.1 | 1.79 |
| > 26 | 10.2 | 1.4 |

The resulting aerodynamic fatigue loads are summarized in Table 11.6 in terms of damage equivalent loads at tower bottom for different inverse slopes m of the S-N curves and a fixed reference number of load cycles of $N_{ref}=10^7$.

Table 11.6: Damage equivalent aerodynamic loads for $N_{ref}=10^7$

| m | ΔFx | ΔFy | ΔFz | ΔMx | ΔMy | ΔMz |
|---|---|---|---|---|---|---|
| [-] | [MN] | [MN] | [MN] | [MNm] | [MNm] | [MNm] |
| 3 | 4.64 | 2.5 | 0.75 | 234.31 | 518.26 | 34.01 |
| 4 | 4.17 | 2.19 | 0.6 | 218.33 | 472.11 | 30 |
| 5 | 4.03 | 2.1 | 0.54 | 217.06 | 459.58 | 28.94 |

The calculation of the hydrodynamic loads is based on the reduced wave distribution in Table 11.7.

Table 11.7: Wave scatter diragram

| $H_s$ | $T_p$ | Probability |
|---|---|---|
| [m] | [m] | [%] |
| 4.19 | 9.53 | 1.1 |
| 3.80 | 9.22 | 1.2 |
| 3.45 | 8.89 | 1.3 |
| 3.10 | 8.52 | 3.5 |
| 2.67 | 8.14 | 4.8 |
| 2.50 | 7.87 | 6.4 |
| 2.20 | 7.53 | 11.3 |
| 1.90 | 7.24 | 10.8 |
| 1.75 | 7.07 | 12.7 |
| 1.50 | 6.92 | 13.3 |
| 1.24 | 6.87 | 10.5 |
| 1.20 | 6.98 | 8.6 |
| 1.15 | 7.10 | 9.1 |

Hydrodynamic fatigue loads are calculated without consideration of any influences from the wind. However, aerodynamic damping has been applied as additional structural damping ratio of 4% in order to address the aero-elastic behavior of the offshore wind turbine resulting in a total structural damping ratio of 4.5% in the model.

The technical availability is assumed to be 100% and wind and waves are applied fully aligned with a directional distribution according to Table 11.8.

Table 11.8: Directional wind and wave distribution

| Directional | N | NNE | ENE | E | ESE | SSE | S | SSW | WSW | W | WNW | NNW |
|---|---|---|---|---|---|---|---|---|---|---|---|---|
| | 0° | 30° | 60° | 90° | 120° | 150° | 180° | 210° | 240° | 270° | 300° | 330° |
| probability [%] | 16.7 | 7.6 | 6.5 | 3.9 | 2.6 | 2.8 | 7.6 | 16.6 | 8.3 | 6.8 | 8.1 | 12.6 |

The total fatigue loads are calculated as the square root of the sum of squares of the individual aerodynamic and hydrodynamic fatigue loads according to:

$$\Delta F_{eq} = (\Delta F_{eq,Wind}^{2} + \Delta F_{eq,Wave}^{2})^{0.5}$$

with $\Delta F_{eq,Wind}$ - damage equivalent wind load
$\Delta F_{eq,Wave}$ - damage equivalent wave load

Based on the total fatigue loads the structure is designed for a lifetime of 20 years in an iterative manner, i.e. hydrodynamic fatigue loads are recalculated in case of structural changes.

## 11.6 Jacket Foundation

The design efforts in this chapter are limited to the jacket and the piles. The turbine and tower have been obtained from upscaling approaches and are used as they are even though that they can be considered by far too heavy and large. Furthermore, representative models of the transition piece and the grouted connection between the jacket and the piles have been applied but not designed at all. It has to be emphasized, that strong interactions between those subsystems exist, which must therefore be addressed for a proper design. Particularly, transition pieces between tubular steel tower and jackets are of high relevance and interest even for today's designs. However, this is considered outside the scope and available resources for the present design study.

The overall design summary of the jacket foundation structure for the 20MW turbine is presented in Table 11.9. Furthermore, Figure 11.4 and Figure 11.5 illustrate the whole support structure as well as the jacket member geometries.

Table 11.9: Dimensions and masses of the 20MW foundation

| Description | Unit | Value |
|---|---|---|
| Base width top | [m] | 28.0 |
| Base width bottom | [m] | 42.0 |
| Pile penetration | [m] | 55.0 |
| Jacket pile diameter | [m] | 5.60 |
| Jacket pile wall thicknesses | [mm] | 50 to 60 |
| Jacket only weight | [tons] | 2736 |
| Transition piece weight (indicative) | [tons] | 1065 |
| Total pile weight | [tons] | 1809 |
| Total weight (jacket, transition piece and piles) | [tons] | 5610 |

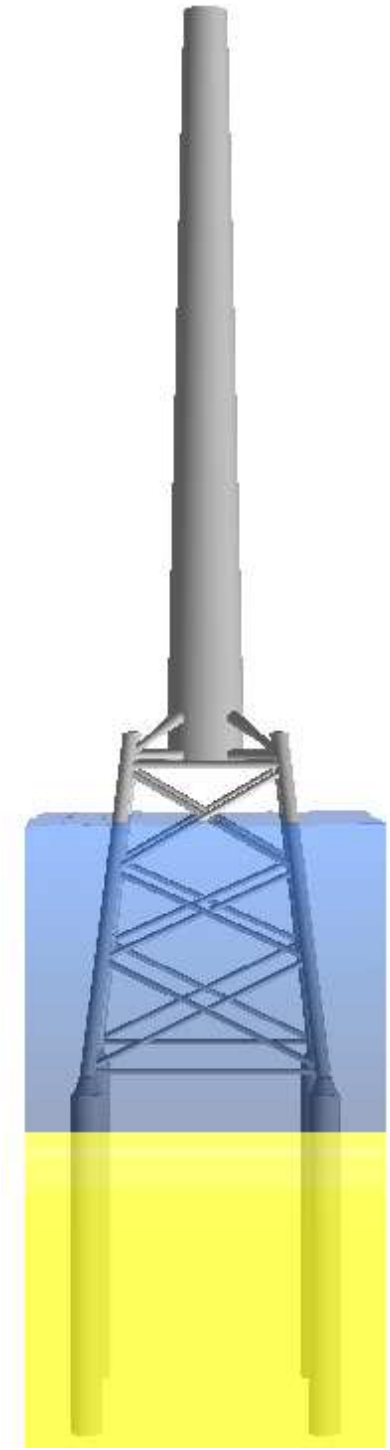

Figure 11.4: Support structure for the 20MW turbine

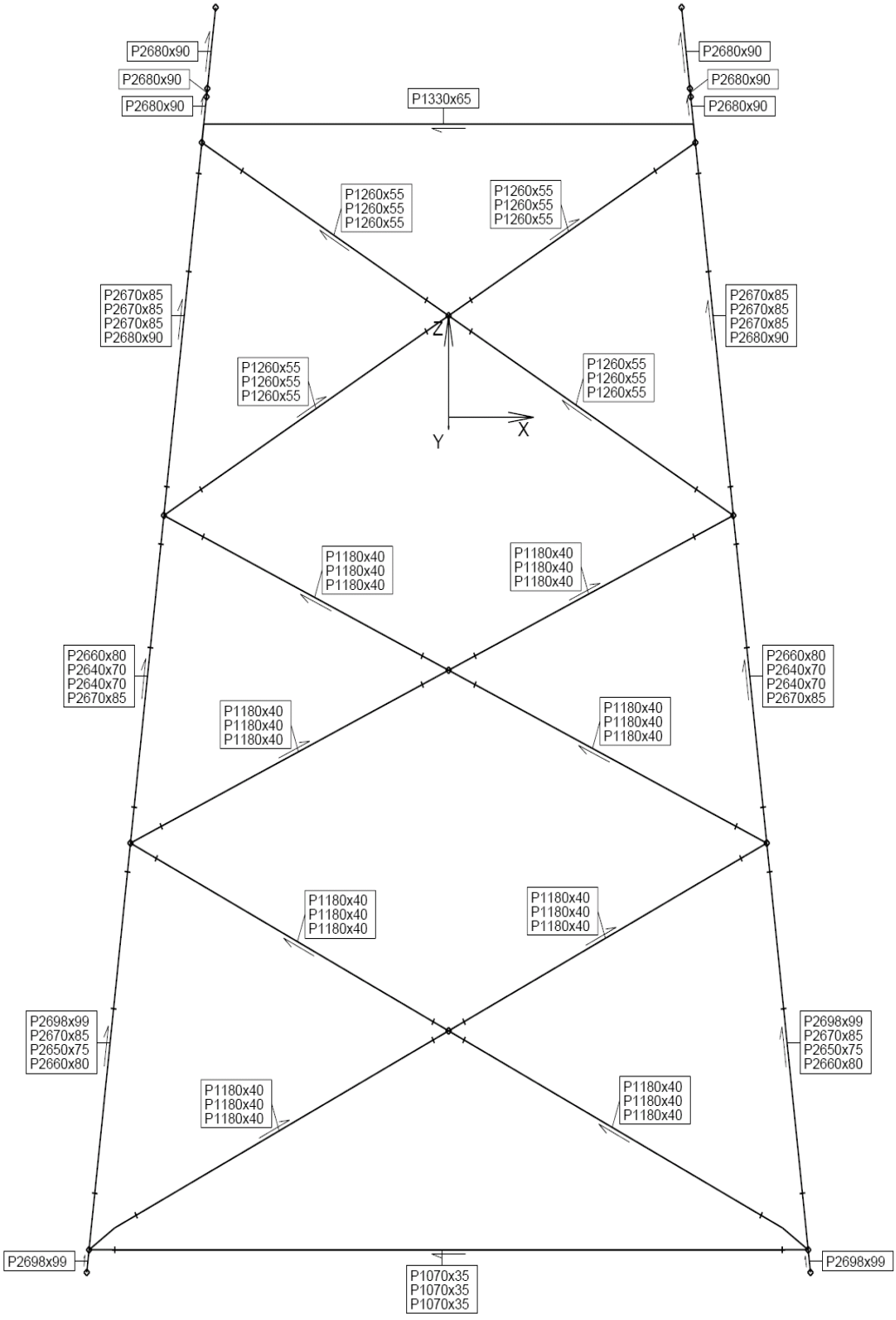


Figure 11.5: Diameter and wall thicknesses of the jacket members

The design verification of the jacket foundation focuses on the Ultimate limit state (ULS) as well as the Fatigue Limit State (FLS).

**Ultimate limit state (ULS)**

1. Maximum utilization ratios of the tension and compression capacity of the soil below 1.0
2. Steel maximum utilization ratios for all sections below 1.0

**Fatigue limit state (ULS)**

The minimum fatigue life for all sections should be above 20 years and above approx. 30 years for the piles in order to accommodate for driving fatigue in the present case.

A brief summary of the results from the natural frequency, extreme and fatigue analysis is provided in Table 11.10.

Table 11.10: Foundation design result summary

| | | |
|---|---|---|
| Natural Frequency [Hz] | | 0.297 |
| Maximum Utilization Ratio [-] | Member | 0.98 |
| | Joints | 0.63 |
| | Soil | 0.98 |
| Minimum Fatigue Life [years] | Member | 172.3 |
| | Joint | 37.1 |

Furthermore, the first eigenmode as well as the maximum steel utilization ratios in the jacket and piles are shown in Figure 11.6.

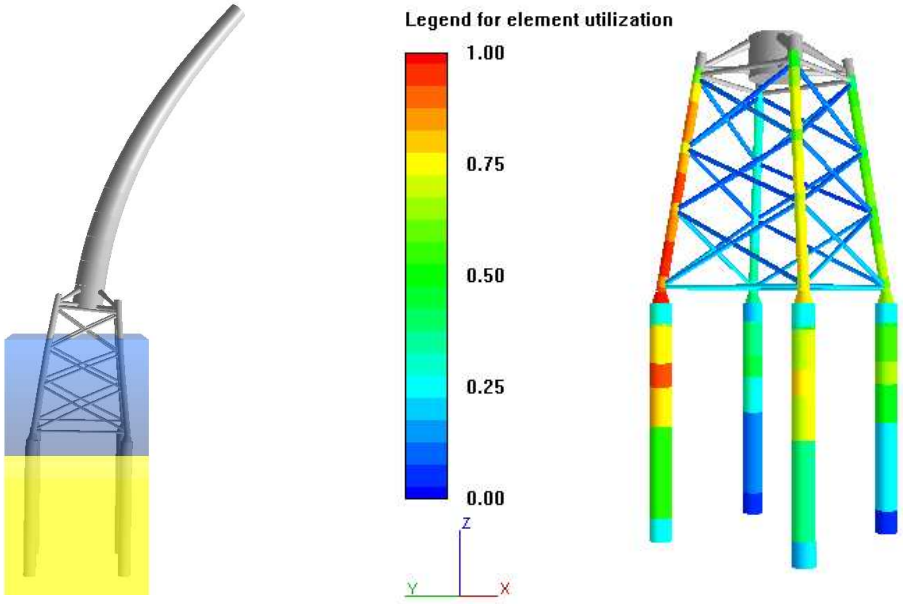


Figure 11.6: First mode shape of the support structure and maximum steel utilization in the jacket and piles

## 11.7 Assessment of the 20MW offshore wind turbine

The main parameters of the turbine, tower, jacket and piles have been introduced in the previous chapters. As mentioned before the present study has limited its scope to the design of the jacket as well as piles for the given configuration of the tower, RNA and their corresponding aerodynamic loads. Nevertheless, this section addresses aspects related to the evaluation of all relevant subsystems as well as of the offshore wind turbine as a whole.

### 11.7.1 Evaluation Approaches for the Design

A typical task of a foundation designer comprises the evaluation of a foundation structure after and within each design iteration loop. Numerous aspects/approaches may be inspected/applied to obtain a measure for this evaluation, including the following exemplary selection:

1. Geometry and masses from structures designed for similar conditions
2. Feasibility of the design with respect to available fabrication, transportation and installation equipment/facilities
3. Influence from alternative design solutions for the main subsystems on the design results, loads and masses
4. Influence from variations of the main structural parameters on the design results, loads and masses
5. Load ratios, e.g. aerodynamic vs. hydrodynamic loads and static vs. dynamic loads
6. Integration of the foundation structure into the overall offshore wind turbine
7. Reserves in terms of fatigue lives and utilization ratios throughout the structure as well as the distance of the natural frequency from the main exciting frequencies (such as 1P, 3P and waves)
8. Visual and numerical comparison of the relation of jacket member and pile dimensions compared to the tower
9. Comparison of the superstructure mass, i.e. tower and RNA, with the mass of the transition piece, jacket and piles

Additional aspects such as influences from met-ocean conditions and other site specific parameters, specific structural influences such as dampers, wind farm influences as well as from fabrication, transportation and installation possibilities and limitations needs to be considered in relation to the aforementioned list of selected aspects/approaches. This list might be taken as a basis for the evaluation of the present foundation structure.

The comparison of geometry and masses of similar structures according to item 1 of the list cannot be properly addressed in this study due to missing references.

Assessment of the fabrication, transportation and installation possibilities according to item 2 is addressed in a limited manner in a latter part of this chapter with reference to available equipment from both, the offshore wind and the offshore oil & gas industry.

Alternative design solutions according to the item 3 are briefly discussed for a selection of main subsystems at a latter part of this chapter.

Influences from variations of the main structural foundation parameters according to item 4 have been assessed for the foundation parameters during the course of the design. However, it has been found that the largest influences are introduced by the superstructure, i.e. tower and RNA which is further elaborated at a latter part of this chapter.

Checking the load ratios according to item 5 reveals a significant dominance of the aerodynamic loads. For example, the maximum absolute integral overturning moment from the hydrodynamic loads at mudline is in the order of 6% of the overturning moment from aerodynamic loads in the extreme load situation. Similar load ratios can be expected for the fatigue loads. However, it has

to be emphasized that the influence of the hydrodynamic load contribution to the total fatigue loads must be weighted differently compared to the extreme load situation. This is due to the fact, that the fatigue damage is tendentially proportional to the $m^{th}$ power of the loads, with $m$ being the inverse slope of the S-N curve for the corresponding fatigue detail. The following numbers may serve as a simplified example:

- Fatigue detail with an inverse slope of the S-N curve of $m = 5$
- Hydrodynamic fatigue loads increase the total fatigue loads by 6% (e.g. damage equivalent loads)
- Fatigue damage increased by a factor of $1.06^5 = 1.34$, due to hydrodynamic contribution

Integration aspects of the foundation into the overall offshore wind turbine according to item 6 as well as the integration of the turbine and tower are discussed throughout this section. One main conclusion of this assessment e.g. is that superstructure design should be revised in order to allow for a cost-efficient foundation design w.r.t. natural frequency requirements. As stated before, the present design of the offshore wind turbine foundation can be seen as the result established within the first design iteration loop of an integrated design.

Certain details on item 7 have already been provided in the previous section. The steel utilization in the extreme load scenario is relatively good throughout the leg(s) of the structure, compare Figure 11.6. Some fatigue reserves in the foundation structure are introduced due to the large and stiff configuration, i.e. lowest fatigue life in joints at 37.1 years and in the members at 172.3 years. The pile design is driven by the soil capacity with a utilization of 0.98. All utilization ratios and fatigue lives indicate a reasonably designed foundation. However, the natural frequency is at 0.297 Hz which is approx. 3.5% below the stiff-stiff design frequency limit i.e. the natural frequency is just 6.5% above the 3P excitation at rated rotor speed. Designing support structures with a natural frequency in the closer vicinity of the 3P excitations introduces a high risk of large aerodynamic loads. Even though that this natural frequency must be considered too low, the foundation structure as a whole has been designed on basis of very high stiffness requirements in order to achieve at least this minimum natural frequency of the integrated system. This is a consequence of the extremely low natural frequency of the superstructure, i.e. the superstructure natural frequency of 0.361 Hz is just 20% above the stiff-stiff frequency limit of 0.307 Hz.

Items 8 and 9 are related to the first item, but require also to a partially subjective judgement of the designer. In this present case, the member diameters, the jacket top and bottom width as well as pile penetration are not considered to be designed unreasonably in relation to the given tower dimensions in Figure 11.4. Only the lower two x-braces seem to have a rather flat slope. However, application of only two rather than three x-braces is not sufficient due to the fact that the very large length of the resulting braces would introduce severe buckling problems. Furthermore, the largest slope can be found at upper x-brace. This has been designed by intention in order to ensure that the lower joints of the upper x-brace as well as the upper joints of the middle x-brace are outside the splash zone and therefore no corrosion allowance needs to be considered at those particular joints according to Figure 1.7.

Further ratios of key parameters and properties for the 20MW offshore wind turbine and, for convenience, also of the 5MW reference turbine [5] are summarized in Table 11.11.

Table 11.11: Ratios of key parameters and properties of the 20MW and 5MW turbine

| Item | 20MW turbine | 5MW turbine |
|---|---|---|
| $mass_{Tower+RNA}/mass_{TransitionPiece+Jacket+Piles}$ | 1.35 | 0.6[5] |
| $mass_{Jacket}$ /$mass_{Piles}$ | 1.5 | 1.2 |
| jacket top width / tower bottom diameter | 2.0 | 1.4 |
| jacket base width / tower bottom diameter | 3.0 | 2.1 |
| tower bottom diameter / jacket leg diameter | 5.2 | 4.7 |
| tower bottom diameter / pile diameter | 2.5 | 2.7 |
| hub height w.r.t mudline/ pile penetration | 3.8 | 2.9 |

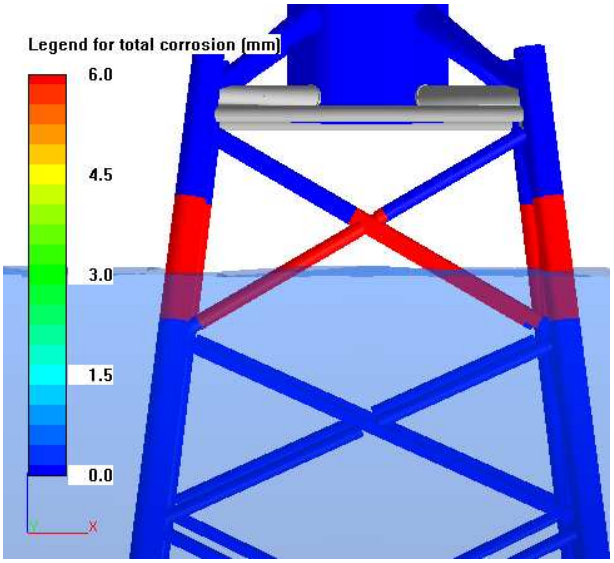


Figure 11.7: Corrosion allowance for the fatigue analysis

The transition piece design has been integrated into the lowest tower section in order to avoid direct wave actions. As a consequence, the vertical blade clearance has become very low. However, increasing the hub height and therefore the tower length would further decrease the superstructure natural frequency which already is extremely low. It must be emphasized for the present structural configuration that even small reductions of the superstructure natural frequencies are related to the need of tremendous amounts of additional foundation material in order to compensate the global stiffness loss, as will be elaborated in the next part. Furthermore, the overall dimensions of the given superstructure are considered unrealistically large. A further increase of the foundation dimensions would therefore not help to get a better understanding of future generations of foundation designs for large wind turbines as well as to identify the corresponding challenges.

The pile diameters and penetration depths are rather large. In fact, a penetration depth of 55m for driven piles is considered to be the upper limit in order to avoid buckling and pile refusal and has therefore be applied as a limit for the present design. The jacket base width as well as the pile diameter and wall thickness has been increased in order to ensure a sufficient soil capacity

[5] No consideration of the concrete transition piece mass

as well as avoid pile buckling as a consequence of the pile penetration limitation. Nevertheless, driven piles with the present dimensions are not necessarily the most efficient solution, alternative e.g. are:

- pile groups at each leg, consisting of 3-4 smaller diameter piles with sufficient distance to each other.
- drilled piles, resulting a in larger penetration depth and/or diameter.

No detailed analysis of the steel/grout interaction in the overlap zone between jacket legs and main piles has been performed within this study. In a real design situation, however, a detailed analysis should be performed in order to verify a sufficient capacity of this connection.

Furthermore, the transition piece has not been properly addressed for the present design due to resource and time limitations. However, it must be stated that transition pieces between tubular steel towers and jackets have a large influence on the global stiffness as well as on the load transfer from the tower to the jacket. They also form a major cost item of the foundation structure. A thorough design of the transition piece as an integrated part of the foundation structure based on a combination of detailed subsystem models and global models must be considered essential for a proper overall design optimization in a real design situation. Additionally, the connection of the transition piece with the jacket legs should be addressed by a more detailed FE analysis.

### 11.7.2 Considerations on the natural frequency of the support structure

As outlined before, the natural frequency of the offshore wind turbine at 0.297 Hz is slightly below the stiff-stiff frequency limit at 0.307 Hz, i.e. the natural frequency is within the safety range of the upper limit 3P excitation. It can be assumed that the turbine is operating at rated speed for a significant amount of the life time and that severe aerodynamic 3P excitations are introduced to the support structure. Therefore, the risk of large aerodynamic fatigue loads is estimated to be very high. This could only be quantified by a proper aero-elastic analysis implying another load iteration which is beyond the scope of this study. The obvious solution would be an increase of the natural frequency by increasing the foundation stiffness since the superstructure properties, i.e. tower and RNA, are fixed. However, implementation of more foundation stiffness can only be achieved on basis of tremendous material efforts due to the very soft superstructure for a stiff-stiff design solution (i.e. 0.361Hz with a rigid foundation). A further increase of the foundation stiffness is neglected for the present design since other options for an increase of the global stiffness and/or decrease of the mass properties are more convenient and probable in reality.

**Tower and transition piece**

A large influence on the global stiffness of the present offshore wind turbine is introduced by the tubular steel tower which has a rather low stiffness-to-mass ratio compared to other structures. Both, the structural layout as well as rather large tower height might be considered as sufficient starting points for modifications of the mass and stiffness properties.

As mentioned before, the transition piece has a large influence on the global stiffness as well as on the load transfers from the tower to the jacket and forms a major cost item of the foundation structure. This requires a thorough design approach and optimization e.g. w.r.t. the fabrication and installation in a real design situation.

An elegant solution for both aspects, increasing the tower stiffness-to-mass ratio as well as avoiding expensive transition pieces, might be introduced by replacement of the tubular steel tower by either jacket or lattice type towers. However, it needs to be noted that the horizontal dimensions of these kinds of braced towers typically exceed those of their corresponding tubular steel tower counterparts which is given by the outer diameter. Braced towers might therefore

become more attractive in combination with downwind turbines in order to satisfy horizontal blade clearance requirements between the blade tip and tower. Furthermore, negative tower shadow effects on downwind turbines will probably be also less pronounced for jacket or lattice towers compared to tubular steel towers.

**Rotor-Nacelle-Assembly**

Influences of the RNA on the first natural frequency of the support structure are mainly introduced by the mass properties. However, additional aspects influence the natural frequency design as well. Here, the rotor diameter could serve as an example:
Reduction of the rotor diameter tendentially reduces the rotor mass and potentially also the hub height. Both reductions correspond to an increased natural frequency of the support structure. On the other hand, it must be considered that the rated rotor speed might very well increase in order to maintain the optimal tip speed ratio .

Another alternative might be introduced by reconsideration of a two-bladed turbine design. Potentially, tremendous costs benefits next to a significant decrease the rotor mass could be achieved by saving one blade. Of course, two-bladed turbines introduce their own challenges such as more severe dynamic loading on the hub. However, the optimal tip speed ratio increases for a two-bladed turbine compared to their three-bladed counterparts. Therefore, it is probable that the frequency limits for soft-stiff and stiff-stiff designs would be shifted as well for a two-bladed turbine.

A further solution to avoid inconvenient 3P excitations for the present design aims at the control system rather than the structural properties. The control system can be used to define a rotor speed exclusion window in the vicinity of the natural frequency. Even though that this solution has successfully been applied for real wind turbine designs it would probably have a significant negative impact on the turbine performance for the present design since the natural frequency under consideration would require an exclusion of the rated rotor speed.

More detailed investigations on the aforementioned aspects related to the RNA are far beyond the scope of the present study and are elaborated in more detail in other work packages of the UpWind project.

### 11.7.3 Evaluation of the RNA and tower

Table 11.1 has introduced upscaling coefficients according to the classical similarity theory as well as more realistic values. The influence of the different upscaling parameters for a 20MW turbine based on the much smaller 5MW configuration is rather large. This is indicated in Table 11.8 for the development of the upscaled RNA mass using the upscaling coefficients from Table 11.1. The difference of the upscaled RNA masses show a clear non-linear trend toward increasing differences with increasing step sizes for the upscaling.

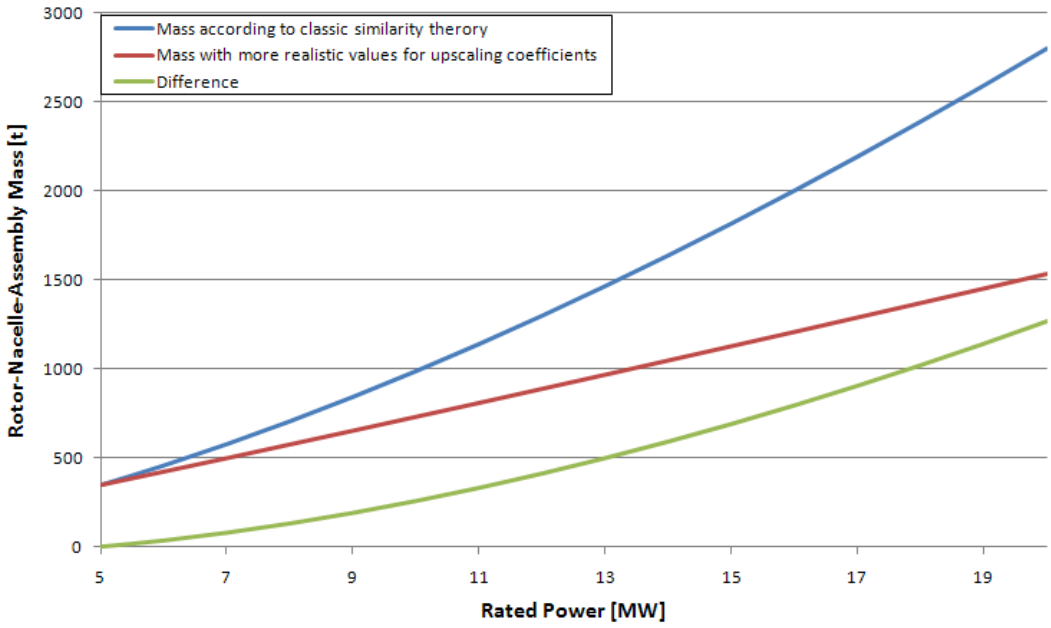


Figure 11.8: Upscaling of the RNA mass for different upscaling coefficients

The influence from the different sets of upscaling coefficients according to Table 11.1 is briefly summarized for selected parameters for two 20MW turbines in Table 11.12. The two turbines are:

- 20MWclassic as used throughout this chapter based on classic theory uspcaling coefficients
- 20MWmod based on the more realistic upscaling coefficients

Furthermore, Table 11.12 also shows the natural frequencies for the both 20MW turbines as well as for the 5MW reference turbine [5] in case of a flexible and rigid foundation. For simplicity, the 20MWmod turbine natural frequencies have been calculated under consideration foundation structure designed for the 20MWclassic turbine and a reduced hub height level according to the reduction of the rotor radius, i.e. 12 m. The hub height change has been incorporated into the model by cutting-off the upper 12m of the tower.

Table 11.12: Turbine parameters and natural frequencies for different upscaling approaches

| Turbine | 5MW (reference structure) | $20MW_{classic}$ (classic upscaling coefficients) | $20MW_{mod}$ (more realistic upscaling coefficients) |
|---|---|---|---|
| Rotor diameter [m] | 126 | 258 | 234 |
| Power [MW] | 5 | 20 | 20 |
| RNA mass [t] | 350 | 3565 | 1536 |
| Natural frequency [Hz] | 0.290 | 0.297 | 0.441 |
| Rigid foundation natural frequency [Hz] | 0.410 | 0.361 | 0.557 |

The table clearly shows that a more realistic design introduces much more beneficial mass properties and modal properties of the superstructure. The integrated support structure natural frequency could therefore easily be designed far beyond the lower limit of the stiff-stiff design

range. However, as mentioned before the reduced rotor diameter of the 20MWmod configuration might also imply an increase of the rated rotor speed and therefore an increase of the frequency limit of the stiff-stiff design range. Nevertheless, the increased stiffness in combination with the tremendously decreased mass of the superstructure ensures a significant reduction on the stiffness requirements of the foundation for the natural frequency design.

Furthermore, the potential hub height reduction of 12 m of the 20MWmod turbine will have a mitigating effect on the aerodynamic loads while the reduced mass of the RNA and tower significantly reduce the dead weight loads as well as inertia loads as a part of the dynamic response. Especially, the decreased aerodynamic loads as well as the increased natural frequency potentially would lead to a foundation design with lower member diameters and/or width of the jacket. This, in turn, will further have a beneficial influence on the hydrodynamic loads due to the following aspects:

- Increased natural frequency of the structure shows larger distance from exciting fatigue wave frequencies and therefore to a less amplified hydrodynamic response.
- Lower member diameters and/or width of the jacket leads to lower hydrodynamic forces on the structure

Both aspects tend to reduce the overall design loads even beyond the reduction of the aerodynamic loads and dead weight load allowing for further design optimizations.

### 11.7.4 Fabrication, Transport and Installation

20MW turbines will only be available on the medium- to long-term scale. Development of these turbines is expected to take place in a number of intermediate steps introducing a more steady increase of the turbine sizes. This steady development will be accompanied be development of facilities and equipment for fabrication, transportation and installation. An assessment of available facilities and equipment as part of an integral design approach will therefore only be relevant as soon as the design process for such a turbine starts.

This part of the 20MW offshore wind turbine study addresses aspects related to the fabrication, transportation and installation of the main components, i.e. piles, jacket, transition piece, tower and RNA. Focus is given to considerations on facilities and equipment as available today. However, it must be kept in mind that the superstructure is considered by far too large for a realistic representation of future 20MW turbines. Therefore, lower requirements on the facilities and equipment are expected for 20MW offshore wind turbines in reality.

#### Rotor-Nacelle-Assembly

Fabrication issues for the large rotor-nacelle-assemblies are not considered in the present study since this is expected to be part of the studies conducted in the UpWind Upscaling work package. Transportation of such large structures is possible offshore. However, limitations might arise in case of fabrication yards far away from the harbour. Here, the dimensions of the rotor blades as well as the mass and dimensions of the assembled nacelle might result in onshore transportation problems. Furthermore, installation of the RNA is not possible with the equipment available today due to the large hub height. The lifting capacities of available cranes are sufficient apart from the aforementioned lifting height limitation.

#### Tower

The tower diameters of the segments are too large for available fabrication facilities, especially the bottom segment with a diameter of 14m. These diameters might introduce similar onshore transportation problems as for the RNA while offshore transportation should not introduce any challenges. Furthermore, installation of the upper tower segment(s) is not possible with the equipment available today due to the large hub height.

**Transition Piece and Jacket**

Both, the transition piece as well as jacket can be fabricated, transported and installed with available equipment as existing structures from the offshore oil and gas industry prove, compare e.g. the Kvitebjørn jacket [49]. The upper part of this modular jacket structure from the offshore oil & gas industry has a base width of 50x50m, a weight of more than 7000t and height of more than 177m. However, onshore transportation problems might occur for the 20MW turbine jacket and transition piece structure as for the tower and rotor-nacelle-assembly. It must furthermore be stressed that offshore structures from the oil & gas industry are specialized and unique designs whereas offshore wind turbine foundations are often subject to mass production, mass transportation and mass installation. In addition, the requirements for cost efficient production, transportation and installations are stricter for offshore wind turbines compared to offshore oil & gas structures. Nevertheless, lessons can be learnt from experiences of the offshore oil & gas industry. For example, jackets designs could consist of two or more modules in order to cope with capacity limitations for fabrication, transportation and installation, but also to utilize benefits from mass production for large wind farms as indicated in Figure 11.9. However, connection solution for modular jackets might have some practical implications on the jacket configuration. For example, the jacket would need to have vertical legs (at least in the lower module) if it should be fabricated in two sections and assembled offshore below water. On the other hand, vertical legs are not a requirement if the jacket is assembled onshore by welding.

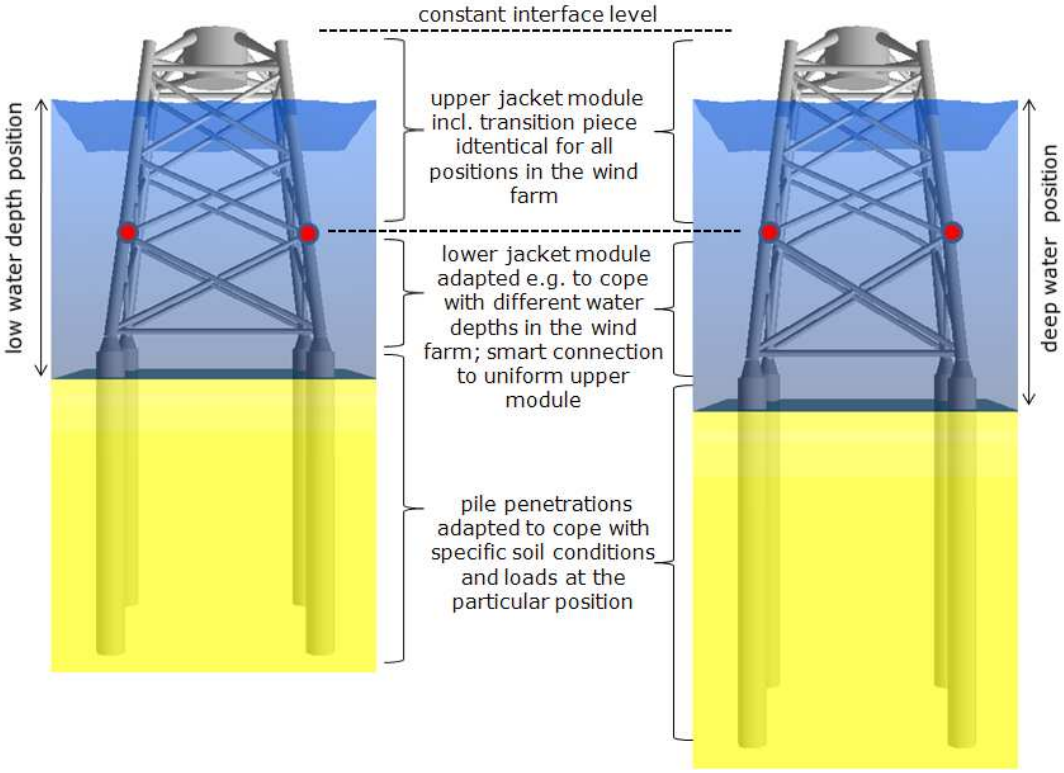


Figure 11.9: Modular jackets at different positions within a wind farm

**Piles**

The main pile dimensions of 5.6m diameter and 60m length are very similar to monopile dimensions of present installations of offshore wind turbines. Therefore, no particular problems are expected in relation to fabrication and transportation of the piles. However, the penetration depth is relatively large compared to monopiles which must not necessarily lead to problems.

## 11.8 Conclusions

This chapter described the design of a 20MW offshore wind turbine foundation at the Upwind offshore reference site [13] and subsequently evaluated the overall offshore wind turbine. For this purpose a 20MW turbine had to be upscaled from the 5MW reference turbine [5] based on classical similarity rules since no other representative turbine was available when the design work had to be conducted. Unfortunately, the resulting turbine is considered by far too large and heavy which is a result of the application of classic upscaling coefficients rather than more realistic values as e.g. obtained from turbine development trends over the last years. Furthermore, the foundation design efforts are mainly limited to the jacket and piles whereas a transition piece representation has been considered in the model but has not properly been designed. Exclusion of the transition piece from more detailed investigations in this study is based the following aspects:

- A proper transition piece design requires major design and modeling efforts which is not reflected by the available resources for this study.
- No standardized solutions for transition pieces between jackets and tubular steel towers do exist even for nowadays jacket designs. In fact, transition pieces are currently subject to major research and development activities.
- The given tubular steel tower structure is not a reasonable representation of future 20MW towers. Here, even solutions without tubular steel towers such as with a jacket or lattice type towers might be more feasible which would make the transition piece obsolete.

Design loads are superimposed from individually calculated aerodynamic and hydrodynamic loads in a reduced load setup compared to the design of the 5MW reference foundation [2]. The superimposed approach is considered sufficient for the purpose of this study and especially due to the fact that the aerodynamic loads show a significant dominance. However, application of damage equivalent aerodynamic loads for the fatigue design in this particular case of a jacket and the dominating aerodynamic loads should be critically evaluated due to the fact that the jacket joint classification depends also on the load constellation. Furthermore, the tower and RNA design has been performed in an isolated manner, i.e. without consideration of foundation requirements. Therefore, the conducted foundation design efforts are on a conceptual design level at best representing only a first design iteration loop.

Some general conclusion can be made on basis of the present design even though that the overall design of the 20MW offshore wind turbine is not considered to be a good representation of real turbines in the future.

Upscaling of the turbine based on the classic similarity theory corresponds in principle to the assumption of using the same technology for the larger turbine as has been used for the reference turbine. However, all trends from recent turbine developments as well as from currently developed technologies, e.g. with respect to lighter material or aerodynamic blade optimizations indicate that realistic upscaling coefficients will be much more beneficial. The influence of wrong assumptions in the upscaling coefficients is significantly amplified by the increased step sizes between the reference turbine and the upscaled turbine. Especially, in the present case of upscaling a 5MW turbine to a 20MW turbine the step size is considered rather large.
Furthermore, simple application of traditional design solutions rather than consideration of more feasible alternatives might lead to even more unfavourable dimensions of the upscaled offshore wind turbine such as for example application of the tubular steel tower instead of a lattice tower.
Both, neglecting technological developments and therefore applying a conservative upscaling approach as well as application of traditional design solutions for the superstructure result in tremendous masses and loads accompanied by the harsh requirements on the foundation for the natural frequency design. This introduces many challenges to the foundation designer and, furthermore points towards an economic dead end for large offshore wind turbines.

In this context, it is also highlighted that the isolated design approach of the superstructure, i.e. RNA and tower, and subsequent integration of a foundation is not considered sufficient when developing larger turbines. Instead, a more integrated approach even at early development stages will be superior to this separated approach since essential subsystem requirements can be identified before the main parameters of e.g. the RNA are fixed.

The foundation design is considered reasonably only in relation to the given tower and RNA configuration, allowing for fabrication, transportation and installation even with nowadays facilities and equipment. Nevertheless, the designed foundation structure is very large and not expected to be a good representation of future jacket foundation structures for 20MW turbines. This is a consequence of the fact that the foundation design strongly depends on the tower and RNA configuration and both subsystems are expected to differ significantly in reality from the given configuration in this study.

Equipment and facilities for fabrication, transportation and installation of the designed foundation components are available even nowadays. Limitations arise in connection to the installation of the given tower and RNA components due to the large hub height as well as for fabrication of the tower segments due to the large diameter. It is suggested to use fabrication yards close to the harbour in order to avoid onshore transportation problems.

# 12. Conclusions

The aim of the task 4.2 is to develop support structure concepts for large offshore wind turbines in the range of 5 to 20 MW and in water depth ranges of 25 to 70 m, including bottom mounted very soft and floating structures. To meet this objective first a survey of existing and proposed support structure concepts has been done. An overview of existing concepts is presented in Figure 12.1, while several proposed concepts are shown in Figure 12.2.

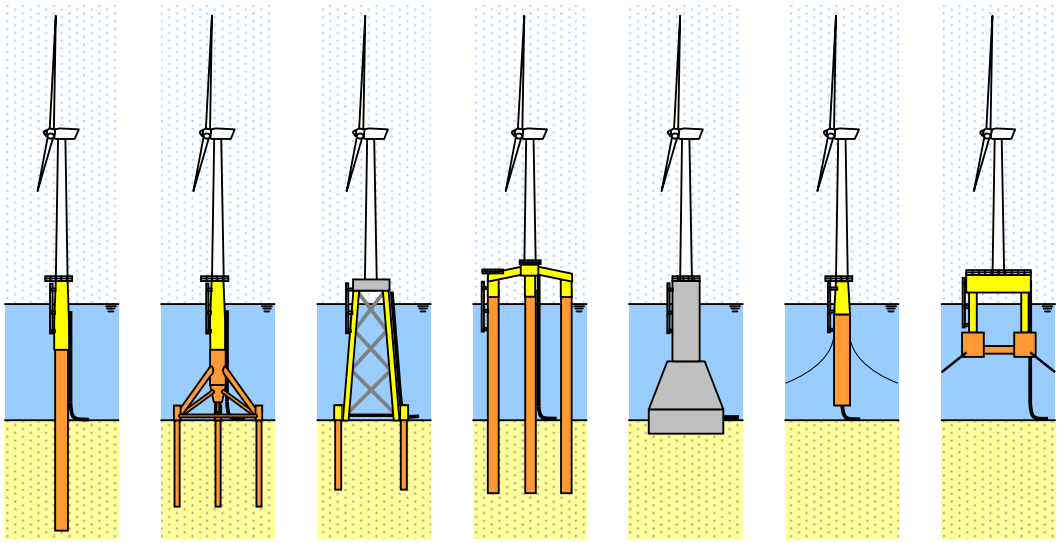


Figure 12.1: Existing support structure concepts

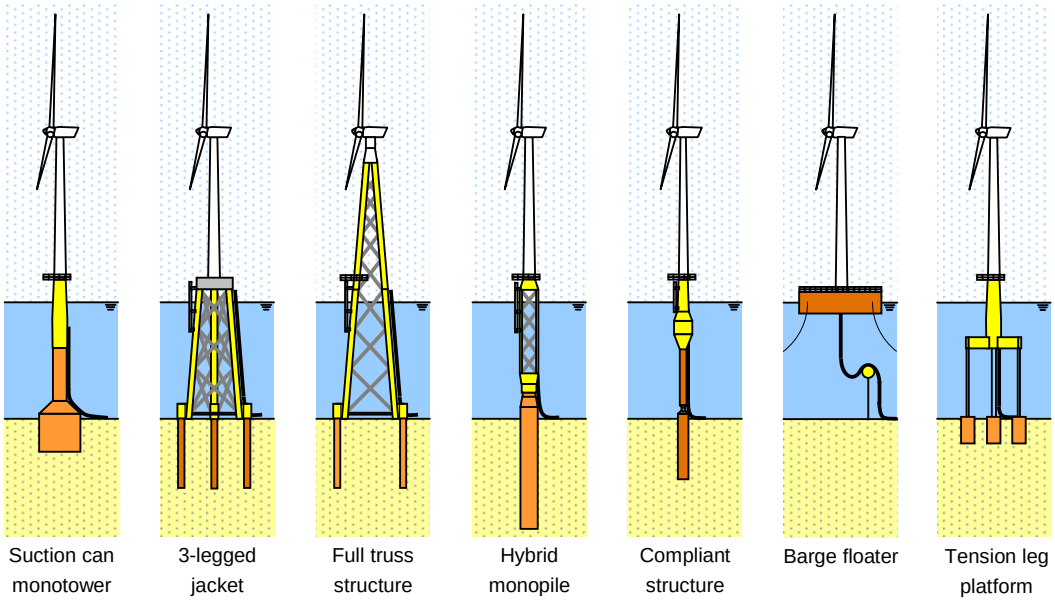


Figure 12.2: Proposed support structure concepts

A reference design was made for a monopile structure in 25 m water depth for the UpWind 5 MW reference turbine. The resulting design comprises a foundation pile with a bottom diameter of 6 m and a conical section tapering to a top diameter of 5.5 m. The embedded length is 24m and the total length is 54 m. The transition piece has an outer diameter of 5.8 m and a total length of 18.7 m. A tower of 68 m length is used, leading to a hub height of 85.2 m. The overall mass of the primary steel for the foundation pile is 542 tonnes and 147 tonnes for the transition piece. The required wall thickness for the monopile and transition piece is driven by fatigue, whereas the penetration depth is driven by ultimate loads and natural frequency requirements.
In general the first natural frequency is strongly influenced by the structure length and to a lesser degree by the turbine mass. When these values are fixed, which is the case when the turbine type and site conditions are known the natural frequency can be influenced by changing pile diameter and penetration depth.
For shallow waters fatigue is predominantly governed by aerodynamic loading, but for deeper waters the increase in diameter causes an increase in the hydrodynamically driven fatigue. However, this is very much dependent on the wave conditions on site and on the turbine size. The structure wall thickness is mostly governed by fatigue.
The structure mass increases following a square relation with the water depth and as this is mainly due to the increase in the length of the structure, this also holds true for increasing hub height. The overall costs for a monopile structure are mainly driven by the material costs, due to the sheer amount of steel required.

A reference jacket structure has been designed for 50 m water depth to support the Upwind 5 MW reference turbine. The interface level and hub height are set at 20.15 m + MSL and 90.55 m + MSL respectively. A simplified transition piece represented by a concrete block is applied with length and width of 9.4 m and 4 m height. A jacket bottom width of 12.0 m is chosen. The overall mass of the jacket structure is 983 tons, the piles accounting for 438 tons and the jacket substructure contributing the remaining 545 tons.
An important feature of jacket structures is their transparency to waves, which significantly reduces the hydrodynamic loading. The support structure's first natural frequency is strongly influenced by the tower length. The base width is an effective parameter to influence the natural frequency, as is increasing the leg diameter. However, the latter measure leads to higher hydrodynamic loading. Jacket structures are relatively insensitive to varying soil conditions if piles are sufficiently long. The overall mass of the substructure increases approximately linearly with increasing water depth.
Costs for fabrication are attributed for the major part to production and only for a minor part to material costs.

Apart from the reference designs for the monopile and jacket structures, several other support structure concepts have been assessed. Preliminary designs were made for a tripod, a three-legged jacket, and a monopile - truss hybrid in 50 m water depth. Also a monopile structure has been designed as a reference. The reference jacket structure is also included in the comparison. The results of this analysis show that the three legged and four legged jacket structures are best suited for the conditions considered. The three-leg jacket concept shows a lower overall mass than the reference jacket. The monopile-truss hybrid structure is only marginally heavier than the four-leg jacket. Compared to an equivalent monopile it experiences significantly lower hydrodynamic loads than and is also significantly lighter. The tripod is significantly heavier than the jacket structures and the monopile-truss hybrid structures. It accumulates high fatigue damage at the connections of the legs and braces to the central column. Finally, the monopile is the heaviest structure, also experiencing high fatigue damage, mainly due to hydrodynamic loading.

Two distinct types of soft-soft structures have been considered, compliant bottom mounted structures and floating structures.
In order to achieve sufficient flexibility for a compliant structure to locate its first natural frequency inside the soft-soft range and below wave frequencies with high energy artificial soft

spots are required. However, it is difficult to achieve strength and stability requirements for such a structure at the same time. Therefore additional restoring force is required. A study in which an extended monopile, a compliant piled tower and an articulated buoyant tower have been evaluated showed that it is possible to design an articulated buoyant tower as a compliant structure in 50 m water depth. The mass savings compared to a soft stiff design for the same conditions were found to be approximately 100 tons in this preliminary assessment. For the other two concepts it has not been found possible to achieve a compliant design for the considered conditions.
Given these requirements it is unlikely that compliant structures will be applied in water depths less than approximately 70m. However, compliant structures may be effective in intermediate water depths, of approximately 70 -100 m, where bottom mounted structures may no longer be viable and floating structures might still need too much buoyancy to be cost effective.
Three floating structure concepts have been compared: a barge floater, a spar buoy and a tension leg platform. The simple design of a barge floater may prove to be cost effective for benign sea conditions. The spar buoy is better suited for harsh sea conditions, but its deep draft and the large ballast make the structure relatively expensive. Regarding ultimate strength and fatigue considerations, the tension leg platform appears to perform best, but the installation procedure and the large mass makes it an expensive structure type.

A design for a jacket foundation for a 20MW turbine has been made. The 20 MW turbine used is the result of the application of classic upscaling coefficients rather than more realistic values as e.g. obtained from turbine development trends over the last years, leading to a very heavy, unrealistic design. Due to the low rotor speed of the 20 MW turbine the upper boundary of the 3P range is at 0.306 Hz. Therefore a stiff-stiff design is considered, rather than the conventional soft-stiff approach.
The foundation design is considered reasonably only in relation to the given tower and RNA configuration. Nevertheless, the designed foundation structure is very large and not expected to be a good representation of future jacket foundation structures for 20MW turbines. The resulting jacket structure has a top width of 28m and a base width of 42m. The overall structure mass, including piles, transition piece and jacket is 5610 tons. The associated first natural frequency is 0.297 Hz. As such the structure's first natural frequency falls within the 10% safety margin at the upper end of the 3P range. However, it is shown that it would be possible to achieve a design with a first natural frequency in the stiff-stiff range when the RNA mass and rotor diameter are scaled in more line with technological developments. Other possibilities for enabling the application of 20 MW wind turbines offshore is by employing lattice towers instead of the tubular tower used in this design.
Equipment and facilities for fabrication, transportation and installation of the designed foundation components are available even nowadays. Limitations arise in connection to the installation of the given tower and RNA components due to the large hub height as well as for fabrication of the tower segments due to the large diameter.

Overall it can be concluded that for water depths less than 25 m the monopile is the most effective solution, due to it relative simplicity in fabrication and installation. However, for larger water depths the hydrodynamic loading on such a structure rapidly increases. In these conditions hydrodynamically transparent structures are more suitable. A monopile-truss hybrid may be a suitable alternative in water depths ranging from 25 m to 40 m. For water depths in the range of 50 m, three leg or four leg jacket structures are most suitable.
For increasing water depths softer structures such as compliant structures or floating structures provide a solution.
Finally for very large turbines a support structure with a natural frequency in the stiff-stiff range is the most likely solution. However, weight reduction in the turbine is essential to enable the deployment of turbines in the range of 20MW offshore and the design of the tower should be performed integrally with the substructure.

# References


[1] DNV-OS-J101. Design of Offshore Wind Turbine Structures, Det Norske Veritas, October 2007.

[2] American Petroleum Institute, Recommended Practice for Planning, Design and Constructing Fixed Offshore Platforms – Working Stress Design, 21st edition, USA, 2000.

[3] Diepeveen, N. de Vries W. Comparison of conventional and hydraulic drive train mass and their influence on support structure design, RERC Trondheim, June 2010

[4] De Vries, W. Assessment of bottom-mounted support structure types with conventional design stiffness and installation techniques for typical deep water sites, Upwind Deliverable report D4.2.1, 2007

[5] Jonkman, J., et al. Definition of a 5-MW reference wind turbine for offshore system development. Technical Report at the National Renewable Energy Laboratory. NREL/TP-500-38060; Golden, CO, USA, 2006.

[6] Bossanyi, E. A state-of-the-art-controller for the UpWind reference wind turbine. Proceedings of the European Wind Energy Conference (EWEC); Marseille, France, 2009.

[7] Jamieson, P. wind turbine cost overview, memo on Upscaling, Upwind WP1B4

[8] IEC 61400-3, Wind turbines – part 3: Design requirements for offshore wind turbines. International Electrotechnical Commission; Geneva, Switzerland, 2009.

[9] Germanischer Lloyd.Rules and regulations; Guideline for the certification of offshore wind turbines; Hamburg, Germany, 2005

[10] Kühn, M. Dynamics and Design Optimisation of Offshore Wind Energy Conversion Systems. PhD thesis - DUWIND 2001.002; Delft, The Netherlands, 2001.

[11] Krolis, V. et al. Determining the embedded pile length for large diameter monopiles, Marine Technology Society Journal, 2010

[12] Fischer, T. et al. Offshore support structure optimisation by means of integrated design and controls,

[13] Fischer, T., de Vries, W., and Schmidt, B.: Design basis - Upwind K13 deep water site, Endowed Chair of Wind Energy, Stuttgart, 2010

[14] Sumer, B.M.; Fredsøe, J., The mechanics of scour in the marine environment, World Scientific Publishing Co., Singapore, 2002

[15] Rambøll Offshore structural Analysis programme package, Version 4.3, January 2009.

[16] GH Bladed, Version 3.81, Garrad Hassan, 2008.

[17] Schmidt, B. Aerodynamic Damping of Offshore Wind Turbines, Dipl. Thesis, Technische Universität Darmstadt, SWE Universität Stuttgart, February 2008

[18] EN10025: 1993 : “Hot rolled products of non-alloy structural steels – Technical delivery conditions, November 1993.

[19] de Vries, W. Krolis, V. Effects of deep water on monopile support structures EWEC, Milan, 2007

[20] Cockerill, T. et. al.Opti-OWECS Final report Vol.3: Comparison of cost of offshore wind energy at European sites, 1998

[21] Efthymiou, M: Development of SCF formulae and generalised influence functions for use fatigue analysis. Proceedings of offshore tubular joint conference, surrey, United Kingdom, October 1988.

[22] NORSOK standard N-004 – Design of steel structures, Rev. 2, October 2004.

[23] Vemula, K., De Vries, W., Fischer, T., Cordle, A. and Schmidt, B. - Design solution for the UpWind reference offshore support structure, UpWind deliverable D4.2.6, 2010.

[24] Passon. P, Design of Offshore Wind Turbine Foundations in Deeper Water - 2010,to be published.

[25] Popko, W., Load analysis and mitigation of an offshore wind turbine with jacket support structure, Master thesis, Risoe-DTU, 2010.

[26] Barltrop, N.; Adams, A.: Dynamics of fixed marine structures, section 6.8.7, MTD / Butterworth-Heinemann 1991

[27] Kaufer, D.; Fischer, T.; Vorpahl, F.; Popko, W.; Kühn, M.:Different approaches to modeling jacket support structures and their impact on overall wind turbine dynamics, Conference paper, DEWEK, Bremen, 2010

[28] Vorpahl, F. R.; Huhn, H.; Busmann, H. and Kleinhansl, S. - A Flexible Aero-elastic Simulation Approach for Offshore Wind Turbines, European Offshore Wind Conference (EOW), 2007

[29] Cordle, A. (editor): Final report for WP4.3: Enhancement of design methods and standards, UpWind deliverable D4.3.6, Bristol, 2011

[30] Vorpahl, F. and Kaufer, D.: Description of a basic model oft he „Upwind reference jacket“ for code comparison in the OC4 project under IEA Wind Annex XXX, Fraunhofer Institute for Wind Energy and Energy System Technology (IWES), 2010

[31] Seidel, M. Jacket substructures for the REpower 5M wind turbine, EOW, Berlin, 2007

[32] Clauss, G. The Conquest of the Inner Space – Challenges and Innovations in Offshore Technology 21st National Congress on Maritime Transportation, Ship Construction and Offshore Engineering, 2006

[33] Gerwick, B. Construction of marine and offshore structures CRC Press ISBN 978-0-8493-3052-0, 2007

[34] Vugts, J. Handbook of bottom founded offshore structures Delft University of Technology, 2002

[35] de Vries,W. Compliant bottom mounted support structure types, UpWind deliverable report D4.2.4, 2009

[36] Oud, M. Compliant structures for offshore wind turbines BSc thesis report, Delft University of Technology, 2010

[37] Sesam Manager 5.3-01, Det Norske Veritas, June 2002

[38] Jonkman, J.: Dynamics Modeling and Loads Analysis of an Offshore Floating Wind Turbine. NREL/TP-500-41958. Golden, US-CO : National Renewable Energy Laboratory, November 2007.

[39] Matha, D.: Model Development and Loads Analysis of an Offshore Wind Turbine on a Tension Leg Platform, with a Comparison to Other Floating Turbine Concepts. NREL/TP-500-45891. Golden, US-CO : National Renewable Energy Laboratory, 2009.

[40] Nakim, H. and Stol, K.,: Control methods for Reducing Pitching Motions of Floating Wind Turbines. Stockholm, Sweden : EOWC 2009, 2009.

[41] Design load cased used for the combined wind, wave load calculation, Garrad Hassan.

**Internet**

[42] Ministerie van Verkeer en Waterstaat: Monitoring van de Waterstaatkundige Toestand des lands (MWTL), data K13 Alpha; www.golfklimaat.nl

[43] http://bildarchiv.alpha-ventus.de/

[44] http://www.all-energy.co.uk/UserFiles/File/Peter_Coutts.pdf#search=%22%22OWEC%20Jacket%20Quattropod%22%20all-energy%22

[45] www.dongenergy.com

[46] www.noordzeewind.nl

[47] www.repower.de

[48] http://www.doris-engineering.com/horizon/images/photos/baldpate.jpg accessed May 8th 2009

[49] http://www.ivt.ntnu.no/imt/courses/tmr4195/literature/(Microsoft%20PowerPoint%20-%20February_7th_Kvitebj.pdf

# Appendix I: Reference monopile dimensions

| Comments | Elevation [m+MSL] | Diameter [m] | Wall thickness [mm] |
|---|---|---|---|
| Tower top | 82.76 | 4 | 20 |
| | 77.76 | 4.12 | 20 |
| | 77.76 | 4.12 | 20 |
| | 68.76 | 4.33 | 20 |
| | 68.76 | 4.33 | 22 |
| | 58.76 | 4.56 | 22 |
| | 58.76 | 4.56 | 27 |
| | 48.76 | 4.8 | 27 |
| | 48.76 | 4.8 | 32 |
| | 36.76 | 5.08 | 32 |
| | 36.76 | 5.08 | 36 |
| | 26.76 | 5.32 | 36 |
| | 26.76 | 5.32 | 40 |
| Tower bottom | 14.76 | 5.6 | 40 |
| Transition piece top | 14.76 | 5.6 | 60 |
| | 13.5 | 5.6 | 60 |
| | 13.5 | 5.6 | 60 |
| | 11 | 5.6 | 60 |
| | 11 | 5.6 | 60 |
| | 8.5 | 5.6 | 60 |
| | 8.5 | 5.6 | 60 |
| | 6.5 | 5.9 | 60 |
| | 6.5 | 5.9 | 70 |
| | 5 | 5.9 | 70 |
| Pile top | 5 | 5.9 | 101 |
| | 2.6 | 5.9 | 101 |
| | 2.6 | 5.9 | 101 |
| | -0.4 | 5.9 | 101 |
| | -0.4 | 5.9 | 101 |
| Transition piece bottom | -3.4 | 5.9 | 101 |
| | -3.4 | 5.9 | 70 |
| | -3.9 | 5.9 | 70 |
| | -3.9 | 5.6 | 65 |
| | -5.4 | 5.6 | 65 |
| Pile cone top | -5.4 | 5.6 | 65 |
| Pile cone bottom | -11.4 | 6.2 | 65 |
| | -11.4 | 6.2 | 65 |
| | -13 | 6.2 | 65 |
| | -13 | 6.2 | 80 |
| | -17 | 6.2 | 80 |
| | -17 | 6.2 | 80 |
| | -21 | 6.2 | 80 |
| | -21 | 6.2 | 80 |
| | -25 | 6.2 | 80 |

| | | | |
|---|---|---|---|
| Mudline | -25 | 6.2 | 80 |
| | -26 | 6.2 | 80 |
| | -26 | 6.2 | 80 |
| | -27 | 6.2 | 80 |
| | -27 | 6.2 | 80 |
| | -28 | 6.2 | 80 |
| | -28 | 6.2 | 80 |
| | -29 | 6.2 | 80 |
| | -29 | 6.2 | 80 |
| | -30 | 6.2 | 80 |
| | -30 | 6.2 | 80 |
| | -31 | 6.2 | 80 |
| | -31 | 6.2 | 80 |
| | -32 | 6.2 | 80 |
| | -32 | 6.2 | 80 |
| | -33 | 6.2 | 80 |
| | -33 | 6.2 | 80 |
| | -34 | 6.2 | 80 |
| | -34 | 6.2 | 80 |
| | -35 | 6.2 | 80 |
| | -35 | 6.2 | 75 |
| | -36 | 6.2 | 75 |
| | -36 | 6.2 | 75 |
| | -37 | 6.2 | 75 |
| | -37 | 6.2 | 75 |
| | -38 | 6.2 | 75 |
| | -38 | 6.2 | 75 |
| | -39 | 6.2 | 75 |
| | -39 | 6.2 | 75 |
| | -40 | 6.2 | 75 |
| | -40 | 6.2 | 60 |
| | -41 | 6.2 | 60 |
| | -41 | 6.2 | 60 |
| | -42 | 6.2 | 60 |
| | -42 | 6.2 | 60 |
| | -43 | 6.2 | 60 |
| | -43 | 6.2 | 60 |
| | -44 | 6.2 | 60 |
| | -44 | 6.2 | 40 |
| | -45 | 6.2 | 40 |
| | -45 | 6.2 | 40 |
| | -46 | 6.2 | 40 |
| | -46 | 6.2 | 40 |
| | -47 | 6.2 | 40 |
| | -47 | 6.2 | 40 |
| | -48 | 6.2 | 40 |
| | -48 | 6.2 | 40 |
| Pile toe | -49 | 6.2 | 40 |

# Appendix II: Side view of mode shapes for Jacket Reference Structure

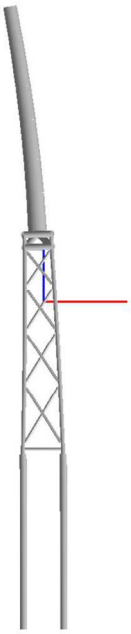

(a) 1st tower fore- aft

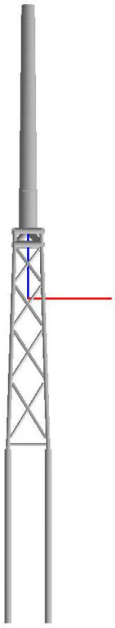

(b) 1st tower side to side

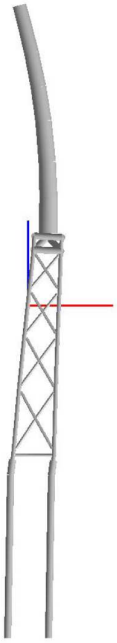

(c) 2nd tower force aft

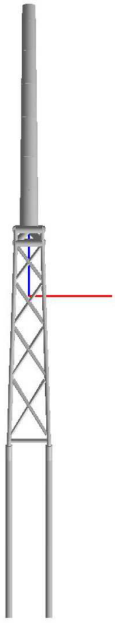

(d) 2nd tower side to side

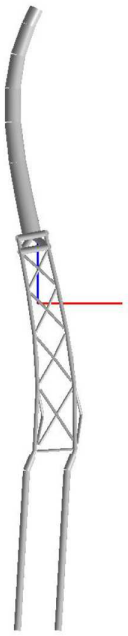

(e) 3rd tower force-aft

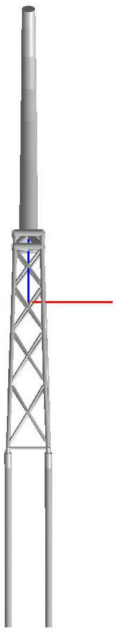

(f) 3rd tower side to side

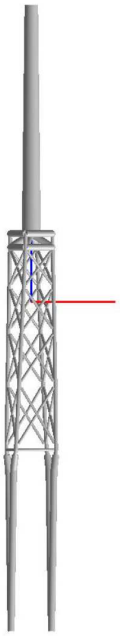

(g) 1st tower torsion

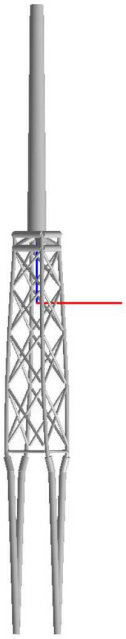

(h) 2nd tower torsion

# Appendix III: Structural drawings of Jacket Reference structure

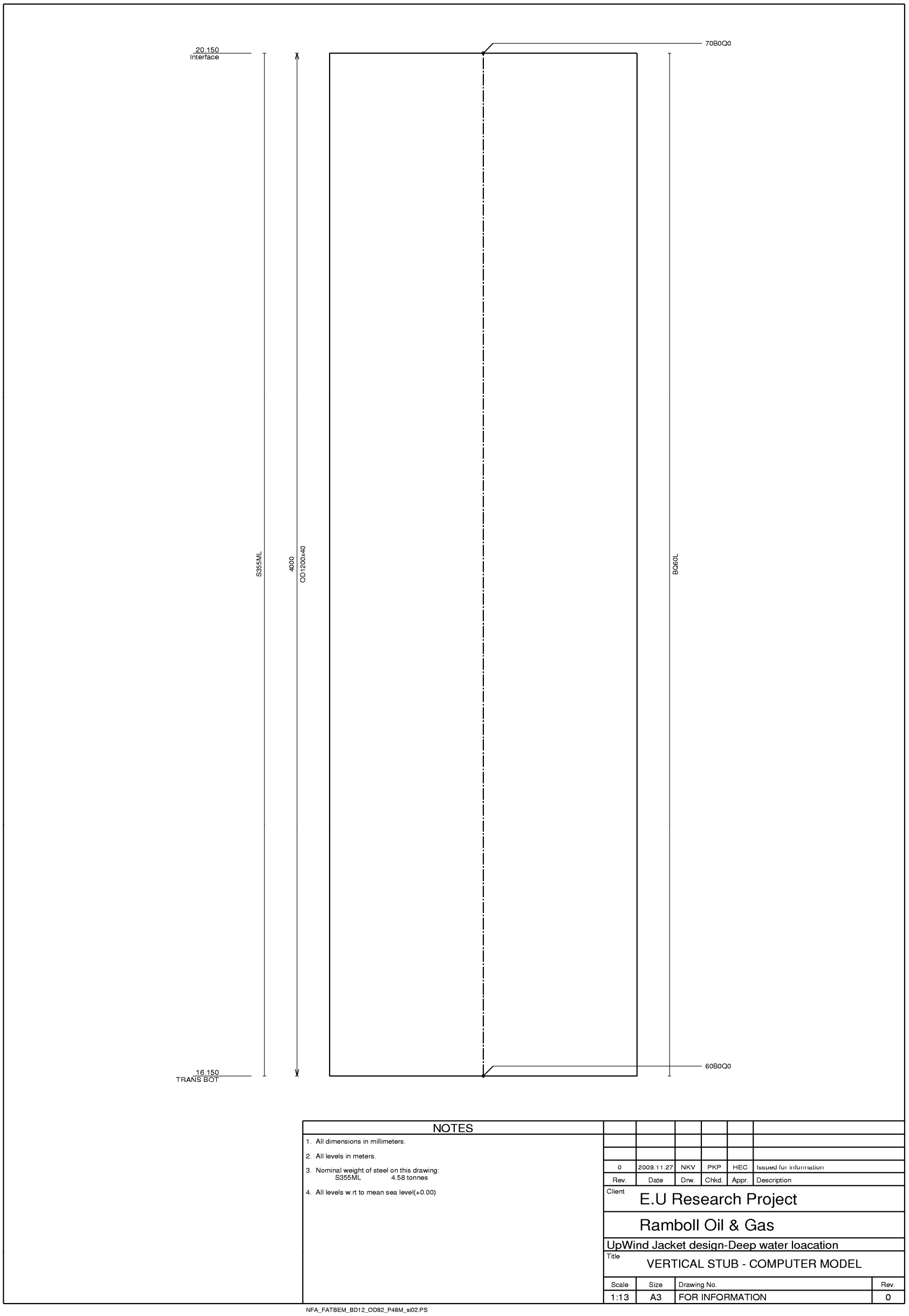


NOTES

1. All dimensions in millimeters.
2. All levels in meters.
3. Nominal weight of steel on this drawing:
   S355ML 4.58 tonnes
4. All levels w.rt to mean sea level(+0.00)

| Rev. | Date | Drw. | Chkd. | Appr. | Description |
|---|---|---|---|---|---|
| 0 | 2009.11.27 | NKV | PKP | HEC | Issued for information |

Client: E.U Research Project

Ramboll Oil & Gas

UpWind Jacket design-Deep water loacation

Title: VERTICAL STUB - COMPUTER MODEL

| Scale | Size | Drawing No. | Rev. |
|---|---|---|---|
| 1:13 | A3 | FOR INFORMATION | 0 |

NFA_FATBEM_BD12_OD82_P48M_si02.PS

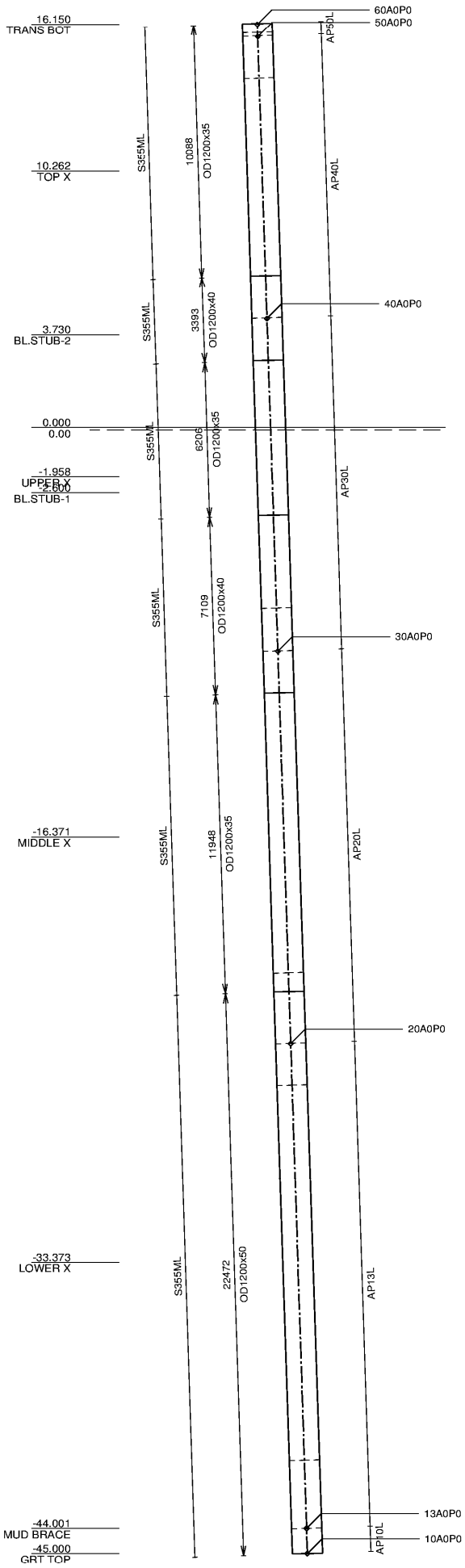


| NOTES |
|---|
| 1. All dimensions in millimeters. |
| 2. All levels in meters. |
| 3. Nominal weight of steel on this drawing:<br>S355ML 72.28 tonnes |
| 4. All levels w.rt to mean sea level(+0.00) |

| Rev. | Date | Drw. | Chkd. | Appr. | Description |
|---|---|---|---|---|---|
| 0 | 2009.11.27 | NKV | PKP | HEC | Issued for information |

Client: E.U Research Project

Ramboll Oil & Gas

UpWind Jacket design-Deep water loacation

Title: JACKET LEG - COMPUTER MODEL

| Scale | Size | Drawing No. | Rev. |
|---|---|---|---|
| 1:194 | A3 | FOR INFORMATION | 0 |

NFA_FATBEM_BD12_OD82_P48M_si02.PS

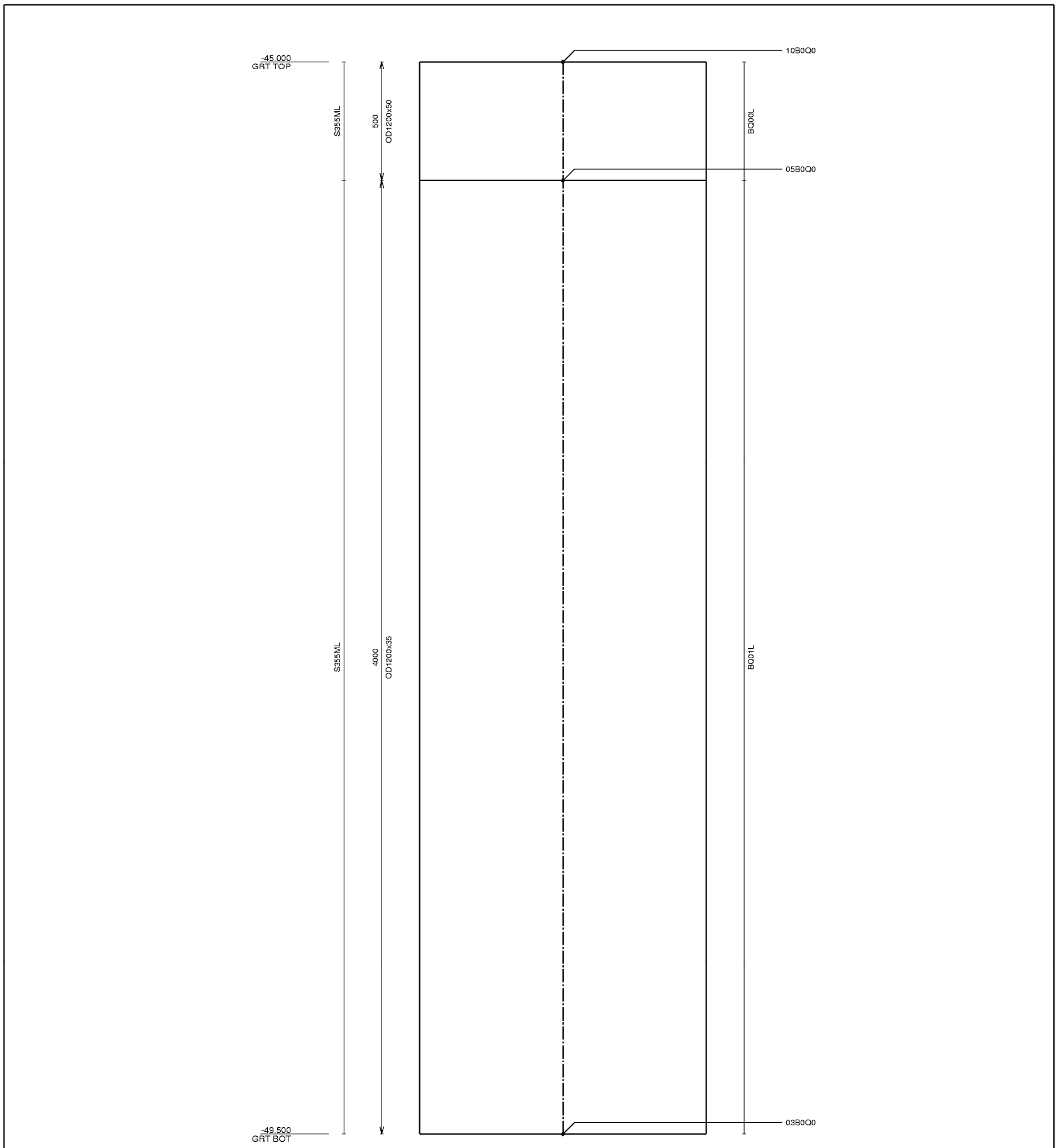


| NOTES |
|---|
| 1. All dimensions in millimeters. |
| 2. All levels in meters. |
| 3. Nominal weight of steel on this drawing:<br>S355ML 4.73 tonnes |
| 4. All levels w.rt to mean sea level(+0.00) |

| Rev. | Date | Drw. | Chkd. | Appr. | Description |
|---|---|---|---|---|---|
| 0 | 2009.11.27 | NKV | PKP | HEC | Issued for information |

Client: E.U Research Project

Ramboll Oil & Gas

UpWind Jacket design-Deep water loacation

Title: TUBULAR LEG SECTION - COMPUTER MODEL

| Scale | Size | Drawing No. | Rev. |
|---|---|---|---|
| 1:16 | A3 | FOR INFORMATION | 0 |

NFA_FATBEM_BD12_OD82_P48M_si02.PS

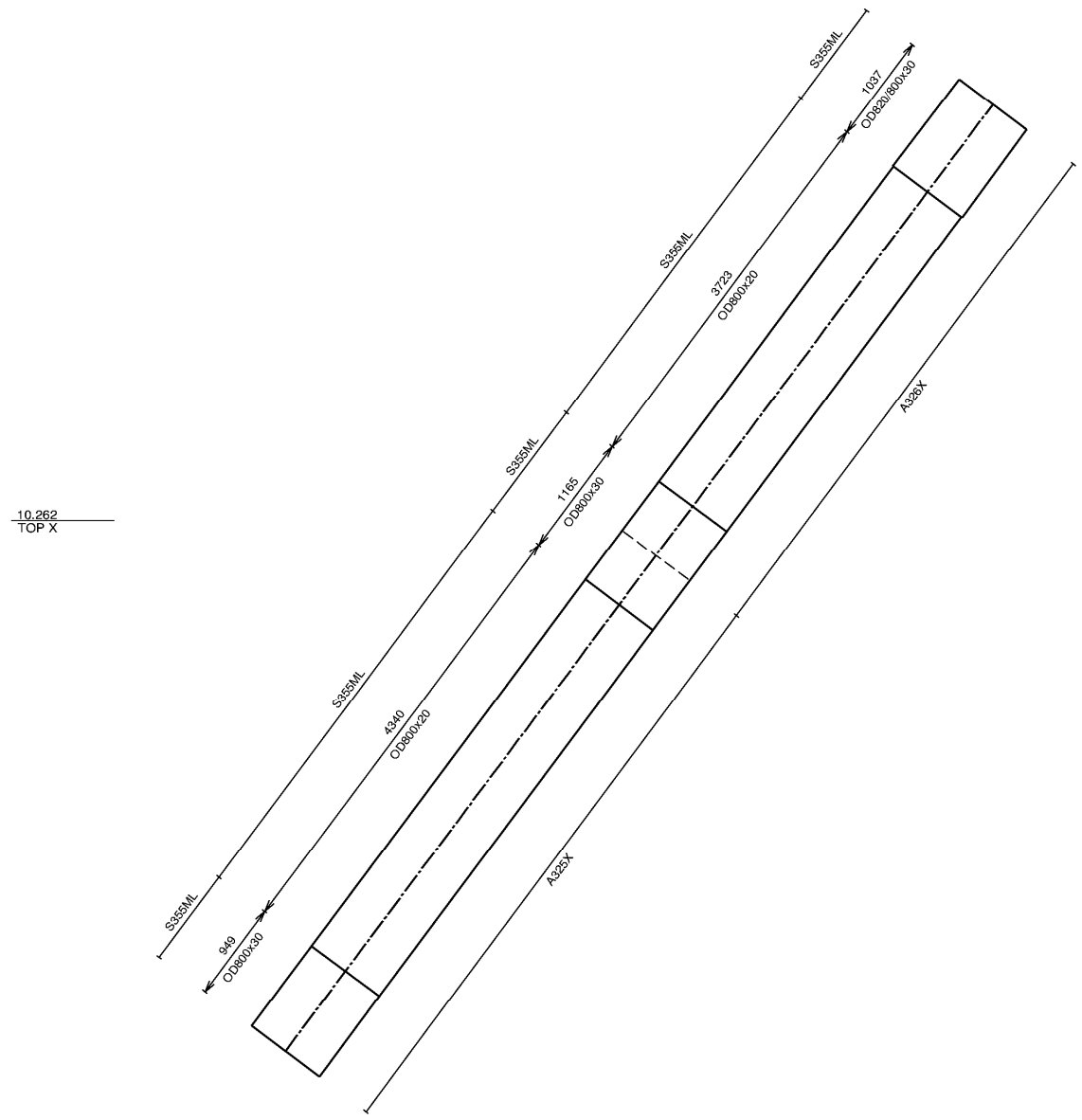


| NOTES |
|---|
| 1. All dimensions in millimeters. |
| 2. All levels in meters. |
| 3. Nominal weight of steel on this drawing:<br>S355ML 4.91 tonnes |
| 4. All levels w.rt to mean sea level(+0.00) |

| Rev. | Date | Drw. | Chkd. | Appr. | Description |
|---|---|---|---|---|---|
| 0 | 2009.11.27 | NKV | PKP | HEC | Issued for information |

Client: E.U Research Project

Ramboll Oil & Gas

UpWind Jacket design-Deep water loacation

Title: TOP X-BRACE - COMPUTER MODEL

| Scale | Size | Drawing No. | Rev. |
|---|---|---|---|
| 1:54 | A3 | FOR INFORMATION | 0 |

NFA_FATBEM_BD12_OD82_P48M_si02.PS

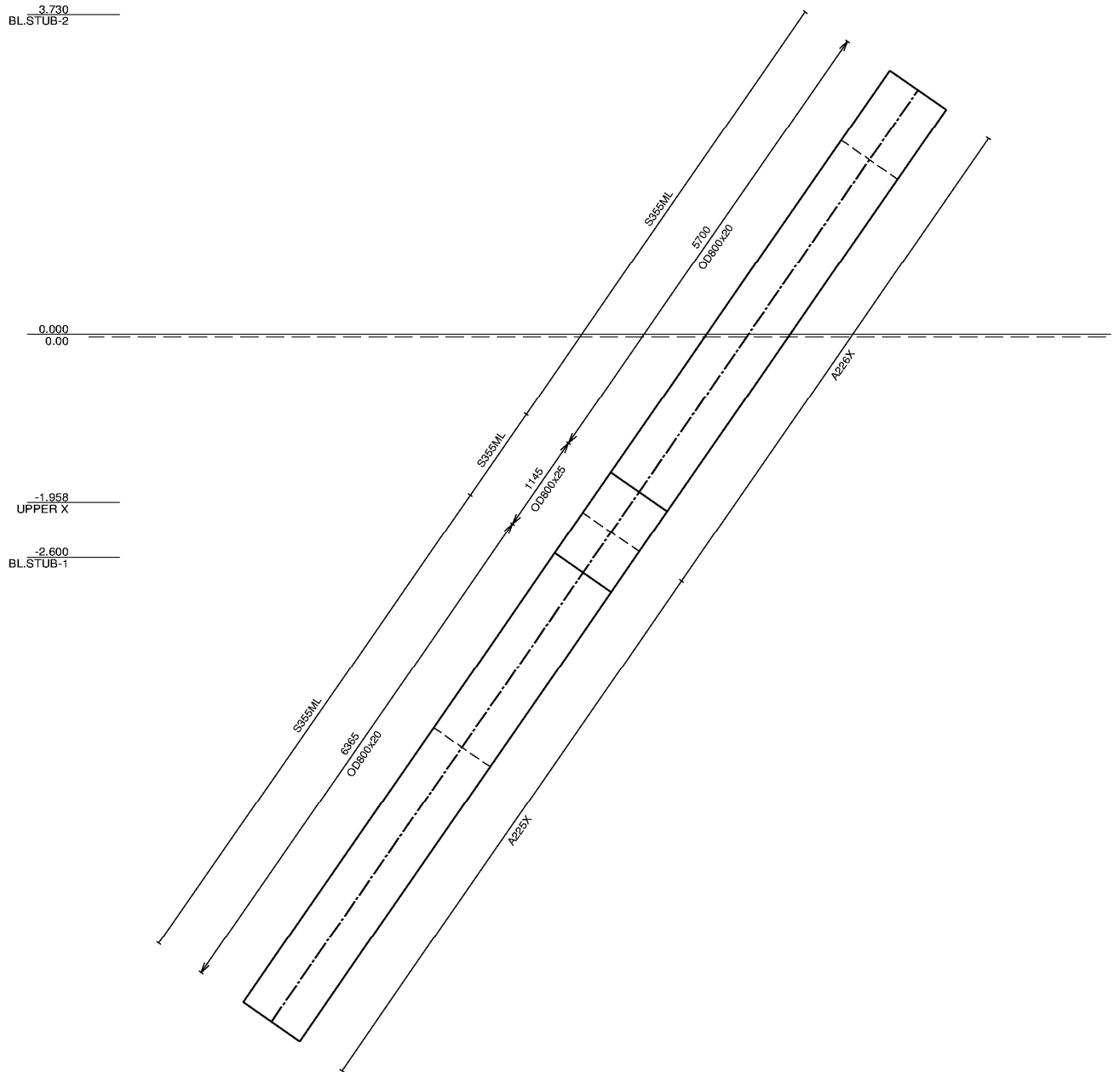


| NOTES |
|---|
| 1. All dimensions in millimeters. |
| 2. All levels in meters. |
| 3. Nominal weight of steel on this drawing:<br>S355ML 5.19 tonnes |
| 4. All levels w.rt to mean sea level(+0.00) |

| Rev. | Date | Drw. | Chkd. | Appr. | Description |
|---|---|---|---|---|---|
| 0 | 2009.11.27 | NKV | PKP | HEC | Issued for information |

Client: E.U Research Project

Ramboll Oil & Gas

UpWind Jacket design-Deep water loacation

Title: UPPER X-BRACE - COMPUTER MODEL

| Scale | Size | Drawing No. | Rev. |
|---|---|---|---|
| 1:60 | A3 | FOR INFORMATION | 0 |

NFA_FATBEM_BD12_OD82_P48M_si02.PS

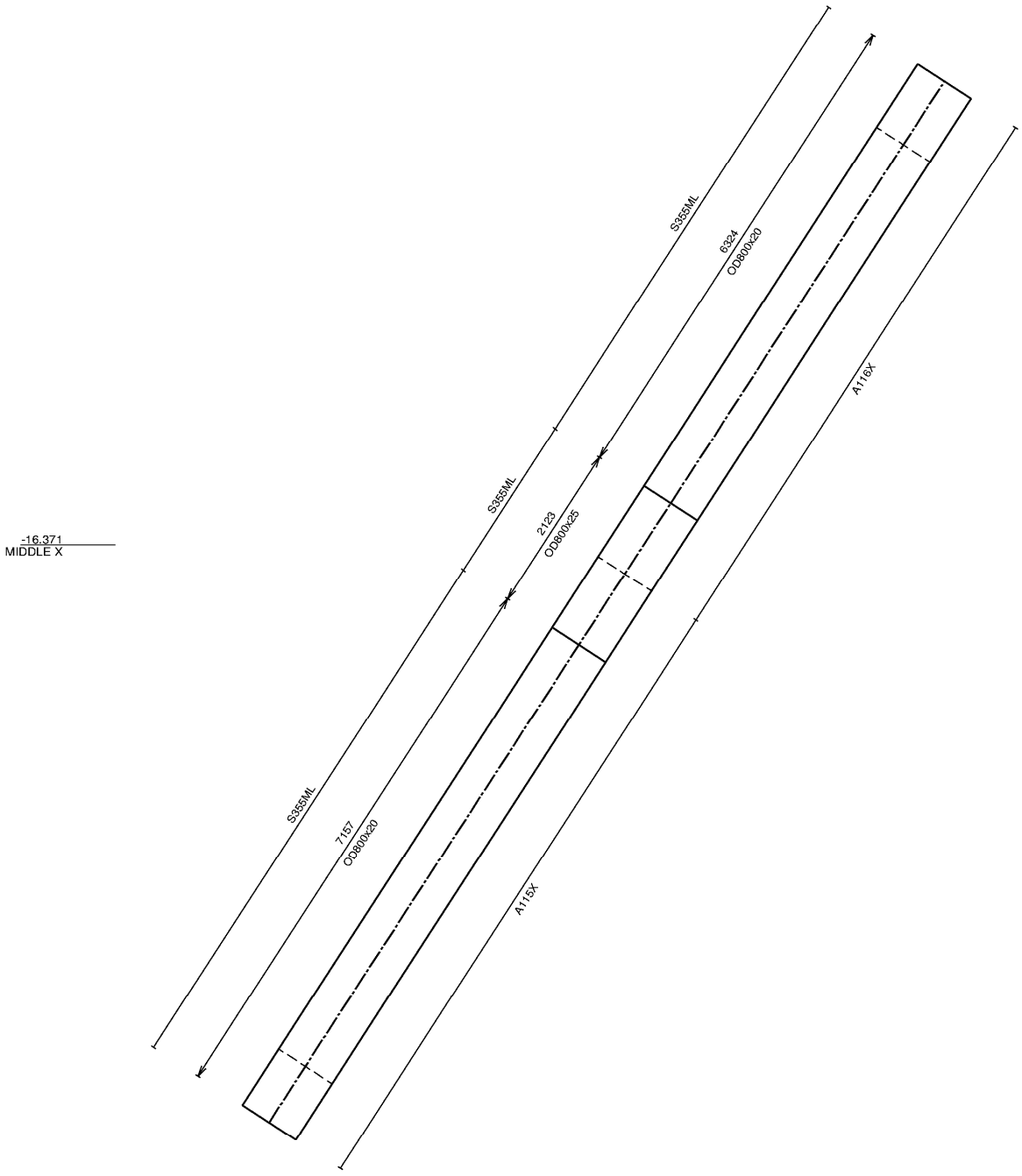


| NOTES |
|---|
| 1. All dimensions in millimeters. |
| 2. All levels in meters. |
| 3. Nominal weight of steel on this drawing:<br>S355ML 6.20 tonnes |
| 4. All levels w.rt to mean sea level(+0.00) |

| Rev. | Date | Drw. | Chkd. | Appr. | Description |
|---|---|---|---|---|---|
| 0 | 2009.11.27 | NKV | PKP | HEC | Issued for information |

Client: E.U Research Project

Ramboll Oil & Gas

UpWind Jacket design-Deep water loacation

Title: MIDDLE X-BRACE - COMPUTER MODEL

| Scale | Size | Drawing No. | Rev. |
|---|---|---|---|
| 1:66 | A3 | FOR INFORMATION | 0 |

NFA_FATBEM_BD12_OD82_P48M_si02.PS

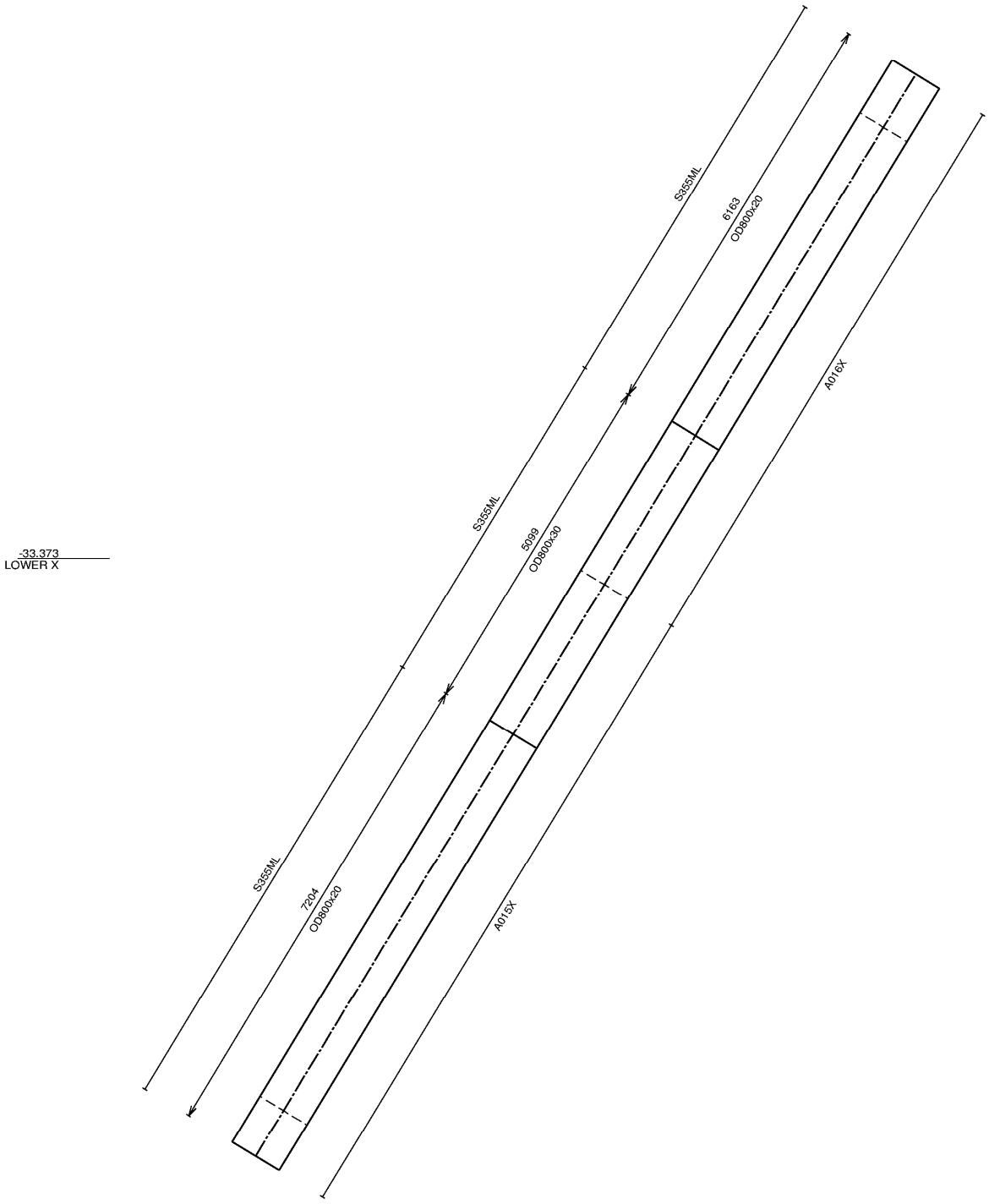


| NOTES |
|---|
| 1. All dimensions in millimeters. |
| 2. All levels in meters. |
| 3. Nominal weight of steel on this drawing:<br>S355ML 8.05 tonnes |
| 4. All levels w.rt to mean sea level(+0.00) |

| Rev. | Date | Drw. | Chkd. | Appr. | Description |
|---|---|---|---|---|---|
| 0 | 2009.11.27 | NKV | PKP | HEC | Issued for information |

Client: E.U Research Project

Ramboll Oil & Gas

UpWind Jacket design-Deep water loacation

Title: LOWER X-BRACE - COMPUTER MODEL

| Scale | Size | Drawing No. | Rev. |
|---|---|---|---|
| 1:74 | A3 | FOR INFORMATION | 0 |

NFA_FATBEM_BD12_OD82_P48M_si02.PS

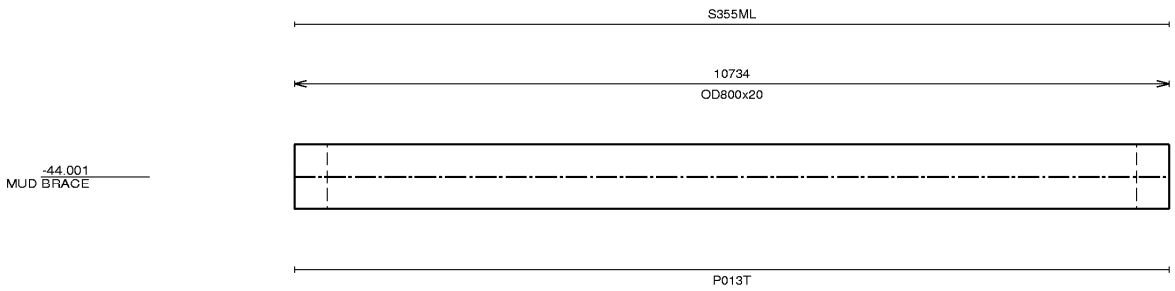


| NOTES |
|---|
| 1. All dimensions in millimeters. |
| 2. All levels in meters. |
| 3. Nominal weight of steel on this drawing:<br>S355ML 4.13 tonnes |
| 4. All levels w.rt to mean sea level(+0.00) |

| Rev. | Date | Drw. | Chkd. | Appr. | Description |
|---|---|---|---|---|---|
| 0 | 2009.11.27 | NKV | PKP | HEC | Issued for information |

Client: E.U Research Project

Ramboll Oil & Gas

UpWind Jacket design-Deep water loacation

Title: MUD BRACE - COMPUTER MODEL

| Scale | Size | Drawing No. | Rev. |
|---|---|---|---|
| 1:74 | A3 | FOR INFORMATION | 0 |

NFA_FATBEM_BD12_OD82_P48M_si02.PS

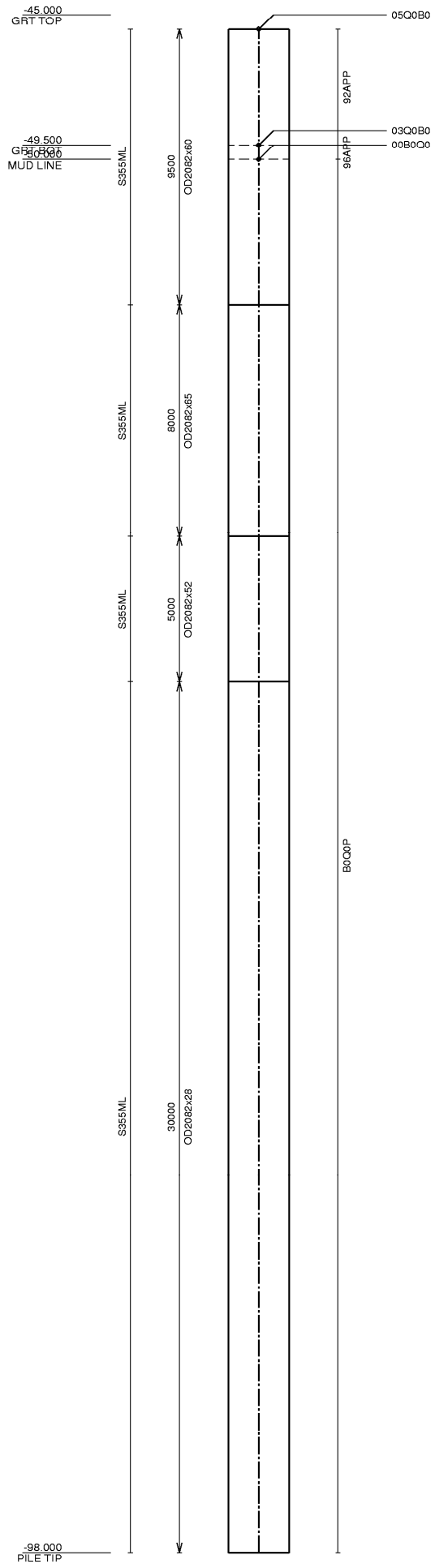


| NOTES |
|---|
| 1. All dimensions in millimeters. |
| 2. All levels in meters. |
| 3. Nominal weight of steel on this drawing:<br>S355ML 109.86 tonnes |
| 4. All levels w.rt to mean sea level(+0.00) |

| Rev. | Date | Drw. | Chkd. | Appr. | Description |
|---|---|---|---|---|---|
| 0 | 2009.11.27 | NKV | PKP | HEC | Issued for information |

Client: E.U Research Project

Ramboll Oil & Gas

UpWind Jacket design-Deep water loacation

Title: PILE - COMPUTER MODEL

| Scale | Size | Drawing No. | Rev. |
|---|---|---|---|
| 1:168 | A3 | FOR INFORMATION | 0 |

NFA_FATBEM_BD12_OD82_P48M_si02.PS

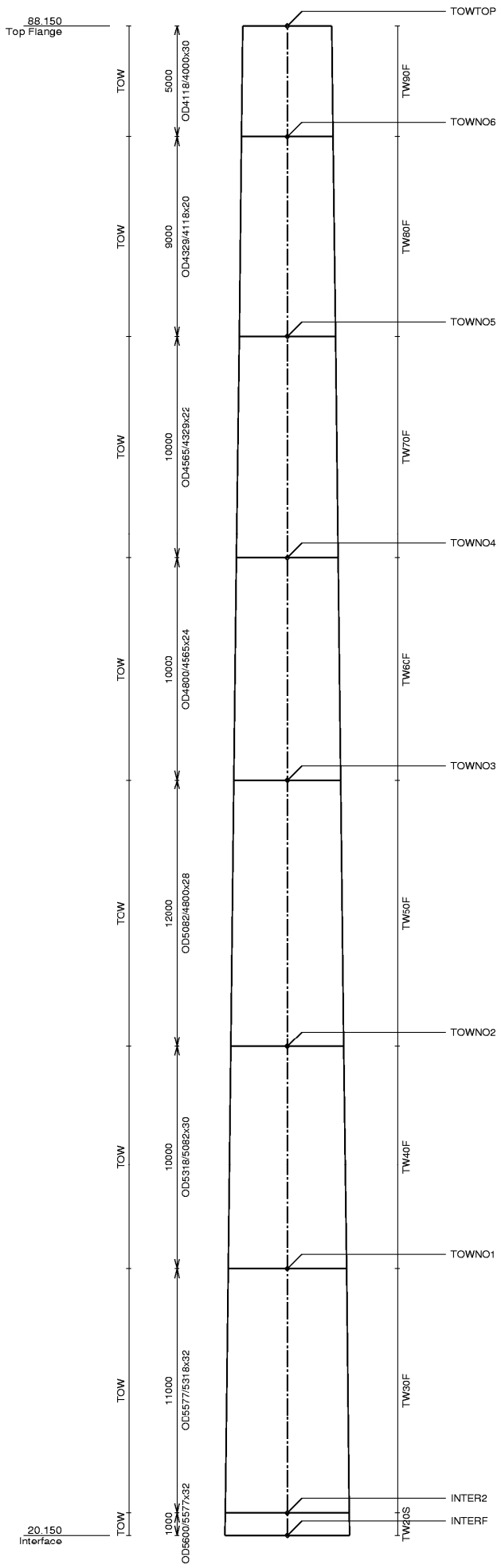


| NOTES |
|---|
| 1. All dimensions in millimeters. |
| 2. All levels in meters. |
| 3. Nominal weight of steel on this drawing:<br>TOW 215.52 tonnes |
| 4. All levels w.rt to mean sea level(+0.00) |

| Rev. | Date | Drw. | Chkd. | Appr. | Description |
|---|---|---|---|---|---|
| 0 | 2009.11.27 | NKV | PKP | HEC | Issued for information |

Client: E.U Research Project

Ramboll Oil & Gas

UpWind Jacket design-Deep water loacation

Title: TOWER - COMPUTER MODEL

| Scale | Size | Drawing No. | Rev. |
|---|---|---|---|
| 1:216 | A3 | FOR INFORMATION | 0 |

NFA_FATBEM_BD12_OD82_P48M_sl02.PS